Diploma Thesis

to obtain the title of

Dipl.–Ing. (FH)

of the University of Applied Sciences – Karlsruhe
— Fakultät für Maschinenbau und Mechatronik (MMT) —

Monitoring of damage on water–cooled cables installed in the Large Hadron Collider (CERN) and research on possible alternatives

---

CERN-THESIS-2011-316
//2011

Defended by
Alexander G. Wollmann (21365)

Thesis Advisor: Prof. Dr. Frank Artinger

Prepared at CERN – Geneva

Date of submission: 2011–02–18

Abstract

To supply the superconducting magnets in the Large Hadron Collider at CERN, several thousand metres of water–cooled cables were installed. These cables consist of a flexible copper core surrounded by a reinforced rubber hose. Although the hose material has been selected carefully, on many cables the rubber hose has suffered from damage.

After giving a general overview on common rubber materials and known reasons for their ageing, the technology of water–cooled cables and their special requirements will be introduced. Then, the aim of this thesis is to present the monitoring of the damage on the rubber hoses. This includes an introduction to the monitoring technique used, followed by an analysis and discussion of the results obtained.

As a different way of investigating the damage, a pressure test for the rubber hose will be proposed and specified; and the possibility of using alternative conductors for the current supply of the LHC main magnets will be examined.

Finally, a series of radiation tests on potential new materials for rubber hoses will be presented.

This thesis contains confidential data disclosed by CERN. It may not be disclosed, published or made known in any other manner – including in the form of extracts – to any third party without the explicit approval of CERN. This thesis may only be disclosed to the supervisors as well as to the members of the examining board of University of Applied Sciences, Karlsruhe.

Hochschule Karlsruhe
Technik und Wirtschaft
UNIVERSITY OF APPLIED SCIENCES

Fakultät für Maschinenbau und Mechatronik

Diplomarbeit für:	**Alexander Wollmann** **Studiengang Mechatronik**
Arbeitsplatz	CERN (European Organization for Nuclear Research) Engineering department, Cabling and Optical Fibre section CH – 1211 GENEVA (Schweiz)
Betreuer am Arbeitsplatz	Jean-Claude Guillaume (jean-claude.guillaume@cern.ch) Daniel Ricci (daniel.ricci@cern.ch)
Betreuender Dozent	Prof. Dr.-Ing. Frank Artinger Technische Informatik
Datum der Ausgabe	19.10.2010 **Abgabetermin** 18.02.2011

Kurzthema: Monitoring of damage on water-cooled cables installed in the Large Hadron Collider (CERN) and research on possible alternatives

Aufgabenstellung

To supply current to the superconducting magnets in the Large Hadron Collider at CERN, several thousand meters of water-cooled cables were installed. These cables consist of a flexible copper core which is surrounded by a reinforced rubber hose. Although the hose material has been selected carefully, on many cables the rubber hose has suffered from damage.

After giving a general overview on common rubber materials and known reasons for their ageing, the aim of this thesis is to introduce the technology of water-cooled cables and their special requirements. Then, the monitoring of the damage on the rubber hose shall be presented. This includes:

- Introduction to the monitoring technique
- Analysis and discussion of the monitoring results
- Proposal and specification of a pressure test for further investigation

Finally, the possibility to use alternative conductors for the current supply to the LHC main magnets shall be examined

Im Einzelnen sind die folgenden Punkte zu bearbeiten:

- Introduction to rubber materials and typical ageing factors
- Description of the operation conditions and technical requirements of water-cooled cables
- Analysis of the monitoring results of the damage occurred before the startup of the LHC
- Research on possible alternatives for water-cooled cables
- Proposal for possible tests to be conducted in the future

Vorsitzender des Prüfungsausschusses

Prof. Dr.-Ing. Peter Weber

Betreuender Dozent

Prof. Dr.-Ing. Frank Artinger

Contents

Definition of task . . . III
Preface . . . IX
Acknowledgements . . . XI
List of Tables . . . XIII
List of Figures . . . XV

1 Introduction **1**
1.1 About CERN . . . 1
1.2 Particle accelerators at CERN . . . 2

2 Introduction to rubber materials **5**
2.1 A brief history . . . 5
2.2 Definition . . . 6
2.3 Rubber types . . . 7
2.4 Premature ageing of rubber . . . 9
2.4.1 Influence of oxygen . . . 9
2.4.2 Influence of ozone . . . 10
2.4.3 Influence of ionizing radiation . . . 11
2.5 Storage of rubber . . . 12

3 Water–cooled cables in the LHC **13**
3.1 Definition . . . 13
3.2 Application . . . 15
3.3 Technical requirements . . . 17
3.4 Qualification tests . . . 19
3.4.1 Fire hazard testing . . . 19
3.4.2 Smoke density . . . 20
3.4.3 Radiation resistance . . . 21

3.5 Environmental conditions in the LHC tunnel 22
3.5.1 Temperature and humidity 22
3.5.2 Ozone 23
3.5.3 Ionizing radiation 25
3.6 Cooling water system 27

4 Damage occurred before the startup of the LHC 29
4.1 Introduction 29
4.2 Presence of halogens 29
4.3 Surface cracks 32

5 Crack monitoring 35
5.1 Monitoring and evaluation methodology 35
5.1.1 Identification and marking of crack–areas 36
5.1.2 Photo documentation 36
5.1.3 Offline measurements 38
5.1.4 Evaluation 41
5.2 Monitoring Point 6 in Summer 2010 44
5.3 Conclusion 47

6 Discussion 49
6.1 Restrictions of monitoring methodology 49
6.1.1 Camera angle 50
6.1.2 Perspective distortion 52
6.1.3 Conclusion 54
6.2 Crack depth 55
6.2.1 Motivation 55
6.2.2 Measurements 57
6.2.3 Summary 59
6.3 Conclusion 59

7 Crack analysis with combined radiation and pressure testing 61
7.1 Test principle 61
7.2 Operational conditions and pressure patterns 63
7.2.1 Initial test 64
7.2.2 Commissioning of the cable 65
7.2.3 Maintenance of the hydraulic system 66

7.2.4 Shutdown of the hydraulic system 68
7.3 Preparation of samples 69
7.3.1 Dimensioning of test pieces 69
7.3.2 Introduction of cracks 70
7.3.3 Irradiation of samples 70
7.3.4 Crack measurement 71
7.4 Definition of the test method 71
7.4.1 Simulated lifetime 71
7.4.2 Environmental conditions 72
7.4.3 Test setup 72
7.4.4 Test pressure sequence 73
7.5 Expression of results 74

8 Research on possible alternatives **77**
8.1 Motivation 77
8.2 Fundamental considerations 78
8.3 Conductor materials 80
8.4 Conductor layouts 82
8.5 Conclusion 85

9 Radiation resistance testing **87**
9.1 Sample preparation 87
9.2 Material testing 88
9.3 Discussion of results 90
9.4 Conclusion 92

Appendices **95**
Bibliography 97
Index 105
Glossary 107
Declaration 113

A Photo monitoring LHC Point 6 **115**
A.1 Photographs of crack–areas Point 6L 115
A.2 Photographs of crack–areas Point 6R 145
A.3 Monitoring protocols 161
A.4 Crack–areas Point 6L 171

A.5 Crack–areas Point 6R 177
A.6 Crack progression Point 6L 181
A.7 Crack progression Point 6R 187
A.8 Affected cables Point 6L 191
A.9 Affected cables Point 6R 195
A.10 Monitoring history Point 6L 199
A.11 Monitoring history Point 6R 213

B Reinforcement layer measurement records 219

C Pressure test profiles 225

D Tensile test results of irradiated rubber hose samples 237

Preface

CERN operates the LHC, a particle accelerator that uses water–cooled cables to supply its superconducting magnets. These cables consist of a flexible copper core surrounded by a reinforced rubber hose. They are constantly flushed by deminieralized cooling water as they transport currents of several kA that generate a large amount of heat in the conductor.

These cables suffered from damage, which was due to chlorine in the hose material and surface cracks. The problem of surface cracks still persists and poses a possible threat to the safe operation of the LHC. CERN and its particle accelerators will be pictured in Chapter 1.

As the surface cracks affect the rubber hose of the cable, an introduction to rubber materials will then be given in Chapter 2. The aim is to give a general overview on different types of rubber, reasons for their premature ageing and common methods to prevent this ageing.

Chapter 3 will then introduce the technology of water–cooled cables, including structure, typical use and technical requirements. The Chapter finishes with a description of the environmental conditions in the LHC.

The problems which have occurred will be addressed in Chapter 4. After a description of the damage patterns, the monitoring methodology and the composition of the "severity–value" used to evaluate the surface cracks is introduced. A monitoring of 86 crack–areas in LHC Point 6 shows an increased severity–value in 14 areas and is presented in Chapter 5.

However, the accuracy of the methodology is restricted; Chapter 6 will cover some of the limitations. Furthermore, the critical crack depth was determined on spot samples. A depth of 2.40 mm was determined to be a good assumption for this value.

As a future prospect, a combined radiation and pressure test for the hoses is defined in Chapter 7. In this test, the monitoring methodology can be applied under optimized conditions.

Then, the possibility of using alternative conductors as a replacement for the water–cooled cables is examined in Chapter 8. However, rubber materials seem inevitable to provide the necessary flexibility of the conductor.

As radiation levels in the LHC will increase in the next years, a radiation resistance test on potential new rubbers is presented in the last Chapter. Results show the influence of radiation, but qualify all tested materials.

Acknowledgements

I am indebted to many people for their long–lasting support and encouragement which was invaluable for the successful completion of this work.

First and foremost, I would like to thank my supervisors at CERN, Jean–Claude Guillaume and Daniel Ricci, who made available their support in a number of ways. I am also indebted to my thesis advisors Prof. Dr–Ing. Frank Artinger and Prof. Dr. rer. nat. Eberhard Halter, for their valuable guidance.

My gratitude shall also be expressed to my former colleagues at CERN, Karim Loukili, Antonio Gonzalez Puertas, Marten Frans, Christoph Janowicz, James Divine, Patrick Lelong, Guillaume Gros, Daniel Schamme, and all the other members of the EN–EL Group. It was great to work in a group of people from so many different nations. C'était un plaisir de faire votre connaissance, et votre bonne compagnie ne sera jamais oubliée.

Furthermore, I would like to thank Serge Deleval for his explanations of both the cooling water circuit and the air handling system, as well as Alexandre Gerardin, who executed the tensile tests on the rubber hose samples. I also owe my gratitude to Vesa Ylamaki, without whose detailed documentation on the crack monitoring, this work would not have been possible.

I also do not want to fail to mention Tom Levens and Daniel Lemon, two of the numerous students I met at CERN who happened to become my neighbours in Ferney–Voltaire. I will not forget the good time we had together.

In this regard, I also express my gratitude to Laura Saulnier, who did a great job in introducing and guiding the new students at CERN.

Among all the people I met at CERN, I am especially grateful to have made the acquaintance of Yu Wang. Thank you for your constant encouragement, your positive attitude and all the inspiring discussions – not to forget the genuine Chinese food. Please keep laughing at the awkward things in life.

The commitment of Oliver Geiger, Dieter Gittel, Raman Chaudhari and Verena Senger at Fraunhofer ICT shall also be emphasized.

Furthermore, I would like to thank John N. Harrison and M. Bert Geraghty BSc, PhD, for taking the task of cross–reading this paper.

Needless to say, I would like to thank my family: my parents, Annelie and Willi Wollmann as well as my two brothers, Martin and Andreas. Thank you for all the support, trust and help I received within the last months. Without you, I wouldn't be the person I am now.

Finally, my deepest and sincere thanks go to my dear friends Sebastian Buccheri, Stefanie Herzberg, Michel Hussong and Jelena Berg. I probably wasn't the most pleasant person to be around during the last weeks, but you were there for me. Thank you for that.

Alexander Wollmann
Karlsruhe, 16th February 2011

List of Tables

2.1 Rubber types found in water–cooled cable hoses 9

3.1 Main parameters of water–cooled cables 18
3.2 Maximum permissible leakage current 18

5.1 File naming system 37
5.2 Crack frequency, assigned category and according factor . . 40
5.3 Crack width, assigned crack depth and according factor . . 40
5.4 Values for crack type, frequency and depth 41
5.5 Inspected cables 44

7.1 Required test time 74

List of Figures

1.1 CERN accelerator complex 2

3.1 Copper core of water–cooled cable 14
3.2 Layers of cable hose 14
3.3 Connection pattern of water–cooled cables 15
3.4 Example of water–cooled cable installation 16
3.5 Test setup for smoke density test 20
3.6 Schematic layout of the air flows in the LHC tunnel 23
3.7 Hose sample after ozone exposure 24
3.8 Exemplary dose map of annual dose in LHC arcs 26
3.9 Water cooling circuit 27

4.1 Corroded connector 31
4.2 Crack types 33
4.3 Affected cables 34

5.1 Monitoring procedure 35
5.2 Examination of cables 36
5.3 Steps of the offline measurement process 38
5.4 Examination of cables 39
5.5 Crack measurements 43
5.6 Increase of severity–value Point 6L 45
5.7 Increase of severity–value Point 6R 46
5.8 Absolute severity–value 46

6.1 Geometric principle of angular misalignment 50
6.2 Error due to angular misalignment 51
6.3 Geometric principle of perspective distortion 52

6.4 Error due to perspective distortion 53
6.5 Crack–area 32: offset of reference object 54
6.6 Cross–section profile of water–cooled cable hose 56
6.7 Depth measurements on 76 mm hose samples 58
6.8 Depth measurements on 86 mm hose samples 58
6.9 Depth measurements on 105 mm hose samples 59

7.1 Radiation and pressure test procedure 62
7.2 Pressure pattern during initial test 64
7.3 Pressure pattern during commissioning 65
7.4 Pressure pattern during maintenance of the hydraulic system 67
7.5 Pressure pattern during hydraulic shutdown 68
7.6 Sample bent through 90° 69
7.7 Test pressure sequence 73

8.1 Water–cooled tubes and cables 79
8.2 Power dissipation per metre for different conductor materials 81
8.3 Flexible conductor with copper tube 83
8.4 Cross–section of the conductor for the MINOS detector coil 84

9.1 Tensile test of water–cooled cable hose 89
9.2 Tensile strength of hose samples 90
9.3 Elongation of hose samples at F_{max} 91
9.4 Relative elongation at F_{max} 92

Chapter 1

Introduction

CERN is a multinational research centre, operating some of the most advanced particle accelerators in the world. This first Chapter will give a short introduction to CERN as a research facility and to the particle accelerators that are used for the experiments.

1.1 About CERN

Straddling the Franco–Swiss border, just outside Geneva, the European Organization for Nuclear Research has been a centre for European collaboration and research into fundamental physics for over fifty years. Founded in 1953, with a convention between twelve European countries, CERN is one of the world's largest and most respected centres for scientific research and now has contributors from twenty European member states and from many universities around the world.

As a scientific institution, CERN designs, builds and operates a chain of "particle accelerators". These machines are used to accelerate particles, such as protons and heavy ions, to close to the speed of light and increase their energy. These particles are then made to collide, either with each other or with a fixed target, and in this collision the energy of the particles can create other particles. Around this collision point, massive detectors are constructed which observe the debris and track any particles that may be produced as a result of these collisions.

Since its first accelerator was commissioned in 1959, CERN has been host to a number of significant scientific discoveries including neutral

currents (1973), the $W^{\pm}$ and Z^0 bosons (1983) and the first observations of antihydrogen (1995). It is also the birth–place of the world–wide–web (1990) [CER11].

1.2 Particle accelerators at CERN

As it is difficult to accelerate particles from rest to a high energy in a single machine, CERN operates a chain of accelerators which are used to gradually increase the energy of particles. Once accelerated in a particular machine, particles are either transferred to a larger machine or supplied to any of a number of experiments. Nowadays, CERN's injector chain consists of six accelerators and a de–accelerator.

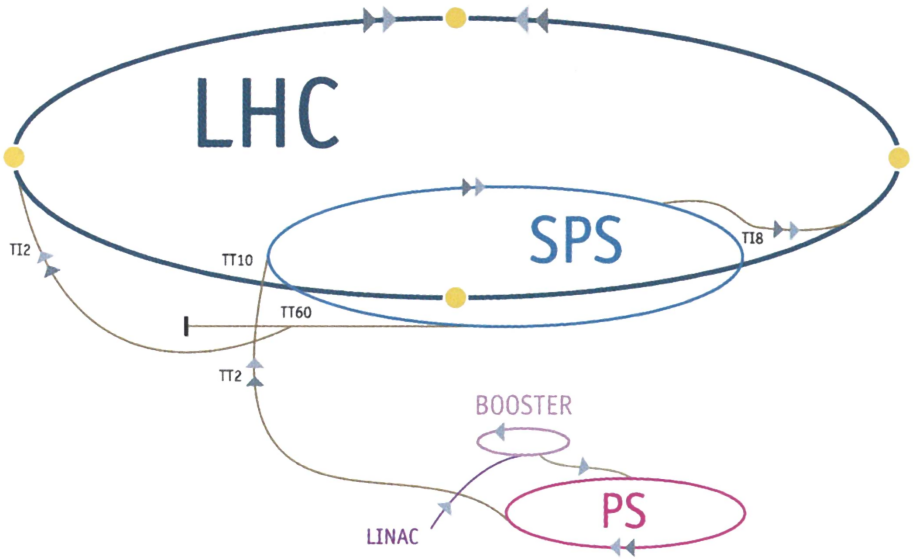

Figure 1.1: Particle accelerator complex at CERN: After initial acceleration in LINAC, particles are further accelerated in the Booster (PSB), passed into the PS and then delivered to the SPS. Finally, they are injected into the LHC. The Figure illustrates the accelerator chain for protons, so LEIR is not shown (image source: [Eva09]).

Currently, two types of particles are accelerated at CERN: protons (H^+), which are hydrogen atoms stripped of their electrons; and lead ions (Pb^{82+}). The initial production and acceleration is different for both protons and ions, however both types start with a source which strips the electrons from the atoms to produce a positively charged ion. In both cases, initial acceleration of the particles is performed using a Linear Accelerator (LINAC): LINAC2

is used for protons, accelerating them to 50 MeV; and LINAC3 is used for ions, accelerating them to 4.2 MeV/u[1]. Protons are then accelerated up to 1.4 GeV by a small, 25 m synchrotron called the PS Booster (PSB) before being passed into the Proton Synchrotron (PS). Ions from LINAC3 are accumulated in a small storage ring called Low–Energy Ion Ring (LEIR) and accelerated to 72 MeV/u before being passed to the PS.

The PS, the oldest machine in CERN's complex, is a 628 m, 26 GeV synchrotron that was commissioned in 1959. Apart from accelerating the particles delivered by the PSB and LEIR, it performs complex RF[2] tasks which split the bunches of particles and ensure they have the correct size and shape for injection into the Super Proton Synchrotron (SPS) and Large Hadron Collider (LHC). As well as serving as an injector, the PS provides the beam for fixed–target experiments.

Particles are then injected into the Super Proton Synchrotron (SPS), which is a 6.9 km synchrotron straddling the Franco–Swiss border. The SPS was commissioned in 1976, as a 300 GeV proton accelerator for fixed–target physics. Since then, it has been used as a proton–antiproton collider (as the Sp$\bar{\text{p}}$S), serving as the final injector for both the Large Electron–Positron Collider (LEP) and now the Large Hadron Collider (LHC), and still provides particles for a number of fixed–target experiments.

The LHC is the largest accelerator in CERN's complex and the primary focus of the current physics programme. This giant synchrotron is located in a 27 km tunnel, 100 m beneath the French countryside and features four major detectors along with a number of smaller experiments. Particles are injected from the SPS at 450 GeV and are accelerated up to 7 TeV in the form of two counter–rotating beams [Eva09].

[1] Energy per nucleon.

[2] Radio Frequency, a rate of oscillation in the range of approximately 30 kHz to 300 GHz.

Chapter 2

Introduction to rubber materials

Components based on rubber materials play a very important part in engineering processes and products; springs and snubbers, seals and gaskets, hoses and belts – items that would be included in a suprisingly long comprehensive listing of essential rubber components.

This Chapter will begin with a brief review of the history and unique properties of rubber materials. Subsequently, common rubber types will be introduced. Finally, reasons for the premature ageing of rubbers and common antidegradants will be covered.

2.1 A brief history

Natural rubber obtained from trees was the only source of rubber until the advent of the synthetic polymers in the early part of the twentieth century. In 1839 Charles Goodyear discovered that when rubber was heated with sulphur it became stronger and more elastic, but more importantly it was no longer susceptible to changes in temperature. This process became known as vulcanization. Almost 50 years later, the pneumatic tyre was patented by John Dunlop in England.

The production of rubber was expensive at that time, as the raw materials had to be imported from South America or Asia. Attempts to duplicate rubber synthetically did not succeed until the 1930s, when synthetic rubbers were first produced in Germany. The United States started

the bulk production of synthetic rubbers when the supply of natural rubber was interrupted during the Second World War.

Since its use by Charles Goodyear, sulphur had been the principal vulcanizing agent, but the rate of vulcanization with sulphur alone was very slow. George Oenslager discovered organic accelerators which could speed up the vulcanization process and improve the elastic properties of the rubber as well[1]. His contribution was crucial for the commercialization of both natural and synthetic rubber.

Over the years, the importance of rubber to modern life has increased constantly. This is not always apparent at first sight as rubber products are mostly used in appliances that are not easily visible. Without rubber, the automobile as well as many other objects of everyday life would not exist in the form familiar to us today.

Up to the present day, research and development work on rubber materials still continues. Existing rubbers are being modified, new rubbers are being discovered, new additives are being adopted and techniques for recycling and reusing waste rubber are beginning to meet environmental and commercial requirements [DW01].

2.2 Definition

With thermoplastics and duromers, rubbers form the third main group of the polymeric materials known as the elastomers. Rubbers are created when the raw materials like caoutchouc are cross–linked during the vulcanization or curing process. In this context, the term "rubber" is ambiguous, as it refers to both the raw material and the finished product[2]. In Section 2.3, the term "rubber" will refer to the uncured polymers.

In most applications for rubber products there are no alternative materials except other rubbers. Rubber has a very high deformability and consists of molecules with a high molecular mass that can be cross–linked to form a network. If the crosslink density is not too high, the material will return to its original dimensions when external forces are

[1] A discovery for which he was awarded with the Perkin Medal in 1933, which is considered to be the highest honour given in the US industrial chemical industry.

[2] The German language distinguishes between "Kautschuk", being the natural or synthetic, uncured polymer and "Gummi", being the finished product.

removed. This ability to recover its original dimensions leads to many applications.

The mechanical properties of rubbers derive from the molecular chains that are assembled into a cross–linked network. When unstressed, the molecular segments between crosslinks are randomly coiled. When a tensile stress is applied, deformation is principally achieved by localized motions of the molecular segments taking new shapes, in which they are stretched out in the direction of the tensile axis [Tre75].

Rubbers are usually formulated with a complex mixture of additives. These are included to promote and control the crosslinking process, to impart beneficial mechanical properties and to inhibit degradation caused by the working environment. Carbon black is a common additive. It causes an increase in stiffness and strength, provides abrasion resistance and reduces UV degradation. This has allowed the development of a huge family of materials with a wide range of properties. [DW01].

2.3 Rubber types

The current range of rubber products comprises a vast amount of different materials. Until now, there is no unified method of categorizing the different types of rubber, so multiple methods coexist [DW01]. Common methods are:

- Classification by *application*: Rubbers are divided into *General Purpose Rubbers* and *Speciality Rubbers*. General Purpose Rubbers are usually cheap and used for mass production. Speciality Rubbers are generally far more expensive and are used for applications demanding special properties from the rubber material. With the expanding use of Speciality Rubbers in recent years, this classification is, however, not clear [DW01].

- Classification by *chemical structure*: According to ISO 1629, rubbers are divided into eight groups, representing the chemical structure of their main molecular chain. The last letter of the abbreviated name refers to this structure, e.g. the R–group contains rubbers with an unsaturated carbon chain (e.g. NBR) [ISO 1629].

- Classification by *polarity*: There is a distinction between nonpolar and polar rubbers. Nonpolar rubbers are pure hydrocarbon polymers, containing no polar groups. They are labile to other hydrocarbon compounds such as gasoline or mineral oils. Polar rubbers contain further atoms or atom groups apart from C and H in their polymer chain. They are, to a differing extent, resistant to gasoline or mineral oils [Nag04].

- Classification by *saturation*: Regarding the degree of saturation of the main polymer group, rubbers are divided into saturated and unsaturated rubbers. Saturated rubbers contain no double bonds but only single bonds in the main chain. Therefore, they have a low reactivity and a good ageing resistance. Unsaturated rubbers contain double bonds in the main chain. With the amount of double bonds rising, they are more reactive and have a lower ageing resistance. The degree of saturation is often used as an indication for the resistance to oxidation [Nag04].

However, giving a description of all the rubber types currently available would go beyond the scope of this thesis. Therefore, only the rubbers used in the water–cooled cables will be covered in this Section.

In 2008, CERN charged LRCCP[3], a laboratory specialised in the analysis of rubber materials, with analysing the composition of rubber materials. Those were, on the one hand, materials which at that time were used for hoses of water–cooled cables, and on the other hand materials which were considered to be used in the future for the same application. Results are available in [HF09], [HTD08] and [HT08].

Three different compositions could be distinguished: hoses composed of a mixture of NR or IR[4], NBR, and SBR rubbers, samples made from AEM rubber and samples made from EPM or EPDM rubber[5]. In Table 2.1, rubber types which were found in this analysis are listed:

[3]LRCCP: **L**aboratoire de **R**echerches et de **C**ontrôle du **C**aoutchouc et des **P**lastiques, Paris, France.

[4]The report states that instead of NR, IR, a synthetic copy of natural rubber, might be part of the composition. The use of IR seems more likely, as the use of synthetic rubbers for the composition is demanded in [CER03].

[5]The last two rubbers were considered as an alternative to the composition currently used.

Abbr.	Name	Saturation	Polarity
NR	Natural Rubber	Unsaturated	Non–polar
IR	Isoprene Rubber	Unsaturated	Non–polar
NBR	Nitrile–Butadiene Rubber	Unsaturated	Polar
SBR	Styrene–Butadiene Rubber	Unsaturated	Non–polar
AEM	Ethylene–Acrylic Rubber[6]	Saturated	Polar
EPM	Ethylene–Propylene Rubber	Saturated	Non–polar
EPDM	Ethylene–Propylene Diene Rubber	Saturated	Non–polar

Table 2.1: Rubber types found in water–cooled cable hoses

2.4 Premature ageing of rubber

A number of factors are responsible for the deterioration of rubber materials, all of which limit the service life of the product. Generally, those factors can be divided into *environmental influences* and the *influence of contact media*. Although the latter is a large field of study, it will not be covered here. The only medium in contact with water–cooled cables is demineralized water far below the boiling point. At this temperature, the water is not a critical factor for rubbers. This Section will rather concentrate on the main environmental factors that seem relevant for water–cooled cables in the LHC.

2.4.1 Influence of oxygen

It is safe to assume that all polymers will degrade when in contact with a potentially oxidising medium (and therefore with air) and that the rate of degradation will increase with increasing temperatures. The degradation process starts with oxygen being absorbed by the rubber. The absorbed oxygen can then either lead to chain scission or crosslinking. Both of these processes occur simultaneously. If chain scission dominates during ageing, the elastomer softens and eventually may become sticky. The ongoing crosslinking process leads, however, to hardening and brittleness during oxidation.

[6]The nomenclature of acronyms for rubbers is not consistent. In AEM, EPM and EPDM, the letter "M" refers to the classification according to ISO 1629. "M–Class" rubbers have a saturated chain of the polymethylene type.

Unsaturated rubbers are generally prone to oxidation, depending on the amount of double links in their molecular chains. Saturated rubbers, however, show a good ageing resistance against oxidation.

For natural rubber, scission of molecular chains usually dominates in the beginning. This results in a softening of the rubber, which will change into hardening with the progression of ageing. With SBR and NBR, the cross–linking process dominates from the beginning.

The principal mechanism of oxygen attack involves an autocatalytic, free radical reaction. The first step is the creation of macroradicals as a result of hydrogen abstraction from rubber chains by a proton acceptor. Oxidation continues by reaction of macroradicals with oxygen and the subsequent formation of peroxy radicals and hydroperoxides [Wri01].

Antioxidants are employed to slow oxidation. There are two types with different functions. The first type, called preventive antioxidants, react with hydroperoxides to form harmless, non–radical products. In the process, the antioxidant is oxidized. The second type, chain–breaking antioxidants, destroy peroxy radicals that would otherwise propagate. Chain–breaking antioxidants are aromatic and contain labile protons, which are donated to the peroxy–radicals [IS09a].

2.4.2 Influence of ozone

Ozone is a very reactive form of oxygen and the strongest known oxidant. Ozone, even when present in the atmosphere at only a few hundred parts per hundred million, readily cleaves carbon–carbon double bonds in elastomers. As a result, unsaturated rubbers can age rapidly when exposed to ozone and a static strain at the same time. In this case, cracks on the surface of the material form perpendicularly to the direction of strain. These typical types of cracks became known as *ozone cracks*. The ozone content in the ambient air and strain of the rubber are the significant factors for the development of ozone cracks.

Physical protection against ozone cracking is provided by the addition of paraffinic waxes that migrate to the surface of the rubber and thereby act as a barrier to ozone ingress. High molecular paraffinic waxes (microcrystalline waxes) form a more cohesive protective layer than low molecular weight waxes. The latter, however, provide protection more rapidly after processing as they reach the surface more quickly. A mixture

of waxes is therefore often beneficial. As a chemical method of protection, phenylenediamine–based additives are used. These react preferentially with ozone and, as with the waxes, migration of the additive to the surface is essential [DW01].

2.4.3 Influence of ionizing radiation

Ionizing radiation includes gamma rays, x–rays, electron beams, protons, neutrons, alpha particles and other nuclear fragments. It interacts with matter by transferring energy to electrons in the atoms of the matter which is present. The electrons may be ejected from the atoms, thus ionizing them. Deposition of energy in the material will eventually appear as heat [CCO98]. The amount of radiation received by matter is referred to as radiation dose. Dose is a quantity describing the amount of energy absorbed by a material. The SI unit for absorbed radiation dose is gray (Gy). One gray is defined as the absorption of one joule of ionizing radiation by one kilogram of matter.

In polymers, ions result directly or indirectly from the respective stripping or excitation of orbital electrons. The ions are unstable and lead to the rupture of covalent bonds. If elastomers are exposed to ionizing radiation, chain scission or cross–linking effects occur simultaneously, although the latter effect usually dominates. With a higher radiation dose, the density of crosslinks increases, leading to an increased hardness of the material. Radiation thus accelerates the long term ductile to brittle transition [IS09b].

However, not only the total dose of radiation but also the *dose rate*, i.e. the quantity of radiation absorbed per unit time, has an influence on the degradation process. Generally speaking, an elastomer irradiated at a low dose rate will require less *total dose* to sustain a certain amount of damage[7] than the same material irradiated at a higher dose rate. By determining this so–called dose to equivalent damage (DED) for different dose rates, the extent of this effect, which is highly dependent on the material, can be evaluated.

The radiation resistance of rubbers can be increased by the use of antirads. Antirad compounds decrease the rate of reactions including both crosslinking and chain scission. Internal and external protection can

[7] For rubber materials, a typical damage criterion would be a reduction of tensile strength by 50 % (see also Section 3.4.3).

be distinguished. Dissipation of the energy of ionizing radiation can be intensified by the insertion of certain structural elements directly into the chemical structure of the rubber (internal protection) or in the form of additives which are not bonded chemically (external protection). Aromatic compounds are often used as antirad agents [Iva01] .

2.5 Storage of rubber

As a matter of fact, the ageing mechanisms covered in the preceding Section apply to rubber materials not only during actual application, but also during storage of the material. If stored correctly, rubbers can maintain their material properties for many years without noticeable degradation. Wrong storage conditions can, however, render the products worthless even before installation. Generally, rubbers should be stored preferably under low strain, e.g. coiled up on a drum of large diameter. Furthermore, the storage temperature should be between 15 and 25 °C. Relative humidity should be below 65 %. The rubber products should be protected from light, especially from direct solar irradiation and artificial light with high content of ultraviolet radiation. Equipment generating ozone such as electric motors or high voltage installations are to be avoided in the storage rooms. No solvents, fuels, or other organic liquids should be kept in the storage space. Rubber products should not get in contact with harmful metals like copper or manganese. Detailed guidelines concerning the correct storage or rubbers are given in [DIN 7716].

Chapter 3

Water–cooled cables in the LHC

In this Chapter, the technology of water–cooled cables will be introduced. The general application and technical requirements are covered in the first part. Section 3.4 will then cover tests for the qualification of the hose material. The Chapter will close with a description of the environmental conditions at the place of installation and the cooling water system to which the cables are connected.

3.1 Definition

Cables for electrical connections usually consist of a conductor which is surrounded by an insulating material. A lug is attached to the end of the cable to allow a proper connection, e.g. with retaining screws. The water–cooled cables used in the LHC have a similar layout. They are composed of a loosely twisted flexible copper core with crimped–on connection lugs at both ends (see Figure 3.1).

The lugs maintain the electrical connection as well as the connection to the cooling water system by internal water channels. This conductor is surrounded by an external flexible rubber hose which maintains the electrical insulation and water–tightness of the cable. The cooling water circulates between the core and the hose, flowing between the individual wires of the core.

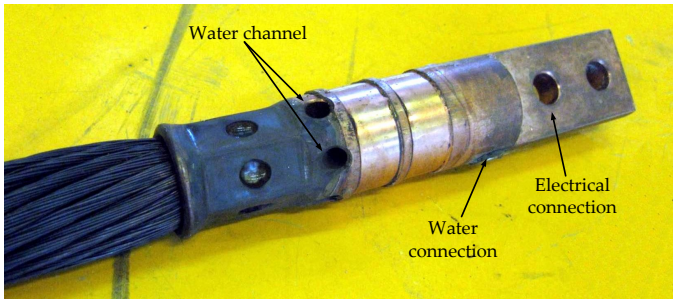

Figure 3.1: Copper core and lug of water–cooled cable. The lug ensures both electrical and water connection. Cooling water is piped to the flexible conductor by water channels.

The different layers of the water–cooled cable hose are presented in Figure 3.2. The cable hose has a multilayer composition to meet the physical and chemical criteria. The inner liner and the cover are reinforced by two layers of braided textile fibre structures. Those reinforcement layers are bonded to the inner liner and the cover by an adhesive layer.

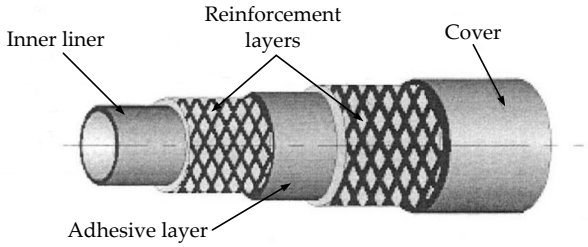

Figure 3.2: Layers of cable hose (image source: [Wyd09]).

The rubber composition of inner liner and cover of hoses currently used in the LHC is a compound of natural rubber (NR) or isoprene rubber (IR), butadiene rubber (BR) and nitrile butadiene rubber (NBR). The reinforcement structures are made of braided polyester fibres [Wyd09].

As the water–cooled cables have to conduct very high currents, large cross–sections are required. In the circuits for the auxiliary quadrupole[1] magnets, cables with conductor cross–sections of 800, 1000 or 1300 mm^2 are used. For the main dipole[2] and main quadrupole magnets, the circuits are composed of water–cooled cables with a conductor cross–section of 2000 mm^2.

[1]Magnets used for focusing and defocusing the two particle beams.

[2]Magnets used for bending the two particle beams.

3.2 Application

The water–cooled cables and tubes[3] described in this Chapter are part of the power supply system for the superconducting magnets of the LHC. They are used to supply the main dipole, main quadrupole and auxiliary quadrupole magnets. Basically, four components are necessary to supply the magnets: power converters, water–cooled cables, Distribution Feed Boxes (DFB) and current leads. The basic connection pattern is illustrated in Figure 3.3.

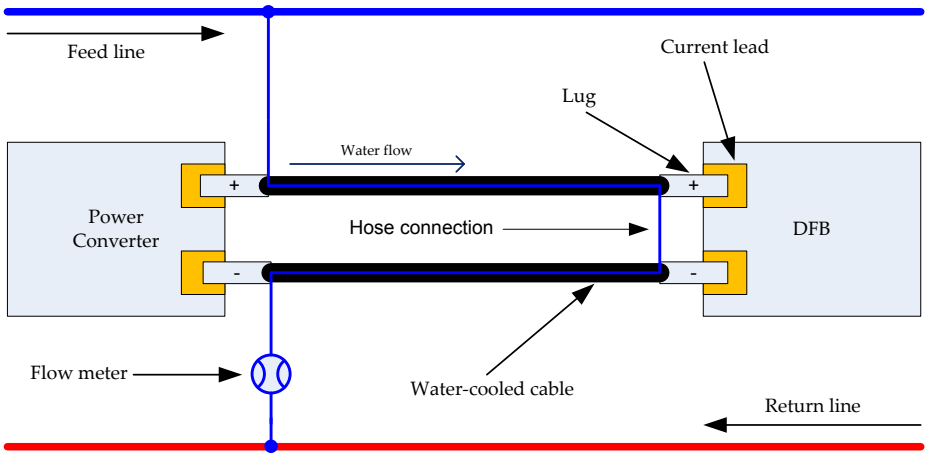

Figure 3.3: Connection pattern between power converter and DFB. Note that both electrical and water connection are established by the lug of the water–cooled cable. Cooling water from the feed line flows through the first cable and is then routed to the second cable by a hose connection. After passing the second cable, it is fed back to the return line. Water flow during operation is monitored with a flow meter (water flow symbolised by the blue line).

The high–precision[4] power converters are located underground and are fed by the main AC supply lines from the surface. Here, the AC supply voltage is converted into the specified DC voltage. The power converters are then connected to the DFBs by water–cooled cables. The main function of the DFBs is to house the current leads which act as a link between the normal conducting water–cooled cables and the superconducting magnets.

This rather complex approach is necessary as the magnets in the LHC

[3]Fixed water–cooled copper tubes are used for the straight sections of the circuit.

[4]The term “precision” is a generic term, covering accuracy, reproducibility and stability of the output current.

have different requirements from those previously installed in the LEP. Magnets in the LEP required high voltage and low currents for their loads. Therefore, it was relatively easy and inexpensive to install the power converters on the surface and cable them to their underground loads. For the LHC, however, this approach would have been prohibitive as the accelerator requires very large currents and rather low voltages for its superconducting magnets.

The electrical resistance of conductors becomes increasingly important in high–current applications like this. It leads to a voltage drop across the conductor whereby heat is generated. As water–cooled cables are the only ohmic resistance in the circuit, cable ways had to be kept as short as possible, which is why the power converters were installed underground close to the magnets. In order to dissipate the heat, the converters as well as the cables used as connections between the converters and the DFBs are cooled by demineralised water [B$^+$04a]. A typical installation of water–cooled cables is shown in Figure 3.4.

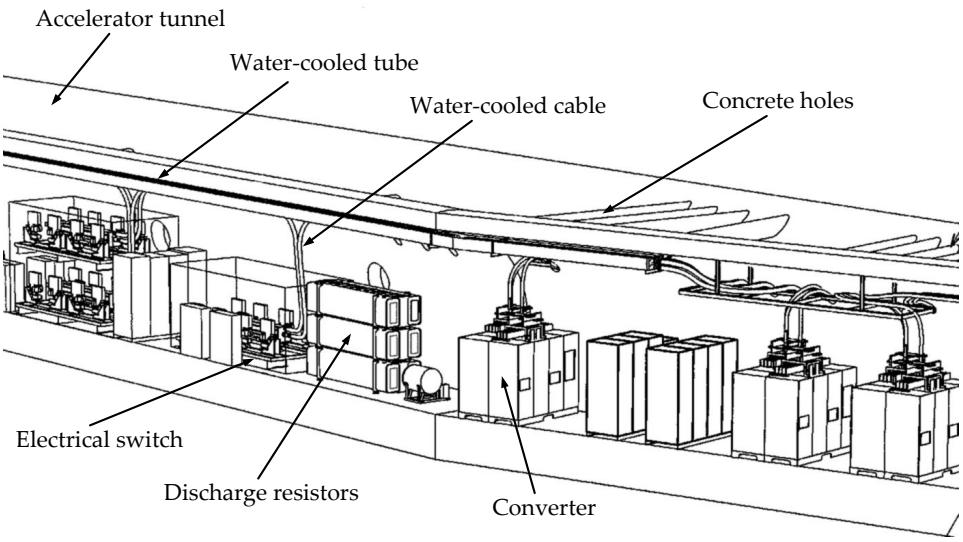

Figure 3.4: Example of water–cooled cable installation. The cables are routed through concrete holes to the DFBs which are located in the accelerator tunnel (image source: [CER03]).

The power converters are installed in service tunnels parallel to the accelerator tunnel which houses the LHC. For the connection to the DFBs which are located in the accelerator tunnel, the cables are led through holes

in the concrete wall. Water–cooled cables are also used to connect the magnets to the electrical switches and dump resistors which are part of the energy extraction system. This safety system is activated if the magnet coils need to be discharged rapidly, e.g. in case of a quench[5]. The dump resistors are then switched into the circuit, thus discharging the magnets [D$^+$00].

3.3 Technical requirements

The core of the water–cooled cables and tubes is made of copper. Copper quality has to be at least equal to IACS[6] 100 %. This standard specifies the unit of electrical conductivity for metals and alloys relative to a standard annealed copper conductor. An IACS value of 100 % equals a conductivity κ of

$$\kappa = 58 \, \frac{S \cdot m}{mm^2} \tag{3.1}$$

which corresponds to a specific electrical resistance ρ of

$$\rho = 0.01724 \, \frac{\Omega \cdot mm^2}{m} \tag{3.2}$$

at 20 °C [KNK01]. The main parameters of the different water–cooled cables are presented in Table 3.1 on the next page. The cross–sections of the cables are specified according to the nominal current and range from 800 mm^2 to 2000 mm^2. The maximum voltages applied to the cables by the converters are 190 V for the dipole circuits, 18 V for the main quadrupole circuits and 8 V for all other electrical circuits using water–cooled cables [ZG05]. The highest transitory voltage is 500 V. The maximum operating temperature is specified with 50 °C.

[5] A quench is an abnormal termination of magnet operation that occurs when part of a superconducting magnet enters the normal conducting state. Thus, it heats up the surrounding regions and pushes them into the normal state as well. This leads to more heating in a chain reaction and is accompanied by a loud noise as the energy in the magnetic field is converted to heat, and rapid boil–off of the cryogenic fluid.

[6] **I**nternational **A**nnealed **C**opper **S**tandard.

Cross–section	Maximum overall diameter	Nominal current	Time constant
800 mm^2	65 mm	6000 A	140 sec
1000 mm^2	76 mm	8000 A	62 sec
1300 mm^2	86 mm	8000 A	62 sec
2000 mm^2	105 mm	13 000 A	110 sec

Table 3.1: Main parameters of water–cooled cables.

Owing to installation constraints, the maximum overall diameter of the cable is limited. The minimum bending diameter with water at nominal pressure shall not be higher than 8 times the overall diameter.

The time constant is defined in regard to the time a cable is able to support an exponentially decaying current with no water flow. In case of leakage or failure of the water circuit, the circuit is shut down and the energy stored in the magnets is discharged by the dump resistors in the energy extraction system. Therefore, the time constant of the cable represents the time constant of the magnet with its dump resistor inserted [B$^+$04a]. During this time, the cable must stay within the specified limits. The external hose of the cable must be manufactured in one piece without discontinuities. Its leakage current[7] must be lower than the values shown in Table 3.2.

Cross–section	Permissible leakage current	Test voltage level
800 mm^2	20 µA/m	1.5 kV
1000 mm^2	20 µA/m	1.5 kV
1300 mm^2	30 µA/m	1.5 kV
2000 mm^2	40 µA/m	3.0 kV

Table 3.2: Maximum permissible leakage current.

For all connections – especially for the conical connectors of the 13 kA circuits – the contact resistance of the connectors has to be taken into account, too. A low contact resistance is a good proof that contact areas are clean and aligned properly. The upper limit for the ohmic resistance at each connection is 2 µΩ.

[7] Undesirable flow of current through or over the surface of an insulating material [MP03].

3.4 Qualification tests

Safety is a major concern for the water–cooled cables, as it is for all installations at CERN. During operation, there is no access to the LHC tunnel which means that all equipment has to meet the highest possible standards. The tests for the qualification of the cable hose material according to CERN's safety instruction [IS 23] will be described in this Section. Apart from these tests, a major obligation for all materials is that they have to be free of halogens and sulphur. This is mainly a safety concern, but the presence of halogens can also lead to technical problems (see Section 4.2).

It should be noted that there is also a large variety of tests for the commissioning of the cables before and after installation in the LHC. This Section, however, will set its focus on the test of the rubber hose material.

3.4.1 Fire hazard testing

The eventuality of a fire is a major safety concern, as access to the underground areas is difficult and the confined space increases the potential danger of fire. Therefore, one aspect to consider when choosing the material is the toxicity of its fire effluents. Prediction of toxic potency is based on mathematical models taking into account analytical results of fire effluents for acute toxicity by inhalation in animal tests. This requires the generation of thermal decomposition products and analytical determination of their toxic components.

A method for the generation of fire effluents and the identification and measurement of its combustion products is described in [IEC 60695–7–50]. In this procedure, a moving sample is combusted in a tube furnace using different temperatures. A current of primary air is passed through the furnace and over the test specimen to support combustion. The effluent is expelled into a mixing and measurement chamber, where it is diluted with secondary air. The effluent is then constantly analysed for toxic combustion products and finally exhausted. This method has been found to be a reasonable model for decomposition conditions in various fire stages, as it is inexpensive, simple to use and offers a good possibility of validation.

Subsequently, the toxic potency of the material is estimated. Assuming a fire scenario where material would be burnt, the contribution of the fire

effluent of the tested material to the toxic threat to life of the total fire effluent if examined. [IEC 60695–7–51] describes the calculation procedure for converting data generated in the combustion test described above into estimated toxic potency data [Tro04].

3.4.2 Smoke density

The measurement of smoke density is an important aspect for evaluating the burning performance of a material. It is related to the evacuation of persons and, especially in the case of the LHC, accessibility for fire–fighting.

The light transmittance for flaming and smouldering conditions can be used for comparing different cables or determining how they comply with specific requirements. A suitable setup for this test method is described in [IEC 61034–1]. The test specimen is placed in a test chamber with sealed windows on two opposite sides. This permits the transmission of a beam of light from a photometric system through the test chamber.

The basic components of the photometric system are a light source, placed at one side of the test chamber, a lens system to focus the emitted light beam and a photocell to measure the intensity of light on the opposite side of the chamber. This detector is placed in a tube with a matt–black surface to prevent reflections. This setup is illustrated in Figure 3.5.

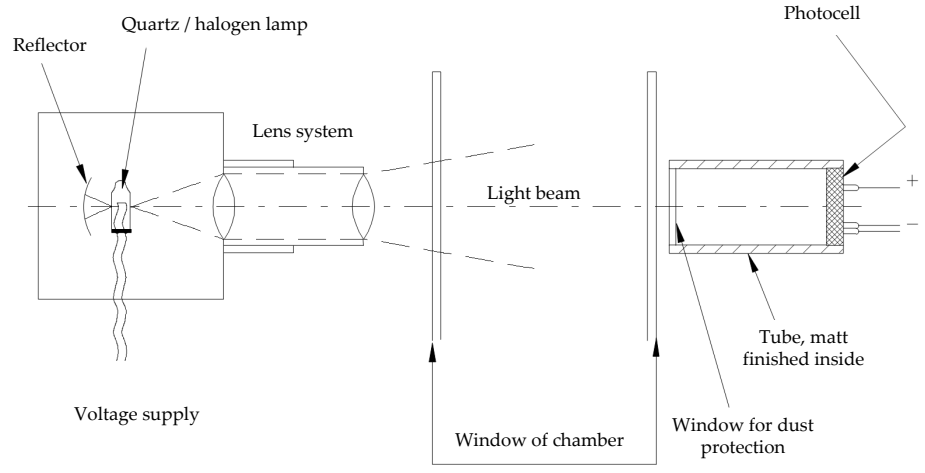

Figure 3.5: Test setup for smoke density test. The sample is combusted inside the test chamber, causing smoke and therefore reduced light transmittance (image source: [IEC 61034–1]).

Additionally, a fan with an air flow rate of 7 to 15 m^3/min is placed in the chamber to ensure uniform distribution of the smoke.

The general test procedure is described in [IEC 61034–2]. The sample is placed in the test chamber above a metal tray containing alcohol which acts as a standard fire source. Before the test, the photometric system is calibrated. The zero and full scale reading of a recorder connected to the photocell is adjusted for light on the detector corresponding to 0 % (absence of light) and 100 % luminous transmission. Immediately before the test, the temperature inside the cube is verified to be within the specified range of $\pm 25\,°C$. For the test, air circulation is started and the alcohol ignited. Now, the light transmittance is recorded continuously. The test is considered finished when there is no more decrease in light transmittance for 5 minutes after the fire source has been extinguished.

The minimum light transmittance that has been recorded is then used for evaluation. A minimum value of 60 % is recommended as a value for a positive evaluation of the test.

3.4.3 Radiation resistance

Exposure to ionizing radiation is an important factor in the premature ageing of rubber materials. This results in reduced flexibility of the rubber. Therefore, the hoses of water–cooled cables are tested for their radiation resistance.

The standard procedure for determining the influence of ionizing radiation on flexible materials is to cut dumb–bell shaped test specimens out of the hose material and to irradiate them with different dose levels. Then, the tensile stress–strain properties of the samples are determined according to [ISO 37]. The elongation at break ϵ is regarded as the critical property. It is determined for each sample and expressed as the relative value ϵ/ϵ_0, with ϵ_0 being the elongation of a non–irradiated reference sample. This relative elongation is then plotted against the dose with which the sample was irradiated [IEC 1244–2]. According to [CER03], the end–point criterion for rubber materials which are used for water–cooled cables is $\epsilon/\epsilon_0 = 0.5$ at an absorbed dose of 20 kGy, indicating that the flexibility of the sample has been reduced by 50 %.

3.5 Environmental conditions in the LHC tunnel

A main factor for the ageing of polymers are the environmental conditions to which they are exposed. Therefore, the main conditions present in the LHC tunnel will be treated in this Section. The first part will outline the air handling system. Subsequently, the ozone and radiation level will be covered. The Section closes with a description of the cooling water circuit.

3.5.1 Temperature and humidity

In order to allow an interference–free operation of all systems in the LHC, controlled air temperature and humidity conditions in the tunnel are also of particular importance. One of the most important aspects in the design of the air handling system is the heat load which can be evacuated via the ventilation air. Although the main part of the heat created by the equipment is removed by cooling water, the heat dissipation to the ambient air can exceed 285 kW in some sectors. In addition to the heat load, the air handling system provides functions such as dehumidification to prevent condensation, fresh air supply for people, filtering of the exhaust air etc.

An elaborate air handling system is used to provide these conditions. Consequently, a great part of the systems previously installed in the LEP has been re–used and modified.

There are two major regions of the LHC that are treated with two separate air handling systems. Those are the LHC tunnel itself and the underground areas such as the service tunnels in which power converters are installed. The main tunnel is divided into eight independent volumes, called “sectors”. Two air handling units provide air supply at each even point of a sector, while two extraction units remove air at the odd points of each sector. The air is transported to the underground areas by air ducts and then pulsed into the tunnel. At each extraction point, partitions separate the air flow coming from the adjacent sectors. The generalised air flow is shown schematically in Figure 3.6.

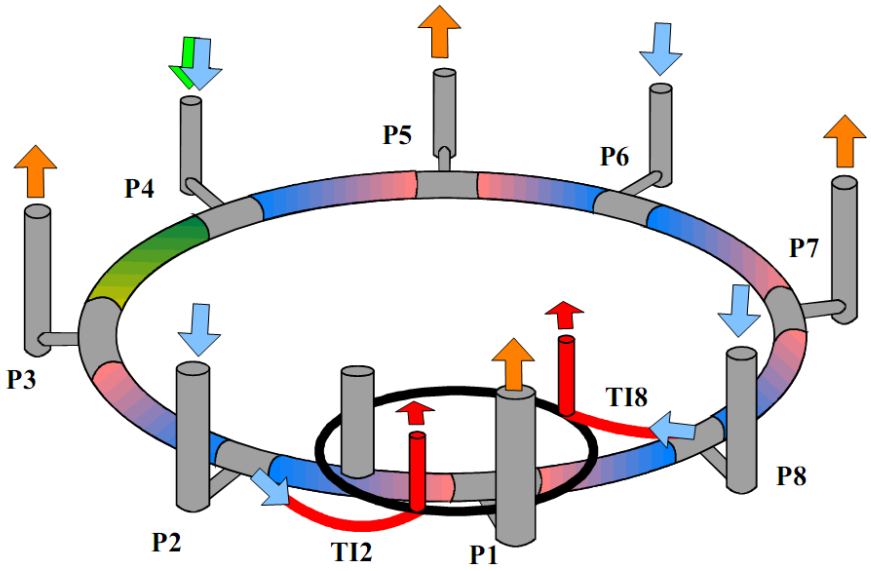

Figure 3.6: Schematic layout of the air flows in the LHC tunnel. Air is provided at each even point and extracted at the odd points of a sector (image source: [Mar03]).

Depending on the actual operation mode, the air flow rate of each supply or extraction unit for one tunnel sector can reach up to 64 000 m^3/hour. The system is designed to guarantee a minimum dry bulb temperature in the underground areas of 19 ± 1 °C in winter and 26 ± 1 °C in summer at a dew point of ≤ 12 °C[8] [Mar03], [B+04b]. These conditions are kept at a constant level and also coincide with the requirements for the storage of rubber according to [DIN 7716] as described in 2.5.

3.5.2 Ozone

As mentioned in Section 2.4, a high ozone concentration is a known factor for premature degradation of rubber materials. In fact, the impact of ozone on water–cooled cable hoses has been proved in [Wyd08a] and [Wyd08b]. In multiple test series, samples of hose material were exposed to a high ozone concentration for up to 312 h. Under these harsh test conditions, very deep and long ozone cracks were produced (see Figure 3.7).

[8]This is equal to a relative humidity of approximately 30–65 %.

Figure 3.7: Hose sample after 312 h exposure to an ozone concentration of 200 pphm O_3 at 40 °C and 55 % relative humidity (image source: [Wyd08a]).

To obtain an overview on ozone concentration at the actual place of installation of the water–cooled cables, a specialized company was assigned to take the following measurements in June 2008:

- Outside, near access points to the LHC tunnel, in order to give an indication of the ozone concentration in the surrounding ambient air
- At two air extraction points: if the ozone concentration at the extraction point is higher than in the ambient air, this would indicate that ozone is generated in the LHC tunnel
- In the underground complex of the LHC at places where water–cooled cables are installed and near converters and transformers
- In rooms where water–cooled cable hoses are stored

These measurements showed that the ozone concentration in the ambient air varied between 0.00 and. 0.03 pphm O_3. The ozone concentration in the LHC tunnel, the air extraction points and the storage rooms was lower than or equal to that value. Nowhere could a higher concentration than 0.02 pphm O_3 be measured. The report concludes that at the time of the measurements, there are no identifiable ozone sources in the LHC tunnel and the underground areas. No ozone — or at least no significant and measurable quantity of ozone — is being produced in the LHC tunnel [Rib08].

3.5.3 Ionizing radiation

All components placed in the LHC will inevitably be subject to radiation during machine operation. The ionizing radiation will affect material properties of insulation materials, electronics components[9], optical fibres etc. Some components are situated in a highly radioactive environment. The RR cavern in Point 7 and the Dispersion Suppressor regions of IR1 and IR5 are locations[10] where these high annual doses may accumulate [FS01a]. Thus, on the one hand, reliable construction materials and components will be required, which have sufficient radiation resistance to survive LHC operation. On the other hand, detailed information regarding the expected radiation environment in the LHC is essential in order to assess the necessary radiation–hardness of components [FS01c], [Li09].

There are two main sources of ionizing radiation in the LHC: Beam–gas interactions and point losses. Dose from beam–gas interactions arises from the secondary particle cascades originating from inelastic interactions of the circulating proton beams with the small amount of residual gas in the vacuum chamber of the collider. In addition to the dose arising from beam–gas interactions, an extra source of radiation is due to collisions of off–momentum protons with the beam–screen installed in the vacuum chamber. These so–called point–losses occur in the beam–pipe in which protons are outgoing from the interaction points where the two proton beams are brought to collision [FS01b].

The total radiation dose to which the installed equipment is exposed is a combination of radiation caused by those two effects and highly dependent on the particular location. Therefore, the estimated radiation doses are simulated at CERN for different regions of the LHC machine and presented in the form of dose ratio maps[11]. Whereas in most regions the annual dose will be several Gy/year to several tens Gy/year, in some local hot–spots very close to the beam–pipe, the radiation level can reach several thousands of Gy/year [FS02].

---

[9] Such as silicon sensors, which are widely used in the LHC detectors.

[10] These regions are close to the interaction points where the particle beams are brought to collision.

[11] Those highly complex simulations are performed with the FLUKA tool, a fully integrated Monte Carlo simulation package for the interaction and transport of particles and nuclei in matter [F$^+$05].

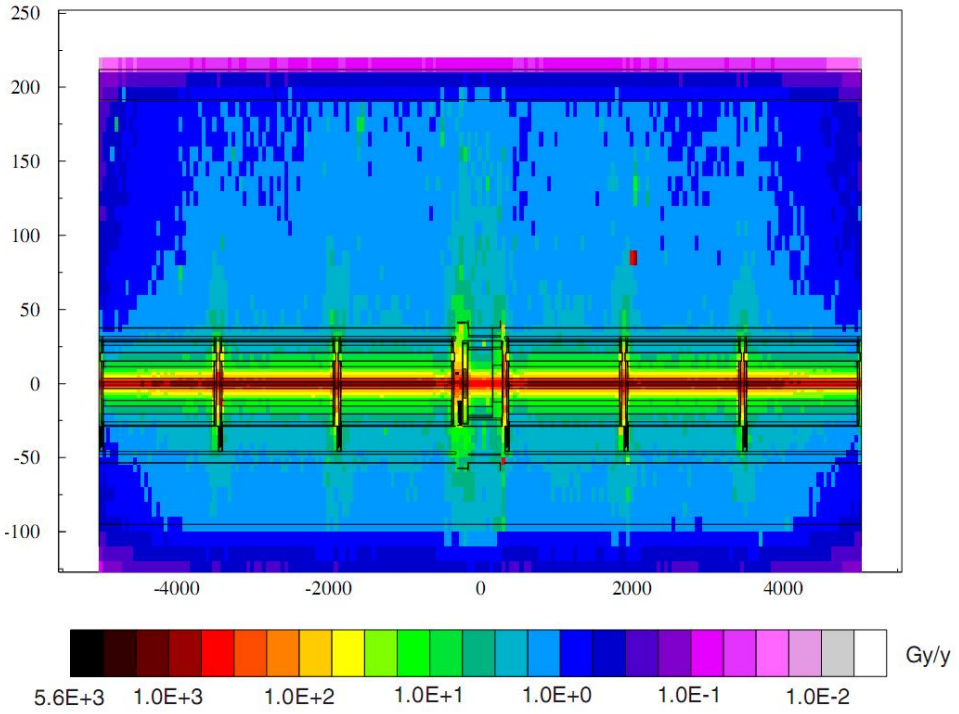

Figure 3.8: Exemplary dose map of annual dose in the LHC arcs. The image shows a longitudinal cut. Dimensions on the x– and y–axis are in cm (image source: [FS01c]).

This also applies to the water–cooled cables which are installed in many different locations within the LHC. Therefore, assuming worst–case operational conditions, the annual dose rate to which the water–cooled cables are exposed is expected to be 20 kGy/year.

Radiation tests for the selection of polymer–based materials used in radiation environments have been performed at CERN for several decades on a variety of materials. Many results have been published in catalogues, e.g. by Schönbacher and Tavlet in [ST89]. A major study was conducted in 1991, when the test methodology was enhanced to allow a lifetime prediction of different cable materials [DST91]. With simulation data available for both the dose and expected lifetime of the material, these data were compared with actual measurements eleven years later. The results show that the accuracy of lifetime prediction is highly dependent on the particular material. It was possible, however, to achieve very good results for rubber materials [ST02].

3.6 Cooling water system

Equipment in the LHC including water–cooled cables and power converters generates a vast amount of heat during operation. This heat load cannot be handled purely by an air cooling system. Therefore a water cooling system is necessary to transport the heat from the tunnel area to the surface and dissipate it to the ambient air. To supply cooling water for the whole LHC machine, primary water is produced at four surface buildings located at LHC points 2, 4, 6 and 8. The general setup of one cooling water circuit is illustrated in Figure 3.9.

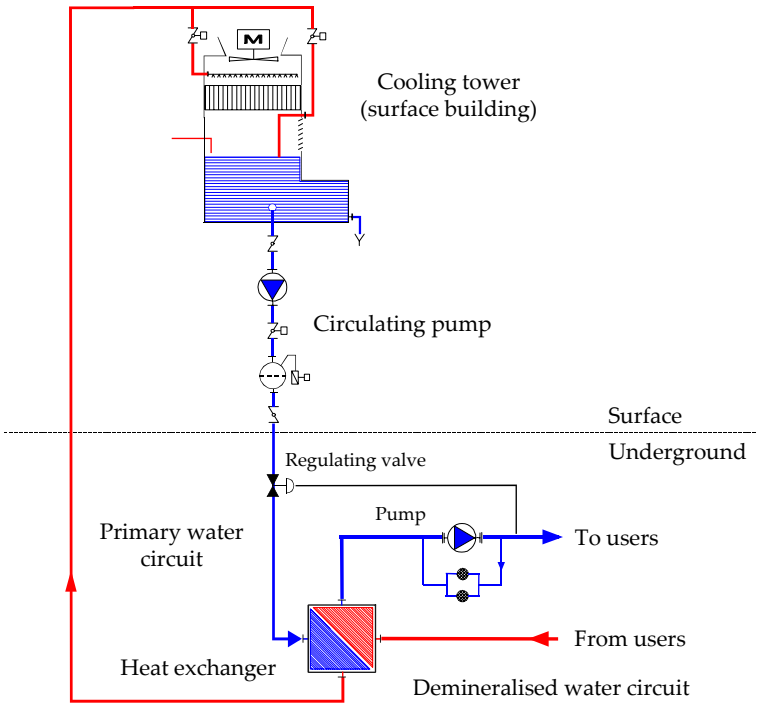

Figure 3.9: Layout of cooling water system in the LHC. The demineralised water circuit (purple) located underground is connected to the primary water circuit (green) by heat exchangers. Heated cooling water is pumped to the surface, where heat is dissipated by cooling towers (image source: [Ann02]).

The system consists of two separate water circuits: the primary water circuit which provides cool water from the surface, and the demineralised water circuit underground. Both circuits are connected by heat exchangers. By means of the heat exchangers, the thermal load of the demineralised water network is extracted to the primary water system and will then be

dissipated by cooling towers on the surface. Altogether, the cooling capacity for all LHC points reaches nearly 55 MW.

Each primary water loop is an open circuit. The water is cooled down by the cooling towers and distributed by pumps installed in pumping stations. The cooling towers are of an atmospheric type, each one having a cooling capacity of 10 MW. They guarantee[12] a maximum outlet temperature of 24 °C with a maximum inlet temperature of 34 ± 1 °C. The available pressure difference on the user side is typically 3 bar. The pumping stations are directly connected to the cooling towers and supply the primary cooling water to the underground areas.

From the underground areas, the demineralised water is distributed to the two adjacent sectors of the LHC machine. Each demineralised water circuit is a closed circuit and equipped with a set of pump, heat exchanger, expansion vessel, filter, ion cartridge for demineralisation and all the necessary control and regulating devices. It operates at a rated pressure of 16 bar with a maximum temperature of 27 °C at the cooled equipment. The conductivity of the demineralised water is $< 5\,\mu S/cm$ [Ann02], [B$^+$04b].

[12] Under normal conditions in the Geneva area (max. 21 °C wet bulb temperature and 32 °C dry bulb temperature).

Chapter 4

Damage occurred before the startup of the LHC

In this Chapter, problems relating to the rubber hoses will be addressed. Beginning with problems caused by halogens in the hose material, the focus will then be set upon the issue of surface cracks on the water–cooled cable hoses.

4.1 Introduction

Despite the careful selection of hose material as described in the previous Chapter, problems occurred with the water–cooled cables even before the startup of the LHC which took place on September 10, 2008. On the one hand, these problems were related to the presence of halogens in the hose material. On the other hand, cracks appeared on the surface of many cable hoses. Around 10 % of the hoses containing halogens have since been replaced. However, the problem of surface cracks is still present and is being pursued up to the present day. The crack growth is monitored at regular intervals, a process which will be discussed in Chapter 5.

4.2 Presence of halogens

Halogens are elements located in the 17th group of the periodic system. There are four main halogens: fluorine (F), chlorine (Cl), bromine (Br) and iodine (I). In addition, the rare astatine (At) and the recently discovered

ununseptium (Uus) are included in this group. All halogens are highly reactive. This is because the atoms are highly electronegative owing to their high effective nuclear charge. They can gain an electron by reacting with atoms of other elements. According to CERN's safety instruction [IS 23], all cable materials used in the LHC have to be halogen and sulphur free.

Nevertheless, in October 2007, chlorine was detected in hoses of water–cooled cables which had already been installed in the LHC. After investigation, it turned out that it was the adhesive layer of the hose that contained a considerable amount of chlorine. In one case, the inner liner of the hose had formed cracks which had reached this layer. Thus, chlorine was released into the cooling water circuit.

For various reasons, the presence of chlorine poses a potential threat to the installation, as it can react with most components contained in the cable and cooling assembly. Chlorine, after fluorine, is one of the most reactive chemical elements. It combines exothermically with nearly all other elements, usually at no higher than room temperature, and still more vigorously at elevated temperatures. It is unreactive only towards oxygen, nitrogen and the noble gases, but chlorine compounds containing these elements may also be prepared by indirect routes [HW01].

Chlorine is highly corrosive to metals. The more reactive the metal, the quicker the corrosion process will be. It can even form compounds with gold, which is unusual as gold is the least reactive of all metals [Wat02]. Corrosion at the copper connector of a water–cooled cable was the first indication that led to the detection of chlorine in the cable hose (see Figure 4.1). The chlorine had been dissolved into the cooling water and corroded the connector.

Furthermore, the presence of chlorine in the cooling water is dangerous owing to several other reasons. With time, it also has the potential to pollute the stainless steel components of the cooling system with the danger of corrosion or even stress corrosion cracking as a result.

Another aspect is the premature ageing of the reinforcement layer of the rubber hose caused by radiation, which is an accelerated process compared to a halogen–free hose. This means that in a radiation environment, the molecular bonds of chlorine can break. The reaction mechanisms of this so–called radiation–induced dechlorination are rather complicated and not yet completely understood. However, it has been shown that extensive

dechlorination can be achieved if the radiation dose is high enough. As an industrial application, the dechlorination of pulp–mill effluents using γ–radiation has been investigated by Taghipour and Evans and proved to be very effective[1] [TE98]. In this application, the premature ageing of the reinforcement layer could lead to a weakening of the cable and therefore poses an immediate threat to a safe operation.

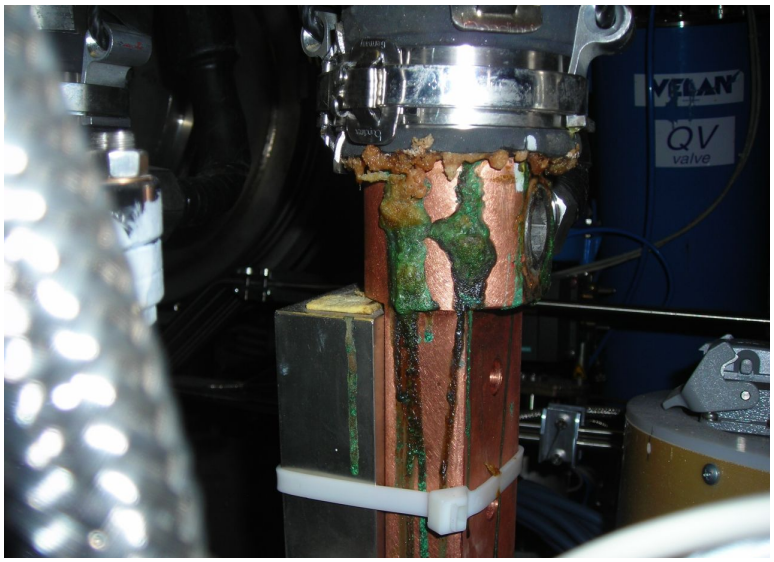

Figure 4.1: Copper oxide on the lug of a water–cooled cable. The connector corroded due to chlorine released from the adhesive layer of the rubber hose.

In case of fire, chlorine in the smoke can also have serious health effects. Chlorine gas is primarily a respiratory irritant. In sufficient concentration, the gas irritates the mucous membrane, the respiratory tract and the eyes. In extreme cases, difficulty in breathing may increase to the point where death can occur from respiratory collapse or lung failure. The effects of chlorine may become more severe for up to 36 hours after exposure. Apart from the health hazards, chlorine is a strong oxidizer. It can support combustion and is a serious fire risk [Ste98].

The presence of chlorine has therefore been treated with high priority by CERN. Further investigations showed that 66% of all water–cooled cables were affected by the problem [Wil08]. As a first attempt to address the

[1] In this study, effluents were treated with gamma rays at a dose rate of 10 kGy/h. The chlorine content was reduced by more than 50% at a total dose of 10 kGy, a radiation level that is also likely to appear in the LHC (see 3.5.3).

problem, a protective resin was applied at the DFB–side of the affected cables. This was a temporary solution owing to the fact that startup of the LHC was imminent. In the long term however, this potential threat is unacceptable. Similar damage might occur during the operation of the LHC and would indeed remain undetected, as access to the water–cooled cables is impossible during LHC operation. This could lead to a failure of the affected cable or even of the whole hydraulic circuit, and would consequently result in a complete shutdown of the LHC machine. Thus, a long–term replacement plan was developed to gradually replace the affected hoses during the scheduled shutdown periods of the LHC.

4.3 Surface cracks

In January 2008, surface cracks were detected on several water–cooled cable hoses. After an initial investigation, it showed that this problem was not a singular case, but affected a large number of the installed cables. It is noticeable that this damage had occurred before the startup of the LHC. This means that the cables had, until then, not been subject to the effects of radiation, high ozone concentration or direct light.

The cracks pose a latent threat to the operation of the LHC. They have the potential to weaken hoses that operate at a water pressure of 16 bar. In the worst case, the cracks could lead to a water leak or even the rupture of the hose. A shutdown of the LHC would be the result of such an event. Therefore, great importance was placed on a further investigation of the matter.

In general, four distinctive crack types could be observed (see Figure 4.2). One type takes the form of cracks that appear transversally to the orientation of the cable. This first pattern of cracks has often been found in the bending radii of the cables, for example in places where cables were led through bushings. The effect is increased in cases where the bending radius is smaller. Another type are longitudinal cracks, which means that the cracks are in parallel direction with the hose. They appear mainly on the straight sections, in some cases in the bent areas of the cable. A combination of transversal and longitudinal cracks could also be observed in some places. The fourth type consists of torn or damaged areas on the hose originating e.g. from faults during installation of the cable. This type

of pattern might occur when the cables are pulled over sharp edges during installation.

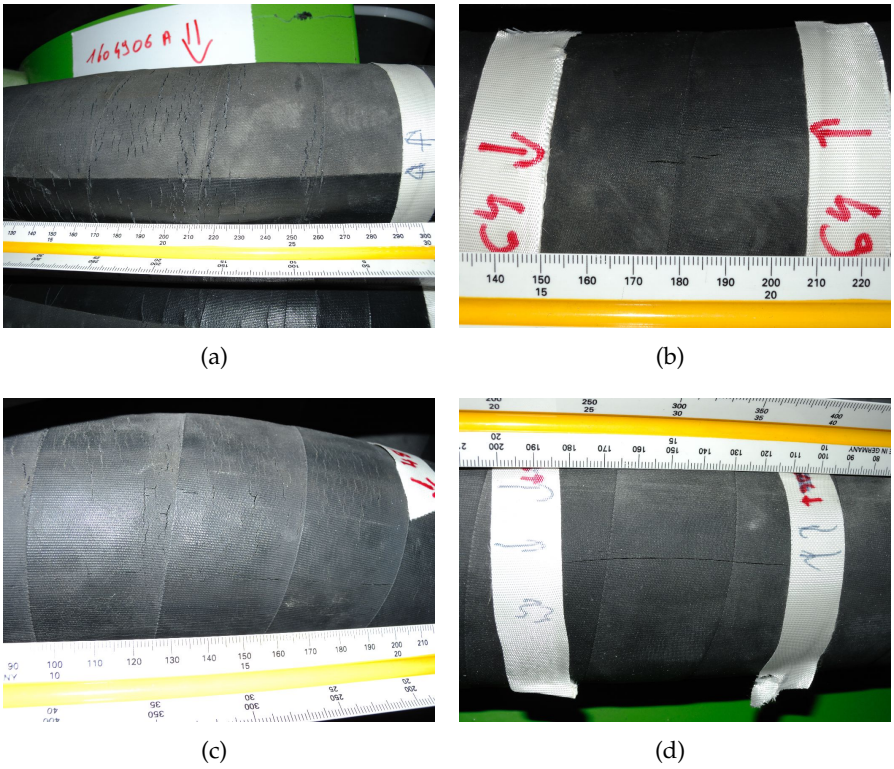

(a) (b)

(c) (d)

Figure 4.2: Different crack types: transversal cracks (a), longitudinal cracks (b), combination of transversal and longitudinal cracks (c), other (d).

To evaluate the extent of the surface cracks, an extensive examination of all cables was conducted. A first inspection was made in 2008, with the aim to determine the number of the cables affected, the seriousness and number of cracks and their types and sizes. In summer 2009, this monitoring was repeated. Figure 4.3 shows the number of affected cables that had been detected during these two monitorings. In 2008, 96 % of the cables had been inspected. 23 % of the cables were affected by cracks, and 4 % had not been controlled. Before the next monitoring in 2009, the cables most affected had been replaced. Altogether, 99 % of all water–cooled cables were controlled during the 2009 monitoring. The number of affected cables rose to 31 %, which is an increase of 8 % compared to the 2008 monitoring.

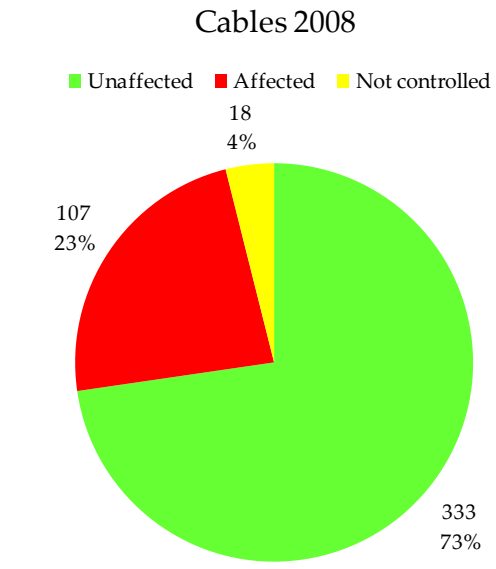

(a)

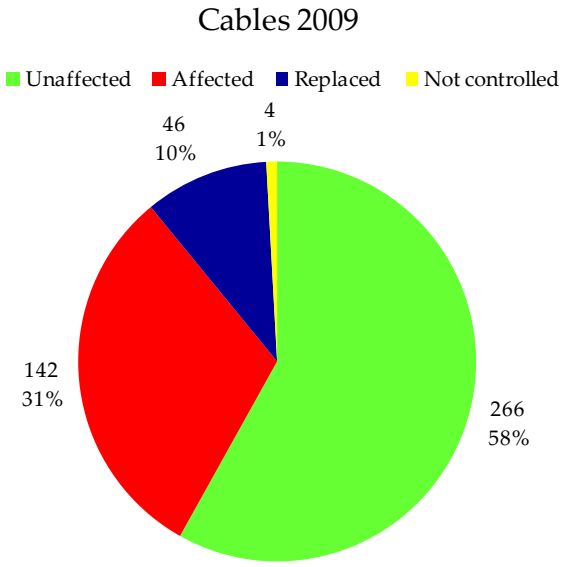

(b)

Figure 4.3: Affected cables in 2008 (a) and 2009 (b). Between these two monitorings, the total number of affected cables increased by 8 %.

Chapter 5

Crack monitoring

With the high number of cables affected, the problem of surface cracks has grown to a large extent. Replacing all the hoses concerned incurs high costs. In addition, exchanging the hoses is very time–consuming and access to the LHC tunnel is only possible during the scheduled stops of the machine. Due to the large number of cables, it is impossible to replace all hoses during one shutdown. Therefore, the priority of replacement is established by monitoring the surface cracks and estimating the severity on each hose.

The monitoring methodology used will be introduced in the first Section of this Chapter. Thereafter, the recent monitoring in LHC Point 6 is presented, followed by a discussion of the results.

5.1 Monitoring and evaluation methodology

The methodology for this monitoring procedure has been specified by Ylamaki in [Yla10a] and will be presented in this Section. Its target is to identify, document and evaluate all existing cracks on the water–cooled cable hoses. The monitoring technique is based on a visual inspection using photographs of the cracks. The hoses are systematically inspected visually and any cracks found are photographed. The severity and the growth of the cracks is then estimated based on photos taken during the monitoring process (see Figure 5.1 for the general procedure).

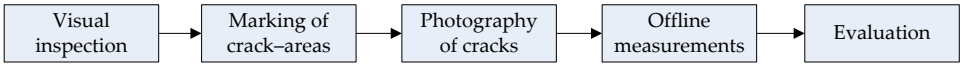

Figure 5.1: Monitoring procedure

5.1.1 Identification and marking of crack–areas

As a first step, the cables are visually examined for cracks. A torch is used to illuminate the surface. The best results are achieved by illuminating the hose from a small angle. If cracks are detected, the area containing the cracks is marked, thus defining a new crack–area on the surface of the hose. The beginning and the end of the crack–area are marked on the hose with a radiation resistant white tape. The tape is wrapped completely around the hose to ensure a good adhesion on the cable. Arrows are then drawn on the tape to show the main concentration of the cracks. Finally, the crack–area is numbered continuously for each LHC point, so as to identify the areas in future monitoring sessions and to follow the progression of the cracks in the area concerned. The number used for new crack–areas is the next free consecutive number for the particular LHC point.

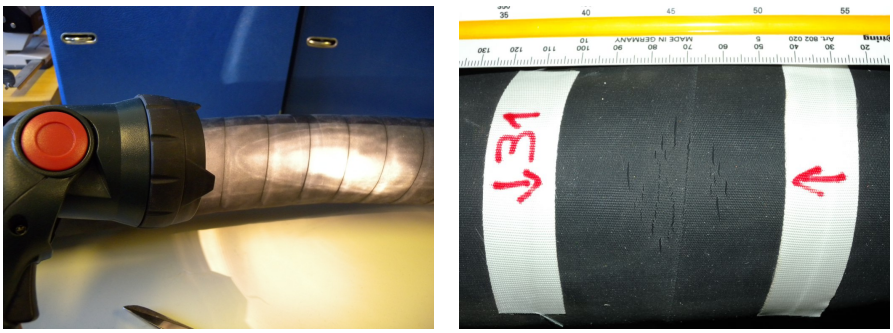

(a) (b)

Figure 5.2: Examination of cables: Illumination from a small angle (a), marked crack–area (b).

If it is not possible to fit all the cracks in one crack–area on one picture, the area is divided into sections. Each section is then documented separately. For example, if the crack–area number is 30 and the area was divided into four sections, those sections are referred to as 30.1, 30.2, 30.3 and 30.4.

5.1.2 Photo documentation

During the monitoring process, a picture of each crack–area is taken. In order to allow a later evaluation of the pictures, a ruler is placed in the image section. The distance between the camera and the surface of the hose should be between 20 and 30 cm. The axis of the camera has to be placed

perpendicularly to the axis of the hose. The ruler must be placed parallel to the axis of the hose and in the same plane with the surface of the hose. The ruler scale has to be readable. Older photos of the current crack–area should be consulted before taking the photo to be sure that the photos will be taken from the same direction and that the same cracks will be shown in the photos.

The settings of the camera are defined in [Yla10a] and have to be checked before taking each picture. This is because the aperture value or the shutter speed might have changed after zooming. The focus must be set on the surface of the hose. All pictures are taken using the self–timer of the camera in order to eliminate vibration when pressing the shutter release button.

Each photo is numbered sequentially on the digital camera. Cable number and crack–area must be noted for each picture number in the monitoring record to allow a later assignment.

Subsequently, the photos are transferred from the digital camera to the computer. The file names of all photos are changed according to a specified naming system. Thereby, the pictures can be arranged logically in order to prevent a mix–up of the images. The name format is *CableNumber.Crack–Area.Date.Extension* (see Table 5.1 for an explanation on the particular attributes).

Attribute	Explanation	Characters
CableNumber	The identification number for the specific cable	8
Crack–Area	Number of the concerned crack–area	5
Date	Date when the photo was taken, format: YYYYMMDD	8
Extension	Extension for the file–type	3

Table 5.1: File naming system.

Following this system, a resulting name for an image file might be *1604860A.32.04.20100721.nrw*. In this example, the photograph refers to section 4 of crack–area 32 on cable number 1604860A. The picture was taken on July 21, 2010 and is available as a raw image file[1].

[1]NRW–files are created by Nikon COOLPIX and digital SLR cameras. It is an uncompressed format that can be processed on a computer after the images are captured.

5.1.3 Offline measurements

Picture processing is the next step after changing the file names. The software "Nikon ViewNX" is used for processing the raw–format images before taking the measurements. First, the images are converted to monochrome colours, as cracks are better visible on a greyscale picture. In the next step, a sharpness filter is applied in order to better accentuate the edges of the cracks. Finally, the images are converted to the JPEG file format. Thus, the file size is reduced and the image can be loaded to CorelDRAW X3[2] which is used for the actual offline measurements. Figure 5.3 shows the basic steps of the process.

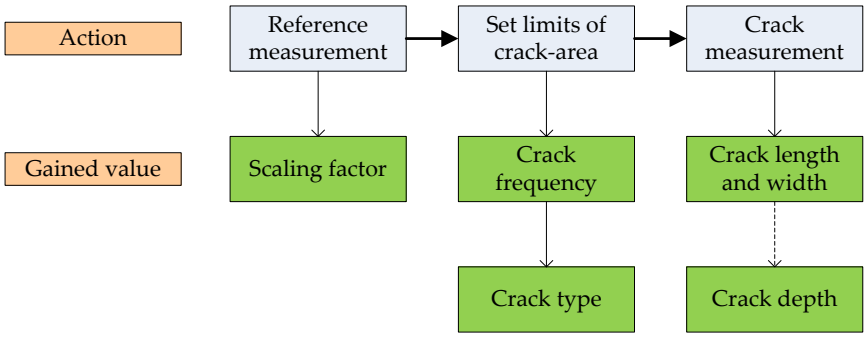

Figure 5.3: Steps of the offline measurement process.

The measurements are made with the "dimension tool" of the software. This tool displays the number of pixels between two reading points, in the following referred to as "pixel count". First, the scaling factor k for later measurements is determined by measuring a reference dimension of 50 mm on the ruler that was placed in the picture frame when taking the picture. Therefore, the start and end points of the "dimension tool" are placed exactly on the corresponding markings of the ruler. The scale factor k can then be determined by

$$k = \frac{d}{p} \tag{5.1}$$

with d being the reference dimension and p being the pixel count.

[2]CorelDRAW is a professional graphic design software developed and marketed by the Corel Corporation located in Ottawa, Canada.

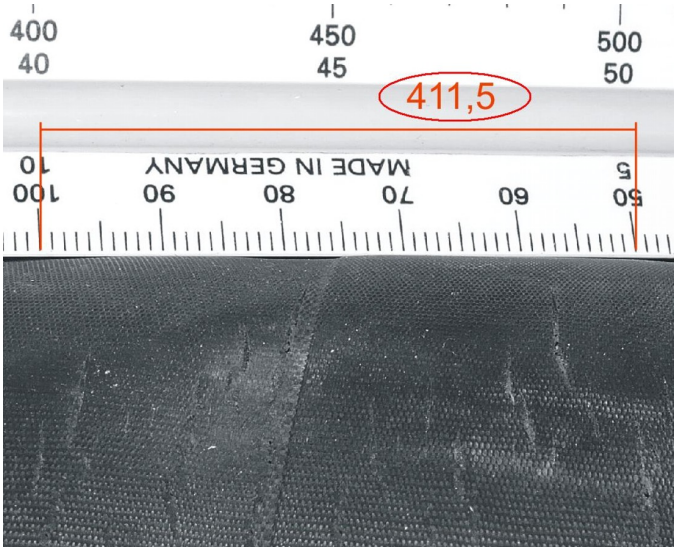

(a)

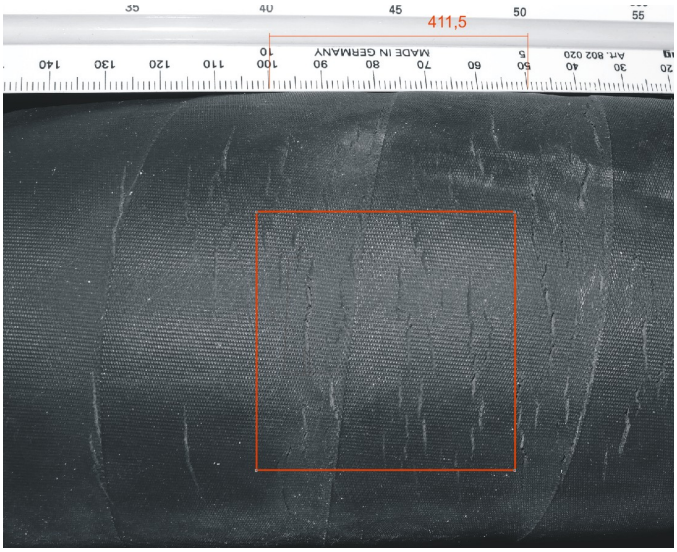

(b)

Figure 5.4: Measurement of reference dimension (a) and marking the inspection area (b).

Subsequently, the crack frequency and type are identified. Therefore, an inspection area of 5 by 5 cm is marked with the Rectangle Tool in the crack–area of the corresponding photo. This square is then placed in the region with the highest crack density. By using this standardized size for every picture, crack–areas with different overall sizes can be compared

with each other. The total amount and type of cracks located in this area are then determined (see Figure 5.4 (a) and (b)). If all cracks in the area were taken into consideration, the process would, on the one hand, be highly time–consuming. On the other hand, a comparison between the different crack–areas would be impossible, as they all differ in size. The crack frequency is then divided into five categories as presented in Table 5.2 which follows:

Crack frequency	Category	Factor
1–2 cracks	1	1.0
3–5 cracks	2	1.5
6–10 cracks	3	2.0
11–20 cracks	4	2.5
$>$ 20 cracks	5	3.0

Table 5.2: Crack frequency, assigned category and according factor.

Finally, the biggest crack in the inspection area is selected. The exact width and length of this crack is then measured with the dimension tool. The resulting dimension of the crack d_{crack} is then determined by multiplying the pixel count of the crack p_{crack} by the determined scale factor k:

$$d_{crack} = p_{crack} \cdot k. \tag{5.2}$$

Hereby, the critical property is the crack width, which is used to estimate the depth of the selected crack. As the actual depth of the crack cannot be measured from the photo, it is evaluated using the measured width of the crack under the hypothesis that deeper cracks are also wider.

Crack width	Assigned depth	Factor
$>$ 0.5 mm	Low	1.0
$\geq$ 0.5 mm	Deep	5.0

Table 5.3: Crack width, assigned crack depth and according factor.

All cracks with a width of at least 0.5 mm are considered to be “deep”, and all other cracks are considered to be “low” (see Figure 5.5 for a close–up of the measurement process).

5.1.4 Evaluation

In order to evaluate the overall condition of the hose, a numeric value called "severity–value" is calculated for each crack–area. The higher the severity–value, the more dangerous a particular crack–area is classified. It is generated from the values obtained for crack type (X_{type}), crack frequency $(X_{frequency})$ and crack depth (X_{depth}). Each of these values is weighted according to its particular criterion. The severity–value is then calculated by

$$X_{severity} = X_{type} \cdot X_{frequency} \cdot X_{depth}. \tag{5.3}$$

Table 5.4 shows the weight for the individual values. For example, a crack–area with transversal cracks with a crack frequency of 11–20 cracks that are assumed to be deep is given the severity–value

$$X_{severity} = 1.0 \cdot 2.5 \cdot 5.0 = 12.5. \tag{5.4}$$

Property	Criterion	Value
Crack type	Transversal	1.0
	Longitudinal	1.0
	Both	1.5
	Other	0.5
Crack frequency	1–2 cracks	1.0
	3–5 cracks	1.5
	6–10 cracks	2.0
	11–20 cracks	2.5
	$>$ 20 cracks	3.0
Crack depth	Low	1.0
	Deep	5.0

Table 5.4: Values for crack type, frequency and depth.

For the crack type, transversal and longitudinal cracks are treated equally. A higher value is assigned if both transversal and longitudinal cracks are found in the crack–area. For the crack type "other", a lower value is selected. The value for crack frequency is increased linearly with the category. The crack depth can only have two different values. For

deep cracks the value is much higher than for the low cracks, because deep cracks are more likely to cause severe damage to the hose than low ones.

The measurement data of the monitoring is then stored in a database that contains information about the cables, crack–areas and photos. Here, all the information is gathered and can be compared.

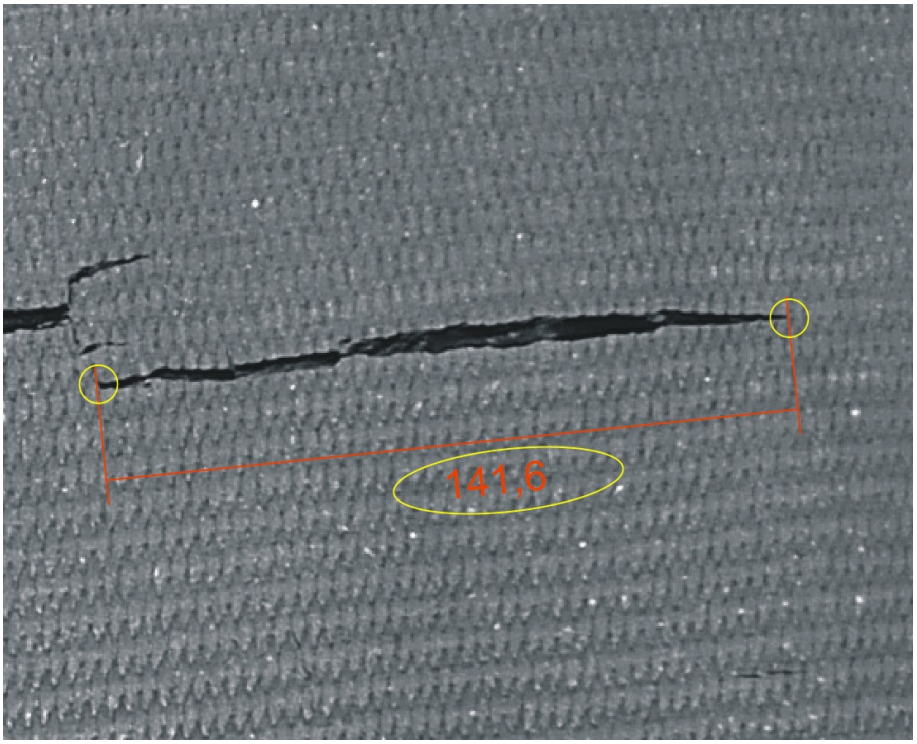

(a)

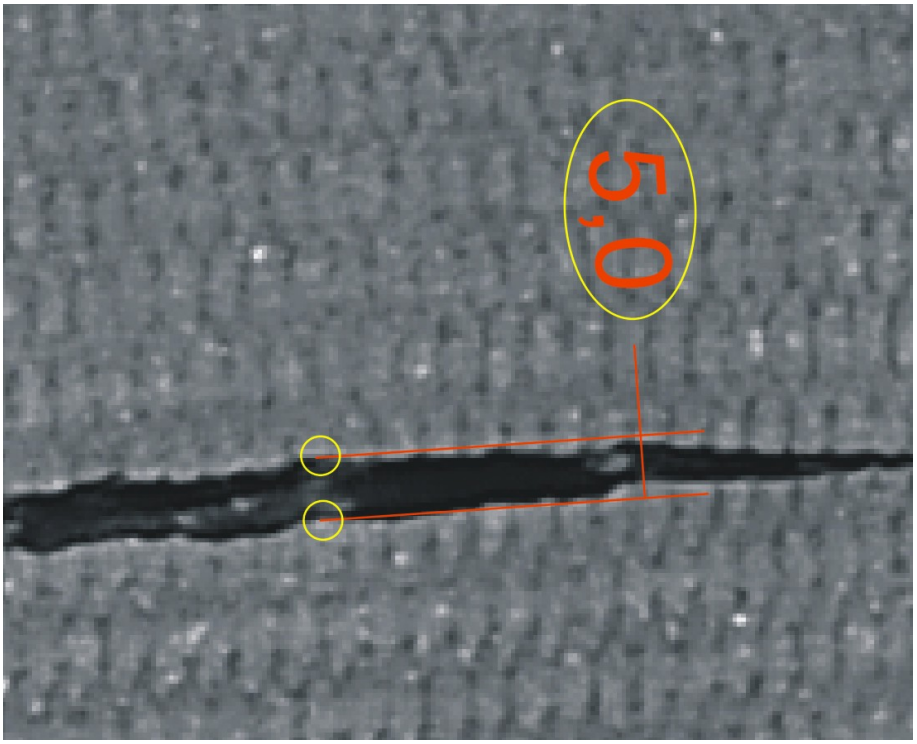

(b)

Figure 5.5: Close–up of crack measurements with the "dimension tool": crack length (a) and crack width (b). The encircled number represents the pixel count, which is the number of pixels between the two measurement points.

5.2 Monitoring Point 6 in Summer 2010

A crack monitoring was conducted by the author in LHC Point 6L and 6R[3] in summer 2010. This location was chosen since a large number of cables are affected by the crack problem in this Point. Based on the last monitoring in 2009, 67 % of the cables in Point 6L and 36 % of the cables in Point 6R showed surface cracks. Furthermore, most of the crack–areas with the highest severity–values are located in this Point.

However, owing to the limited time available, not all cables could be inspected. The monitoring results presented therefore only cover the cables that actually have been inspected. An overview of the inspected cables is given in Table 5.5.

Point 6L		Point 6R	
Cable Number	1604860A	Cable Number	1604893A
	1604861A		1604894A
	1604862A		1604895A
	1604863A		1604896A
	1604864A		1604897A
	1604865A		1604898A
	1604869A		1604905A
	1604870A		1604906A
	1604871A		1604907A

Table 5.5: Inspected cables.

Overall, on the cables inspected a total of 56 crack–areas in Point 6L and 27 crack–areas in Point 6R were monitored. The inspection was conducted following the methodology described in the preceding Section. Photos of the previous monitorings were examined in order to achieve a good comparability. In this respect, special attention was paid to finding exactly the same picture frame and angle for each crack–area.

Especially on large crack–areas, this was not always easy, as multiple photos have to be taken and no exact reference marks can be found on the cables. Several photos taken in Point 6L showed a deviant viewing angle compared to the pictures taken in 2009. The pictures concerned were shot

[3]The suffixes L and R refer to the left or right sector of the LHC access point. See also Figure 3.6.

again to allow a direct comparison. Sometimes, even a series of photos was shot of which the best was selected for comparison.

After image selection and processing, the cracks were measured. The data obtained were gathered in the database. By comparing the new data with those obtained in the last monitorings, the crack development for each area was visualized.

Of the 56 crack–areas monitored in Point 6L, a total of 30 areas show an increase in the crack length and/or crack width. Regarding the estimation of crack severity, the crack growth leads to a increase of the severity–value in 10 crack–areas. Figure 5.6 shows the crack–areas concerned and the relative increase of severity–value since the last monitoring. For example, the severity–value of crack–area 32.2 increased from "3" in the last monitoring to "15" in the current monitoring, resulting in a relative increase of "12".

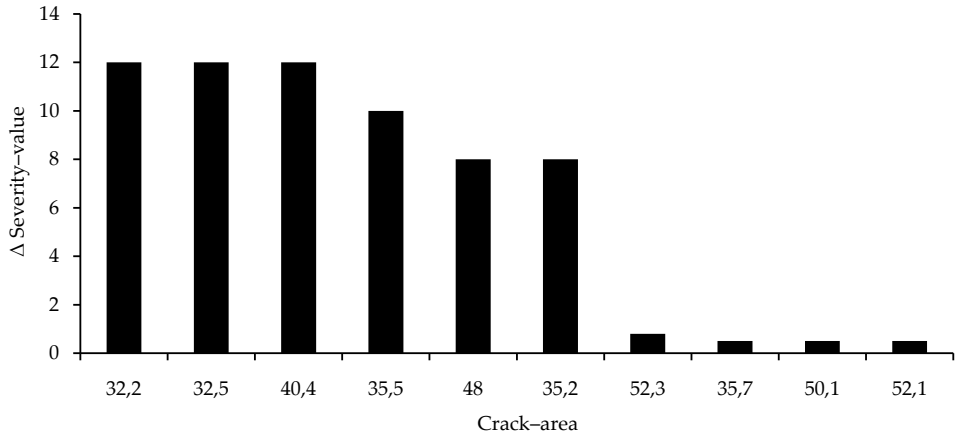

Figure 5.6: Increase of severity–value Point 6L.

The crack–areas with the highest increase are located on three cables: Number 1604860A (32.2 and 32.5), 1604862A (35.2, 35.5, 35.7 and 48) and 1604863A (40.4, 52.1 and 52.3). Crack–area 50.1 is located on cable number 1604863A.

In point 6R, 24 of the 27 crack–areas inspected show a small crack growth. The increase in length and/or width, however, is rather small, leading to an increased severity–value in four areas only (see Figure 5.7 for the areas concerned).

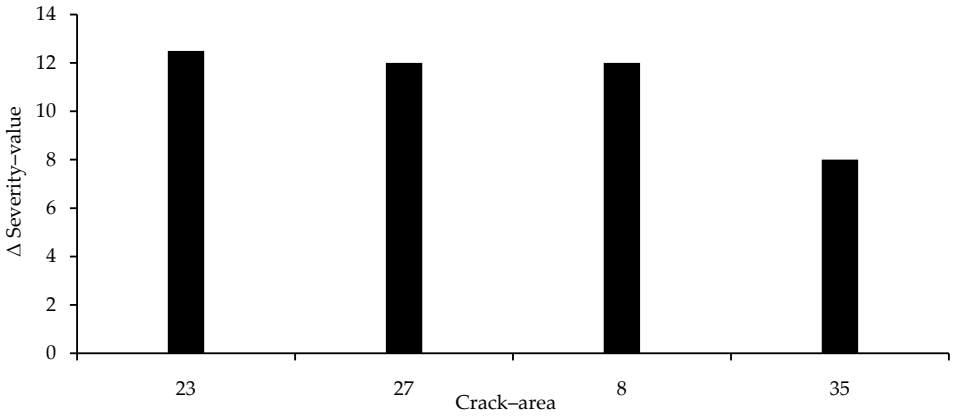

Figure 5.7: Increase of severity–value Point 6R.

Here, the crack–areas are located on four different cables: 1604893A (23), 1604894A (27), 1604897A (8) and 1604898A (35).

With this new data, it is possible to give an overview of the overall situation of the cables inspected. Therefore, the severity–values of all crack–areas located on one cable are added up. The cables with the highest overall severity–value are considered to have the highest priority for replacement. Figure 5.8 shows this stacked value for all the water–cooled cables that had been included in this monitoring.

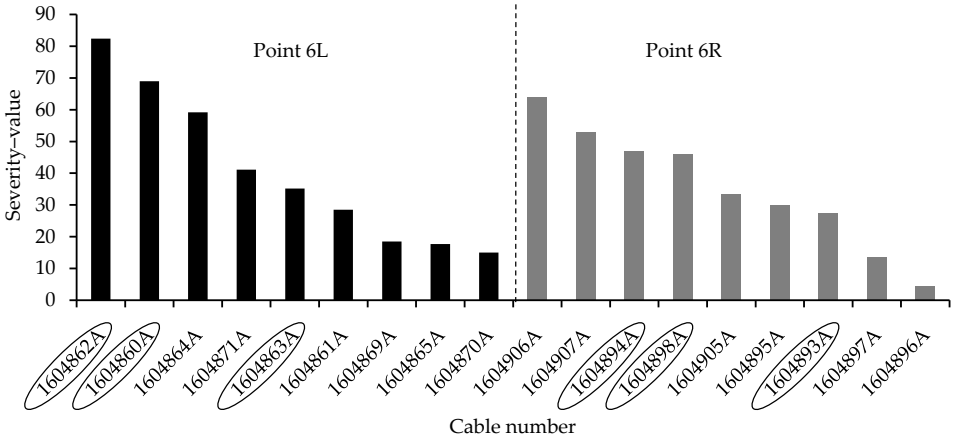

Figure 5.8: Total severity–value by cable. The graph shows the stacked severity–values of all crack–areas on a cable.

Cables containing the crack–areas with the highest growth of severity–value are marked in this graph. It should be noted that this Figure is

based on data collected during all monitorings. Therefore, it contains data from both the current and the preceding monitorings. The crack–areas on cable Nr. 1604864A, for example, showed no crack growth in the current monitoring. Nevertheless, it ranks as the third most affected cable in Point 6L. Therefore, it is displayed in this statistic, as the aim of the monitoring is to show the general condition of the cables.

5.3 Conclusion

In this monitoring, 56 crack–areas in LHC Point 6L and 27 crack–areas in Point 6R were monitored. No new cracks were detected on the cables. Some crack–areas show an extensive increase in the severity–value. For example, for the crack–areas 32.2, 32.5 and 40.4, the value rose from 3 to 15. For the crack–areas 8, 23 and 27, the value rose from 2.5 to 12.5. In all cases, this leap can be explained by the increase in the measured crack width. Even though the absolute increase was rather small in these areas, the resulting severity–value is increased by a factor of 5 as the crack width reaches the "threshold–value" of 0.5 mm. With the width reaching this value, the cracks are assumed to be deep. This results in a corresponding increase in the severity–value (see Table 5.4).

Nevertheless, all crack–areas showing a high increase in severity–value are located on cables with a very high absolute severity–value. Most of these cables already showed a high number of cracks in the preceding monitorings. Therefore, using the given monitoring procedure, they must be assumed to be the cables with the highest damage within the monitoring of 2010.

During the monitoring process, however, various limitations of the methodology became evident. The first difficulty occurs when trying to find exactly the same picture frame of an assigned crack–area. Reference marks that clearly define the outline of the area are not present on the cable. Having an assigned camera position for each area would partly solve this problem. However, given the high number of crack–areas, the effort would be vast. Furthermore, some crack–areas are difficult to access and therefore unsuitable for such an approach.

Basically, the only source available to determine the picture frame is images from previous monitorings. From these, the necessary horizontal

and vertical camera angles have to be estimated. As the camera positions will never be exactly identical, each photo is affected by an angle error. Also, the ruler acting as a reference mark will never be placed identically, leading to deviations in determining the scaling factors. These two problems will be further discussed in Chapter 6. Other problems concerning the accessibility of the cables are mentioned by Ylamaki in [Yla10b]. As access to cables was generally good during this monitoring, this issue will not be further addressed [Wol10b].

Chapter 6

Discussion

Crack monitoring with the described methodology has shown that several limitations are involved, especially in regard to reproducibility. These include, for example, deviations in camera angle and different position of the measurement reference. These issues, along with a closer inspection of the cable material, will be addressed to in this Chapter.

6.1 Restrictions of monitoring methodology

The monitoring methodology used can in the broadest sense be categorized as a digital image processing procedure. For this type of application, consistent lighting conditions and a fixed, exactly aligned camera are usually basic requirements for achieving reproducible and accurate measurement results. In industrial applications, great efforts are taken to meet these demands.

Lighting conditions in the LHC tunnel are, however, not very good and the use of the internal flashlight of the camera often creates uneven illumination. Furthermore, sharpness of the images is an issue. On the one hand, the camera's autofocus has problems working on the black surface of the rubber hose. On the other hand, the camera's aperture is opened wide due to the bad lighting conditions, resulting in a narrow depth of field. Therefore, parts of the image are blurred to some extent. With the hoses being cylindrical objects, this phenomenon becomes apparent when taking the measurements on the pictures at a close range.

6.1.1 Camera angle

One factor which influences the accuracy of the measurement is the angle of the camera to the object (i.e. the hose). Generally, the camera should be positioned perpendicularly to the object to allow an accurate measurement. This means that the object resides on a plane which is parallel to the image plane. Assuming the principle of a pinhole camera[1], the object will then be represented on the image plane. However, in case of an angular misalignment between the object plane and the image plane, the object will appear reduced in size. The extent of this reduction can be expressed by

$$h_2 = h_1 \cdot \cos(\alpha) \tag{6.1}$$

with h_1 being the height and h_2 the apparent height of the object and α being the misalignment angle. The geometric principle is shown in Figure 6.1. In the current application, h_1 represents the width of a crack on the hose surface.

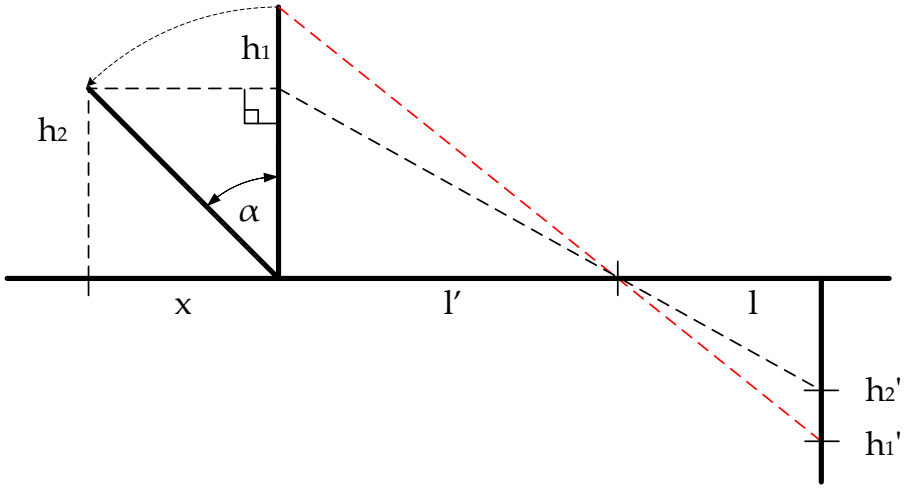

Figure 6.1: Geometric principle of measurement error due to angular misalignment. The object appears reduced in size, depending on the misalignment angle α.

If the camera alignment is correct, h_1 will be represented on the image as h_1', scaled by the factor

[1] Although the pinhole camera nowadays has no relevance for optical applications, it provides a usable model for the description of the fundamental elements of optical projection.

$$h_1' = h_1 \cdot \frac{l}{l'}. \tag{6.2}$$

Accordingly, the apparently reduced object h_2 is represented as h_2'. On closer inspection, the distance of the object from the camera l' is increased by the distance x, which is calculated by the equation

$$x = h_1 \cdot \sin(\alpha). \tag{6.3}$$

However, with the crack width h_1 having a dimension of several tenths of a millimetre and the distance l_1 being around 300 mm in the actual application, this factor is assumed to be negligible. Figure 6.2 shows the dependent relationship of the error expressed in percent and the misalignment angle α.

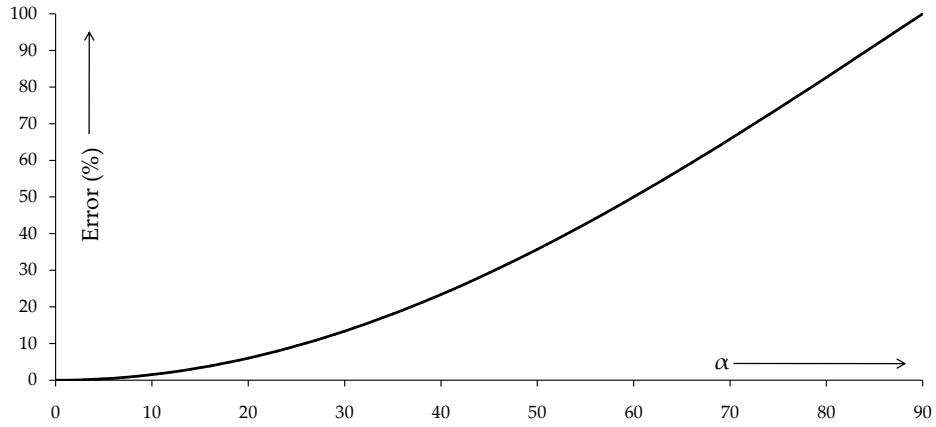

Figure 6.2: Error due to an angular misalignment of the object plane to the image plane. The error increases with the misalignment angle α. At an angle of 90°, the object becomes completely invisible.

The deviation increases with the misalignment angle. For an angle of 30°, a value that can be regarded as quite realistic in the monitoring process, the resulting error is already 13 %. If the angle reaches 90°, the object becomes completely invisible.

The effect of an angular misalignment on the result of the measurement is, however, heavily dependent on the orientation of the measured object, bearing in mind that the critical property influencing the severity–value is the width of a crack (see Table 5.3). If the dimension h_1 in Figure 6.1 represents the height of a crack, the measurement of the corresponding

crack width will not be influenced by the angular misalignment. If, in this example, crack orientation is reversed, the error will affect the measurement of the crack width, not the crack length. Therefore, in reality the resulting error will differ from this idealised model to some extent.

Finally, it should be noted that not only a misaligned camera, but also an angular orientation of the cable and the round shape of the cable itself can lead to this type of measurement inaccuracy.

6.1.2 Perspective distortion

As described in Section 5.1.2, during the picture taking process a ruler is placed in the picture frame, acting as a reference object for measurements during evaluation. In order to achieve an accurate measurement, the reference object has to be placed on the object plane. This ideal condition, however, cannot be achieved in the monitoring process. When taking a photo, the camera will focus on the surface of the cable, thus creating the object plane. The ruler is placed at the side of the cable. It is therefore safe to assume that, in this case, the reference object is placed in a position offset from the object plane. This inevitably leads to a perspective distortion of the reference dimension and therefore of the scaling factor k, that is used to transform the number of pixels to a physical dimension (see 5.1.3). In Figure 6.5 this offset becomes visible, along with the angular misalignment described in the preceding Section.

It becomes evident from Figure 6.5 that the reference object is placed to the crack–area with an offset. In other words, both objects reside on different planes, with the plane of the reference object (reference plane) placed behind the object plane of the crack–area. This results in the reference object appearing smaller due to perspective distortion. The geometric principle is presented in Figure 6.3.

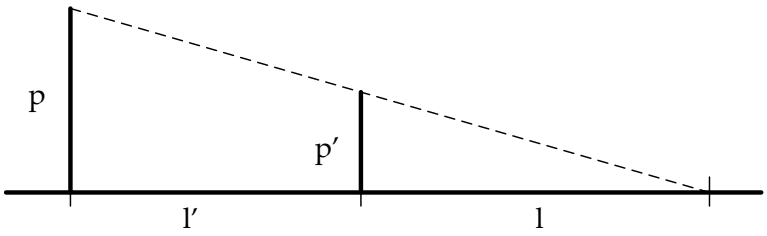

Figure 6.3: Geometric principle of perspective error due to perspective distortion.

Applied to the monitoring methodology, the scale of this transformation is dependent on the distance from the camera to the object plane l and the distance from the object plane to the reference plane l'. The object p is then represented on the object plane as p':

$$p' = \frac{p \cdot l}{l + l'}. \tag{6.4}$$

In order to evaluate the dimension of this error on the monitoring process in a sample calculation, the following values will be assumed: reference dimension $p = 1\,\text{mm}$, camera distance $l = 300\,\text{mm}$. The resulting error for an increasing distance from the reference plane to the object plane l' is presented in Figure 6.4.

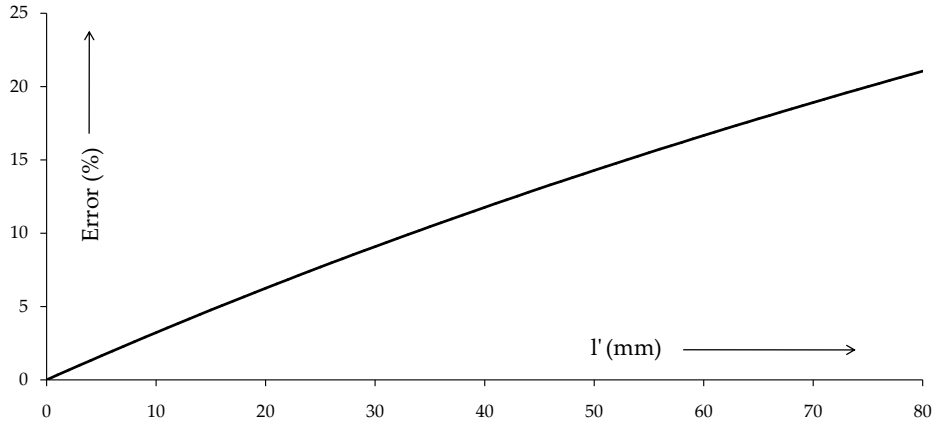

Figure 6.4: Error due to perspective distortion for a camera distance $l = 300\,mm$ and an increasing offset distance l'.

As expected, the error increases with the offset distance l'. At a distance of 40 mm, a dimension that is safe to assume as realistic, the resulting error is almost 12 %. In the first instance, this error affects the calculation of the scale factor k used in the offline measurements. In this case, p' represents the pixel number for the reference dimension d. This pixel count is reduced by the perspective error. Consequently, k is increased, as it is calculated by

$$k = \frac{d}{p'}. \tag{6.5}$$

A higher scaling factor will accordingly lead to increased values of the measured crack dimensions.

Figure 6.5: Photograph of crack–area 32 in Point 6L during the monitoring 2010. Angular misalignment and offset of reference object to crack–area are clearly visible.

6.1.3 Conclusion

Two possible errors which might occur in the measurement process have been described. These fundamental examinations do not claim to describe all possible errors and especially their influence on the measurement process. Instead, the aim is to give a view of the principal influence of the inevitable factors that occur during the process of picture taking and conducting measurements on the pictures themselves.

Neither angle and orientation of an angular misalignment are known, nor is the offset distance between the reference object and the measured object. The possibility of determining the exact extent of the measurement error therefore seems very unlikely. However, the given examples show that under realistic conditions, the resulting error can reach a double–digit percentage.

One question that has not been covered yet is how the combination of possible errors will influence the measurement results. Generally, single uncertainties in combination will form an absolute error, in which they either potentiate or lessen each other in effect. In the given examples, angular misalignment and perspective distortion influence the measurement

results in opposite directions. While an angular misalignment can decrease the measured value, the perspective distortion leads to an increase of the measurement result. In this case, the particular uncertainties eliminate each other to some extent. This case must be considered as prevalent, as both conditions are likely to appear together. Figure 6.5 may serve as a good example of this situation occurring.

One aspect, however, that needs further investigation is the critical crack depth. This value has the highest impact on determining the severity–value for a particular crack–area. It is, however, merely estimated from the measured crack width, since no information about the actual physical dimensions of a critical crack had been available. This issue will be discussed in the following Section.

6.2 Crack depth

The severity–value is mainly influenced by the depth of the cracks in a particular crack–area. In this case, deep cracks are considered to be more dangerous than low cracks. Furthermore, cracks are considered to be of a critical depth once they reach the reinforcement layers of the cable. In this Section, the internal structure of the cable hoses will be examined more closely. Next, a value for the critical crack depth based on a series of measurements will be determined.

6.2.1 Motivation

There are different ways of evaluating the severity of cracks on the hose surface. One possibility is to base the evaluation on the width of the crack as described in Chapter 5, thus drawing conclusions about the crack depth. However, this method gives no information about the actual depth of the crack, especially as the visible width of a crack on the surface is highly dependent on factors such as the bending radius of the cable. A crack located on the straight section of the hose may show an entirely different width from that of a crack of the same depth located on a bent area.

A method of directly determining the depth of a crack would therefore be favourable. Although no suitable method has so far been found for conducting these measurements on the installed cables, one important

factor is to define a critical crack depth in the first place. The value of this critical depth can then be used to evaluate the risk potential of cracks.

Although even deep cracks have proved not to have a direct impact on the burst pressure of the cable in the first place [Wyd08a], they are generally assumed to be of a critical depth when they reach the second reinforcement layer of the cable. When a crack reaches that depth, the reinforcement fibres which mainly determine the structural integrity of the hose are no longer protected by the outer rubber liner of the cable, but are exposed to the environment. This might lead to a premature ageing of the reinforcement material, and thus to a water leak or even a burst hose.

In order to define this critical crack depth, it was therefore essential to determine the actual distance from the second reinforcement layer to the surface of the hose, d_r. The general layout of the hose material has already been presented in Figure 3.2, but no data concerning the actual physical dimensions of the different layers were available at CERN or from the hose manufacturer. Therefore, the rubber hose was inspected for its internal layout. On a first visual inspection, it became clear that the different layers of the hoses were not aligned evenly within the cross–section of the cable. Accordingly, the depth varies within the circumference of the hose as shown in Figure 6.6. This might be caused by an excentric alignment of the reinforcement layers themselves, e.g. during the production process of the hose, or due to an irregular overall thickness of the hose.

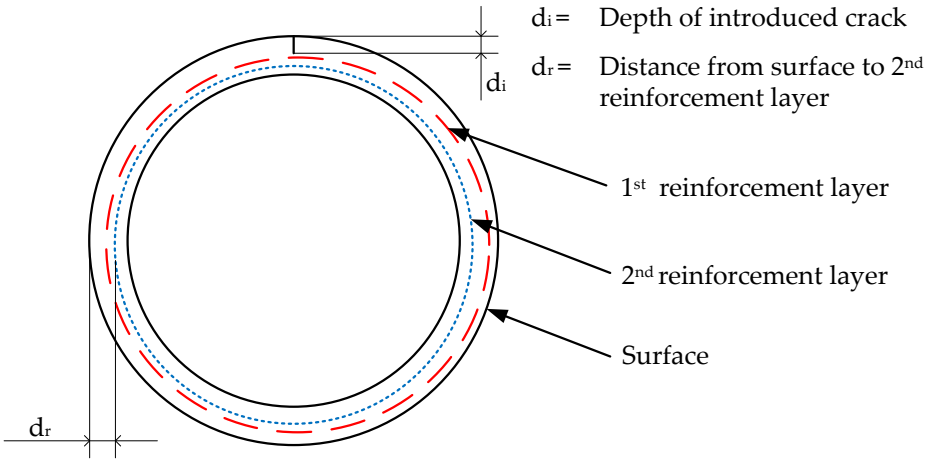

Figure 6.6: Cross–section profile of water–cooled cable hose[2]. Note the excentric alignment of the two reinforcement layers.

It is therefore obvious that a fixed depth cannot be assumed for d_r. Accordingly, a series of measurements on spot samples was conducted to obtain an indication on the distribution of the reinforcement layer within the hose. Hence, a value for d_r can be determined which is valid for a high percentage of the hose surface.

6.2.2 Measurements

Specimens of hoses with an outer diameter of 76 mm, 86 mm and 105 mm were inspected. These are hoses used to replace the hoses with chlorine in the reinforcement layer. They have an identical internal structure, but contain no chlorine. Three samples were taken from each hose. In order to achieve good measurement results, the surface of the specimens needs to be flat, which is not an easy task when dealing with a flexible rubber material. Therefore, a water–jet cutter was used to cut the samples from the hoses. The specimens were then cut open to allow a straight alignment on the test bench. From these nine samples, the distance d_r was then determined using a measurement microscope. The measurement accuracy was ± 0.1 mm. Measurement reports are available in Appendix B.

The distributions of measurement results are presented in Figures 6.7 to 6.9, where the frequency of measured values is plotted against the corresponding measurement value for all three hose types. Values for d_r range between 3.40 and 4.70 mm on the hose samples with 76 mm diameter, and between 3.10 and 4.60 mm on the hose with 86 mm diameter. The distribution of values is approximately the same, with an arithmetic average of 4.00 and 3.90 mm respectively. The 105 mm samples, however, show a different internal layout. The hose material is generally thinner, with d_r only ranging between 2.30 and 3.50 mm with an arithmetic average of 2.87 mm. With the reinforcement layers being closer to the surface, this hose type must be considered as one that suffers from surface cracks more rapidly. Hence, it was chosen as the reference to determine a critical value for d_r. Covering around 90 % of the co–domain, a value of 2.40 ± 0.1 mm is assigned to d_r.

[2]The parameter d_i will be of interest in Chapter 7.

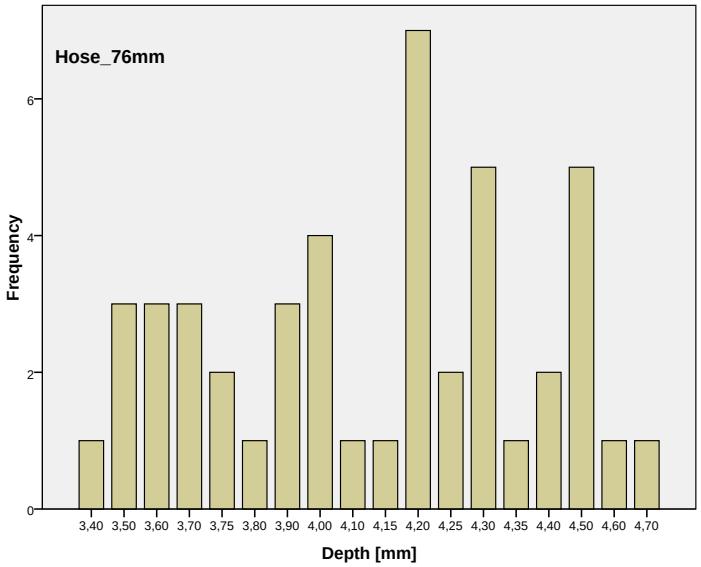

Figure 6.7: Distribution of measurement results for d_r (hose samples with 76 mm diameter).

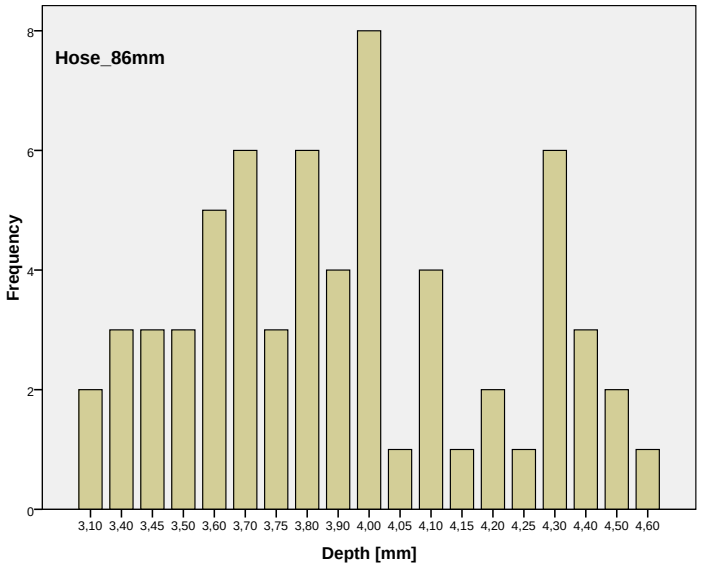

Figure 6.8: Distribution of measurement results for d_r (hose samples with 86 mm diameter).

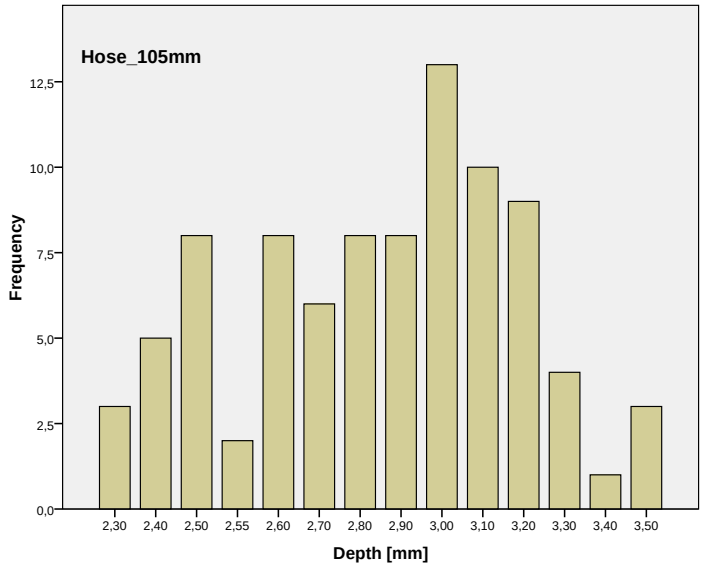

Figure 6.9: Distribution of measurement results for d_r (hose samples with 105 mm diameter).

6.2.3 Summary

The crack depth is a factor that influences the severity–value of a crack–area to a high degree. Cracks are considered to be critical once they reach the second reinforcement layer of the hose, but information on the dimension of this critical crack depth was not available.

Therefore, the critical crack depth d_r has been determined by conducting measurements on spot samples of three different cable types. Two of those materials showed a similar internal structure. In the third cable type, however, the reinforcement layers are located at a significantly lower depth. This cable type was then used as a reference to determine the critical value for d_r. A dimension of 2.40 ± 0.1 was chosen, as it is a valid value for around 90 % of the cable's circumference.

6.3 Conclusion

The monitoring methodology used seems to be a valid method of investigating the progress of cracks on water–cooled cables. For cracks developing

in the visible range, a good qualitative comparison between the photos taken during two monitorings is possible. This is a definite advantage of the method, as significant changes become obvious very quickly.

Results of the more time–consuming process of generating quantitative data from the obtained images, however, must be interpreted carefully. The fact that all measurement results are affected by an inaccuracy of unknown extent must always be considered when evaluating the data. Bearing in mind that the aim of the monitoring is to determine a reasonable replacement order for the affected cables, drastic change in severity–value should be validated by a visual evaluation. A good example is crack–area 17 in Point 6R (see Figure A.83 in Appendix A.2). Here, very large cracks are visible, furthermore the measurements indicate a considerable increase in severity–value. Therefore, giving the corresponding cable a high priority for replacement is a plausible deduction.

Thus, it is a combination of visual evaluation and critical assessment of gathered measurement data that is required for the successful application of this methodology.

Chapter 7

Crack analysis with combined radiation and pressure testing

The purpose of the test described in this Section is to simulate the operational conditions of the cables installed in the LHC in respect of radiation level and water pressure conditions. Both of these factors might have an effect on the crack growth on the cable hoses. The radiation and pressure conditions occurring during operation are simulated for a lifetime of up to 15 years. The aim of this test is to observe if under the given conditions the impact on the crack growth is so high that the hoses have to be replaced prematurely.

7.1 Test principle

A variety of standards already exists, describing test methods to determine the safety of tubing and hoses under a pressure load. In general, they can be divided into tests applying a constant pressure for a certain time (static test) and test procedures applying a certain pressure profile to the specimen (dynamic test). An example of a static test is the hydrostatic testing according to [ISO 1402]. This test method is applied to the water–cooled cable hoses by the hose manufacturer to verify pressure stability, dimensional stability and water–tightness of the product.

The test specified here, however, is a dynamic test, as a changing pressure profile will be applied to the sample. An example of the specification of a dynamic test is [ISO 6803], where the effect of pressure

impulses on a test sample is determined. This standard cannot be applied directly as it is designed to test cables or tubing for high–pressure hydraulic systems. In these applications, the working pressure reaches up to several hundred bars. Also, the rate of pressure rise defined in this standard is much too high. However, in regard to the dimensioning of the specimens and the general setup of the test–rig, this standard provides a basis for the definition of the test method.

The test is designed as a non–destructive test procedure. It is supposed to simulate the influence of ionizing radiation and different pressure conditions occurring during the operation of the water–cooled cable. As there is probably no laboratory where these two conditions can be applied simultaneously, they have to be applied sequentially. Test pieces of hose material, either used pieces already showing surface cracks, or specimens with artificially introduced cracks, are first irradiated to a specific total dose. Then, they are submitted to a cycle of pre–defined pressure loads. These are derived from different pressure patterns which occur during the operation of water–cooled cables. After the test, the impact of the test procedure on the growth of the cracks is investigated (see Figure 7.1 for the general test sequence).

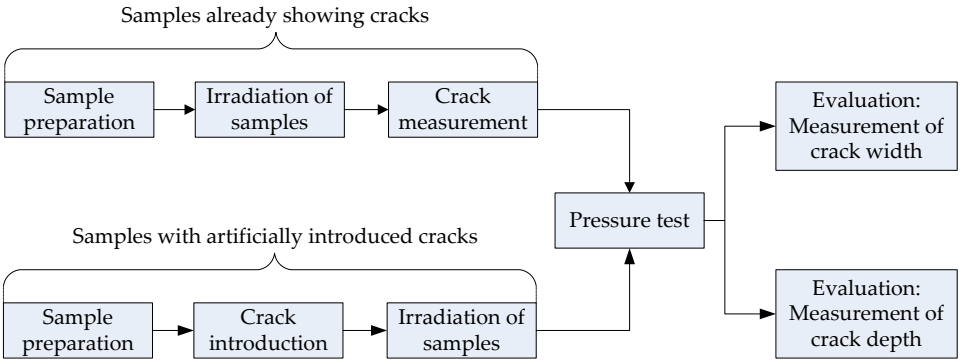

Figure 7.1: Radiation and pressure test procedure.

There are two possible types of samples for this test method. On the one hand, cable samples already showing cracks can be tested. As the exact depth of the cracks is unknown on these specimens, they can be evaluated in regard to the increase in length and/or width of the cracks. From these values, the depth of the cracks has to be estimated. On the other hand, samples with artificially introduced surface cracks can be used for testing.

As the crack depth is a known factor on these samples, they allow a better evaluation of the radiation and pressure influence on the crack growth.

7.2 Operational conditions and pressure patterns

In order to determine the parameters of the pressure test, the operating conditions of the water–cooled cables are being used as a reference. The general parameters and operating conditions are presented in Section 3.3. Important factors for the definition of this test are the minimum bending radius of the different water–cooled cables (see Table 3.1), the operation pressure of 16 bar (see Section 3.6) and the exposure to ionizing radiation (see Section 3.4.3), which is assumed to be 20 kGy per year.

During operation, the cables are connected to the demineralised water circuit. The basic connection pattern is presented in 3.3. The circuit in this graphic shows the water–cooled cables with positive and negative polarity connecting a power converter to a DFB. The lugs on the end of the cables maintain both the electrical connection to the current leads and the hydraulic connection to the cooling water circuit. The cooling water is fed through the first cable, then routed to the second cable by a hose connection and finally fed back to the return line.

There, the water in the cooling system is maintained at a constant pressure level of 16 bar. However, in addition to the constant pressure load during operation, four specific pressure profiles might appear during operation. Those profiles will be described in the graphs in the following Section. Note that for a better visualization of the pressure profiles, the graphs are not true to scale and the time axis in the graphs is not to scale for the periods of constant pressure. Furthermore, in the actual application the pressure rise or fall rate is not exactly linear. In this test, however, pressure changes will be applied at a linear rate.

In this Section, the individual pressure profiles are described. For the actual test sequence, these profiles are combined (see Section 7.4.4 for a description of the test pressure sequence and Appendix C for a graph of the complete test pressure sequence).

7.2.1 Initial test

In order to verify the water–tightness of the cable, the initial test is performed after installation of the cable. During this test, the cable is loaded with a pressure of 24 bar by using a manual pump (see Figure 7.2 for the relevant pressure pattern). The pressure is applied for a period of 10 minutes, resulting in a pressure rise rate of 0.04 bar/s (1). This pressure level is then maintained for a period of one hour to verify the water–tightness of the tested cable. Finally, the pressure is released at a rate of 0.4 bar/s (2) (see Figure 7.2).

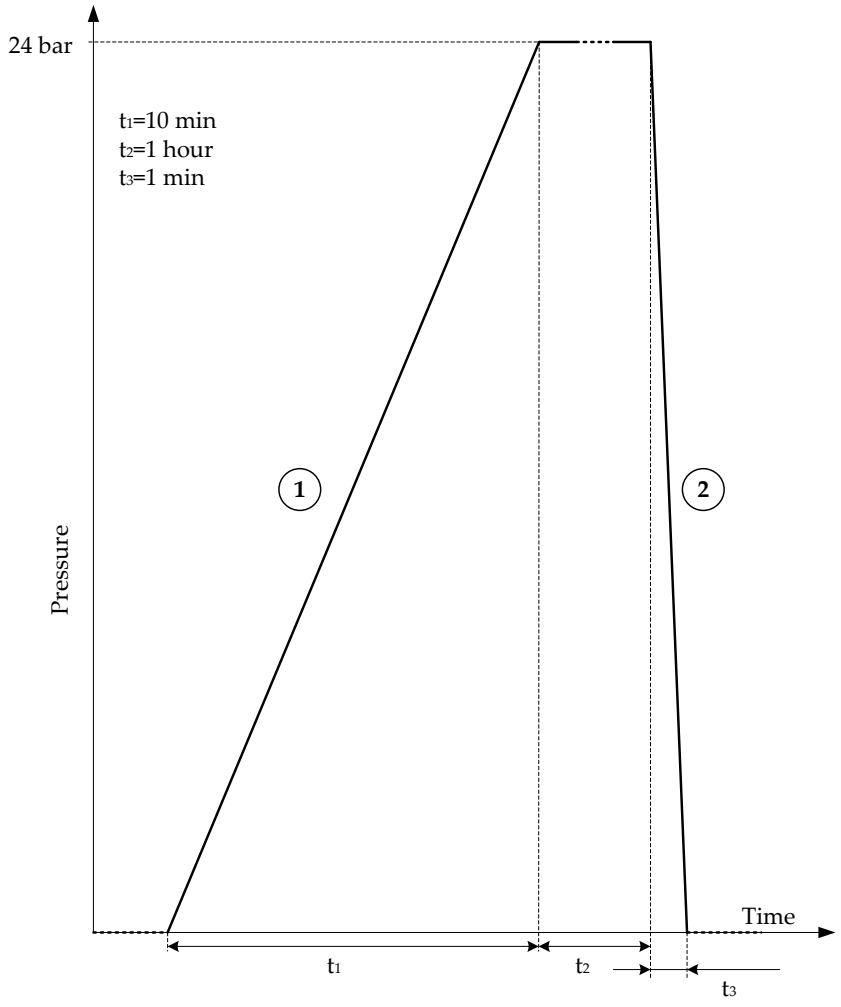

Figure 7.2: Pressure pattern during initial test.

7.2.2 Commissioning of the cable

The pressure profile during the commissioning of the cables in a circuit is presented in Figure 7.3. The beginning of the graph shows the cables connected to the cooling water circuit with the valves of the feed line and the return line both still closed. The operator then first opens the valve of the return line to fill the cable with water. This action takes one minute. The pressure will rise to 3 bar, which is the pressure level present in the return line of the circuit (3). The pressure in the circuit will rise at a rate of 0.05 bar/s . In a second step, the operation pressure of 16 bar is applied to the cables by slowly opening the feed line valve for a period of 10 minutes (4). The pressure rise rate is 0.02 bar/s. After that, the commissioning is completed and the cables stay under the constant operating pressure of 16 bar (see Figure 7.3).

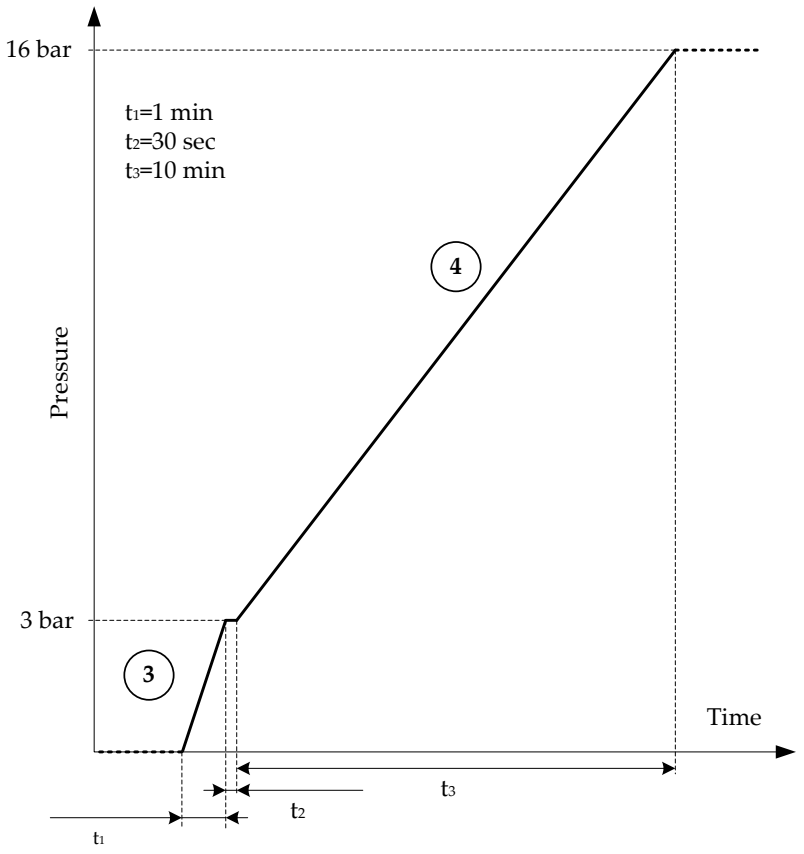

Figure 7.3: Pressure pattern during commissioning.

7.2.3 Maintenance of the hydraulic system

This pressure pattern appears when the hydraulic system has to be shut down for maintenance, e.g. cleaning a water filter or replacing the pump. Although the hydraulic system is very reliable and maintenance work is not likely to be necessary during normal operation, this event has to be taken into consideration for the pressure test.

The pressure patterns presented previously referred to the local circuits of water–cooled cables according to Figure 3.3. In contrast to that, the pressure conditions which are present during the maintenance of the hydraulic system concern the whole hydraulic circuit, i.e. they concern the feed and return line.

Out of normal operation, the valves of the system are closed first, resulting in a reduced water flow and hence in a pressure rise in the system for 30 seconds from 16 bar to 23 bar (5). The resulting pressure rise rate is approximately 0.02 bar/s. After that, the pump is shut down, decreasing the pressure in the system at a rate of 0.8 bar/s. (6). The following time span of 30 seconds with zero pressure in the system represents the actual maintenance work. The restart of the pump (7) is carried out with the valves in the system still closed, again resulting in a pressure peak at a rise rate of 0.7 bar/s. Finally, the valves are opened (8) and the pressure drops to the operating level of 16 bar at a rate of 0.1 bar/s (see Figure 7.4).

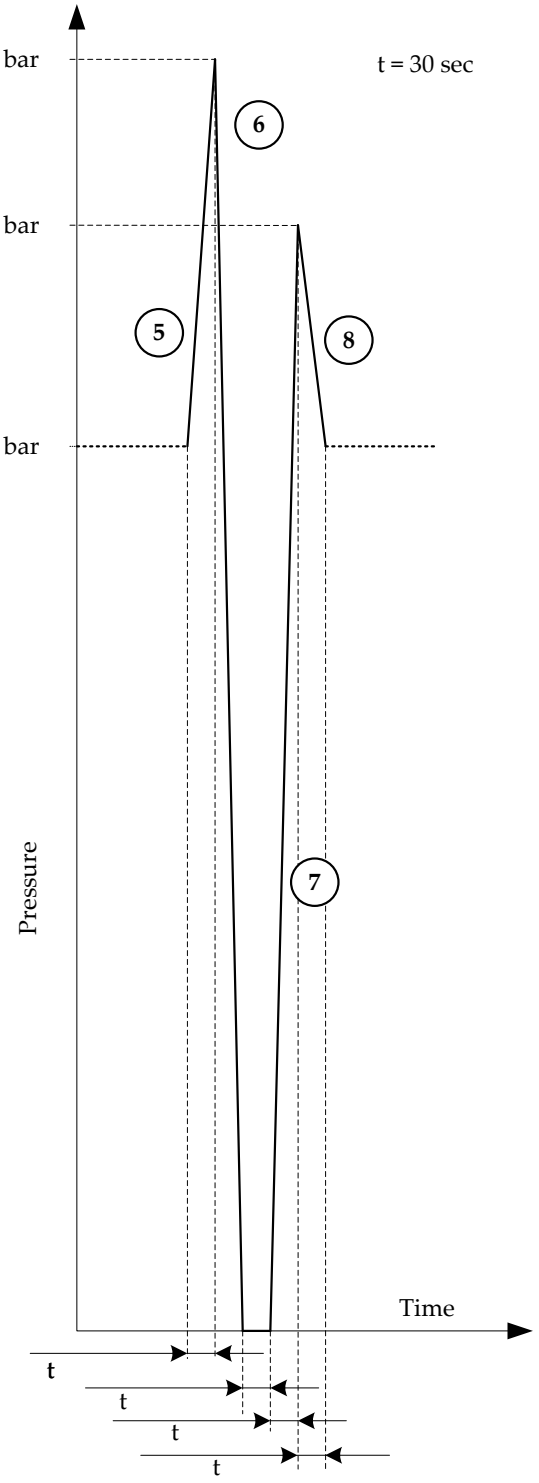

Figure 7.4: Pressure pattern during maintenance of the hydraulic system.

7.2.4 Shutdown of the hydraulic system

If one cooling circuit of the water–cooled cables has to be shut down, e.g. in order to replace the hose of a cable, this is done in two steps. The resulting pressure pattern is presented in Figure 7.5. First, the valve of the feed line and then the valve of the return line are closed (9) , resulting in a pressure drop at a rate of 0.2 bar/s. Then, the residual pressure in the cables is released (10). The pressure drop is 0.05 bar/s.

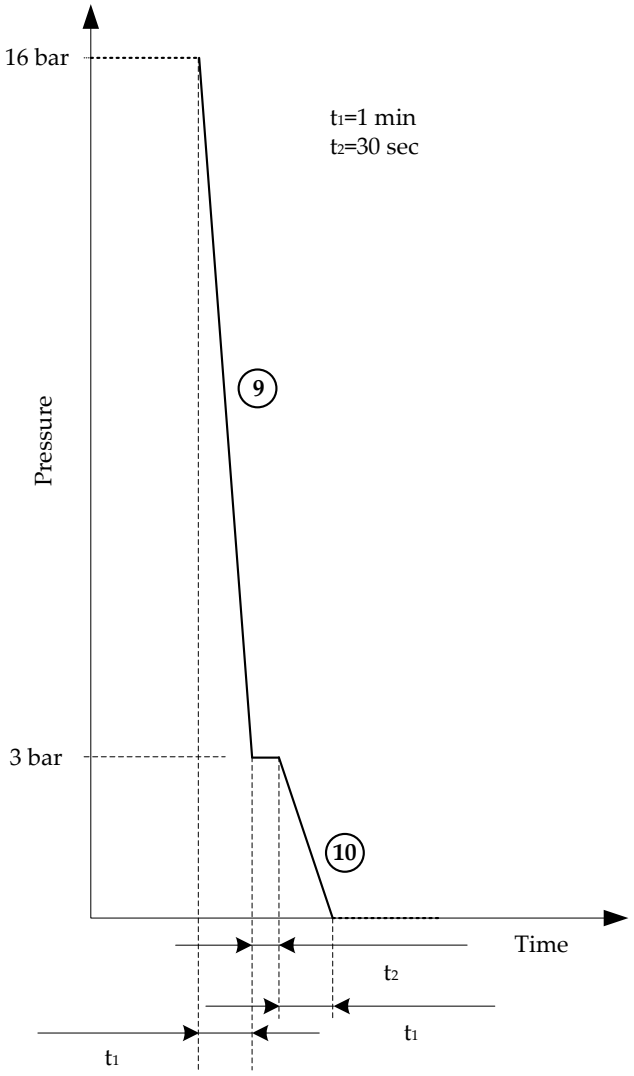

Figure 7.5: Pressure pattern during hydraulic shutdown.

7.3 Preparation of samples

As mentioned previously, the test pieces shall consist of complete hose assemblies or pieces of hose with suitable fittings attached. Following [ISO 6803], four test pieces should be tested. The samples can either be hose pieces already showing surface cracks or hose pieces with artificially introduced cracks. Samples already showing cracks are selected from hose pieces that had already been installed in the LHC and were replaced because of the presence of surface cracks. New or stocked hoses are used for samples on which cracks will be introduced artificially.

7.3.1 Dimensioning of test pieces

Following [ISO 6803], the tests shall be conducted on samples that have been bent through an angle of 90° (see Figure 7.6). This alignment represents the maximum bending angle which can occur in the installation in which the cables are exposed to the highest surface strain. The free length l of the sample is dependent on the maximum overall diameter d and the minimum bending radius r of the tested hose. Both values are specified in Section 3.3.

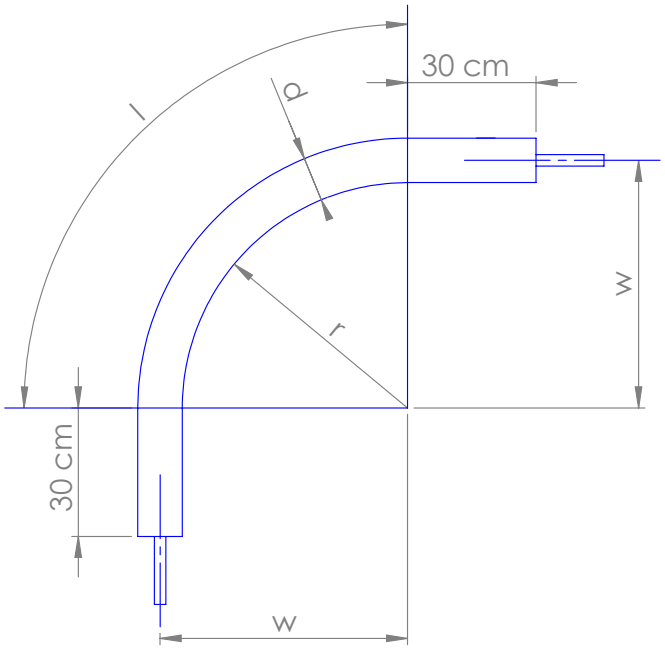

Figure 7.6: Sample bent through 90°.

The overall free length l of the sample is calculated as follows:

$$l = 0.5 \cdot \pi \cdot r + 2 \cdot d + 60\,\text{cm}. \tag{7.1}$$

To obtain the desired bending radius of 90°, the mounting distance w shall be:

$$w = r + 0.5 \cdot d. \tag{7.2}$$

7.3.2 Introduction of cracks

A major factor for the evaluation of the test is whether a crack reaches the second reinforcement layer of the hose or not. Therefore, the depth of the introduced crack shall be related to the critical distance from the surface of the hose to the second reinforcement layer d_r. Figure 6.6 in Section 6.2 shows a simplified cross–section profile of the tested hose. In this Section, the critical crack depth d_r has already been discussed. The cracks introduced shall be an equal combination of transversal and longitudinal cracks. The depth of the introduced crack d_i shall be

$$d_i = \frac{d_r}{2}. \tag{7.3}$$

The artificial cracks shall be created using a suitable cutting device that allows an exact and reproducible introduction of cracks. The cracks shall be introduced at $l/2$, i.e. in the middle of the test sample, covering the whole circumference of the hose. Especially when bending the sample through 90° during the test, this is the region in which the highest change of crack growth is expected to appear. Depth and length of the introduced cracks shall be recorded for later comparison.

7.3.3 Irradiation of samples

After cutting of the samples to the required length and, if desired, the introduction of cracks, the samples shall be irradiated with a total dose representing the lifetime period that is to be simulated. The radiation dose to expect in the LHC tunnel has already been discussed in Section 3.5.3. A dose of 20 kGy has been found to occur in the worst case. This value will be used to simulate one year of lifetime. Accordingly, the dose for a

simulated lifetime of two years shall be 40 kGy, for three years 60 kGy etc. Although the yearly dose will be much lower in most parts of the LHC tunnel, this high dose is used to test the cable under the hardest conditions likely to appear.

7.3.4 Crack measurement

If samples already showing surface cracks are used, the length and width of those cracks shall be determined for later evaluation of the test. If the sample shows a very high amount of cracks, only the cracks with the largest dimensions shall be measured. A total of 20 cracks shall be considered sufficient for the evaluation of the test. This number was chosen as it also represents the highest crack frequency to be taken into consideration for the severity–value (see Table 5.2).

Measurement of cracks can be made by the photo monitoring method described in Section 5.1. This method is based on a comparison of photographs. They show the areas in which cracks appear and a reference mark. When evaluating the photos, the reference mark allows the measurement of the crack dimensions. By taking pictures before and after the test, the growth rate of the cracks can be determined.

As already discussed, when using this method for the crack measurements on test samples, it is important to take the photos from exactly the same distance and viewing angle. This can be achieved by installing the camera on a tripod next to the test setup. The reference mark shall be attached to the test sample. Photos of the crack–areas shall be taken before and after the pressure test. During the test, the camera shall not be moved. By taking the pictures from exactly the same location, the conditions for the later crack measurements are optimal.

7.4 Definition of the test method

7.4.1 Simulated lifetime

Concerning the lifetime to be simulated in the test, there are two possible approaches. One possibility is to conduct a single test, simulating the estimated lifetime period of 15 years by applying the expected radiation dose and pressure deviations. The evaluation of the test will then give

information about whether the samples meet the end–point criterion or not.

On the other hand, it is possible to conduct a series of tests, simulating different lifetime periods. Typical periods could be 5, 10 and 15 years. The resulting crack growth can then be plotted against the simulated lifetime, giving a better understanding of the crack growth during the simulated lifetime of the sample. If the crack growth shows approximately linear behaviour, this methodology even allows a simple graphical extrapolation for time periods exceeding the simulated lifetimes.

7.4.2 Environmental conditions

According to [ISO 471], the following test conditions shall be applied. The test temperatures to be applied are the maximum temperatures specified in [CER03] and [Mar03].

Standard temperature The standard temperature shall be 26 ± 4 °C.

Standard humidity Standard humidity shall be 50 % relative humidity. The normal tolerance shall be 5 % relative humidity. The average relative humidity of the environment shall be as close as practicable to the specified relative humidity.

7.4.3 Test setup

Based on [ISO 6803], the test setup shall fulfil the following requirements:

Apparatus The apparatus shall be capable of applying an internal pressure to the test piece using the test fluid which circulates through the test piece. The fluid shall be maintained at the required test temperature.

Each pressure cycle shall be conducted as described in Section 7.4.4 . A suitable graphical recorder is required to enable the pressure cycle to be checked against this specification. The rate of pressure rise and drop depends on the individual pressure profile and is defined in Section 7.2.

Test fluid The test fluid shall be demineralised water as specified in Section 3.6.

Test temperature The temperature of the test fluid shall be $50 \pm 3\,°C$. According to [CER03], this is the highest temperature to occur during the operation of the water–cooled cable. The test fluid shall be circulated through the test pieces at the specified temperature.

The test fluid temperature shall be measured at the inlet and the outlet of the test pieces and the test temperature is defined as the mean value of the two measured temperatures. None of the measured values may deviate from the test temperature by more than 3 °C.

7.4.4 Test pressure sequence

In Section 7.2, four distinctive pressure profiles which can occur during operation have been defined. These are:

- Initial test (Figure 7.2)
- Commissioning of the cable (Figure 7.3)
- Maintenance of hydraulic system (Figure 7.4
- Shutdown of hydraulic system (Figure 7.5)

The actual pressure sequence to be applied to the cable by the test apparatus is a combination of the pressure profiles mentioned above. Figure 7.7 shows the test sequence for the simulation of one year of usage.

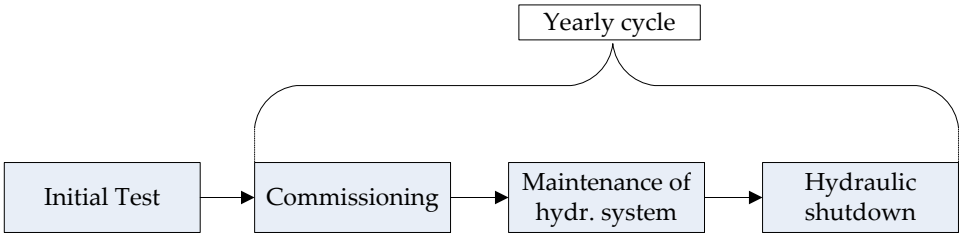

Figure 7.7: Test pressure sequence.

Every pressure test begins with the "initial test" profile, followed by a sequence of profiles called "yearly cycle". Usually, several years of service shall be simulated during the test. In this case, the "yearly cycle" has to be repeated, each cycle representing one year of usage. A graph of the complete test pressure sequence is presented in Appendix C. Each pressure rise or decrease has been marked by a continuously numbered point in the

graph. Between the pressure profiles in the yearly cycle, a time period of one hour has been specified to represent the normal operation of the cable.

Simulated lifetime [years]	5	10	15
Required test time [hh:mm]	12:41	24:11	35:41

Table 7.1: Required test time.

Between the different pressure profiles, the current pressure shall be kept for a period of two minutes. The resulting overall time required for the test is 01:11 hours for the initial test and 02:18 hours for the yearly cycle. According to that, the total required test time for different simulated lifetimes is shown in Table 7.1.

7.5 Expression of results

The growth of surface cracks on the test samples is used as the criterion for the evaluation of the test. For this reason, samples already showing cracks before the test and samples with artificially introduced cracks have to be treated differently. The methodology for the evaluation of these two different sample types is described in this Section.

Samples already showing cracks

After the tests, the length and width of the cracks concerned shall be measured, thus showing the growth of the cracks. Hereby, the growth in crack width is assumed to be of higher importance than the growth in crack length. [Yla10a] Therefore, the growth in crack width is taken as the critical property to define the endpoint criterion.

The results of the measurements shall then be presented as the relation w_0/w, where w_0 is the width of the crack before the test and w is the width of the crack after the test. This value shall be taken as the endpoint criterion and then be plotted over the number of lifetime cycles with which the sample has been tested. A typical endpoint criterion could be

$$\frac{w_0}{w} = 0.5, \tag{7.4}$$

indicating that the crack width has doubled.

Samples with artificially introduced cracks

When using samples with induced cracks, the crack depth is the critical property used to evaluate the test. After the test, the hose has to be cut perpendicularly to the crack orientation. Then, the depth of the cracks is determined and compared to the depth of the induced crack.

The result shall then be presented as the relation d_i/d, where d_i is the depth of the induced crack before the test and d is the depth of the crack after the test. This value shall be taken as the endpoint criterion and then plotted over the number of lifetime cycles the hose has been tested with. A typical endpoint criterion might be

$$\frac{d_i}{d} = 0.5. \tag{7.5}$$

If the crack was introduced with respect to the distance of the surface to the 2nd reinforcement layer as described in Section 6.2, this value means that the crack must be supposed to have reached the reinforcement layer [Wol10a].

Chapter 8

Research on possible alternatives

The preceding Chapters showed that the technology of water–cooled cables is not without problems. In this Chapter, possible alternatives shall therefore be investigated.

At this point, it shall be emphasized that this Chapter does not claim to present technical solutions that can be applied directly. The complex structure of the LHC and the vast effort gone into its design prohibit such pretensions. It shall rather be a reflection about how the problems which occurred could be avoided. Therefore, after engaging fundamental considerations on the topic and possible conductor materials, different conductor layouts will be examined.

8.1 Motivation

After thorough selection, water–cooled cables were installed as high–current conductors in the LHC. However, even before the startup of the LHC, problems occurred which can be ascribed to the rubber material of the hoses, as described in Chapter 4. The problem of surface cracks still requires a continuous updating and estimation of its potential danger. This represents a time–consuming task which, however, is absolutely necessary as the consequential damage in case of cable failure would be immense.

Hence, the question arose how the operational reliability could be guaranteed on a sustained basis and how surface cracks could be avoided

in the future. In this regard, possible alternatives for the fault–prone conductors currently in use shall be examined.

8.2 Fundamental considerations

The application of these conductors is special in many ways. To begin with, very high currents have to be conducted. The specified currents range from 3.5 to 13 kA. As a consequence, the conductor will heat up during operation, as every normal conducting material shows an electrical resistivity of some extent. Cooling the conductor during operation will therefore be inevitable.

Furthermore, access to the confined space in the underground areas of the LHC must be considered in regard to both the initial installation and the eventuality of replacing a cable before the scheduled lifetime. When the water–cooled cables were first installed, special equipment was used to pull the cables through the bends to their desired location. Considering the weight of the cables, this work could not be done manually[1]. This fact requires the use of auxiliary equipment, which, at the same time, must be suitable for use in the LHC tunnel, as space and accessibility are very limited.

Along with the latter factor goes the necessity for the conductor to have a certain flexibility. It is used for the sections of a circuit that involves bends and does not allow the usage of rigid, straight connections. In places where this type of connection is possible, water–cooled tubes are used already. This setup is illustrated in Figure 8.1.

The last and most important aspects to be taken into consideration are maintenance effort and reliability of the conductor. As the conducting material itself can be regarded as maintenance–free, the focus must be on the insulation material as the critical factor. In most cases, this will be a polymeric material of some sort, which by its nature is subject to a certain level of degradation over time. Of course, this fact influences the selection of a material, which keeps its necessary properties for the aspired lifetime under assumed influence conditions.

[1] Copper has a very high density. For a 10 m–section of 2000 mm^2 water–cooled cable, the copper core alone has a weight of 178 kg.

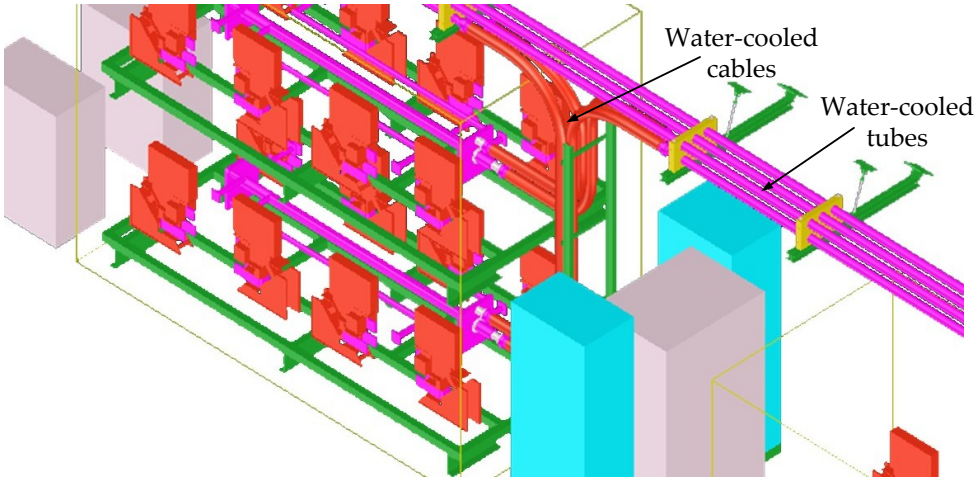

Figure 8.1: CAD–drawing of water–cooled cables and tubes in the LHC. Tubes are used to cover the straight sections, whereas flexible cables are utilized in areas involving bends (image source: CERN internal).

Unfortunately, the previous Chapters show that there is always a danger of unexpected premature degradation. In the particular case of water–cooled cables, this danger is of exceptional importance, as the polymeric material is not only responsible for electric insulation, but also ensures the water–tightness of the cable. While a defective electric insulation will not necessarily result in an imminent failure of the concerned circuit, water leakage certainly will.

In consequence, this leads to several different methods of resolution. One possibility would be to use insulation material that is generously overdimensioned in terms of expected degradation, so that even in case of premature ageing it will stay within the desired limits. Another way would be to avoid these susceptible materials altogether, which would ensure the highest level of reliability. This, however, seems virtually impossible, but based on this assumption a valid way would be to reduce the usage of these materials to the absolute minimum.

Bearing in mind the effort that is currently taken to address the problem of surface cracks, a restricted number of rubber hoses would not only reduce considerably the degree of monitoring required, but also the time and money needed to replace cables which are affected.

Finally, another means of reducing the damage potential dramatically would be to limit the use of polymeric materials to electrical insulation only,

and to obtain water–tightness of the conductor with a material resistant to environmental stress. This, however, will at the same time most likely limit the flexibility of the conductor, as rubber materials are unique regarding flexibility.

At this point, it becomes obvious that an "ideal" conductor has to meet demands that are difficult to combine. The main aspects to consider are temperature rise, current–carrying capability, flexibility, and finally maintenance effort and reliability of the conductor. A valid solution must therefore cover both the individual strengths and weaknesses of each aspect in such a way, that the result is a compromise solution meeting the overall requirements.

8.3 Conductor materials

The choice of conductor material can be the first step for the selection of a conductor. Without doubt, silver is the best conductor, but its high price prohibits its use on a large scale. The choice is therefore narrowed to a variety of copper alloys. As mentioned before, conductivity is a major factor to be considered. For commercial coppers, conductivity ranges from 102 % IACS to less than 20 % IACS, the particular value being determined by factors such as type and degree of alloying and heat treatment [Cal11]. Conductivity is a critical factor for the dimensioning of the cable, as together with the cross–section it determines the electrical resistivity of the circuit and therefore the expected power dissipation.

To give an impression of the magnitude of these influencing factors, a short example will be given: a cable made from copper with 100 % IACS conductivity will show a specific resitance of $\rho = 0.01724\ \frac{\Omega \cdot mm^2}{m}$ at 20 °C. At a cross–section of 2000 mm^2, the cable's electric resistance will therefore be 8.62 µΩ/m. Given the rated current $I = 13$ kA for this cable type, the dissipated power P can be calculated by

$$P = I^2 \cdot R. \tag{8.1}$$

The resulting value is surprisingly high: for each metre of cable, the power dissipation is almost 1.5 kW. Bearing in mind that several thousand metres of these high–current cables are currently installed in the LHC, the magnitude of this effect becomes obvious. The expected power dissipation

in a 13 kA circuit for copper 100 % IACS compared to copper 75 % IACS and silver is visualised in Figure 8.2. The latter two materials are included in the graph to illustrate the influence of conductivity on the power dissipation.

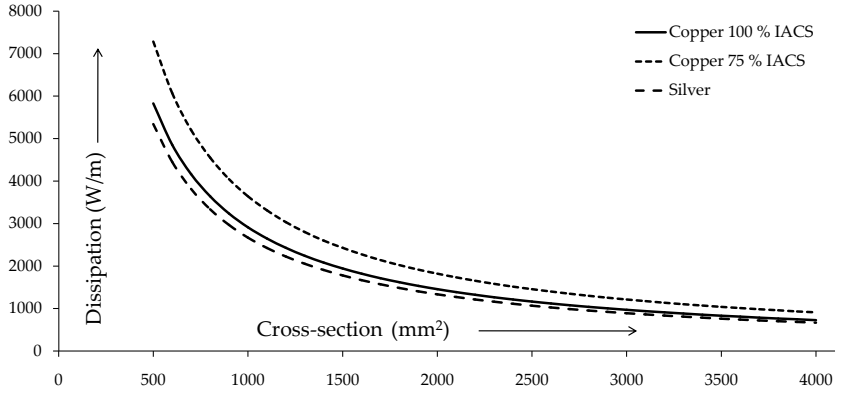

Figure 8.2: Power dissipation per metre for different conductor materials at a current of 13 kA (temperature dependence is ignored).

A further aspect to consider is the temperature dependence of the conductor material. Like most physical properties, the specific resistance, too, will change with temperature. Copper – like all metals – has a positive temperature coefficient, i.e. its resistance will increase with rising temperature. Although this temperature dependency is not exactly linear, a linear approximation can be made that will give a sufficient description for the temperature dependent specific resistance ρ_T for a wide temperature range:

$$\rho_T = \rho_0 \cdot \alpha \cdot \Delta T + \rho_0 \tag{8.2}$$

with α being the temperature coefficient which for copper is

$$\alpha_{Cu} = 3.9 \cdot 10^{-3} \cdot K^{-1}, \tag{8.3}$$

ρ_0 being the specific resistance according to 100 % IACS at 20 °C and ΔT being the temperature difference. The maximum operation temperature is defined as 50 °C (see 3.3), so the maximum ΔT to expect is 30 °C. Applying these values to the formula given above results in an increase of specific resistance by 12 % and in consequence to a proportional increase in

dissipated power[2].

The main aspect, however, is the conductor's cross–section, which not only has the highest influence on power dissipation, but is also the main parameter to adjust in the actual application. Taking into account the limited conductivity, and considering a given integration (and as such given lengths for the conductor and a limited capacity of the cooling system), the parameter to be changed is the cross–section [Gug04], [ZG05], [HRW07].

8.4 Conductor layouts

A first layout imaginable could therefore be a solid copper bar with a cross–section that would be high enough to support the specified current without considerable temperature rise. Although this conductor type would be maintenance–free and very reliable, for obvious reasons the cross–section cannot be increased arbitrarily. The exponentially decaying influence of cross–section on the heating of the conductor furthermore limits the current–carrying capability in case the conductor is dependent on releasing the heat to the ambient air. In terms of conductor flexibility, this solution must also be regarded as inapplicable.

A way to address the problem of heat is to incorporate one or multiple coolant channels in the conductor design. Water–cooled copper tubes represent such a layout, and incorporating the advantages of a solid copper connection with forced cooling, they are a very good solution in places where flexibility of the conductor is not an issue. In this case, the cooling channels can be chosen sufficiently large to dissipate the generated heat to the cooling medium. This type of conductor is already used in the LHC for straight high–current connections. However, the problem of insufficient flexibility remains with this layout.

A way of incorporating a certain level of flexibility in the conductor design can therefore be to use a solid, thin–walled tube as a cooling channel only and to design the electrical conductor as a flexible core. The cooling channel is surrounded by the core, thus dissipating the heat generated.

[2]This, of couse, is a worst–case consideration. When the water–cooled cables were dimensioned, the calculations were performed for an average temperature of 40 °C and therefore for a ΔT of 20 °C.

This type of conductor is also used at CERN for particle accelerators other than the LHC (see Figure 8.3 for the conductor layout).

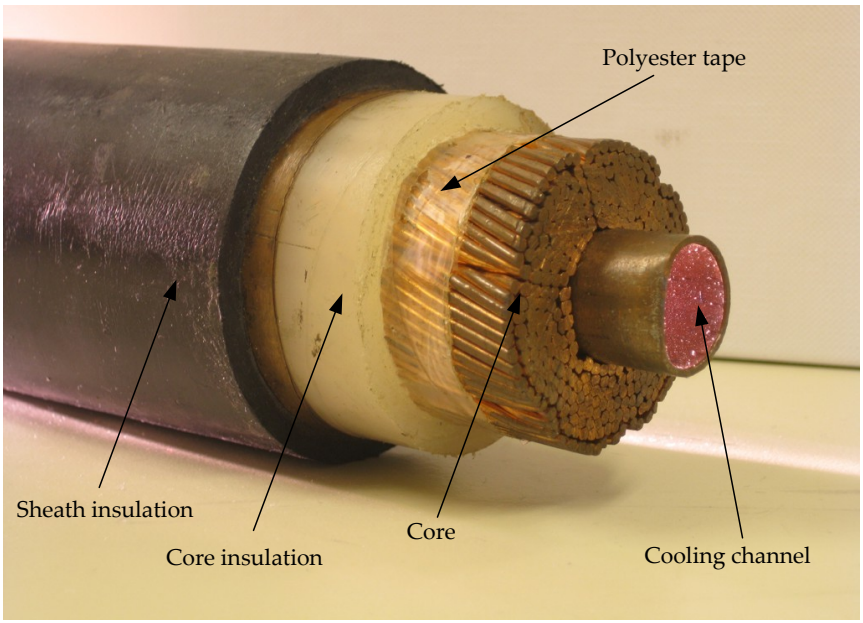

Figure 8.3: Water–cooled conductor with flexible copper core and copper pipe as cooling channel. This layout offers a certain flexibility, but cooling capacity is limited.

In this layout, a copper pipe was chosen for the cooling channel. The core was built up of six stranded sectors which were shaped to ensure good contact with the cooling pipe. To facilitate the fabrication of the cable, the sectors were fixed with a polyester tape. One of the problems encountered was, however, the required flexibility which is reduced as the cross section of the cable increases. The possible current to carry with this type of cable is therefore limited if a specified bending radius has to be maintained. In addition, with this layout heat can only be dissipated in the border area of the core where the core is in contact with the cooling channel. In the application of the conductor shown in Figure 8.3, these problems could only be solved by splitting up the required cross–section into two cables each having half of the required cross–section [PRW70].

A next step to increase the cooling of the conductor and therefore the current–carrying capability can therefore be to incorporate multiple cooling channels in the layout. By increasing the total cross–section of the cooling channel, the possible mass flow rate and therefore the cooling capacity of

the conductor will be higher. Furthermore, the heat transfer to the coolant is distributed more evenly throughout the conductor. A design of this type was used for magnet coils installed in the MINOS[3] experiment at Fermilab[4]. This conductor was dimensioned to provide a current of 15 kA. The cross–section of the conductor is illustrated in Figure 8.4 which follows:

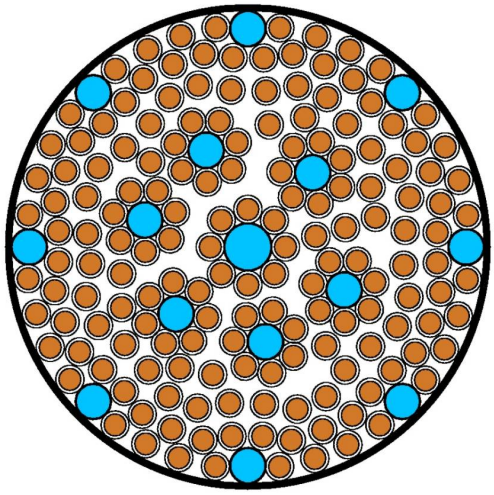

Figure 8.4: Cross–section of the conductor used for magnet coils in the MINOS detector. The larger diameter circles represent the copper cooling channels. The smaller circles are the copper conductor core. The outer circumference is a copper jacket directly cooled by eight cooling tubes (image source: [NK99]).

The conductor in general consists of two parts: an outer jacket and the coil. Each coil is fabricated from stranded copper wires and is housed inside the water–cooled copper jacket. The outer jacket is cooled by water flowing through eight copper tubes. Seven additional tubes provide cooling near the centre of the coil. By dividing the conductor into an outer jacket and the inner coil, the fabrication and installation could be simplified. This type of conductor shows very good thermal properties, which were evaluated by first conducting ANSYS FEA[5] calculations and then verifying the results obtained with an experimental setup [Tan98].

However, although this design provides the necessary current in a small

[3]**M**ain **I**njector **N**eutrino **O**scillation **S**earch, a particle physics experiment which is installed at Fermilab.

[4]Fermi National Accelerator Laboratory, a national laboratory of the US Department of Energy specializing in high–energy particle physics.

[5]Software used for Finite Element Analysis (FEA).

package and uses fault–prone copper tubes for the cooling channels, it is a very rigid construction. In fact, flexibility was not an issue for the layout as the detector structure provided smooth bores through which the magnet coils could be inserted [NK99].

In terms of flexibility, the layout with a flexible copper core surrounded by a rubber hose as it is currently used for the water–cooled cables must be considered as state of the art. Manufacturing a conductor core with sufficient flexibility would be relatively easy by splitting the required cross–section into multiple wires. This, however, is much more difficult to achieve for the required cooling channels. As a certain cross–section is necessary to guarantee sufficient water flow and the wall–thickness of the channels cannot be reduced arbitrarily, their flexibility is limited. This effect is increased if multiple cooling channels are required to achieve a suitable heat conductance. The overall flexibility of the conductor is then determined by the flexibility of the cooling channels.

In the water–cooled cables, this problem is addressed by choosing rubber as the material for the cooling channel, as it can provide the necessary flexibility. Furthermore, in this design the cooling medium flows around the individual wires of the conductor, thus providing the maximum surface possible for heat conduction. These advantages are gained by accepting the restrictions of the rubber material in terms of ageing resistance [And97].

8.5 Conclusion

The selection of a suitable conductor layout is determined by factors that are difficult to combine. Material composition, cross–section and cooling capacity must be adequate to guarantee a demanded current–carrying capability. The method of providing the cooling capacity at the same time determines the resulting flexibility of the conductor. cooling channels made from solid tubing ensure a high operation reliability, but also limit the resulting possible flexibility of the conductor.

However, if flexibility is a major concern – like it is for the conductors needed in the LHC – using a rubber material to form the cooling channel in order to gain the required flexibility seems to be ineluctable. This, at the same time, entails the circumstance that the conductor will be subject to

a certain amount of ageing over time. This fact may not be of exceptional importance in general industrial applications, as access to the conductor will probably not be as restricted as it is in the LHC. In consequence, the effort to monitor the state of the conductor and to replace it if necessary will be much lower.

For the application in the LHC, however, the aspects of reliability as well as flexibility are crucial for the conductor layout. Consequentially, the selection of the hose material becomes a key aspect in meeting these requirements. Saturated rubbers like EPDM have already been considered for future use. They show a high resistance to the ageing factors described in Section 2.4 and therefore seem to be a reasonable material choice.

Chapter 9

Radiation resistance testing

The previous Chapter showed that currently there are no direct alternatives for the water–cooled cables which are used at the moment. Hence, choosing the right rubber material for the hose is crucial.

Radiation is the main factor to change within the following years. Until now, the LHC has been operated with up to 3.5 TeV, but in the following years, beam energy will be increased to the projected level of 7 TeV. Thus, the radiation level in the LHC tunnel will rise as well.

For this reason, eleven different hose materials made from EPDM rubber were tested for their radiation resistance in summer 2010. Material was provided from three different suppliers, in the following referred to as S1, S2[1] and S3. A detailed description of the sample preparation, the test cycle and an analysis of the test results was published at CERN in [WY10] and will in extracts be presented in this Chapter.

9.1 Sample preparation

The relative elongation ϵ/ϵ_0 is used as the end–point criterion for the validation of the hoses. In accordance with [IS 23] and [IEC 1244–2], for an absorbed dose of 20 kGy, ϵ/ϵ_0 must not be less than 0.5, which is equal to a 50 % loss of elasticity. The test pieces were irradiated to five different dose levels: 22 kGy, 100 kGy, 250 kGy, 300 kGy and 330 kGy. The top dose levels were set based on the estimation of the maximum doses that the

[1] Hoses with reinforcement fibres made from Nylon and Rayon were supplied by S2. Accordingly, the samples are referred to as S2–N and S2–R.

water–cooled cables could receive during their life cycle in the LHC. From each hose type, three samples were tested, resulting in a total number of 198 test specimens[2]. The samples were labelled according to the following pattern: *WCC–Supplier–Hose diameter (mm)–Dose (kGy)*. For example, a sample labelled *WCC–S1–90* refers to a hose with a diameter of 90 mm supplied by S1.

The test samples were irradiated in two different facilities: CEA–Saclay[3] and IONISOS Dagneux[4]. Both facilities use gamma rays for irradiation and a ^{60}Co source for radiation. In CEA–Saclay all test samples are placed in the irradiation vault at the same time and the distance from the radiation source determines the total dose. At IONISOS, a conveyor carries the samples and passes the radiation source on regular intervals. In this case, it is the number of passes that determines the total dose to the samples. The received total dose was verified by dosimeters placed close to each set of specimens [Rou10].

9.2 Material testing

The mechanical properties of the materials were then determined by conducting a tensile test according to [ISO 37], where tensile strength σ and elongation at maximum force ϵ are determined.. The test specimen is mounted between the jaws of the test machine (see Figure 9.1). The machine then pulls the jaws apart at a speed of 50 mm/min until the test piece breaks. Simultaneously, the machine measures the force applied to the test piece and the elongation length on the narrow part of the test piece.

The tensile strength σ is determined at the point where the highest amount of stress F_{max} can be applied to the sample (see Figure 9.1(b)). The tensile strength is then calculated by

$$\sigma = \frac{F_{max}}{B \cdot D} \tag{9.1}$$

with B being the width and D being the thickness of the sample. Accor-

[2]Eleven materials irradiated to five dose levels plus reference sample, three samples each results in $11 \cdot (5+1) \cdot 3 = 198$ samples.

[3]Research facility of the **C**ommissariat à l'**é**nergie **a**tomique (French Atomic Energy Commission), Saclay, France.

[4]Laboratory specialized in the treatment by ionizing radiation, Dagneux, France.

dingly, this is the point at which the value for the maximum elongation ϵ is recorded. The elongation is defined as the ratio between the final length l and the initial length L, so

$$\epsilon = \frac{(l - L)}{L}. \tag{9.2}$$

Of course, with the beginning of the break the specimen will still elongate (see Figure 9.1(c)) before actually breaking into two parts. But having already lost its integrity, this further elongation is not significant for the evaluation of the sample.

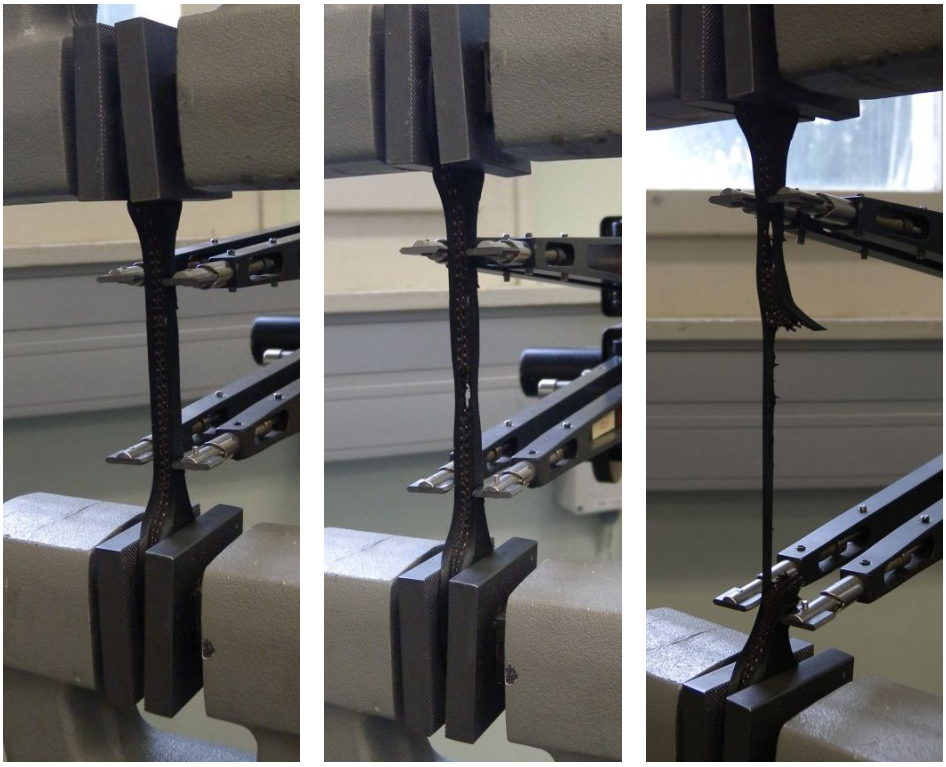

(a) (b) (c)

Figure 9.1: Tensile test of water–cooled cable hose: Elastic deformation (a), peak level of tensile force has been achieved and sample starts to break (b), end of the tensile test (c).

9.3 Discussion of results

The raw data of the tensile test results is available in [Ger10]. Following graphs visualize the impact of the radiation on the samples.

As the tested hose consists of rubber material in which layers of fibres are embedded for reinforcement, it is this reinforcement layer that primarily determines the stability of the hose. However, as the sample pieces have not been cut in parallel to the fibre orientation, the reinforcement fibres must be considered to have little or no influence on the tensile strength and elongation value. Thus, the values determined represent the material properties of the rubber material itself. In Figure 9.2, the y–axis of each data point represents the maximum tensile strength of the sample. The corresponding total dose with which the sample was irradiated is then plotted on the x–axis of the graph. The radiation dose of 0 kGy represents the non–irradiated reference sample.

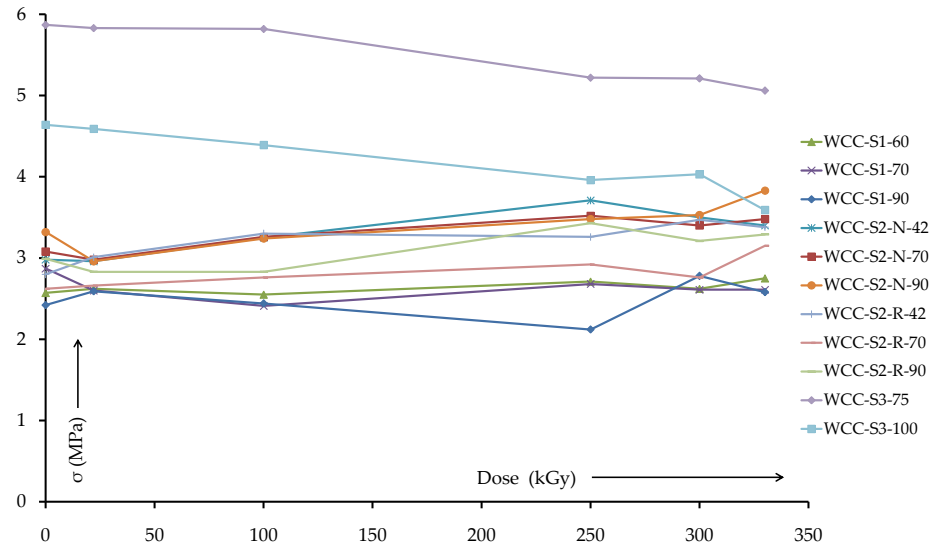

Figure 9.2: Tensile strength of hose samples.

It is noticeable that the S3 samples, especially at low dose rates, show a much higher tensile strength than the specimens of S1 and S2. One possible explanation for that might be the rather homogenous distribution of the reinforcement fibres in the hose material. In the other samples, the reinforcement structure is connected to the surrounding rubber by an

adhesive layer (S1) or is rather concentrated in the middle of the sample (S2). A general trend concerning the influence of the radiation on the tensile strength of the samples could not be detected. All S2 samples as well as S1–60 and S1–90 show a slight increase of tensile strength at higher radiation doses. Further cross–linking of the material might be an explanation for this behaviour. In contrast to that, the tensile strength of the S3 samples tends to decrease as the radiation dose increases. The sample S1–70 shows the same behaviour. However, with almost every test series showing upper and/or lower outliers, it is difficult to derive a universally valid tendency from this data.

Regarding the change in elongation values, however, a clear relation between radiation dose and flexibility of the hose sample is noticable (see Figure 9.3). In general, with an increasing irradiation dose, all samples show a more or less distinctive degradation of elasticity compared to the non–irradiated references. Also, three "bunches" of curves are noticeable that clearly can be assigned to the samples of the three manufacturers.

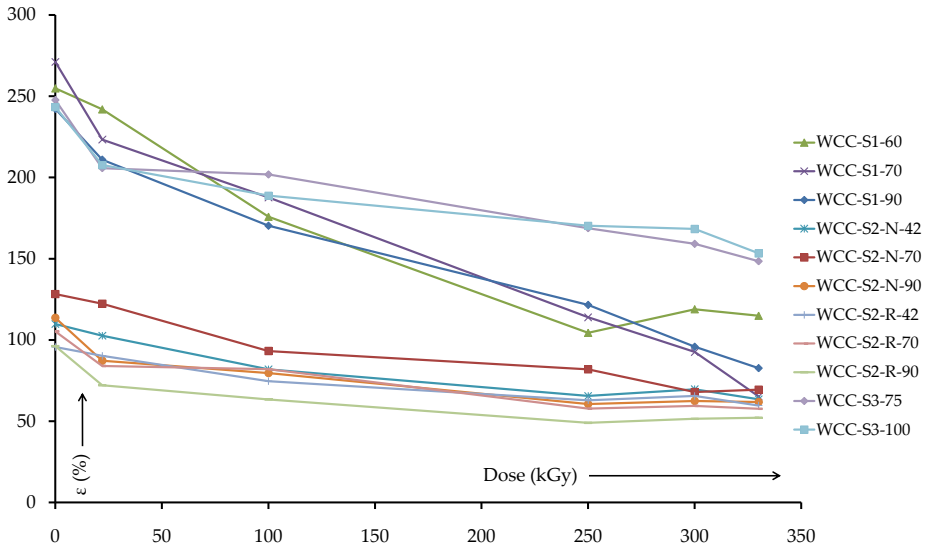

Figure 9.3: Elongation of hose samples at F_{max}. With radiation dose rising, the rubber embrittles and elasticity is decreased. The three "bunches" of curves clearly can be assigned to the three manufacturers.

The S1 and S3 samples show a higher overall elasticity than the samples supplied by S2, with the elongation of the reference specimen being about twice as large as that of S2. The impact of the radiation on the S2 samples

(indicated by the slope of the graph) is comparable to the samples supplied by S3. The highest effect of the radiation can be observed on the S1 samples.

To further illustrate this change of material properties, the relative elongation ϵ/ϵ_0 is presented in Figure 9.4. In this Graph, the end–point criterion of 0.5 is marked with a dotted line.

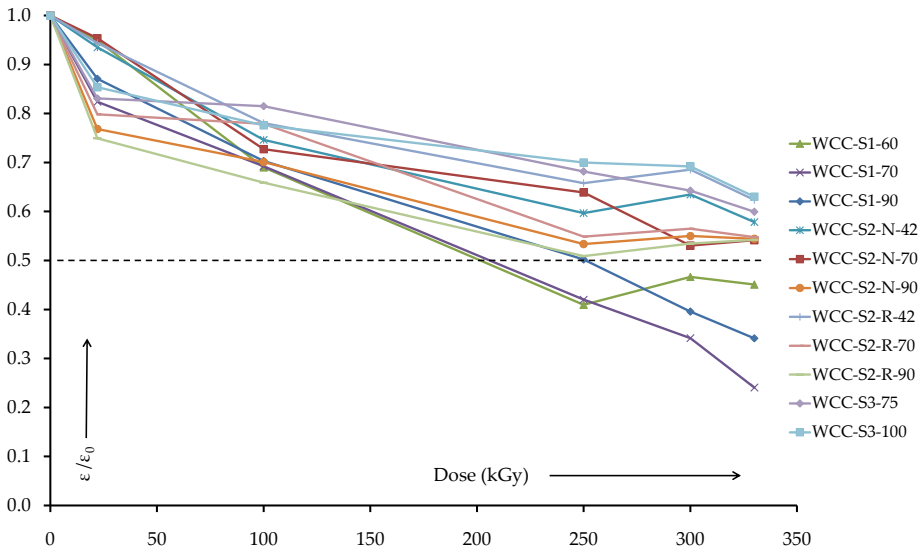

Figure 9.4: Relative elongation ϵ/ϵ_0 at F_{max}.

During this test series, all of the tested samples met the demands, as the end–point criterion is not reached at a dose of 20 kGy. Nevertheless, the influence of radiation on the flexibility of the material is obvious. The highest influence can be noted on the samples supplied by S1 which reach the end–point criterion at a total dose of 250 kGy. At the same dose, the relative elongation of the S2 and S3, as well as the S1–60 samples, seems to saturate. This might indicate the dose level at which the highest deterioration of the material has been reached. However, the possibility that much higher doses might lead to a further degradation of the material cannot be excluded.

9.4 Conclusion

A series of tests to determine the radiation resistance by evaluating tensile stress–strain properties has been conducted on eleven types of rubber hose

samples. The specimens have been irradiated with different doses from 22 kGy to 330 kGy. Compared to a non–irradiated sample, those tests show a clear influence of the radiation on the material properties. Regarding the change in tensile stress properties, a general distinctive tendency is not noticeable. Only the hose samples of S3 show a constant degradation in tensile strength with rising radiation dose, whereas for all other samples a slight increase in tensile strength is noticeable.

Regarding the change of elongation properties, however, the tendency for all test samples seems to be clear. Apparently, with higher radiation doses the hose material becomes stiffer and more brittle. This leads to a decrease in elasticity of the rubber hose test sample. This tendency is consistent with the tests already conducted in the past, where the tests show an even higher decrease in elasticity [ST89], [Ger98]. This effect is strongest on the samples supplied by S1; the effect on the S2 and S3 samples is about the same. Among the samples supplied by S2, a distinctive difference between the R–type and the N–type could not be recognized.

As for the different suppliers, all test samples were able to meet the requirement defined in [CER03]. However, for higher doses the S1 samples cannot meet this demand. The endpoint criterion is reached at a total dose of 250 kGy. The S2 and S3 samples stay within the threshold, with S3 showing the highest overall elasticity as well as the lowest change in elasticity at the maximum irradiation dose.

Appendices

Bibliography

[And97] George J. Anders. *Rating of electric power cables: ampacity computations for transmission, distribution and industrial applicatons*, pages 5, 11, 13. IEEE Press power engineering series. McGraw–Hill, New York, 1997.

[Ann02] Leena Annila. *LHC demineralised water circuit*. Engineering specification, CERN, Geneva, July 2002. EDMS doc. No. 335008.

[B+04a] Oliver Sim Brüning et al. *LHC Design Report*, volume I – The LHC Main Ring, chapter 10: Power Converter System. CERN, Geneva, June 2004.

[B+04b] Oliver Sim Brüning et al. *LHC Design Report*, volume II – The LHC Infrastructure and General Services, chapter 8: Cooling and Ventilation. CERN, Geneva, November 2004.

[Cal11] Vin Callcut. *High Copper Alloys – High Strength Coppers for Demanding Electrical Applications*. Available: `http://www.copper.org/publications/newsletters/innovations/2006/09/high_cu_alloys.html#electr` Accessed: February 5, 2011.

[CCO98] William J. Cooper, Randy D. Curry, and Kevin E. O'Shea, editors. *Environmental Applications of Ionizing Radiation*, pages 2–3. John Wiley & Sons, New York, 1st edition, November 1998.

[CER03] CERN. *Supply and installation of water–cooled tubes and cables*, 2003. EDMS doc. No. 387065.

[CER11] CERN. *CERN history highlights*. Available: `http://public.web.cern.ch/public/en/about/About-en.html` Accessed: January 5, 2011.

[D+00] K. Dahlerup–Petersen et al. *Energy extraction resistors for the main dipole and quadrupole circuits of the LHC*. Proceedings of EPAC 2000, Vienna, Austria, 2000.

[DIN 7716] DIN 7716. *Erzeugnisse aus Kautschuk und Gummi – Anforderungen an die Lagerung, Reinigung und Wartung*, 1982.

[DST91] H. Danielsson, H. Schönbacher, and M. Tavlet. *Estimate of lifetime of cables in the radiation environment of LEP200*. Technical report, CERN, Geneva, September 1991.

[DW01] Sadhan K. De and Jim R. White, editors. *Rubber technologist's handbook*, pages 1–4, 11–86. Rapra Technology, Shrewsbury, 1st edition, 2001.

[Eva09] Lyndon Evans. *The Large Hadron Collider: a Marvel of Technology*, pages 8–15. CRC Press, Boca Raton, 2009.

[F+05] Alfredo Ferrari et al. *FLUKA: a multi–particle transport code*. Technical report, CERN, Geneva, October 2005.

[FS01a] Claire A. Fynbo and Graham R. Stevenson. *Compendium of annual doses in the LHC arcs*. LHC Project Note 251, CERN, Geneva, April 2001.

[FS01b] Claire A. Fynbo and Graham R. Stevenson. *Estimation of extra dose contribution in the LHC arcs arising from proton losses far downstream of the high luminosity interaction points IP1 & IP5*. LHC Project Note 295, CERN, Geneva, May 2001.

[FS01c] Claire A. Fynbo and Graham R. Stevenson. *Radiation environment in the main ring of the LHC*. LHC Project Seminar, CERN, Geneva, Novenber 2001.

[FS02] Claire A. Fynbo and Graham R. Stevenson. *Radiation Environment in the Dispersion Suppressor regions of IR1 and IR5 of the LHC*. LHC Project Note 296, CERN, Geneva, May 2002.

[Ger98] Alexandre Gerardin. *Mechanical characterisation of cable sheath (4)*. Technical report, CERN, Geneva, 1998. EDMS doc. No. 964199.

[Ger10] Alexandre Gerardin. *Tensile tests of water cooled cable sheath*. Report – Quality Test, CERN, Geneva, April 2010. EDMS doc. No. 1070954.

[Gug04] Paolo Guglielmini. *Water–cooled electrical cables – check of the fluid–dynamic constraints*. Technical report, CERN, Geneva, June 2004. EDMS doc. No. 475222.

[HF09] May Le Huy and Benjamin Ferchaud. *Analyse de 3 réferénces de gaines en caoutchouc*. Technical report, LRCCP, Vitry–sur–Seine, January 2009.

[HRW07] David Halliday, Robert Resnick, and Jearl Walker. *Physik: Bachelor–Edition*, page 567. WILEY–VCH, Weinheim, 2007.

[HT08] May Le Huy and Orianne Triquenaux. *Analyse complementaire de trois gaines*. Technical report, LRCCP, Vitry–sur–Seine, September 2008.

[HTD08] May Le Huy, Orianne Triquenaux, and Etiennise Dupé. *Analyse de gaines fissurees de cables refroidis*. Technical report, LRCCP, Vitry–sur–Seine, July 2008.

[HW01] A.F. Holleman and Nils Wiberg. *Inorganic Chemistry*, pages 402–412. Academic Press, San Diego, 2001.

[IEC 1244–2] IEC 1244–2. *Determination of long–term radiation ageing in polymers – Part 2: Procedures for predicting ageing at low dose rates*, 1996.

[IEC 60695–7–50] IEC 60695–7–50. *Fire hazard testing – Part 7–50: Toxicity of fire effluent – Estimation of toxic potency – Apparatus and test method*, 2002.

[IEC 60695–7–51] IEC 60695–7–51. *Fire hazard testing – Part 7–51: Toxicity of fire effluent – Estimation of toxic potency – Calculation and interpretation of test results*, 2002.

[IEC 61034–1] IEC 61034–1. *Measurement of smoke density of cables burning under defined conditions – Part 1: Test apparatus*, 1997.

[IEC 61034–2] IEC 61034–2. *Measurement of smoke density of cables burning under defined conditions – Part 2: Test procedure and requirements*, 1997.

[IS 23] IS 23. *Criteria and Standard Test Methods for the Selection of Electric Cables and Wires with Respect to Fire Safety and Radiation Resistance*, 3rd edition, CERN, Geneva, 2005. EDMS doc. No. 335745.

[IS09a] Sorin Ilie and Radu Setnescu. *Polymeric Materials Review on Oxidation, Stabilization and Evaluation using CL and DSC Methods*. Technical Note, CERN, Geneva, August 2009.

[IS09b] Sorin Ilie and Radu Setnescu. *Radiation Induced Aging Effects in Polymeric Cable Insulators at CERN*. Technical report, CERN, Geneva, 2009. EDMS doc. No. 1055599.

[ISO 1402] ISO 1402. *Rubber and plastics hoses and hose assemblies – Hydrostatic testing*, 2009.

[ISO 1629] ISO 1629. *Rubber and latices – Nomenclature*, 1995.

[ISO 37] ISO 37. *Rubber, vulcanized or thermoplastic – Determination of tensile stress-strain properties*, 2005.

[ISO 471] ISO 471. *Rubber – Standard temperatures, humidities and times for conditioning and testing of test pieces*, 1983.

[ISO 6803] ISO 6803. *Rubber or plastics hoses and hose assemblies – Hydraulic pressure impulse test without flexing*, 1983.

[Iva01] V.S. Ivanov, editor. *Radiation Chemistry of Polymers*, pages 201–212. VSP, Utrecht, 1st edition, 2001.

[KNK01] Friedrich Kießling, Peter Nefzger, and Ulf Kaintzyk. *Freileitungen: Planung, Berechnung, Ausführung; [nach EN 50341]*, page 75. Springer, Berlin, 5th edition, 2001.

[Li09] Zheng Li. *Radiation damage effects in Si materials and detectors and rad–hard Si detectors for SLHC*. *Journal of Instrumentation*, March 2009.

[Mar03] Christophe Martel. *Air handling of the LHC tunnel and its underground areas*. Engineering specification, CERN, Geneva, October 2003. EDMS doc. No. 344211.

[MP03] McGraw–Hill and Sybil P. Parker. *McGraw–Hill dictionary of scientific and technical terms*. McGraw–Hill, New York, 6th edition, 2003.

[Nag04] Khairi Nagdi. *Gummi–Werkstoffe: Ein Ratgeber für Anwender*, pages 41, 45–47, 119–125, 182. Gupta, Ratingen, 3rd edition, 2004.

[NK99] J.K. Nelson and J. Kilmer. *MINOS Far–Detector Coil Design*. Technical report, FERMILAB, Batavia, August 1999.

[PRW70] S. Pichler, S. Richter, and M. Wilck. *Water–cooled cables as interconnecting element for magnets*. To be presented at the third International Conference on Magnet Technology, Hamburg, CERN, Geneva, March 1970.

[Rib08] Enrico Riboni. *Ozone Concentration Measurements in the LHC Tunnel*. Technical report, ozone.ch, Bourdry, June 2008.

[Rou10] Sophie Rouif. *Irradiation exposure trials*. Quotation, IONISOS, Dagneux, April 2010.

[Sou92] Anne H Soukhanov, editor. *The American heritage dictionary of the English language*. Houghton Mifflin, Boston, 3rd. edition, 1992.

[ST89] H. Schönbacher and M. Tavlet. *Compilation of radiation damage test data*, page 7. CERN, Geneva, 2nd edition, December 1989.

[ST02] H. Schönbacher and M. Tavlet. *Absorbed doses and radiation damage during the 11 years of LEP operation*. Technical report, CERN, Geneva, December 2002. EDMS doc. No. 350794.

[Ste98] Jeanne Mager Stellman. *Encyclopaedia of occupational health and safety*. Internat. Labour Office, Geneva, 4th edition, 1998.

[Tan98] Z. Tang. *Thermal analysis of the MINOS far detector coil*. Technical report, FERMILAB, Batavia, September 1998.

[TE98] Fariborz Taghipour and Greg J. Evans. *Radiolytic degradation of chloroorganics and AOX in bleached pulp–mill effluents*, pages 477–494. In Cooper et al. [CCO98], 1st edition, November 1998.

[Tre75] Leslie R. G. Treloar. *The physics of rubber elasticity*. Monographs on the physics and chemistry of materials. Clarendon Press, Oxford, third edition, 1975.

[Tro04] Jürgen Troitzsch, editor. *Plastics flammability handbook: principles, regulations, testing and approval*, pages 521–530. Hanser, München, third edition, 2004.

[Wat02] Susan Watt. *The Elements: Chlorine*, pages 10–11. Benchmark Books, New York, 2002.

[Wil08] Mats Wilhelmsson. *Hoses for water–cooled cables with Halogen content*. Minutes of the meeting, CERN, Geneva, July 2008.

[Wol10a] Alexander Wollmann. *Combined radiation and pressure test for water–cooled cable hoses*. Technical report, CERN, Geneva, 2010.

[Wol10b] Alexander Wollmann. *Monitoring of the LHC water–cooled cables in Point 6 / July 2010*. Technical report, CERN, Geneva, September 2010.

[Wri01] David Wright. *Failure of plastics and rubber products: causes, effects and case studies involving degradation*, pages 25–48, 129–149. RAPRA Technology, Shrewsbury, 1st edition, 2001.

[WY10] Alexander Wollmann and Vesa Ylamaki. *Irradiation tests for new water–cooled cable hose types*. Technical report, CERN, Geneva, 2010.

[Wyd08a] Wolfgang Wydra. *Burst pressure test after ozone exposure at different concentrations and time*. Technical report, ContiTech Schlauch GmbH, Korbach, June 2008.

[Wyd08b] Wolfgang Wydra. *Ozonetest on hose types CERN Kabelschutzschlauch*. Technical report, ContiTech Schlauch GmbH, Korbach, April 2008.

[Wyd09] Wolfgang Wydra. *Cooling hoses for CERN*. Fluid Technology presentation, ContiTech Schlauch GmbH, Korbach, March 2009.

[Yla10a] Vesa Ylamaki. *Instructions for monitoring water–cooled cables*. Technical report, CERN, Geneva, April 2010. EDMS doc. No. 1054451.

[Yla10b] Vesa Ylamaki. *Monitoring of the LHC water–cooled cables*. Technical report, CERN, Geneva, March 2010. EDMS doc. No. 1054449.

[ZG05] Markus Zerlauth and Jean-Claude Guillaume. *Choice of length and cross section of water cooled cables and tubes for the electrical circuits of the LHC*. Engineering specification, CERN, Geneva, April 2005. EDMS doc. No. 571043.

Index

AEM, 8
Air handling system, 22
Antidegradants, 5
Antioxidant, 10
Antiozonant, 10
Antirad, 11

Chain scission, 9, 11
Conditions in the LHC, 22–26
    Ionizing radiation, 25–26
    Ozone, 23–24
    Temperature / humidity, 22–23
Conductor alternatives, 77–86
    Conclusion, 85–86
    Conductor layouts, 82–85
    Conductor materials, 80–82
    Considerations, 78–80
    Motivation, 77–78
Contact media, 9
Cooling tower, 28
Cooling water system, 27–28
Crack
    Area, 36
    Depth, 40
    Frequency, 40
    Width, 40
Current lead, 15

Damage, 29–34
    Introduction, 29
    Presence of halogens, 29–32
    Surface cracks, 32–34
Dew point, 23
DFB, 15
Dipole magnet, 14, 15
Dose rate, 11
Dry Bulb Temperature, 23
Dump resistor, 17, 18

EPDM, 8
EPM, 8

Fire hazard testing, 19

Heat exchangers, 27

IACS, 17
Ionizing radiation, 25–26
    Influence on rubber, 11
IR, 8

LEIR, 3
LEP, 3
LHC, 3
    Tunnel, 19
LINAC, 2
Lug, 13

Methodology, 49–60
    Camera angle, 50–52
    Conclusion, 54–55
    Perspective distortion, 52–54

Restrictions, 49–55
Monitoring, 35–48
Methodology , 44
Point 6 , 44–48

NBR, 8
NR, 8

Oxidation, 9
Oxygen, 9
Ozone, 23
Influence on rubber, 10

Particle accelerator, 2
Pressure testing, 61–75
Conditions, 63–68
Definition, 71–74
Expression of results, 74–75
Sample preparation, 69–71
Test principle, 61–63
Proton Synchrotron, 3
PSB, 3

Quadrupole magnet, 14, 15
Quench, 17

Radiation, *see* Ionizing radiation
Rubber, 5–12
Ageing, 9–12
Definition, 6–7
History, 5–6
Storage, 12
Types, 7–9

SBR, 8
Smoke density, 20
SPS, 3
Sulphur, 6, 19
Synchrotron, 3

Vulcanization, 5, 6

Water–cooled cables
Application, 15–17
Definition, 13–14
Introduction, 15
Qualification tests, 19–22
Technical requirements, 17–18
Waxes, 10

Glossary

AC **A**lternating **C**urrent.

AEM Ethylene–Methyl Acrylate Rubber.

ANSYS Software used for Finite Element Analysis (FEA).

Antihydrogen The antimatter equivalent of hydrogen.

Antioxidant A chemical compound or substance which can be added to rubber that inhibits oxidation.

Antiozonant A protective agent which can be added to rubber to diminish the deteriorating effects of ozone.

Antirad Additives incorporated into rubber to reduce the degrading effects of radiation.

BR Butadiene Rubber.

CEA **C**ommissariat à l'**E**nergie **A**tomique, French Atomic Energy Commission located in Saclay, France.

CERN **C**onseil **E**uropéen pour la **R**echerche **N**ucléaire, European Organization for Nuclear Research located in Geneva, Switzerland. CERN is one of the world's largest centres for nuclear research.

Chain scission The cleavage of polymer chains.

Commissioning Series of tests and initial trial–runs before putting components into operation.

CorelDRAW Professional graphic software.

Cross–linking The setting up of chemical links between the molecular chains of polymers.

Curing See: vulcanization.

Current lead Element serving as a connector between normal conducting cables and superconducting elements.

DC **D**irect **C**urrent.

Dechlorination Removal of chlorine from a substance.

DED **D**ose to **E**quivalent **D**amage.

Dew Point Temperature The temperature at which moisture begins to condensate out of the air.

DFB Electrical **D**istribution **F**eed **B**ox. The main function of the DFBs is to house the current leads which transfer high currents from room temperature cables to superconducting elements of the LHC.

Dimension tool Tool in CorelDraw (see there) displaying the number of pixels between two measuring points.

Dipole magnet Magnet used for bending the two particle beams in the LHC.

Dry Bulb Temperature The sensible heat level of air that is taken with an ordinary thermometer. It does not take into account the moisture content of the air.

Dump resistor Water–cooled resistor which is part of the energy extraction system. It is used to rapidly discharge the superconducting magnet coils, e.g. in case of a quench (see there).

Elastomer Any of various polymers having the elastic properties of natural rubber. With thermoplasts and duromers, elastomers form the third main group of the polymeric materials.

Electronvolt (eV) Unit of energy. 1 eV is the amount of kinetic energy gained by a single unbound electron when it accelerates through an electric potential difference of one volt. 1 eV is equal to $1.6022 \cdot 10^{-19}$ Joule.

End point criterion Criterion to evaluate test results.

Energy extraction system Safety system which is activated if the magnet coils need to be discharged rapidly, e.g. in case of a quench.

EPDM Ethylene–Propylene Diene Rubber.

EPM Ethylene–Propylene Rubber.

Fermilab Fermi National Accelerator Laboratory, a national laboratory of the US Department of Energy specializing in high–energy particle physics.

Free radical An atom or group of atoms that has at least one unpaired electron and is therefore unstable and highly reactive.

GeV See: Electronvolt (eV).

Gray (Gy) SI unit of absorbed radiation dose of ionizing radiation. The dose in gray is the energy deposition per unit mass of material. $1Gy = \frac{1Joule}{kg}$.

IACS **I**nternational **A**nnealed **C**opper **S**tandard, a specified unit of electrical conductivity for metals and alloys relative to a standard annealed copper conductor. An IACS value of 100 % is equal to a conductivity of $\sigma = 58\ \frac{S \cdot m}{mm^2}$ which corresponds to an electric resistance of $0.01724\ \frac{\Omega \cdot mm^2}{m}$.

IONISOS Laboratory specialized in the treatment by ionizing radiation located in Dagneux, France.

Ionizing radiation High–energy radiation capable of producing ionization in substances through which it passes. It includes radiation by gamma rays, x–rays, electron beams, protons, neutrons, alpha particles and other nuclear fragments.

kGy See: Gray.

kW See: Watt.

Leakage current Undesirable flow of current through or over the surface of an insulating material.

LEIR **L**ow **E**nergy **I**on **R**ing. See also: Particle accelerator.

LEP **L**arge **E**lectron–Positron **C**ollider. The tunnel in which LEP was installed is now used for the LHC. See also: Particle accelerator.

LHC **L**arge **H**adron **C**ollider, world's larges particle accelerator installed at CERN, Geneva. See also: Particle accelerator.

LINAC **Lin**ear **Ac**celerator. See also: Particle accelerator.

LRCCP **L**aboratoire de **R**echerches et de **C**ontrôle du **C**aoutchouc et des **P**lastiques, a laboratory specialised in the analysis of rubber materials which is located in Paris, France.

Lug A copper or fitting to which electrical wires can be connected. The lugs used for water–cooled cables ensure both the electrical and water connection.

Macromolecule A very large molecule, such as a polymer, consisting of many smaller structural units linked together.

MeV See: Electronvolt (eV).

MINOS **M**ain **I**njector **N**eutrino **O**scillation **S**earch, a particle physics experiment which is installed at Fermilab (see there).

MW See: Watt.

NBR Nitrile–Butadiene Rubber.

NR Natural Rubber.

Ozone cracks Cracks appearing as a result of ozone and static strain.

Particle accelerator Device that accelerates charged subatomic particles to high energies.

pphm **P**arts **p**er **h**undred **m**illion.

ppm **P**arts **p**er **m**illion.

PS **P**roton **S**ynchrotron. See also: Particle accelerator.

PSB **P**roton **S**ynchrotron **B**ooster. See also: Particle accelerator.

Pulp–mill Facility producing fibre materials, e.g. for later use in paper manufacturing.

Quadrupole magnet Magnet used for focusing and defocusing the two particle beams in the LHC.

Quench Abnormal termination of magnet operation that occurs when part of a superconducting magnet enters the normal conducting state, thus heating up the surrounding regions and pushing them into the normal state as well. This leads to more heating in a chain reaction and is accompanied by a loud noise as the energy in the magnetic field is converted to heat, and rapid boil–off of the cryogenic fluid.

Radiation See: Ionizing radiation.

Radical See: Free radical.

SBR Styrene–Butadiene Rubber.

SPS **S**uper **P**roton **S**ynchrotron. See also: Particle accelerator.

Superconductivity The flow of electric current without resistance in certain metals at temperatures near absolute zero.

Synchrotron A particle accelerator in which charged particles are accelerated around a fixed circular path by an electric field and held to the path by an increasing magnetic field.

TeV See: Electronvolt.

Vulcanization Chemical reaction of sulphur or other vulcanizing agents with rubber to cause cross–linking of the polymer chains.

Watt A SI unit of power; the power required to do work at the rate of 1 J/s, which is equal to the power dissipated in an electric circuit in which a potential difference of 1 volt causes a current of 1 ampere to flow.

Declaration

I certify that the thesis has been written by me. Any help that I have received in my research work and the preparation of the thesis itself has been acknowledged. In addition, I certify that all information sources and literature used are indicated in the thesis.

I also certify that the work in this thesis has not previously been submitted for a degree nor has it been submitted as part of requirements for a degree except as fully acknowledged within the text.

Eidesstattliche Erklärung

Hiermit versichere ich, die vorliegende Arbeit selbstständig und unter ausschließlicher Verwendung der angegebenen Literatur und Hilfsmittel erstellt zu haben.

Die Arbeit wurde bisher in gleicher oder ähnlicher Form keiner anderen Prüfungsbehörde vorgelegt und auch nicht veröffentlicht.

Karlsruhe, 16th February 2011 _____

Signature

Appendix A

Photo monitoring LHC Point 6

A.1 Photographs of crack–areas Point 6L

Figure A.1: 1604860A.32.01.20100721

Figure A.2: 1604860A.32.02.20100721

Figure A.3: 1604860A.32.03.20100721

Figure A.4: 1604860A.32.04.20100831

Figure A.5: 1604860A.32.05.20100721

Figure A.6: 1604860A.32.06.20100831

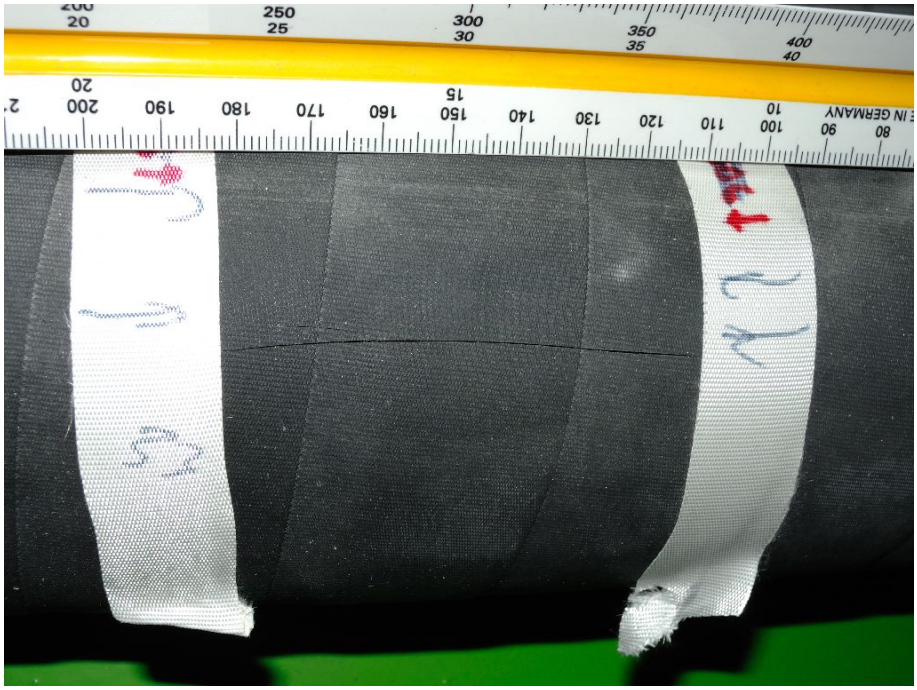

Figure A.7: 1604860A.33.01.20100721

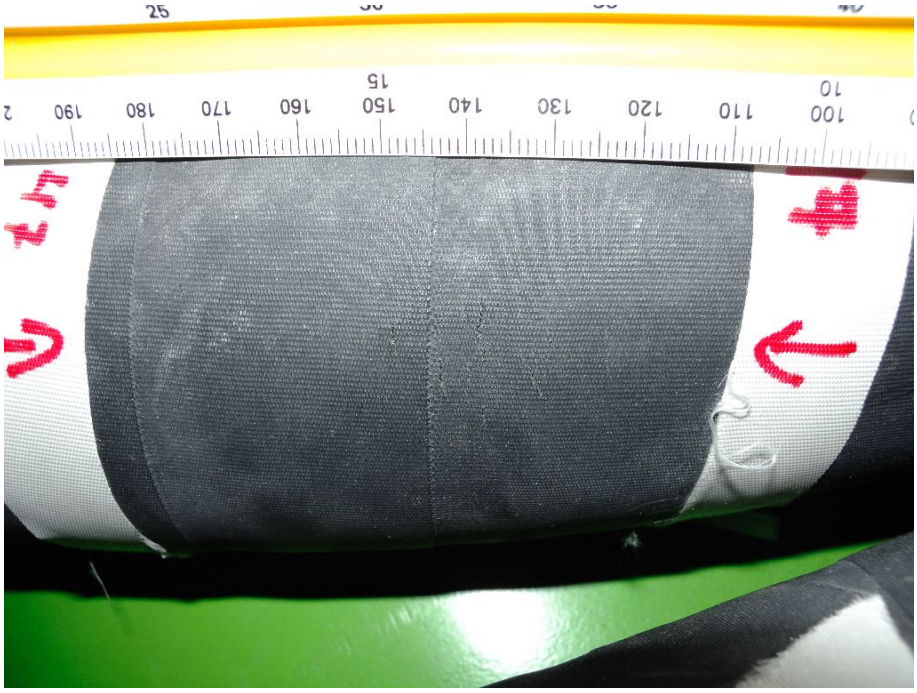

Figure A.8: 1604860A.47.01.20100720

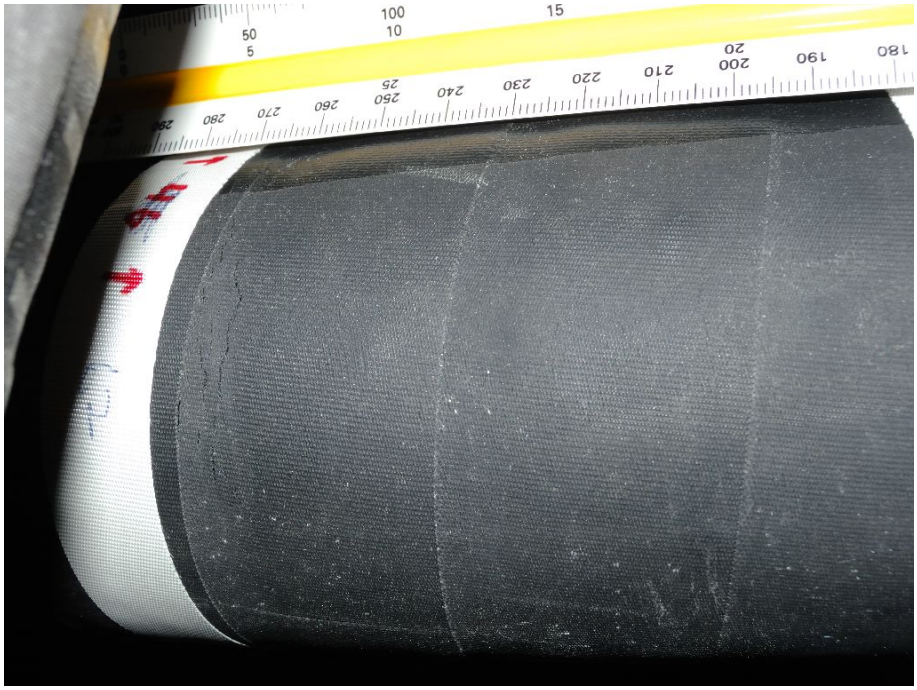

Figure A.9: 1604860A.62.01.20100831

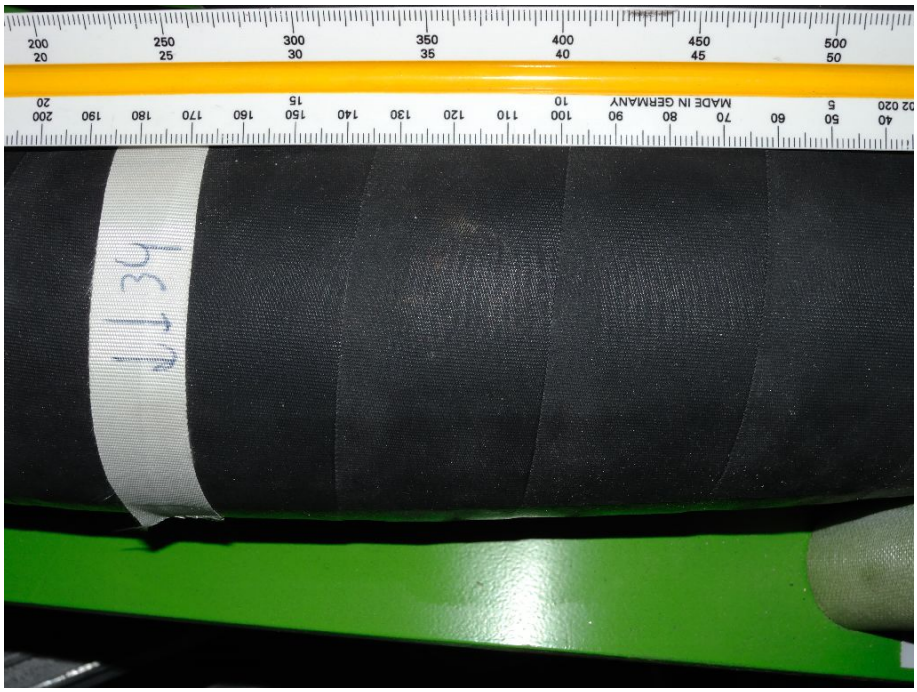

Figure A.10: 1604861A.34.01.20100721

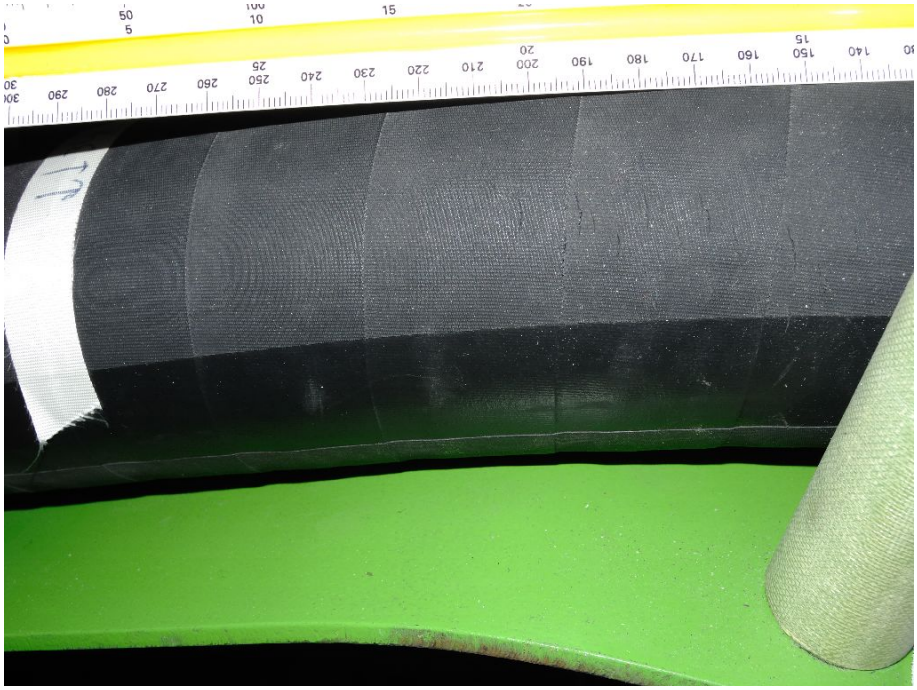

Figure A.11: 1604861A.34.02.20100721

Figure A.12: 1604861A.34.03.20100721

Figure A.13: 1604861A.34.04.20100721

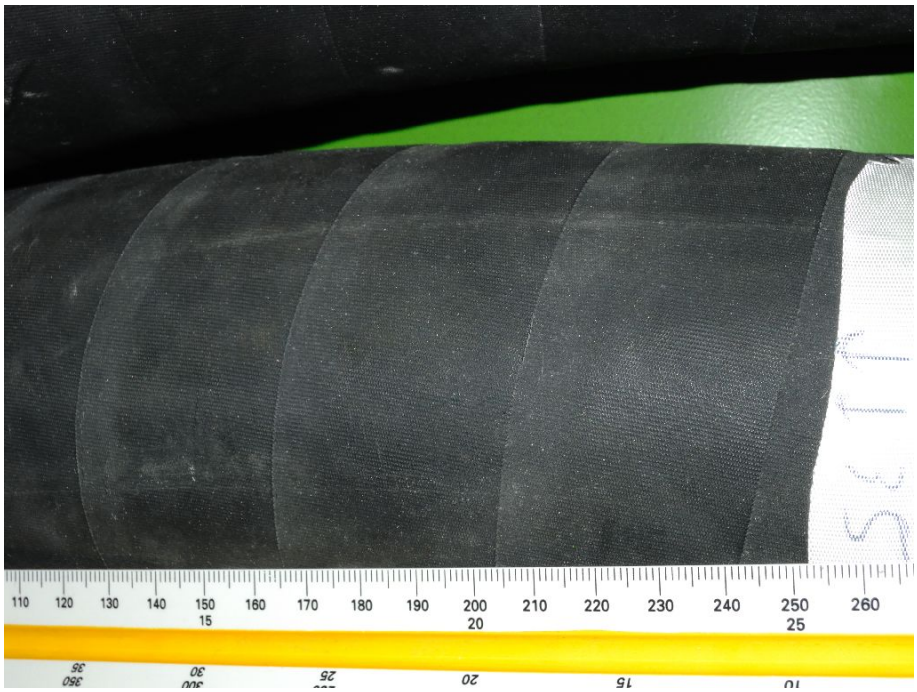

Figure A.14: 1604862A.35.01.20100720

Figure A.15: 1604862A.35.02.20100720

Figure A.16: 1604862A.35.03.20100831

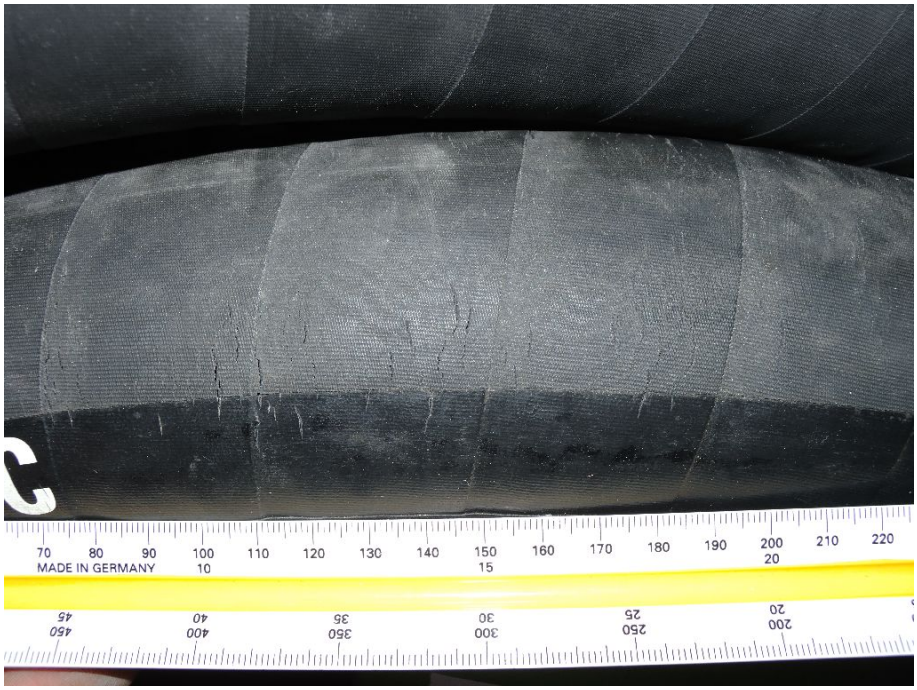

Figure A.17: 1604862A.35.04.20100720

Figure A.18: 1604862A.35.05.20100831

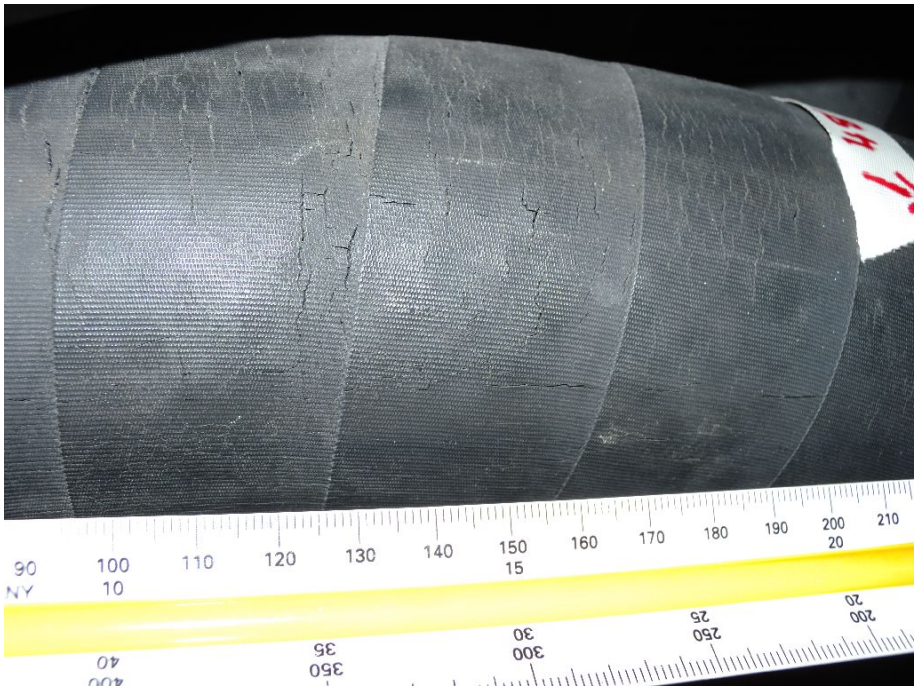

Figure A.19: 1604862A.35.06.20100720

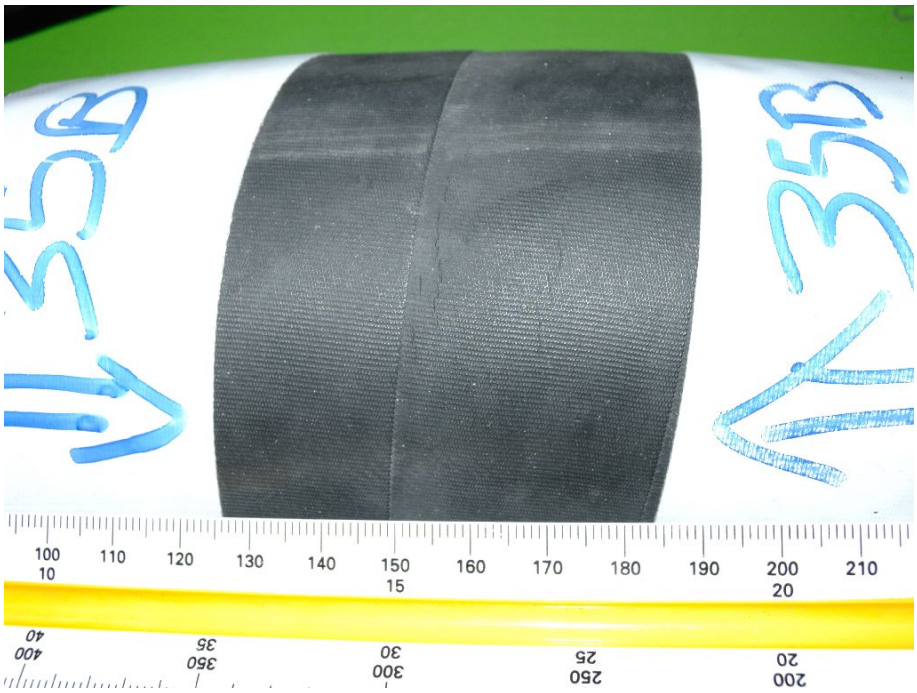

Figure A.20: 1604862A.35.07.20100720

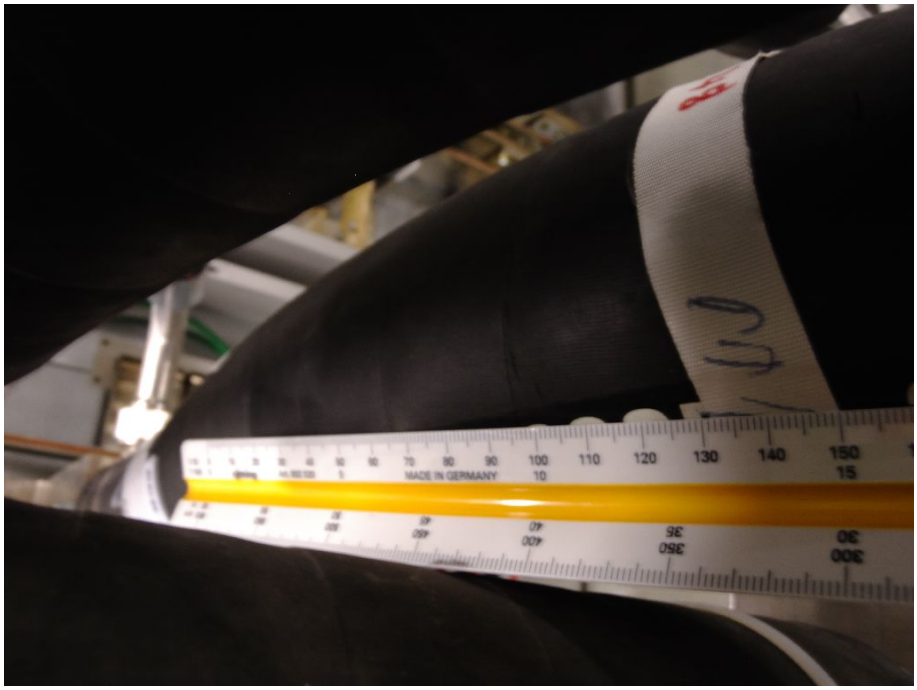

Figure A.21: 1604862A.48.01.20100720

Figure A.22: 1604862A.49.01.20100720

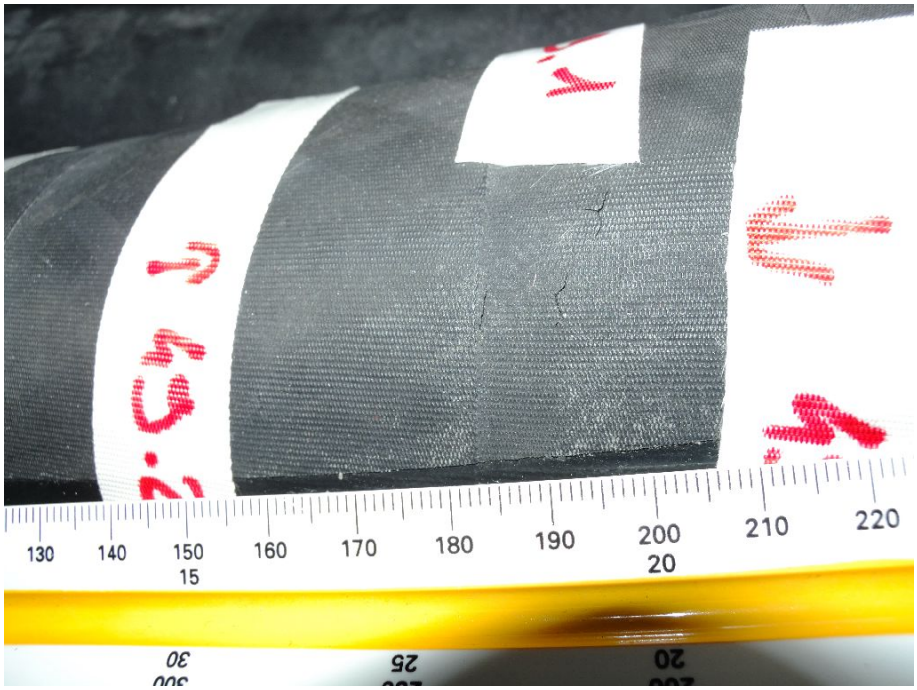

Figure A.23: 1604862A.49.02.20100720

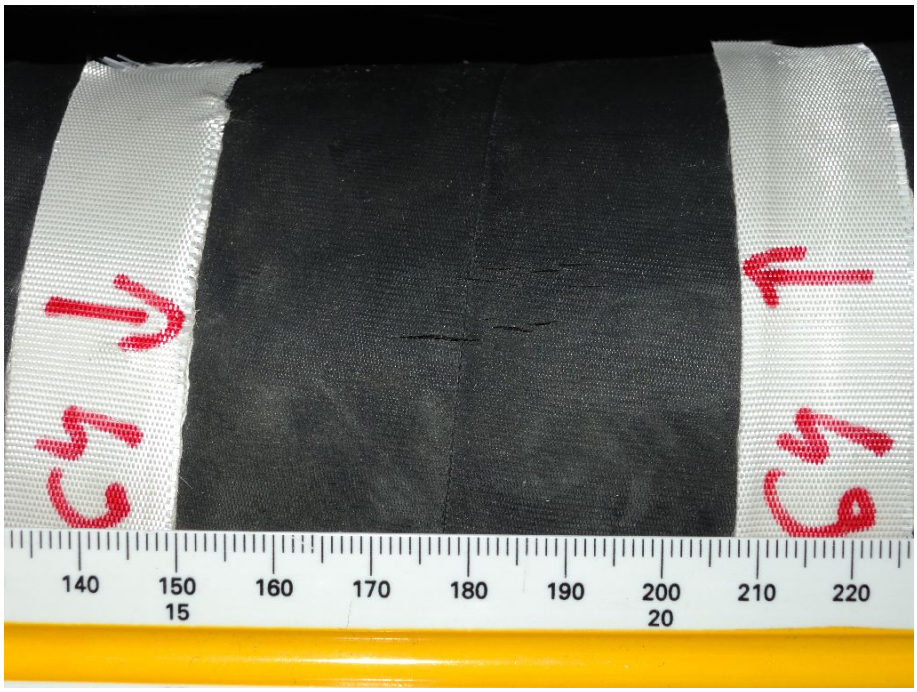

Figure A.24: 1604862A.49.03.20100720

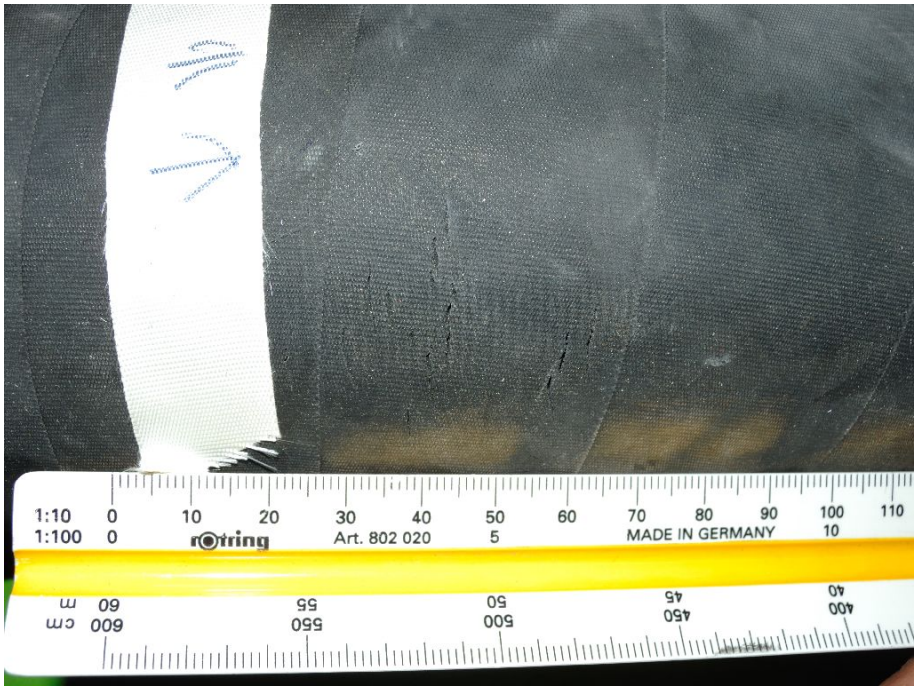

Figure A.25: 1604863A.39.01.20100721

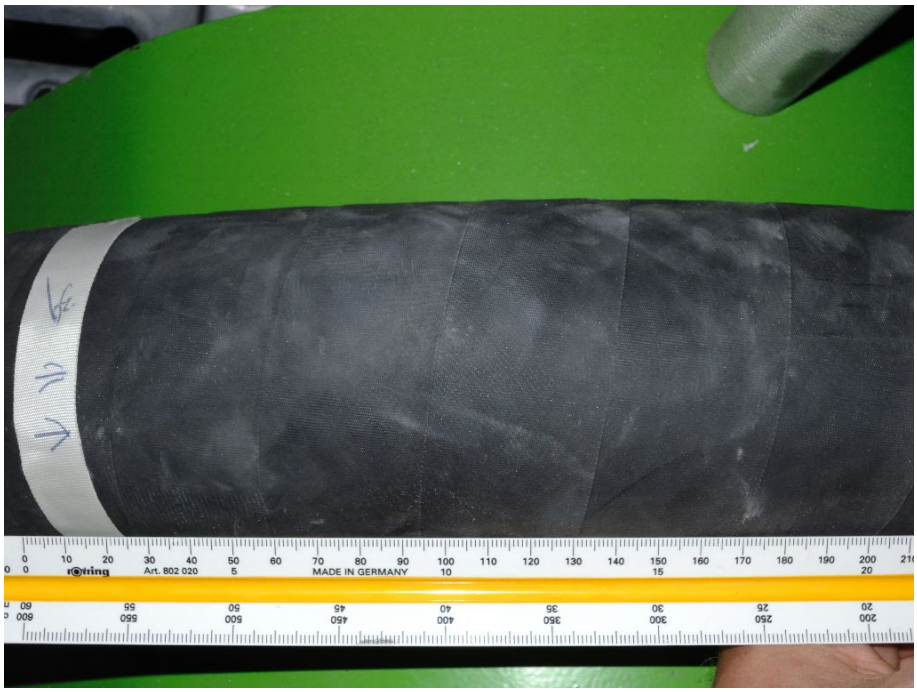

Figure A.26: 1604863A.39.02.20100721

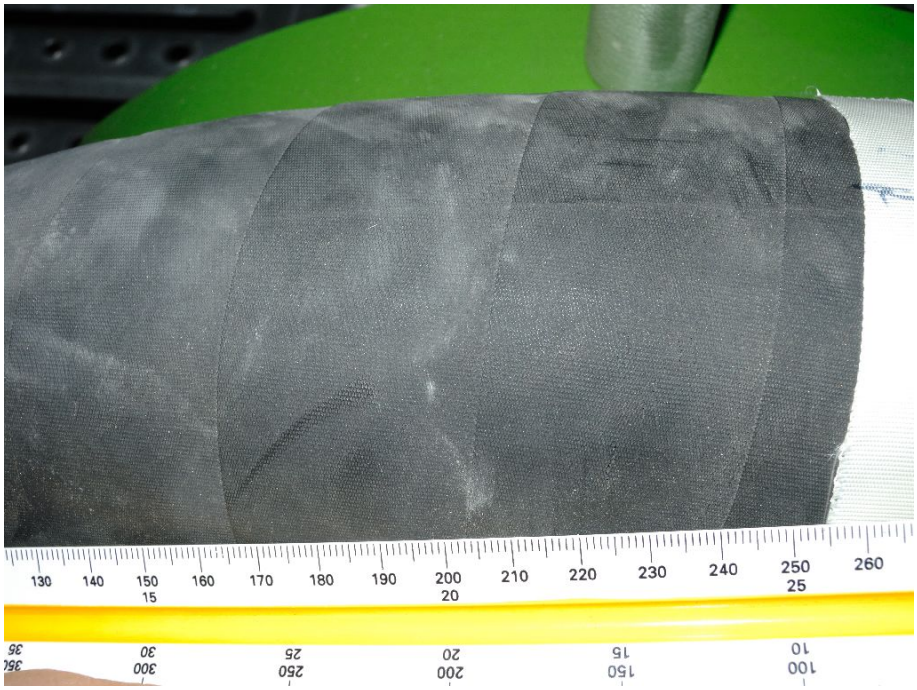

Figure A.27: 1604863A.39.03.20100721

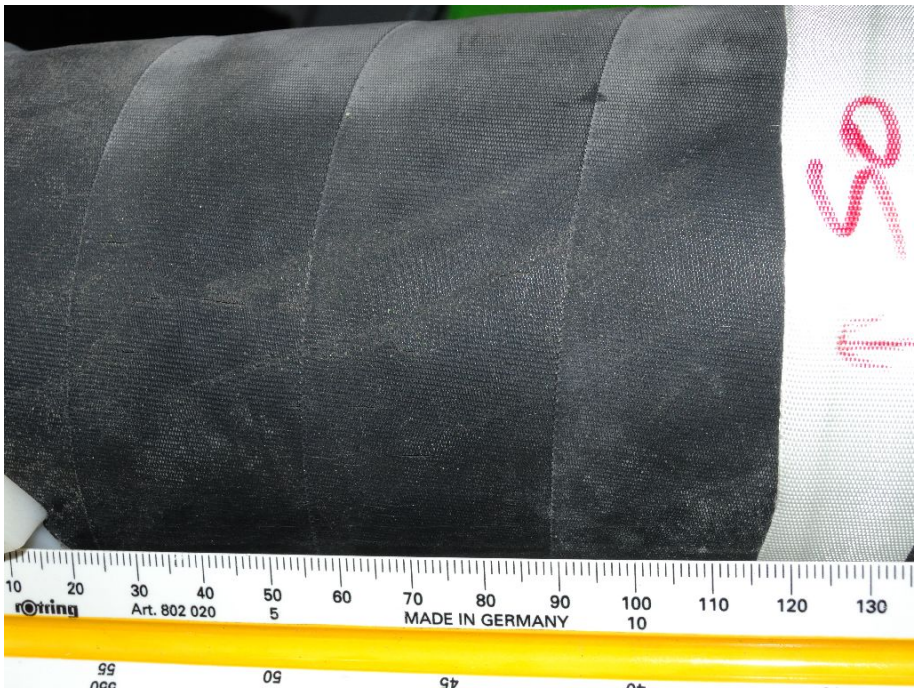

Figure A.28: 1604863A.50.01.20100721

Figure A.29: 1604863A.50.02.20100721

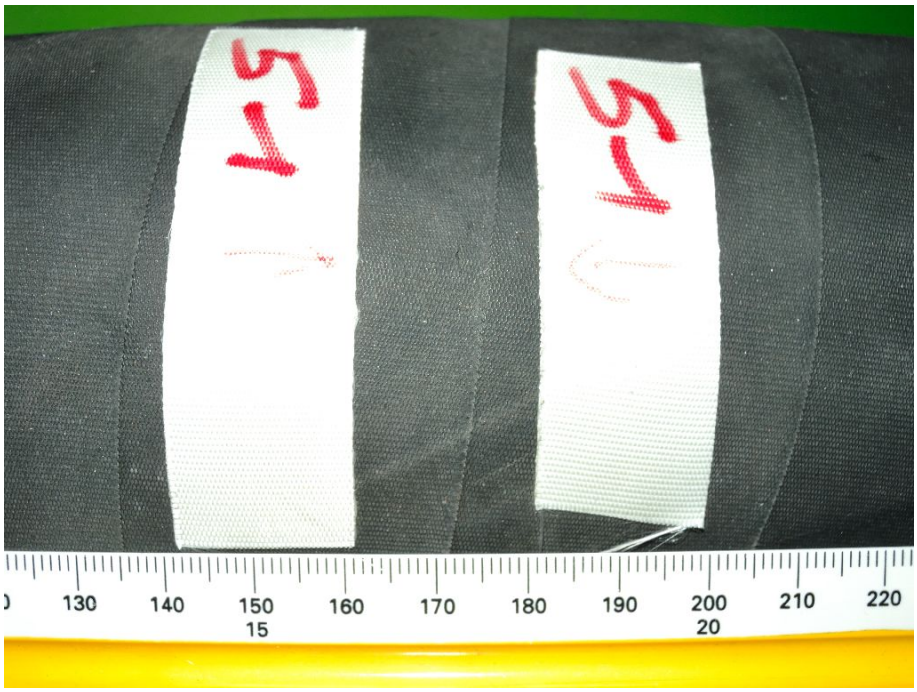

Figure A.30: 1604863A.51.01.20100721

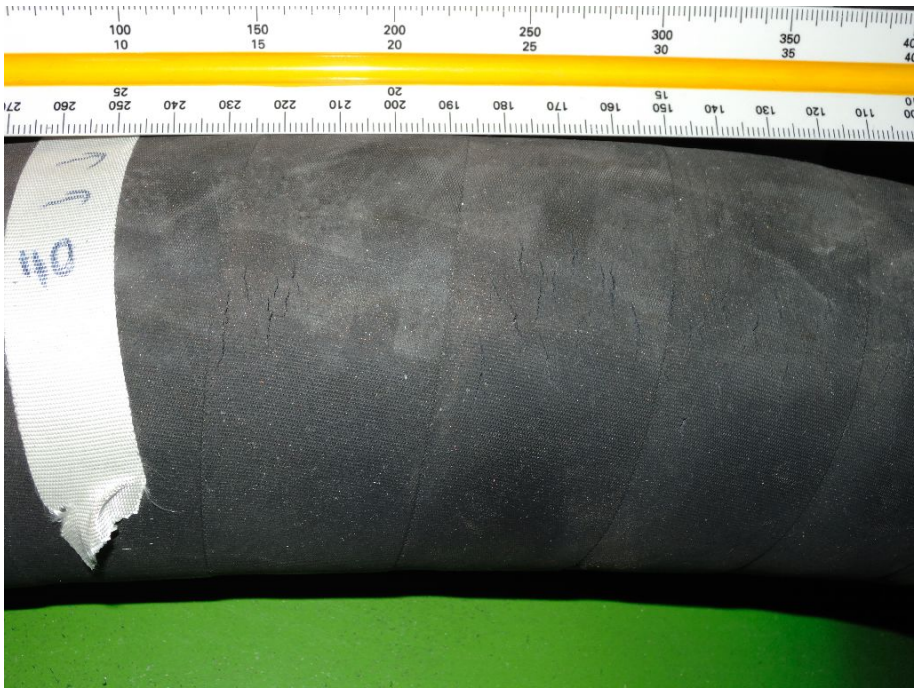

Figure A.31: 1604864A.40.01.20100721

Figure A.32: 1604864A.40.02.20100721

Figure A.33: 1604864A.40.03.20100831

Figure A.34: 1604864A.40.04.20100831

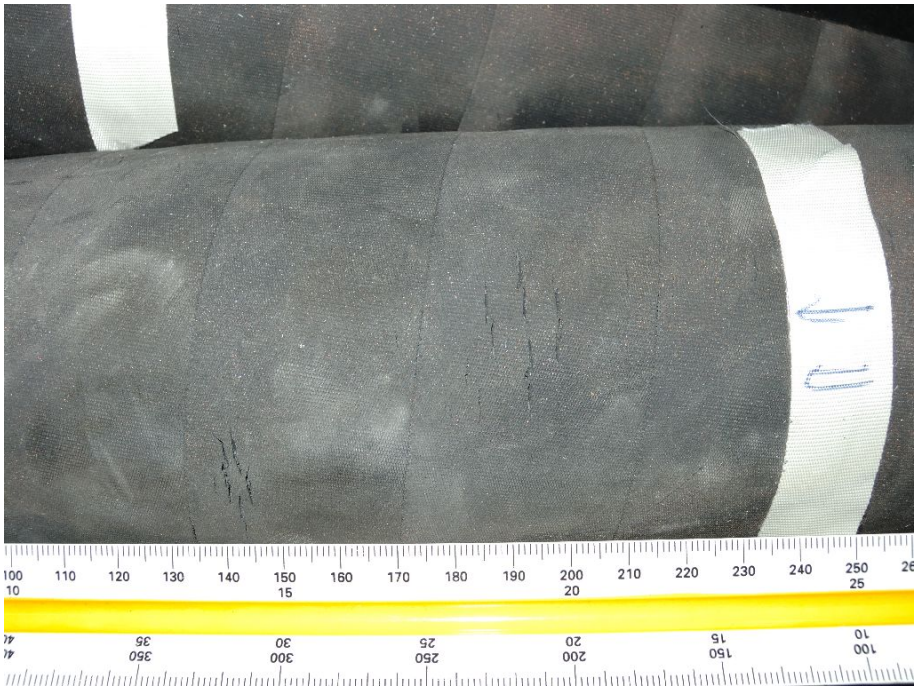

Figure A.35: 1604864A.40.05.20100831

Figure A.36: 1604864A.44.01.20100721

Figure A.37: 1604864A.52.01.20100721

Figure A.38: 1604864A.52.02.20100721

Figure A.39: 1604864A.52.03.20100721

Figure A.40: 1604864A.52.04.20100721

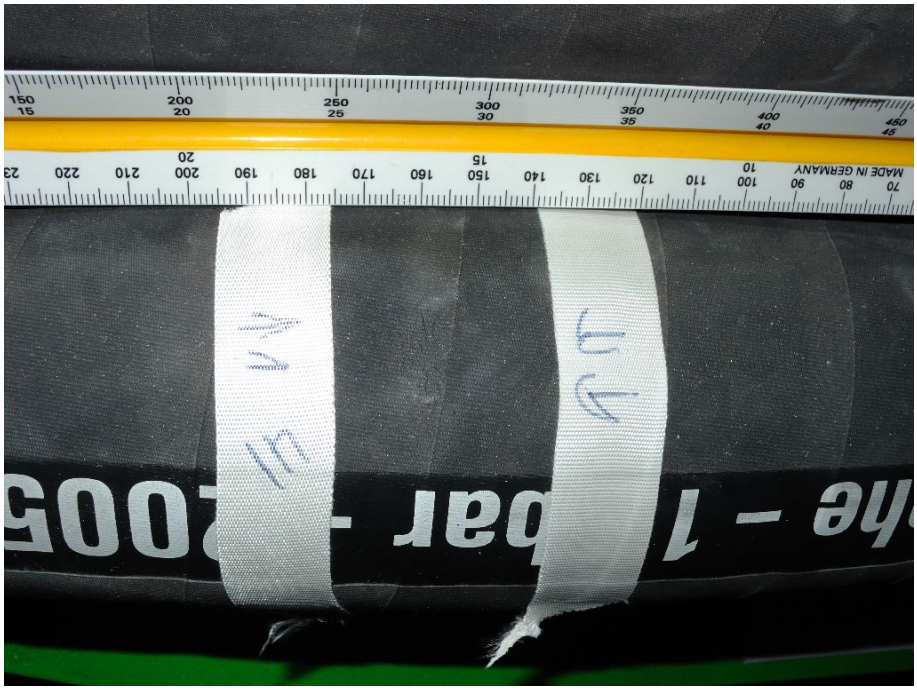

Figure A.41: 1604865A.41.01.20100831

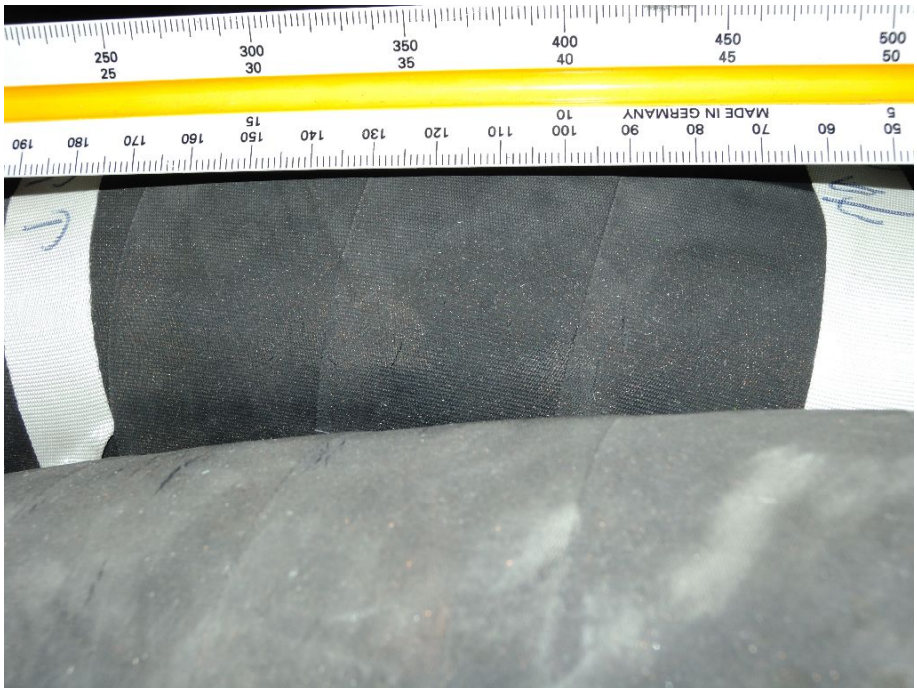

Figure A.42: 1604865A.42.01.20100831

Figure A.43: 1604865A.45.02.20100831

Figure A.44: 1604865A.53.01.20100721

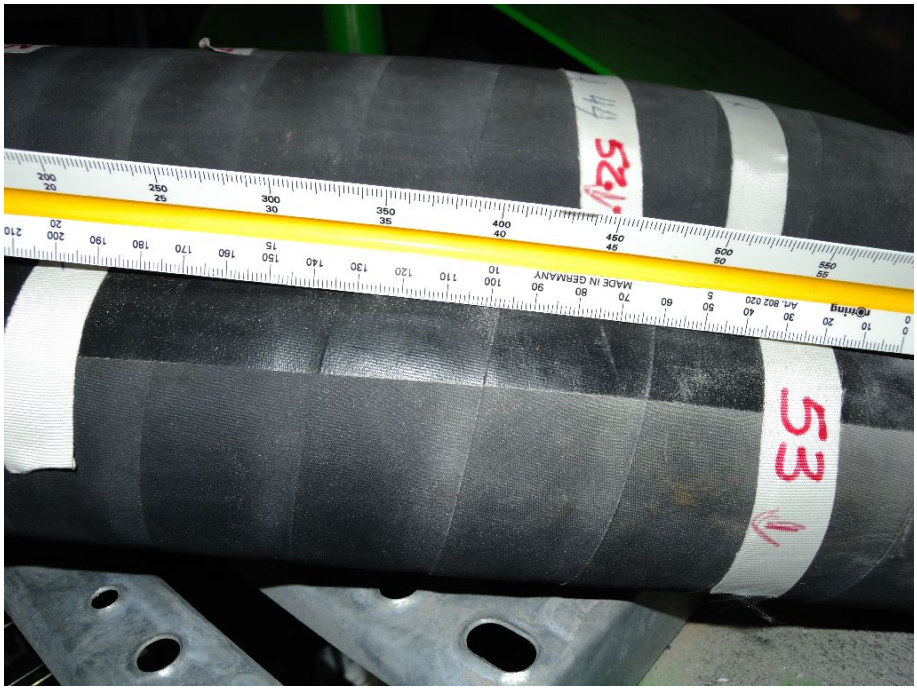

Figure A.45: 1604865A.53.02.20100831

Figure A.46: 1604865A.54.01.20100721

Figure A.47: 1604869A.38.01.20100720

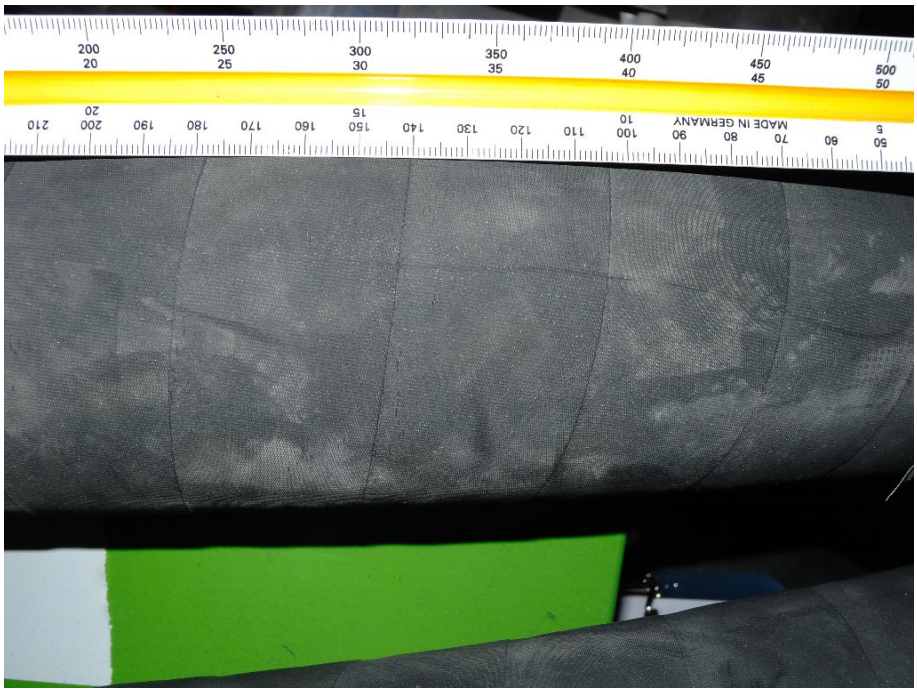

Figure A.48: 1604869A.38.02.20100720

Figure A.49: 1604869A.38.03.20100720

Figure A.50: 1604870A.37.01.20100720

Figure A.51: 1604870A.37.02.20100720

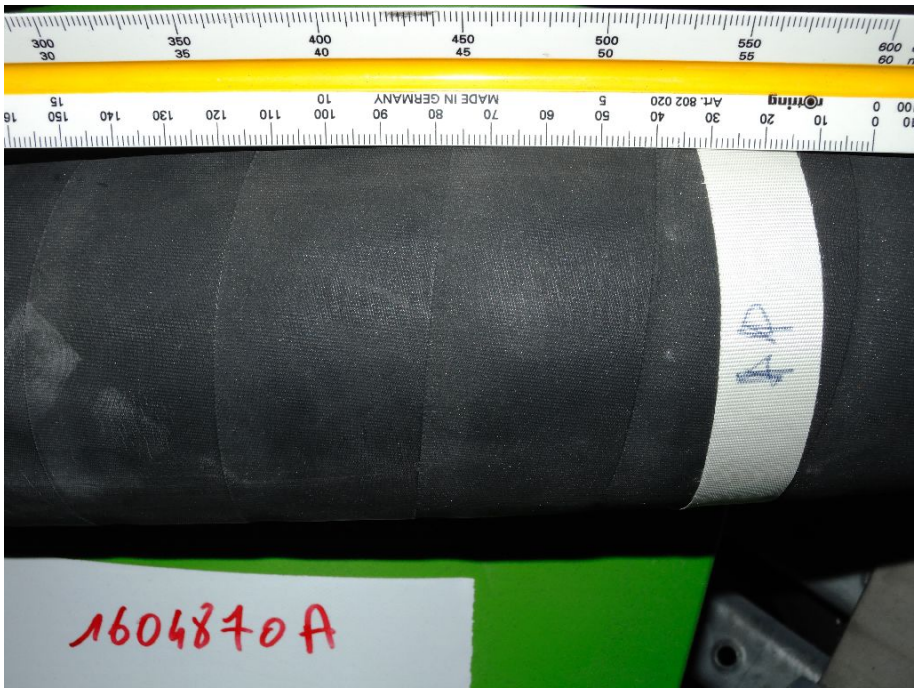

Figure A.52: 1604870A.37.03.20100831

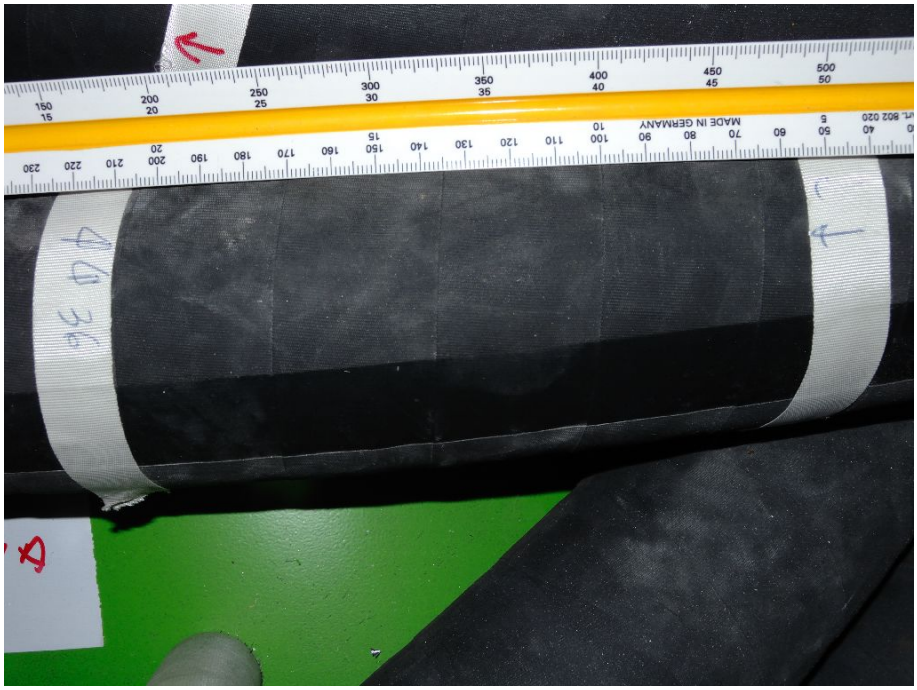

Figure A.53: 1604871A.36.01.20100720

Figure A.54: 1604871A.36.02.20100831

Figure A.55: 1604871A.36.03.20100720

Figure A.56: 1604871A.36.04.20100720

A.2 Photographs of crack–areas Point 6R

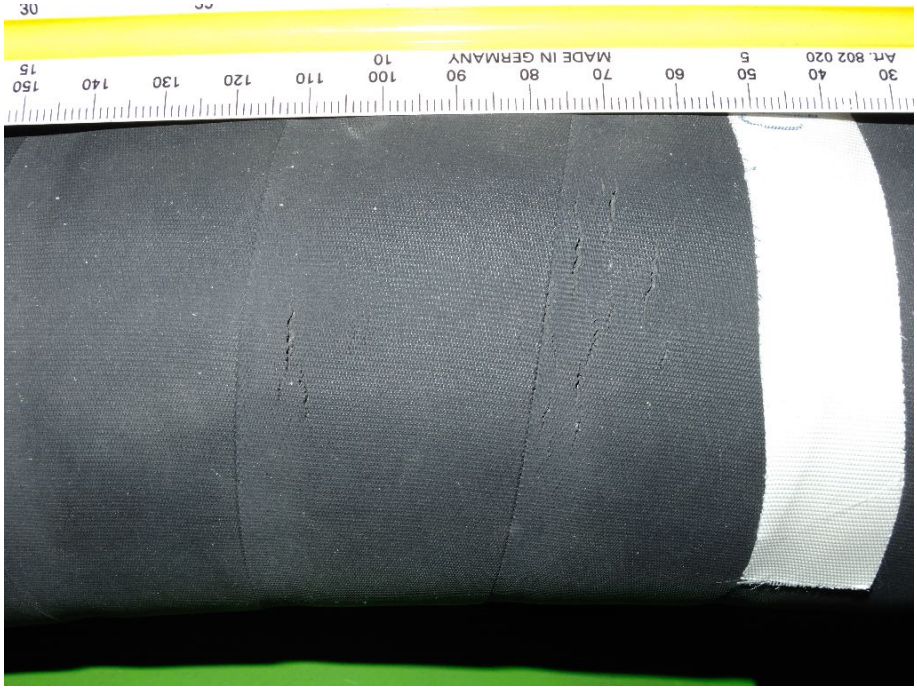

Figure A.57: 1604893A.22.01.20100831

Figure A.58: 1604893A.23.01.20100831

Figure A.59: 1604894A.25.01.20100831

Figure A.60: 1604894A.27.01.20100831

Figure A.61: 1604894A.30.01.20100831

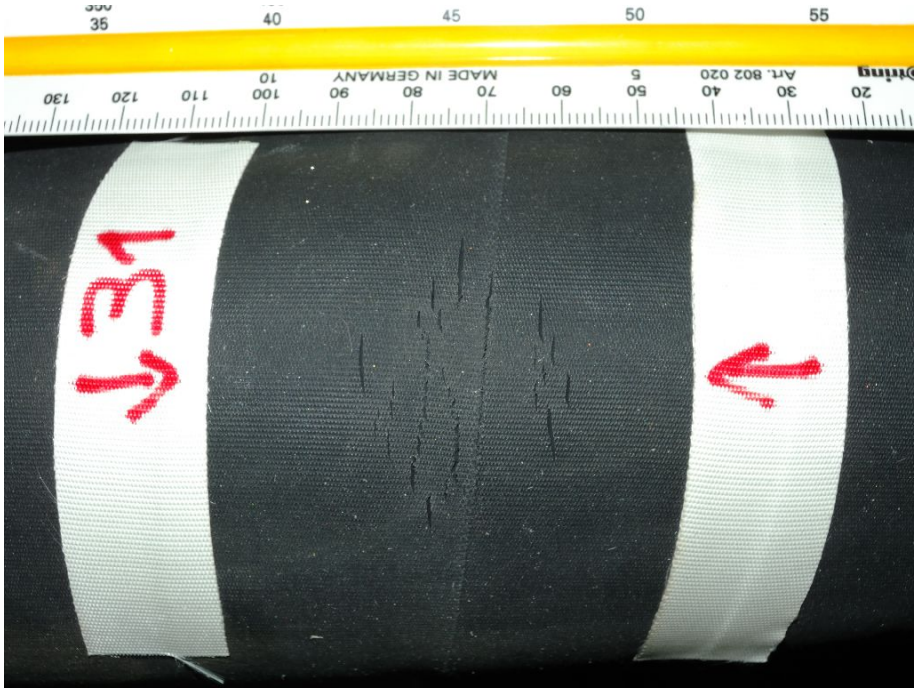

Figure A.62: 1604894A.31.01.20100831

Figure A.63: 1604895A.28.01.20100831

Figure A.64: 1604895A.29.01.20100831

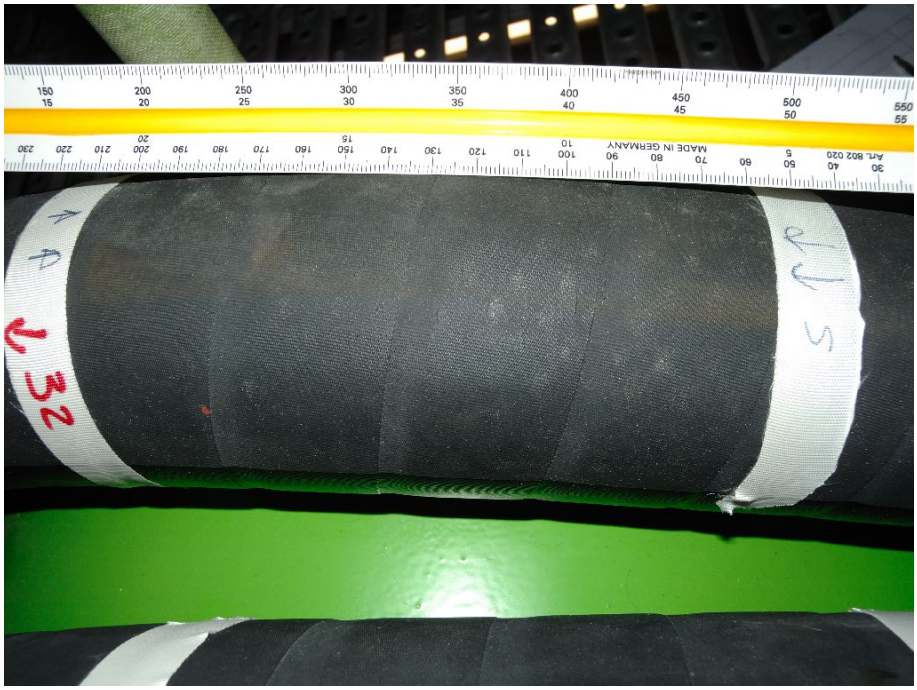

Figure A.65: 1604896A.05.01.20100831

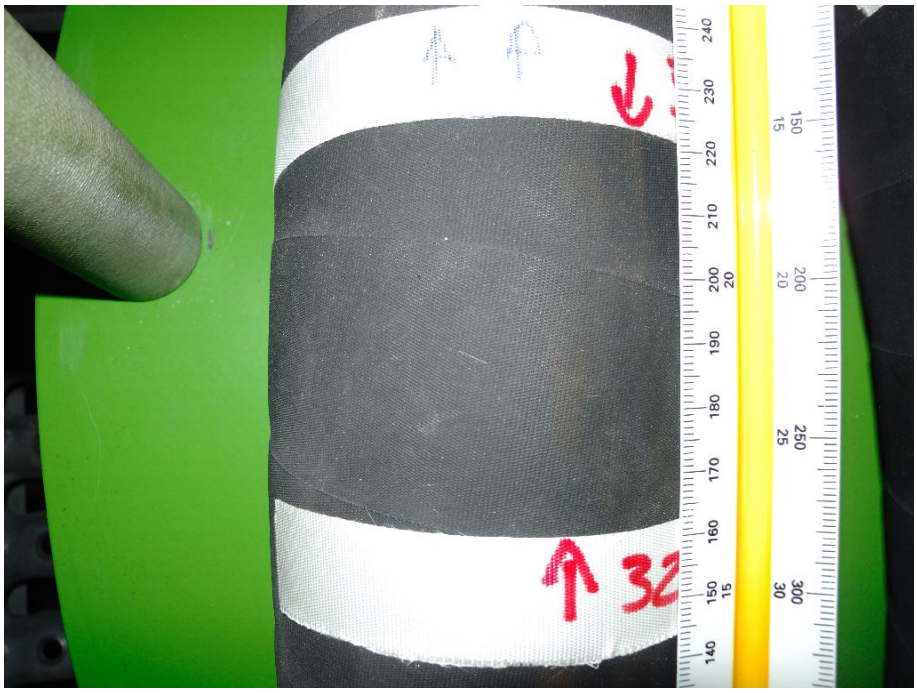

Figure A.66: 1604896A.32.01.20100831

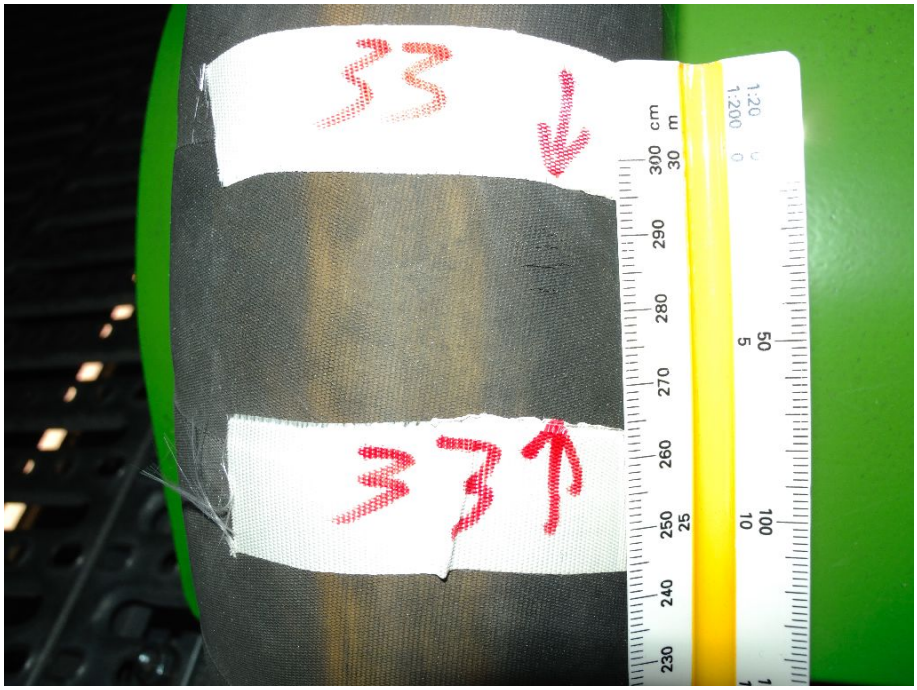

Figure A.67: 1604896A.33.01.20100831

Figure A.68: 1604897A.04.01.20100831

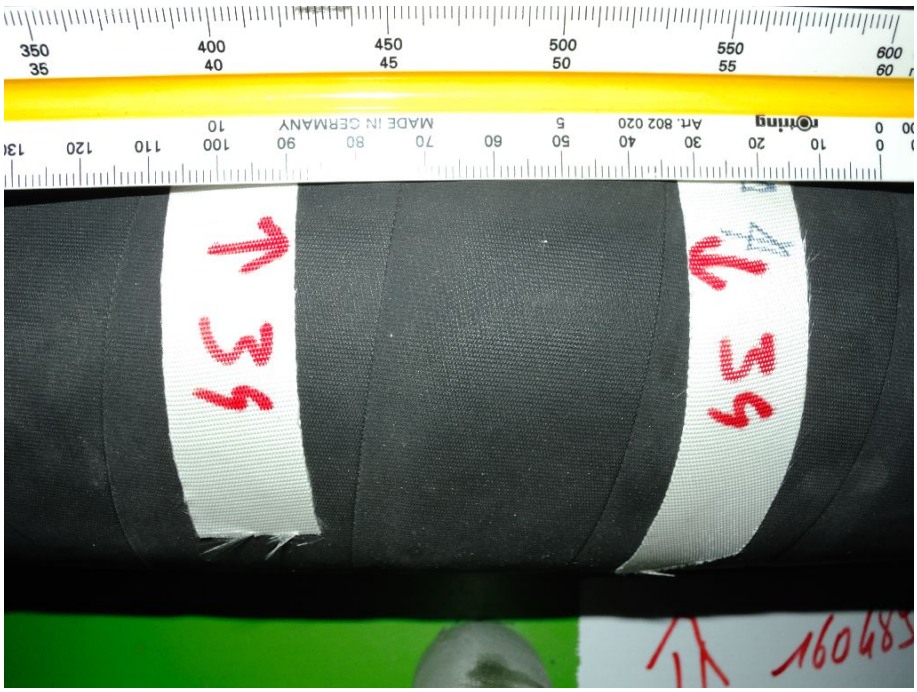

Figure A.69: 1604897A.34.01.20100831

Figure A.70: 1604897A.35.01.20100831

Figure A.71: 1604898A.06.01.20100831

Figure A.72: 1604898A.07.01.20100831

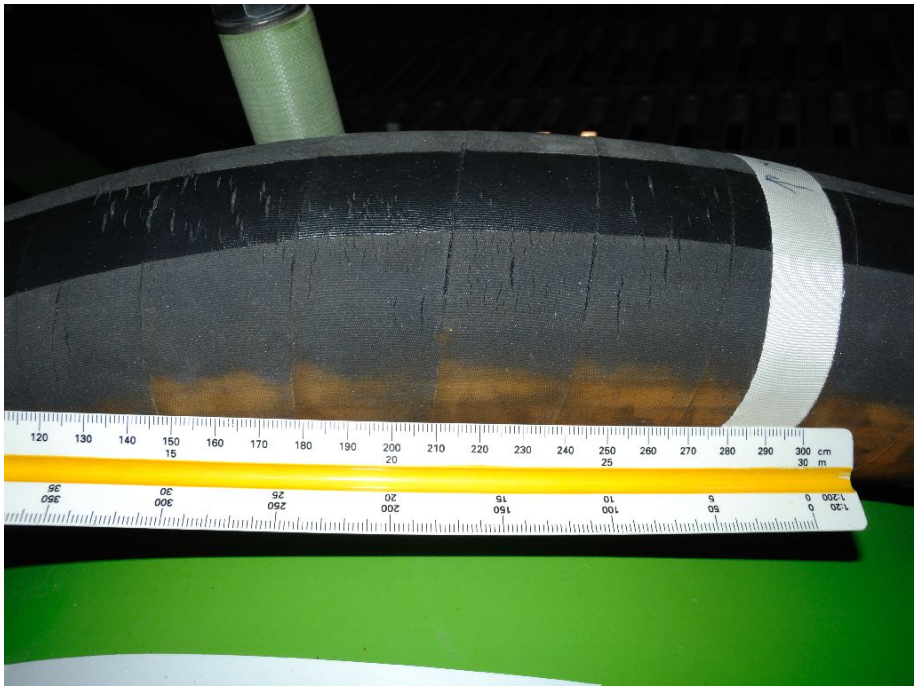

Figure A.73: 1604898A.08.01.20100831

Figure A.74: 1604905A.18.01.20100831

Figure A.75: 1604905A.19.01.20100831

Figure A.76: 1604905A.20.01.20100831

Figure A.77: 1604905A.21.01.20100831

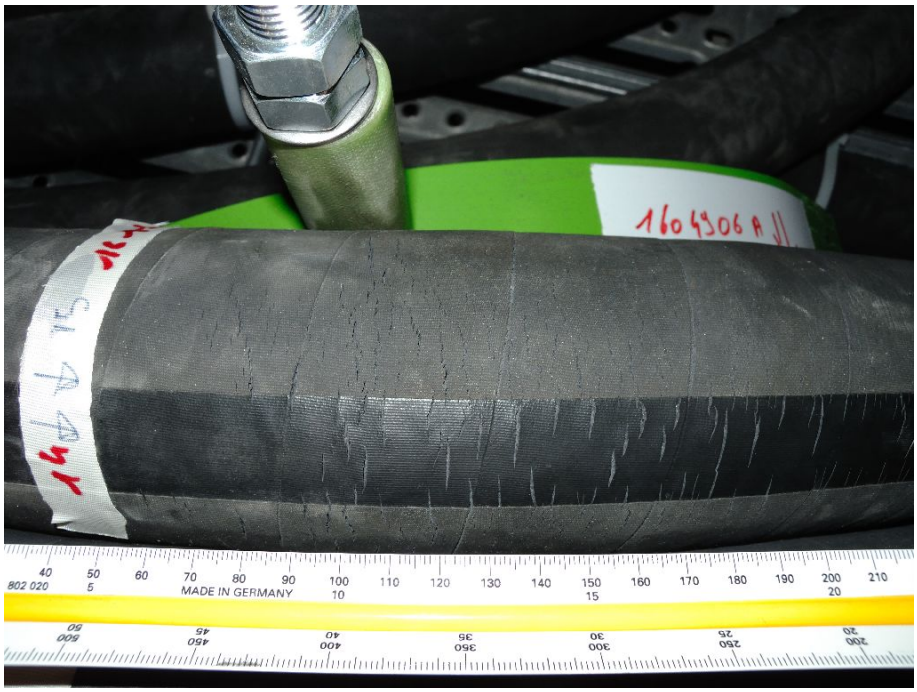

Figure A.78: 1604906A.15.01.20100831

Figure A.79: 1604906A.16.01.20100831

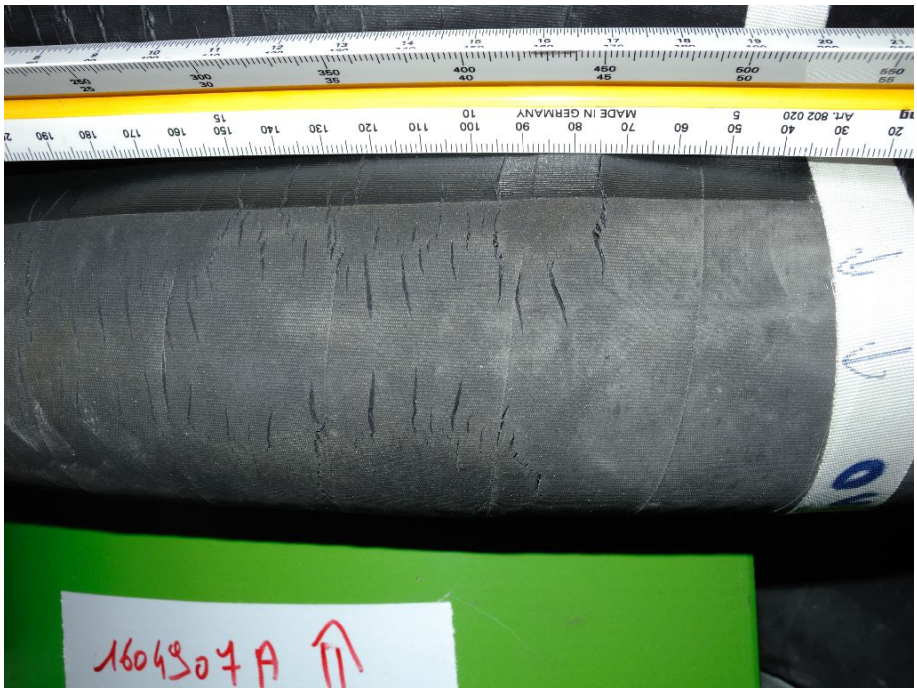

Figure A.80: 1604907A.10.01.20100831

Figure A.81: 1604907A.11.01.20100831

Figure A.82: 1604907A.12.01.20100831

Figure A.83: 1604906A.17.01.20100831

A.3 Monitoring protocols

Date: 20.07.2010			Access Point: 6L
Name: Alexander Wollmann			Page 1 of 4
Crack area	**Photo number**	**New?**	**Comment**
37.01	1740 - NRW	✓	~~50mm = 475,5~~ 6-10 L = 82,6 B = 2,3 ✓
37.02	1743 - NRW	✓	50mm = 347,6 20+ L = 45,6 B = 2,6 ✓
~~37.03~~	1744 - NRW	✓	~~50mm = 371,5~~ !
38.01	1747 - NRW	✓	50mm = 452,9 6-10 L = 72,2 B = 7,8 ✓
38.02	1748	✓	50mm = 441,3 20+ L = 77,8 B = 7,2 ✓
38.03	1750	✓	50mm = 486,9 6-10 L = 55 B = 3,7 ✓
36.01	1757	✓	~~50~~mm = 368,0 3-5 L = 11,4 B = 0,8 ✓
36.02	~~1752~~ 1753	✓	50mm = 422,2 11-20 L = 40,9 B = 1,9 ✓
36.03	1755	✓	50mm = 743,5 20+ L = 222,8 B = 7,9 ✓
~~36.04~~	~~1757~~	✓	
47	1760	✓	50mm = 701.01 6-10 L = ~~56,6~~ 47,63 B = 2,53
49.01	1761	✓	50mm = 529,1 6-10 L = 84,4 B = 1,9 ✓
49.02	1764	✓	50mm = 813,3 3-5 L = 85,5 B = 2,1 ✓
49.03	1765	✓	50mm = 795,4 11-20 L = 170,0 B = 7,1 ✓

Date: 20.07.2020			Access Point: 6L
Name: Alexander Wellmann			Page 2 of 4
Crack area	**Photo number**	**New?**	**Comment**
✓ 35.01 ✓	1768	/	50mm = ~~524,5~~ 7-2 L=30,44 B=2,70 ✓
✓ 35.02 ✓	1771	/	50mm = 626,93 6-10 L=142,8 B=5,69 ✓
✓ 35.03 ✓	1773	X	50mm = 340,6 20+ L=53.4 B=4,0 ✓
✓ 35.04 ✓	1774	/	50mm = 469,6 20+ L=85,4 B=5,2 ✓
✓ 35.05 ✓	1775	X	50mm = 487,6 ~~10~~ 20 L=198,2 B=6,5 ✓
✓ 35.06 ✓	1776	/	50mm = 632,7 20+ L=278.15 B=1,8 ✓
✓ 35.07 ✓	1778	/	50mm = 602,0 11-20 L62.71 B=1,17
~~34-01~~ ✓	1798	X	[redacted] D.
34.02 ✓	1799	/	50mm = 456,21 11-20 L=59.75 B=2,36 ✓
34.03 ✓	1802	/	50mm = 357.26 20+ L=76,64 B=2,23 ✓
34.04 ✓	1803	/	50mm = 386.14 20+ L105.09 B=4.57 ✓
36.04 ✓	~~1799~~ 1787	/	50mm = 487,5 3-5 L=186,3 B=8,1 ✓
33.07 ✓	1782	/	50mm = 555 1-2 ✓ L=774.28 B=2,76
62 ✓	1797	X	50mm = 357,50 20+ L=87.32 B=1.49 ✓
48 ✓	(1808) 1806	X	50mm = 420.08 6-10 L=48,12 B=3,99 ✓
47 ✓	1812	X	!

Date: 27.07.2010			Access Point: 6L
Name: Alexander Wollmann			Page 3 of 4
Crack area	**Photo number**	**New?**	**Comment**
32.01 ✓	1783	/	50mm = 387.85, 11-20 L=115.28, B=13.31 ✓
32.02 ✓	1785	/	50mm = 438.859 20+ L=93.67 B=6.42 ✓
32.03 ✓	1786	/	50mm = 353,7 20+ L=45.23 B=2,0 ✓
~~32.04 ✓~~	~~1788~~	~~X~~	~~50mm = 386,0 20+~~ ~~L=57.87 B=3.97~~ ✓ !
32.05 ✓	1789	/	50mm = 386,0 20+ L=57.87 B=3.97 ✓
32.06 ✓	~~1790~~ 1791	X	~~50mm = 438,9~~ !
~~32.07~~	~~1791~~		
42 ✓	1814	X	50mm = 447,9 6-10 L=59,5 B=1,6 ✓
40.01 ✓	1816	/	50mm = 447,0 11-20 L=26,0 B=1,6 ✓
40.02 ✓	1818	/	50mm = 498,9 6-10 L=7,7 B=2,5 ✓
40.03 ✓	1819	X	50mm = 519,6 20+ L=130,7 B=5,0 ✓
40.04 ✓	1820	X	50mm = 596,3 20+ L=111,2 B=5,3 ✓
40.05 ✓	1828	X	≥81,0 11-20 L=73,0 B=2,9 ✓
54 ✓	1832	/	50mm = 603,2 1-2 L=73,0 B=1,3 ✓
45.2 ✓	1835	X	50mm = 393,0 11-20 L=45,6 B=1,2 ✓
44.01 ✓	1839	/	50mm = 513,5 11-20 L=12,4 B=2,7 ✓

Date: 27.07.2020			Access Point: 6L	
Name: Alexander Wollmann			Page 4 of 4	
Crack area	**Photo number**	**New?**	**Comment**	
53.01 ✓	1836	/	50mm = 474,0 1-2 L = 26,7 B = 1,4	✓
53.02 ✓	1837	X	50mm = [redacted] 3054 1-2 L = 53,8 B = 3,1	✓
52.01 ✓	7840.	/	50mm = 602,5 11-20 L = 57,0 B = 3,3	✓
52.02 ✓	1841	/	50mm = 537,8 11-20 L = 143,0 B = 1,4	✓
52.03 ✓	7842	/	50mm = 543,8 20t L = 67,3 B = 2,3	✓
52.04 ✓	7843	/	50mm = 537,1 P 3-5 L = [redacted] 79,9 B = [redacted] 2,3	✓
39.01 ✓	7846	/	50mm = 616,3 11-20 L = 77,6 B = 10,12	✓
39.02 ✓	7849	/	(50mm = L = [redacted] B =	) ✓
39.03 ✓	[redacted] 1858	/	50mm = 467,1 L = 89,7 B = 1,4	✓
51.01 ✓	1859	/	[redacted]mm = 744,5 1-2 15,4 1,5	✓
50.07 ✓	1860	/	50mm = 595,8 20t L = 73,9 B = 3,0	✓
50.02 ✓	1861	/	50mm = 592,5 11-20 L 71,6 B = 2,6	✓

Date: 31.08.2020			Access Point: 6L
Name: Wollmann			Page 1 of 1
Crack area	**Photo number**	**New?**	**Comment**
X 32.06 60	1878 ✓ 1878 – 1882	/	50mm = 507,0 1-2 ✓ L = 67,1 B = 2,7
X 32.04 60	1875 1877 – 1875	/	50mm = 377,9 20+ ✓ L = 75,5 B = 4,5
X 62 60	1887 1883 – 1887	/	50mm = 480,0 20+ ✓ L = 136,2 B = 2,3
! ~~34.1~~ 61	~~1888 – 1892~~	/	
X 35.3 62	1865 1862 – 1865	/	50mm = 400,0 20+ ✓ L = 47,3 B = 5,5
X 35.5 62	1870 1866 – 1870	/	50mm = 423,3 11-20 ✓ L = 164,7 B = 4,5
! ~~48~~ 62	~~1887 – 1887~~	/	50mm = L = B =
X 37.03 70	1893 1893 – 1900	/	50mm = 450,5 6-10 ✓ L = 87,1 B = 2,4
X 36.2 77	1904 1901 – 1904	/	50mm = 432,4 11-20 L = 44,7 B = 1,8
X 41 65	1906 1905 – 1907	/	50mm = 464,8 11-20 ✓ L = 49,2 B = 2,0
X 42 65	1912 1908 – 1914	/	50mm = 507,6 6-10 ✓ L = 66,6 B = 1,7
X 53.2 65	1919 1917 – 1919	/	50mm = 340,8 1-2 ✓ L = 46,2 B = 2,6
X 45.2 65	1924 1920 – 1925	/	50mm = 367,0 11-20 ✓ L = 49,2 B = 1,1
X 42.3 64	1928 1926 – 1928	/	50mm = 463,8 20+ ✓ L = 127,4 B = 4,9
X 40.4 64	1929 1929 – 1933	/	50mm = 554,0 20+ ✓ L = 112,1 B = 5,2
X 40.5 64	1935 1934 – 1937	/	50mm = 470,5 6-10 ✓ L = 69,5 B = 5,2

Date: 01.09.2020			Access Point: OR
Name: Wollmann			Page 1 of 2
Crack area	**Photo number**	**New?**	**Comment**
X 15	1940 1938–1941	/	50mm = 409,8 20+ L = 72,0 B = 5,9
X 16	1944 1942–1945	/	50mm = 423,3 20+ L = 97,5 B = 5,7
X 17	1947 1946–1950	/	50mm = 423,6 20+ L = 254,1 B = 17,1
X 10	1955 1957–1959	/	50mm = 417,4 20+ L = 126,8 B = 7,2
X 11	1963 1960–1965	/	50mm = 389,9 20+ L = 161,2 B = 4,8
X 12	1968 1966–1971	/	50mm = 571,7 6-10 L = 93,4 B = 4,4
X 18	1975 1972–1975	/	50mm = 406,5 20+ L = 98,5 B = 3,5
X 19	1980 1976–1980	/	50mm = 428,8 20+ L = 52,6 B = 3,4
X 20	1985 1987–1987	/	50mm = 360,2 20+ L = 48,2 B = 4,6
X 21	1991 1988–1992	/	50mm = 425,3 11-20 L = 71,3 B = 4,3
X 06	1995 1993–1996	/	50mm = 500,1 20+ L = 129,3 B = 6,9
X 07	2001 1997–2001	/	50mm = 369,5 20+ L = 111,5 B = 8,3
X 08	2003 2002–2007	/	50mm = 352,8 20+ L = 52,4 B = 4,3
X 05	2009 2008–2010	/	50mm 361,4 3-5 L = 20,0 B = 0,7
X 32	2014 2010–2014	/	50mm = 524,0 1-2 L = 25,0 B = 2,8
X 33	2015 2015–2016	/	50mm = 605,7 6-10 L = 56 B = 3,8

Date: 01-09.2020			Access Point: 6R
Name: Wollmann			Page 2 of 2
Crack area	**Photo number**	**New?**	**Comment**
X 04	2018 2017-2019	/	50mm = 448,9 11-20 L= 51,3 B= 2,8 ✓
X 34	2020 2020-2022	/	50mm = 504,1 1-2 L= 32,6 B= 2,0 ✓
X 35	2027 2023-2027	/	50mm = 530,2 6-10 L=63,2 B= 6,6 ✓
X 28	2030 2028-2032	/	50mm = 405,2 20+ L= 173,1 B= 7,3 ✓
X 29	2033 2033-2036	/	50mm = 497,8 20+ L= 123,4 B= 6,3 ✓
X 22	2039 2037-2042	/	50mm = 601,7 11-20 L= 180,5 B= 9,0 ✓
X 23	2044 2043-2046	/	50 mm = 420,4 20+ L= 48,0 B= 3,8 ✓
X 25	2047 2048 -2050	/	50mm = 411,5 20+ L= 184,0 B= 7,2 ✓
X 27	2057 2051-2054	/	50mm = 501,0 20+ L= 242,6 B= 6,2 ✓
X 30	2055 2055-2056	/	50mm = 598,1 6-10 L= 67,1 B= 3,2 ✓
X 31	2060 2057-2060	/	50mm = 614,6 20+ L= 107,8 B= 6,3 ✓

A.4 Crack–areas Point 6L

Crack-areas

Point LHC	Cable number	Label	Type	Frequency	Depth	Severity value	Crack length	Crack width
6L								
	1604860A							
		32,1	Transversal	11-20	Deep	12,5	15,1	1,7
		32,2	Transversal	over 20	Deep	15	11	0,8
		32,3	Transversal	over 20	Low	3	6,4	0,3
		32,4	Transversal	over 20	Deep	15	10	0,6
		32,5	Transversal	over 20	Deep	15	7,5	0,5
		32,6	Transversal	1-2	Low	1	6,7	0,3
		33	Other fault	1-2	Low	0,5	69,8	0,2
		47	Transversal	6-10	Low	2	3	0,2
		62	Transversal	over 20	Low	3	14,2	0,2
		73,1	Transversal	6-10	Low	2		
		73,2			Low			
	1604861A							
		31	Longitudinal	over 20	Low	3	7,9	0,1
		34,1	Transversal	3-5	Low	1,5	6,1	0,1
		34,2	Transversal	11-20	Low	2,5	6,5	0,3
		34,3	Transversal	over 20	Low	3	10,7	0,3
		34,4	Transversal	over 20	Deep	15	13,6	0,6
		75	Longitudinal	11-20	Low	2,5	6,6	0,3
		76	Longitudinal	1-2	Low	1		
	1604862A							
		30	Transversal & Longitudinal	3-5	Low	2,2	4,7	0,2
		35,1	Transversal	1-2	Low	1	2,9	0,3
		35,2	Transversal	6-10	Deep	10	11,4	0,5
		35,3	Transversal	over 20	Deep	15	5,9	0,7
		35,4	Transversal	over 20	Deep	15	9,1	0,6
		35,5	Transversal	11-20	Deep	12,5	19,5	0,5
		35,6	Transversal & Longitudinal	over 20	Low	4,5	17,2	0,1
		35,7	Transversal	11-20	Low	2,5	5,2	0,1
		48	Transversal	6-10	Deep	10	5,7	0,5
		49,1	Longitudinal	6-10	Low	2	8	0,2
		49,2	Transversal & Longitudinal	3-5	Low	2,2	5,3	0,1
		49,3	Longitudinal	11-20	Low	2,5	10,7	0,4
		74	Transversal	over 20	Low	3	2	0,2

Point LHC	Cable number	Label	Type	Frequency	Depth	Severity value	Crack length	Crack width
	1604863A							
		23	Transversal & Longitudinal	3-5	Deep	11,2	2	0,5
		24	Longitudinal	11-20	Low	2,5	8,1	0,2
		39,1	Transversal	11-20	Deep	12,5	7,5	0,8
		39,2			Low			
		39,3	Transversal	11-20	Low	2,5	9,7	0,2
		50,1	Longitudinal	over 20	Low	3	6,2	0,3
		50,2	Longitudinal	11-20	Low	2,5	6	0,2
		51	Transversal	1-2	Low	1	1	0,1
	1604864A							
		40,1	Transversal	11-20	Low	2,5	14,1	0,2
		40,2	Transversal	6-10	Low	2	7,2	0,3
		40,3	Transversal	over 20	Deep	15	13,7	0,5
		40,4	Transversal	over 20	Deep	15	10,1	0,5
		40,5	Transversal	6-10	Deep	10	7,4	0,6
		44,1	Transversal	11-20	Low	2,5	11,9	0,3
		52,1	Transversal	11-20	Low	2,5	4,7	0,3
		52,2	Transversal & Longitudinal	11-20	Low	3,7	13,4	0,1
		52,3	Transversal & Longitudinal	over 20	Low	4,5	6,2	0,2
		52,4	Longitudinal	3-5	Low	1,5	7,5	0,2
	1604865A							
		25	Longitudinal	11-20	Low	2,5	4,3	0,2
		26	Transversal & Longitudinal	3-5	Low	2,2	2,9	0,1
		41	Transversal	11-20	Low	2,5	5,3	0,2
		42	Transversal	6-10	Low	2	6,6	0,2
		45,2	Transversal	11-20	Low	2,5	6,7	0,1
		53,1	Transversal	1-2	Low	1	2,8	0,1
		53,2	Transversal	1-2	Low	1	6,8	0,4
		54	Transversal	1-2	Low	1	6,1	0,1
		66	Transversal & Longitudinal	6-10	Low	3	7	0,1
	1604866A							
		20	Longitudinal	6-10	Low	2	3,9	0,1
	1604866C							
		81	Other fault	1-2	Deep	2,5	9,1	0,9
	1604867A							
		21,1	Transversal & Longitudinal	over 20	Low	4,5	12,8	0,2
		21,2	Transversal & Longitudinal	over 20	Low	4,5	9,2	0,3
		21,3	Longitudinal	over 20	Low	3	6,5	0,2

Point LHC	Cable number	Label	Type	Frequency	Depth	Severity value	Crack length	Crack width
	1604869A							
		28	Longitudinal	over 20	Low	3	4,3	0,2
		38,1	Transversal	6-10	Low	2	8	0,2
		38,2	Transversal	over 20	Low	3	2	0,1
		38,3	Transversal	6-10	Low	2	5,6	0,4
		70	Transversal	over 20	Low	3	6,7	0,2
		71,1	Transversal	over 20	Low	3	10,6	0,2
		71,2	Transversal	11-20	Low	2,5	6,3	0,2
	1604870A							
		29	Transversal	6-10	Low	2	9,3	0,1
		37,1	Transversal	6-10	Low	2	8,7	0,2
		37,2	Transversal	over 20	Low	3	6,6	0,4
		37,3	Transversal	6-10	Low	2	9,7	0,3
		72,1	Transversal	11-20	Low	2,5	13,7	0,2
		72,2	Transversal	11-20	Low	2,5	10	0,3
		80	Longitudinal	1-2	Low	1		
	1604871A							
		27	Longitudinal	over 20	Low	3	4,1	0,1
		36,1	Transversal	3-5	Low	1,5	1,5	0,1
		36,2	Transversal & Longitudinal	11-20	Low	3,7	5,1	0,2
		36,3	Transversal	over 20	Deep	15	15,5	0,6
		36,4	Transversal	3-5	Deep	7,5	19,1	0,8
		67	Transversal & Longitudinal	11-20	Low	3,7	2,3	0,1
		68	Transversal & Longitudinal	3-5	Low	2,2	4,6	0,2
		69	Transversal	6-10	Low	2	7,4	0,2
		77	Longitudinal	3-5	Low	1,5	6	0,3
		78	Longitudinal	1-2	Low	1	4,1	0,2
	1604872C							
		43,1	Longitudinal	11-20	Low	2,5	15,6	0,2
		43,2	Longitudinal	11-20	Low	2,5	11,4	0,2
		55,1	Longitudinal	over 20	Low	3	13,3	0,2
		55,2	Longitudinal	11-20	Low	2,5	5,7	0,1
		55,3	Longitudinal	11-20	Low	2,5	16,1	0,2
		56,1	Longitudinal	11-20	Low	2,5	8,2	0,3
		56,2	Longitudinal	11-20	Low	2,5	6,7	0,3
		57,1	Longitudinal	6-10	Low	2	4,2	
		57,2	Longitudinal	over 20	Low	3	5,4	0,2
		58,1	Longitudinal	11-20	Low	2,5	17,1	0,1
		58,2	Longitudinal	6-10	Low	2	7	0,1

Point LHC	Cable number	Label	Type	Frequency	Depth	Severity value	Crack length	Crack width
	1604873A							
		44,2	Longitudinal	1-2	Low	1	1,5	0,1
		59	Longitudinal	6-10	Low	2	4,1	0,1
		60	Longitudinal	11-20	Low	2,5	6,1	0,3
		61,1	Transversal & Longitudinal	11-20	Low	3,7	17,8	0,1
		61,2	Longitudinal	1-2	Low	1	8,3	0,2
	1604874A							
		22	Longitudinal	1-2	Low	1	2,7	0,2
	1604874C							
		82	Longitudinal	3-5	Low	1,5		
	1604875C							
		45,1	Longitudinal	3-5	Low	1,5	10,8	0,1
	1604876A							
		46,1	Longitudinal	11-20	Low	2,5	7,6	0,2
		46,2	Longitudinal	over 20	Low	3	4,7	0,2
		46,3	Longitudinal	11-20	Low	2,5	5,5	0,2
		46,4	Longitudinal	over 20	Low	3	8,8	0,1
	1604877A							
		83	Longitudinal	1-2	Low	1		
	1604878A							
		15	Longitudinal	6-10	Low	2	5,7	0,2
		16	Longitudinal	6-10	Low	2	6,7	0,1
		17	Longitudinal	11-20	Low	2,5	5,7	0,2
		18	Transversal & Longitudinal	over 20	Low	4,5	14,6	0,2
	1604879A							
		19	Longitudinal	over 20	Low	3	7,4	0,3
		63	Transversal	6-10	Low	2	4,5	0
		64	Longitudinal	6-10	Low	2	7,2	0,2
		65	Longitudinal	11-20	Low	2,5	5,7	0,3
	1604880A							
		13	Longitudinal	6-10	Low	2	7,6	0,3
		14	Longitudinal	over 20	Low	3	5,7	0,3
		79	Transversal	3-5	Low	1,5		

Crack-areas: 122

Total crack-areas: 122

A.5 Crack–areas Point 6R

Crack-areas

Point LHC	Cable number	Label	Type	Frequency	Depth	Severity value	Crack length	Crack width
6R								
	1604892C							
		45	Other fault	1-2	Low	0,5		
	1604893A							
		22	Transversal	11-20	Deep	12,5	15	0,7
		23	Transversal	over 20	Deep	15	5,7	0,5
	1604894A							
		25	Transversal	over 20	Deep	15	22,4	0,9
		27	Transversal	over 20	Deep	15	24,2	0,6
		30	Transversal	6-10	Low	2	5,1	0,3
		31	Transversal	over 20	Deep	15	8,3	0,5
	1604895A							
		28	Transversal	over 20	Deep	15	21,4	0,9
		29	Transversal	over 20	Deep	15	12,8	0,8
	1604896A							
		5	Transversal	3-5	Low	1,5	2,8	0,1
		32	Transversal	1-2	Low	1	2,4	0,3
		33	Transversal	6-10	Low	2	4,6	0,3
	1604897A							
		4	Transversal	11-20	Low	2,5	5,7	0,3
		34	Transversal	1-2	Low	1	2,9	0,3
		35	Transversal	6-10	Deep	10	6	0,6
	1604898A							
		6	Transversal	over 20	Deep	15	12,9	0,7
		7	Transversal	over 20	Deep	15	15,1	1,1
		8	Transversal	over 20	Deep	15	7,4	0,6
		43	Longitudinal	1-2	Low	1		
	1604905A							
		18	Transversal	over 20	Low	3	12,1	0,4
		19	Transversal	over 20	Low	3	6,1	0,4
		20	Transversal	over 20	Deep	15	7,3	0,7
		21	Transversal	11-20	Deep	12,5	8,4	0,5
	1604906A							
		15	Transversal	over 20	Deep	15	8,8	0,7
		16	Transversal	over 20	Deep	15	11,5	0,7
		17	Transversal	over 20	Deep	15	30	2
		36	Transversal	3-5	Low	1,5	5,8	0,3
		38,1	Transversal	11-20	Low	2,5	3,6	0,3
		38,2	Transversal	over 20	Deep	15	8,8	0,6

Point LHC	Cable number	Label	Type	Frequency	Depth	Severity value	Crack length	Crack width
	1604907A							
		10	Transversal	over 20	Deep	15	15,5	0,9
		11	Transversal	over 20	Deep	15	20,7	0,6
		12	Transversal	6-10	Deep	10	10,5	0,5
		12	Transversal	6-10	Low	2	8,5	0,4
		37	Transversal	6-10	Deep	10	13,8	0,6
		44	Longitudinal	1-2	Low	1		
	1604911A							
		39	Transversal	over 20	Low	3		
		40	Longitudinal	1-2	Low	1		
	1604912A							
		41	Transversal	11-20	Deep	12,5	8,5	0,7
		42	Longitudinal	1-2	Low	1		

Crack-areas: 39

Total crack-areas: 39

A.6 Crack progression Point 6L

Crack-areas - Progression

Summer 2009 - Summer 2010

Point LHC	Cable number	Label	Type value increase	Frequency value increase	Depth value increase	Severity value increase	Crack length increase [mm]	%	Crack width increase [mm]	%
6L										
	1604860A									
		32,1	0	0	0	0	0	0	0,3	21
		32,2	0	0	4	12	1,5	16	0,4	100
		32,3	0	0	0	0	0,3	5	0	0
		32,4	0	0	0	0	0	0	0,1	20
		32,5	0	0	4	12	0	0	0,1	25
		32,6	0	0	0	0	0	0	0,1	50
		33	0	0	0	0	0	0	0	0
		47	0	0	0	0	0	0	0	0
		62	0	0	0	0	3,3	30	0	0
		73,1	0	0	0	0				
		73,2			0					
	1604861A									
		31	0	0	0	0	0	0	0	0
		34,1	0	0	0	0	0	0	0	0
		34,2	0	0	0	0	0,3	5	0	0
		34,3	0	0	0	0	0	0	0,1	50
		34,4	0	0	0	0	0,6	5	0	0
		75	0	0	0	0	0	0	0	0
		76	0	0	0	0				
	1604862A									
		30	0	0	0	0	0	0	0	0
		35,1	0	0	0	0	0	0	0	0
		35,2	0	0	4	8	0,2	2	0,1	25
		35,3	0	0	0	0	0	0	0,1	17
		35,4	0	0	0	0	0,9	11	0,1	20
		35,5	0	0	4	10	1,7	10	0,1	25
		35,6	0	0	0	0	0	0	0	0
		35,7	0	0,5	0	0,5	0	0	0	0
		48	0	0	4	8	0,6	12	0,2	67
		49,1	0	0	0	0	1	14	0	0
		49,2	0	0	0	0	0	0	0	0
		49,3	0	0	0	0	0	0	0,1	33
		74	0	0	0	0	0	0	0	0

Point LHC	Cable number	Label	Type value increase	Frequency value increase	Depth value increase	Severity value increase	Crack length increase [mm]	%	Crack width increase [mm]	%
	1604863A									
		23	0	0	0	0	0	0	0	0
		24	0	0	0	0	0	0	0	0
		39,1	0	0	0	0	0,4	6	0	0
		39,2			0					
		39,3	0	0	0	0	0,6	7	0	0
		50,1	0	0,5	0	0,5	0,1	2	0,1	50
		50,2	0	0	0	0	0	0	0	0
		51	0	0	0	0	0	0	0	0
	1604864A									
		40,1	0	0	0	0	0,1	1	0	0
		40,2	0	0	0	0	0	0	0	0
		40,3	0	0	0	0	1,3	10	0	0
		40,4	0	0	4	12	0,7	7	0,1	25
		40,5	0	0	0	0	0	0	0	0
		44,1	0	0	0	0	1,3	12	0	0
		52,1	0	0,5	0	0,5	0	0	0,1	50
		52,2	0	0	0	0	1,1	9	0	0
		52,3	0	0,5	0	0,8	0,4	7	0	0
		52,4	0	0	0	0	0,2	3	0	0
	1604865A									
		25	0	0	0	0	0	0	0	0
		26	0	0	0	0	0	0	0	0
		41	0	0	0	0	0,1	2	0	0
		42	0	0	0	0	1,6	32	0,1	100
		45,2	0	0	0	0	1,1	20	0	0
		53,1	0	0	0	0	0,2	8	0	0
		53,2	0	0	0	0	0,6	10	0,2	100
		54	0	0	0	0	0	0	0	0
		66	0	0	0	0	0	0	0	0
	1604866A									
		20	0	0	0	0	0	0	0	0
	1604866C									
		81	0	0	0	0	0	0	0	0
	1604867A									
		21,1	0	0	0	0	0	0	0	0
		21,2	0	0	0	0	0	0	0	0
		21,3	0	0	0	0	0	0	0	0

Point LHC	Cable number	Label	Type value increase	Frequency value increase	Depth value increase	Severity value increase	Crack length increase [mm]	%	Crack width increase [mm]	%
	1604869A									
		28	0	0	0	0	0	0	0	0
		38,1	0	0	0	0	0	0	0	0
		38,2	0	0	0	0	0	0	0	0
		38,3	0	0	0	0	0,4	8	0	0
		70	0	0	0	0	0	0	0	0
		71,1	0	0	0	0	0	0	0	0
		71,2	0	0	0	0	0	0	0	0
	1604870A									
		29	0	0	0	0	0	0	0	0
		37,1	0	0	0	0	1	13	0	0
		37,2	0	0	0	0	0,6	10	0	0
		37,3	0	0	0	0	0	0	0	0
		72,1	0	0	0	0	0	0	0	0
		72,2	0	0	0	0	0	0	0	0
		80	0	0	0	0				
	1604871A									
		27	0	0	0	0	0	0	0	0
		36,1	0	0	0	0	0,2	15	0	0
		36,2	0	0	0	0	0,2	4	0	0
		36,3	0	0	0	0	0	0	0	0
		36,4	0	0	0	0	1,2	7	0,1	14
		67	0	0	0	0	0	0	0	0
		68	0	0	0	0	0	0	0	0
		69	0	0	0	0	0	0	0	0
		77	0	0	0	0	0	0	0	0
		78	0	0	0	0	0	0	0	0
	1604872C									
		43,1	0	0	0	0	0	0	0	0
		43,2	0	0	0	0	0	0	0	0
		55,1	0	0	0	0	0	0	0	0
		55,2	0	0	0	0	0	0	0	0
		55,3	0	0	0	0	0	0	0	0
		56,1	0	0	0	0	0	0	0	0
		56,2	0	0	0	0	0	0	0	0
		57,1	0	0	0	0	0	0		
		57,2	0	0	0	0	0	0	0	0
		58,1	0	0	0	0	0	0	0	0
		58,2	0	0	0	0	0	0	0	0

Point LHC	Cable number	Label	Type value increase	Frequency value increase	Depth value increase	Severity value increase	Crack length increase [mm]	%	Crack width increase [mm]	%
	1604873A									
		44,2	0	0	0	0	0	0	0	0
		59	0	0	0	0	0	0	0	0
		60	0	0	0	0	0	0	0	0
		61,1	0	0	0	0	0	0	0	0
		61,2	0	0	0	0	0	0	0	0
	1604874A									
		22	0	0	0	0	0	0	0	0
	1604874C									
		82	0	0	0	0				
	1604875C									
		45,1	0	0	0	0	0	0	0	0
	1604876A									
		46,1	0	0	0	0	0	0	0	0
		46,2	0	0	0	0	0	0	0	0
		46,3	0	0	0	0	0	0	0	0
		46,4	0	0	0	0	0	0	0	0
	1604877A									
		83	0	0	0	0				
	1604878A									
		15	0	0	0	0	0	0	0	0
		16	0	0	0	0	0	0	0	0
		17	0	0	0	0	0	0	0	0
		18	0	0	0	0	0	0	0	0
	1604879A									
		19	0	0	0	0	0	0	0	0
		63	0	0	0	0	0	0	0	#Error
		64	0	0	0	0	0	0	0	0
		65	0	0	0	0	0	0	0	0
	1604880A									
		13	0	0	0	0	0	0	0	0
		14	0	0	0	0	0	0	0	0
		79	0	0	0	0				

A.7 Crack progression Point 6R

Crack-areas - Progression

Summer 2009 - Summer 2010

Point LHC	Cable number	Label	Type value increase	Frequency value increase	Depth value increase	Severity value increase	Crack length increase [mm]	%	Crack width increase [mm]	%
6R										
	1604892C									
		45	0	0	0	0				
	1604893A									
		22	0	0	0	0	0,3	2	0,1	17
		23	0	0,5	4	12,5	0	0	0,1	25
	1604894A									
		25	0	0	0	0	1,5	7	0,2	29
		27	0	0	4	12	1,3	6	0,2	50
		30	0	0	0	0	0,8	19	0,1	50
		31	0	0	0	0	0	0	0	0
	1604895A									
		28	0	0	0	0	3,3	18	0,1	12
		29	0	0	0	0	0	0	0,1	14
	1604896A									
		5	0	0	0	0	0,2	8	0	0
		32	0	0	0	0	0,4	20	0	0
		33	0	0	0	0	0,3	7	0,1	50
	1604897A									
		4	0	0	0	0	0	0	0,1	50
		34	0	0	0	0	0,1	4	New	New
		35	0	0	4	8	0	0	0,2	50
	1604898A									
		6	0	0	0	0	0,2	2	0	0
		7	0	0	0	0	0	0	0	0
		8	0	0	4	12	0,3	4	0,2	50
		43	0	0	0	0				
	1604905A									
		18	0	0	0	0	0	0	0	0
		19	0	0	0	0	0,1	2	0,1	33
		20	0	0	0	0	0,1	1	0	0
		21	0	0	0	0	0,1	1	0	0
	1604906A									
		15	0	0	0	0	0	0	0	0
		16	0	0	0	0	0,4	4	0	0
		17	0	0	0	0	1,1	4	0,3	18
		36	0	0	0	0	0	0	0	0
		38,1	0	0	0	0	0	0	0	0
		38,2	0	0	0	0	0	0	0	0

Point LHC	Cable number	Label	Type value increase	Frequency value increase	Depth value increase	Severity value increase	Crack length increase [mm]	%	Crack width increase [mm]	%
	1604907A									
		10	0	0	0	0	0	0	0	0
		11	0	0	0	0	0,8	4	0	0
		12	0	0	0	0	0	0	0	0
		37	0	0	0	0	0	0	0	0
		44	0	0	0	0				
	1604911A									
		39	0	0	0	0				
		40	0	0	0	0				
	1604912A									
		41	0	0	0	0	0	0	0	0
		42	0	0	0	0				

A.8 Affected cables Point 6L

Cables

Point LHC	Cable number	Circuit ID	Nominal diameter	Transversal cracks	Longitudinal cracks	Other faults	Severity value	Crack-areas	Max. crack length
6L									
	1604860A	RQ10.L6B2	DN 70	Yes		Yes	69	11	69,8
	1604861A	RQ10.L6B1	DN 70	Yes	Yes		28,5	7	13,6
	1604862A	RQ10.L6B1	DN 70	Yes	Yes		82,4	13	19,5
	1604863A	RQ8.L6B2	DN 70	Yes	Yes		35,2	8	9,7
	1604864A	RQ8.L6B1	DN 70	Yes	Yes		59,2	10	14,1
	1604865A	RQ8.L6B1	DN 70	Yes	Yes		17,7	9	7
	1604866A	RQF.A56-C5	DN 90		Yes		2	1	3,9
	1604866C	RQF.A56-C6	DN 90			Yes	2,5	1	9,1
	1604867A	RQF.A56-C1	DN 90	Yes	Yes		12	3	12,8
	1604867C	RQF.A56-C2	DN 90				0	0	
	1604868A	RQF.A56-C3	DN 90				0	0	
	1604868C	RQF.A56-C4	DN 90				0	0	
	1604869A	RQ9.L6B1	DN 70	Yes	Yes		18,5	7	10,6
	1604870A	RQ9.L6B1	DN 70	Yes	Yes		15	7	13,7
	1604871A	RQ9.L6B2	DN 70	Yes	Yes		41,1	10	19,1
	1604872A	RB.A56-C1	DN 90				0	0	
	1604872C	RB.A56-C2	DN 90		Yes		27,5	11	17,1
	1604873A	RB.A56-C3	DN 90	Yes	Yes		10,2	5	17,8
	1604873C	RB.A56-C4	DN 90				0	0	
	1604874A	RB.A56-C5	DN 90		Yes		1	1	2,7
	1604874C	RB.A56-C6	DN 90		Yes		1,5	1	
	1604875A	RQD.A56-C1	DN 90				0	0	
	1604875C	RQD.A56-C2	DN 90		Yes		1,5	1	10,8
	1604876A	RQD.A56-C3	DN 90		Yes		11	4	8,8
	1604876C	RQD.A56-C4	DN 90				0	0	
	1604877A	RQD.A56-C5	DN 90		Yes		1	1	
	1604877C	RQD.A56-C6	DN 90				0	0	
	1604878A	RQ5.L6B1	DN 70	Yes	Yes		11	4	14,6
	1604879A	RQ5.L6B1	DN 70	Yes	Yes		9,5	4	7,4
	1604880A	RQ5.L6B2	DN 70	Yes	Yes		6,5	3	7,6
	1604881A	RQ4.L6B2	DN 70				0	0	
	1604882A	RQ4.L6B2	DN 70				0	0	
	1604883A	RQ4.L6B1	DN 70				0	0	
	Cables:	33			**Affected:**	22			
Total cables:		33			**Total affected:**	22			

A.9 Affected cables Point 6R

Cables

Point LHC	Cable number	Circuit ID	Nominal diameter	Transversal cracks	Longitudinal cracks	Other faults	Severity value	Crack-areas	Max. crack length
6R									
	1604890A	RQD.A67-C5	DN 90				0	0	
	1604890C	RQD.A67-C6	DN 90				0	0	
	1604891A	RQD.A67-C1	DN 90				0	0	
	1604891C	RQD.A67-C2	DN 90				0	0	
	1604892A	RQD.A67-C3	DN 90				0	0	
	1604892C	RQD.A67-C4	DN 90			Yes	0,5	1	
	1604893A	RQ8.R6B2	DN 70	Yes			27,5	2	15
	1604894A	RQ8.R6B2	DN 70	Yes			47	4	24,2
	1604895A	RQ8.R6B1	DN 70	Yes			30	2	21,4
	1604896A	RQ10.R6B2	DN 70	Yes			4,5	3	4,6
	1604897A	RQ10.R6B2	DN 70	Yes			13,5	3	6
	1604898A	RQ10.R6B1	DN 70	Yes	Yes		46	4	15,1
	1604899A	RQF.A67-C1	DN 90				0	0	
	1604899C	RQF.A67-C2	DN 90				0	0	
	1604900A	RQF.A67-C3	DN 90				0	0	
	1604900C	RQF.A67-C4	DN 90				0	0	
	1604901A	RQF.A67-C5	DN 90				0	0	
	1604901C	RQF.A67-C6	DN 90				0	0	
	1604902A	RB.A67-C1	DN 90				0	0	
	1604902C	RB.A67-C2	DN 90				0	0	
	1604903A	RB.A67-C3	DN 90				0	0	
	1604903C	RB.A67-C4	DN 90				0	0	
	1604904A	RB.A67-C5	DN 90				0	0	
	1604904C	RB.A67-C6	DN 90				0	0	
	1604905A	RQ9.R6B1	DN 70	Yes			33,5	4	12,1
	1604906A	RQ9.R6B2	DN 70	Yes			64	6	30
	1604907A	RQ9.R6B2	DN 70	Yes	Yes		53	6	20,7
	1604908A	RQ4.R6B1	DN 70				0	0	
	1604909A	RQ4.R6B1	DN 70				0	0	
	1604910A	RQ4.R6B2	DN 70				0	0	
	1604911A	RQ5.R6B1	DN 70	Yes	Yes		4	2	
	1604912A	RQ5.R6B2	DN 70	Yes	Yes		13,5	2	8,5
	1604913A	RQ5.R6B2	DN 70				0	0	
	Cables:	33			**Affected:**	12			
Total cables:		33			**Total affected:**	12			

A.10 Monitoring history Point 6L

Photos

Point LHC	Cable number	Label		Photo name	Period	Date	Old
6L							
	1604860A						
		32,1					
				1604860A.32.01.20100721	Summer 2010	21.07.2010	☐
				1604860A.32.01.20090806	Summer 2009	06.08.2009	☑
				1604860.32.4.semaine 22 2008	Summer 2008	03.07.2008	☑
		32,2					
				1604860A.32.02.20100721	Summer 2010	21.07.2010	☐
				1604860A.32.02.20090810	Summer 2009	10.08.2009	☑
				1604860.32.3.semaine 22 2008	Summer 2008	03.07.2008	☑
		32,3					
				1604860A.32.03.20100721	Summer 2010	21.07.2010	☐
				1604860A.32.03.20090806	Summer 2009	06.08.2009	☑
		32,4					
				1604860A.32.04.20100831	Summer 2010	31.08.2010	☐
				1604860A.32.04.20090810	Summer 2009	10.08.2009	☑
		32,5					
				1604860A.32.05.20100721	Summer 2010	21.07.2010	☐
				1604860A.32.05.20090810	Summer 2009	10.08.2009	☑
		32,6					
				1604860A.32.06.20100831	Summer 2010	31.08.2010	☐
				1604860A.32.06.20090806	Summer 2009	06.08.2009	☑
		33					
				1604860A.33.01.20100721	Summer 2010	21.07.2010	☐
				1604860A.33.01.20090806	Summer 2009	06.08.2009	☑
				1604860.33.semaine 22 2008	Summer 2008	03.07.2008	☑
		47					
				1604860A.47.01.20100720	Summer 2010	20.07.2010	☐
				1604860A.47.01.20090810	Summer 2009	10.08.2009	☑
		62					
				1604860A.62.01.20100831	Summer 2010	31.08.2010	☐
				1604860A.62.01.20090810	Summer 2009	10.08.2009	☑
		73,1					
				1604860A.73.01.20090813	Summer 2009	13.08.2009	☐
		73,2					
				1604860A.73.02.20090813	Summer 2009	13.08.2009	☐

Point LHC	Cable number	Label		Photo name	Period	Date	Old
	1604861A						
		31					
				1604861A.31.01.20090813	Summer 2009	13.08.2009	☐
				1604861.31.1.semaine 22 2008	Summer 2008	03.07.2008	☑
		34,1					
				1604861A.34.01.20090810	Summer 2009	10.08.2009	☐
		34,2					
				1604861A.34.02.20100721	Summer 2010	21.07.2010	☐
				1604861A.34.02.20090810	Summer 2009	10.08.2009	☑
				1604861.34.2.semaine 22 2008	Summer 2008	03.07.2008	☑
		34,3					
				1604861A.34.03.20100721	Summer 2010	21.07.2010	☐
				1604861A.34.03.20090810	Summer 2009	10.08.2009	☑
				1604861.34.4.semaine 22 2008	Summer 2008	03.07.2008	☑
		34,4					
				1604861A.34.04.20100721	Summer 2010	21.07.2010	☐
				1604861A.34.04.20090810	Summer 2009	10.08.2009	☑
				1604861.34.3.semaine 22 2008	Summer 2008	03.07.2008	☑
		75					
				1604861A.75.01.20090813	Summer 2009	13.08.2009	☐
		76					
				1604861A.76.01.20090813	Summer 2009	13.08.2009	☐

Point LHC	Cable number	Label		Photo name	Period	Date	Old
	1604862A						
		30					
				1604862A.30.01.20090813	Summer 2009	13.08.2009	☐
				1604862.30.semaine 22 2008	Summer 2008	03.07.2008	☑
		35,1					
				1604862A.35.01.20100720	Summer 2010	20.07.2010	☐
				1604862A.35.01.20090810	Summer 2009	10.08.2009	☑
				1604862.35.semaine 22 2008	Summer 2008	03.07.2008	☑
		35,2					
				1604862A.35.02.20100720	Summer 2010	20.07.2010	☐
				1604862A.35.02.20090810	Summer 2009	10.08.2009	☑
				1604862.35.2.semaine 22 2008	Summer 2008	03.07.2008	☑
		35,3					
				1604862A.35.03.20100831	Summer 2010	31.08.2010	☐
				1604862A.35.03.20090810	Summer 2009	10.08.2009	☑
				1604862.35.3.semaine 22 2008	Summer 2008	03.07.2008	☑
		35,4					
				1604862A.35.04.20100720	Summer 2010	20.07.2010	☐
				1604862A.35.04.20090810	Summer 2009	10.08.2009	☑
				1604862.35.6.semaine 22 2008	Summer 2008	03.07.2008	☑
		35,5					
				1604862A.35.05.20100831	Summer 2010	31.08.2010	☐
				1604862A.35.05.20090810	Summer 2009	10.08.2009	☑
				1604862.35.5.semaine 22 2008	Summer 2008	03.07.2008	☑
		35,6					
				1604862A.35.06.20100720	Summer 2010	20.07.2010	☐
				1604862A.35.06.20090810	Summer 2009	10.08.2009	☑
		35,7					
				1604862A.35.07.20100720	Summer 2010	20.07.2010	☐
				1604862A.35.07.20090810	Summer 2009	10.08.2009	☑
		48					
				1604862A.48.01.20100720	Summer 2010	20.07.2010	☐
				1604862A.48.01.20090810	Summer 2009	10.08.2009	☑
		49,1					
				1604862A.49.01.20100720	Summer 2010	20.07.2010	☐
				1604862A.49.01.20090810	Summer 2009	10.08.2009	☑
		49,2					
				1604862A.49.02.20100720	Summer 2010	20.07.2010	☐
				1604862A.49.02.20090810	Summer 2009	10.08.2009	☑
		49,3					
				1604862A.49.03.20100720	Summer 2010	20.07.2010	☐
				1604862A.49.03.20090810	Summer 2009	10.08.2009	☑
		74					
				1604862A.74.01.20090813	Summer 2009	13.08.2009	☐

Point LHC	Cable number	Label		Photo name	Period	Date	Old
	1604863A						
		23					
				1604863A.23.01.20090813	Summer 2009	13.08.2009	☐
				1604863.23.semaine 22 2008	Summer 2008	03.07.2008	☑
		24					
				1604863A.24.01.20090813	Summer 2009	13.08.2009	☐
		39,1					
				1604863A.39.01.20100721	Summer 2010	21.07.2010	☐
				1604863A.39.01.20090810	Summer 2009	10.08.2009	☑
				1604863.39.1.semaine 22 2008	Summer 2008	03.07.2008	☑
		39,2					
				1604863A.39.02.20100721	Summer 2010	21.07.2010	☐
				1604863A.39.02.20090810	Summer 2009	10.08.2009	☑
		39,3					
				1604863A.39.03.20100721	Summer 2010	21.07.2010	☐
				1604863A.39.03.20090810	Summer 2009	10.08.2009	☑
				1604863.39.3.semaine 22 2008	Summer 2008	03.07.2008	☑
		50,1					
				1604863A.50.01.20100721	Summer 2010	21.07.2010	☐
				1604863A.50.01.20090810	Summer 2009	10.08.2009	☑
		50,2					
				1604863A.50.02.20100721	Summer 2010	21.07.2010	☐
				1604863A.50.02.20090810	Summer 2009	10.08.2009	☑
		51					
				1604863A.51.01.20100721	Summer 2010	21.07.2010	☐
				1604863A.51.01.20090810	Summer 2009	10.08.2009	☑

Point LHC	Cable number	Label		Photo name	Period	Date	Old
	1604864A						
		40,1					
				1604864A.40.01.20100721	Summer 2010	21.07.2010	☐
				1604864A.40.01.20090810	Summer 2009	10.08.2009	☑
				1604864.40.1.semaine 22 2008	Summer 2008	03.07.2008	☑
		40,2					
				1604864A.40.02.20100721	Summer 2010	21.07.2010	☐
				1604864A.40.02.20090810	Summer 2009	10.08.2009	☑
		40,3					
				1604864A.40.03.20100831	Summer 2010	31.08.2010	☐
				1604864A.40.03.20090810	Summer 2009	10.08.2009	☑
		40,4					
				1604864A.40.04.20100831	Summer 2010	31.08.2010	☐
				1604864A.40.04.20090810	Summer 2009	10.08.2009	☑
				1604864.40.2.semaine 22 2008	Summer 2008	03.07.2008	☑
		40,5					
				1604864A.40.05.20100831	Summer 2010	31.08.2010	☐
				1604864A.40.05.20090810	Summer 2009	10.08.2009	☑
				1604864.40.4.semaine 22 2008	Summer 2008	03.07.2008	☑
		44,1					
				1604864A.44.01.20100721	Summer 2010	21.07.2010	☐
				1604864A.44.01.20090810	Summer 2009	10.08.2009	☑
		52,1					
				1604864A.52.01.20100721	Summer 2010	21.07.2010	☐
				1604864A.52.01.20090810	Summer 2009	10.08.2009	☑
		52,2					
				1604864A.52.02.20100721	Summer 2010	21.07.2010	☐
				1604864A.52.02.20090810	Summer 2009	10.08.2009	☑
		52,3					
				1604864A.52.03.20100721	Summer 2010	21.07.2010	☐
				1604864A.52.03.20090810	Summer 2009	10.08.2009	☑
		52,4					
				1604864A.52.04.20100721	Summer 2010	21.07.2010	☐
				1604864A.52.04.20090810	Summer 2009	10.08.2009	☑

Point LHC	Cable number	Label		Photo name	Period	Date	Old
	1604865A						
		25					
				1604865A.25.01.20090813	Summer 2009	13.08.2009	☐
				1604863.24.semaine 22 2008	Summer 2008	03.07.2008	☑
		26					
				1604865A.26.01.20090813	Summer 2009	13.08.2009	☐
				1604865.25.semaine 22 2008	Summer 2008	03.07.2008	☑
		41					
				1604865A.41.01.20100831	Summer 2010	31.08.2010	☐
				1604865A.41.01.20090810	Summer 2009	10.08.2009	☑
				1604865.41.1.semaine 22 2008	Summer 2008	03.07.2008	☑
		42					
				1604865A.42.01.20100831	Summer 2010	31.08.2010	☐
				1604865A.42.01.20090810	Summer 2009	10.08.2009	☑
				1604865.42.2.semaine 22 2008	Summer 2008	03.07.2008	☑
		45,2					
				1604865A.45.02.20100831	Summer 2010	31.08.2010	☐
				1604865A.45.02.20090810	Summer 2009	10.08.2009	☑
		53,1					
				1604865A.53.01.20100721	Summer 2010	21.07.2010	☐
				1604865A.53.01.20090810	Summer 2009	10.08.2009	☑
		53,2					
				1604865A.53.02.20100831	Summer 2010	31.08.2010	☐
				1604865A.53.02.20090810	Summer 2009	10.08.2009	☑
		54					
				1604865A.54.01.20100721	Summer 2010	21.07.2010	☐
				1604865A.54.01.20090810	Summer 2009	10.08.2009	☑
		66					
				1604865A.66.01.20090813	Summer 2009	13.08.2009	☐
	1604866A						
		20					
				1604866A.20.01.20090813	Summer 2009	13.08.2009	☐
				1604866.20.semaine 22 2008	Summer 2008	03.07.2008	☑
	1604866C						
		81					
				Picture 362	Winter 2008	21.02.2008	☐
	1604867A						
		21,1					
				1604867A.21.01.20090813	Summer 2009	13.08.2009	☐
				1604868.21.semaine 22 2008	Summer 2008	03.07.2008	☑
		21,2					
				1604867A.21.02.20090813	Summer 2009	13.08.2009	☐
		21,3					
				1604867A.21.03.20090813	Summer 2009	13.08.2009	☐

Point LHC	Cable number	Label		Photo name	Period	Date	Old
	1604869A						
		28					
				1604869A.28.01.20090813	Summer 2009	13.08.2009	☐
				1604869.28.semaine 22 2008	Summer 2008	03.07.2008	☑
		38,1					
				1604869A.38.01.20100720	Summer 2010	20.07.2010	☐
				1604869A.38.01.20090810	Summer 2009	10.08.2009	☑
				1604869.38.1.semaine 22 2008	Summer 2008	03.07.2008	☑
		38,2					
				1604869A.38.02.20100720	Summer 2010	20.07.2010	☐
				1604869A.38.02.20090810	Summer 2009	10.08.2009	☑
				1604869.38.2.semaine 22 2008	Summer 2008	03.07.2008	☑
		38,3					
				1604869A.38.03.20100720	Summer 2010	20.07.2010	☐
				1604869A.38.03.20090810	Summer 2009	10.08.2009	☑
		70					
				1604869A.70.01.20090813	Summer 2009	13.08.2009	☐
		71,1					
				1604869A.71.01.20090813	Summer 2009	13.08.2009	☐
		71,2					
				1604869A.71.02.20090813	Summer 2009	13.08.2009	☐
	1604870A						
		29					
				1604870A.29.01.20090813	Summer 2009	13.08.2009	☐
				1604870.29.1.semaine 22 2008	Summer 2008	03.07.2008	☑
		37,1					
				1604870A.37.01.20100720	Summer 2010	20.07.2010	☐
				1604870A.37.01.20090810	Summer 2009	10.08.2009	☑
				1604870.37.1.semaine 22 2008	Summer 2008	03.07.2008	☑
		37,2					
				1604870A.37.02.20100720	Summer 2010	20.07.2010	☐
				1604870A.37.02.20090810	Summer 2009	10.08.2009	☑
		37,3					
				1604870A.37.03.20100831	Summer 2010	31.08.2010	☐
				1604870A.37.03.20090810	Summer 2009	10.08.2009	☑
				1604870.37.2.semaine 22 2008	Summer 2008	03.07.2008	☑
		72,1					
				1604870A.72.01.20090813	Summer 2009	13.08.2009	☐
		72,2					
				1604870A.72.02.20090813	Summer 2009	13.08.2009	☐
		80					
				1604870A.80.01.Observation	Winter 2008		☐

Point LHC	Cable number	Label		Photo name	Period	Date	Old
	1604871A						
		27					
				1604871A.27.01.20090813	Summer 2009	13.08.2009	☐
				1604871.27.semaine 22 2008	Summer 2008	03.07.2008	☑
		36,1					
				1604871A.36.01.20100720	Summer 2010	20.07.2010	☐
				1604871A.36.01.20090810	Summer 2009	10.08.2009	☑
				1604871.36.1.semaine 22 2008	Summer 2008	03.07.2008	☑
		36,2					
				1604871A.36.02.20100831	Summer 2010	31.08.2010	☐
				1604871A.36.02.20090810	Summer 2009	10.08.2009	☑
		36,3					
				1604871A.36.03.20100720	Summer 2010	20.07.2010	☐
				1604871A.36.03.20090810	Summer 2009	10.08.2009	☑
		36,4					
				1604871A.36.04.20100720	Summer 2010	20.07.2010	☐
				1604871A.36.04.20090810	Summer 2009	10.08.2009	☑
		67					
				1604871A.67.01.20090813	Summer 2009	13.08.2009	☐
		68					
				1604871A.68.01.20090813	Summer 2009	13.08.2009	☐
		69					
				1604871A.69.01.20090813	Summer 2009	13.08.2009	☐
		77					
				1604871A.77.01.20090813	Summer 2009	13.08.2009	☐
		78					
				1604871A.78.01.20090813	Summer 2009	13.08.2009	☐

Point LHC	Cable number	Label		Photo name	Period	Date	Old
	1604872C						
		43,1					
				1604872C.43.01.20090811	Summer 2009	11.08.2009	☐
		43,2					
				1604872C.43.02.20090811	Summer 2009	11.08.2009	☐
				1604872c.43.2.semaine 22 2008	Summer 2008	03.07.2008	☑
		55,1					
				1604872C.55.01.20090811	Summer 2009	11.08.2009	☐
		55,2					
				1604872C.55.02.20090811	Summer 2009	11.08.2009	☐
		55,3					
				1604872C.55.03.20090811	Summer 2009	11.08.2009	☐
		56,1					
				1604872C.56.01.20090811	Summer 2009	11.08.2009	☐
		56,2					
				1604872C.56.02.20090811	Summer 2009	11.08.2009	☐
		57,1					
				1604872C.57.01.20090811	Summer 2009	11.08.2009	☐
		57,2					
				1604872C.57.02.20090811	Summer 2009	11.08.2009	☐
		58,1					
				1604872C.58.01.20090811	Summer 2009	11.08.2009	☐
		58,2					
				1604872C.58.02.20090811	Summer 2009	11.08.2009	☐
	1604873A						
		44,2					
				1604873A.44.02.20090811	Summer 2009	11.08.2009	☐
				1604873a.44.3.semaine 22 2008	Summer 2008	03.07.2008	☑
		59					
				1604873A.59.01.20090811	Summer 2009	11.08.2009	☐
		60					
				1604873A.60.01.20090811	Summer 2009	11.08.2009	☐
		61,1					
				1604873A.61.01.20090811	Summer 2009	11.08.2009	☐
		61,2					
				1604873A.61.02.20090811	Summer 2009	11.08.2009	☐
	1604874A						
		22					
				1604874A.22.01.20090813	Summer 2009	13.08.2009	☐
				1604874.22.semaine 22 2008	Summer 2008	03.07.2008	☑
	1604874C						
		82					
				Picture 358	Winter 2008	21.02.2008	☐

Point LHC	Cable number	Label		Photo name	Period	Date	Old
	1604875C						
		45,1					
				1604875C.45.01.20090811	Summer 2009	11.08.2009	☐
				1604876a.45.1.semaine 22 2008	Summer 2008	03.07.2008	☑
	1604876A						
		46,1					
				1604876A.46.01.20090811	Summer 2009	11.08.2009	☐
				1604876a.45.2.semaine 22 2008	Summer 2008	03.07.2008	☑
		46,2					
				1604876A.46.02.20090811	Summer 2009	11.08.2009	☐
				1604876a.45.3.semaine 22 2008	Summer 2008	03.07.2008	☑
		46,3					
				1604876A.46.03.20090811	Summer 2009	11.08.2009	☐
		46,4					
				1604876A.46.04.20090811	Summer 2009	11.08.2009	☐
	1604877A						
		83					
				1604877A.83.01.Observation	Winter 2008		☐
	1604878A						
		15					
				1604878A.15.01.20090812	Summer 2009	12.08.2009	☐
				1604878.15.semaine 22 2008	Summer 2008	03.07.2008	☑
		16					
				1604878A.16.01.20090812	Summer 2009	12.08.2009	☐
				1604878.16.1.semaine 22 2008	Summer 2008	03.07.2008	☑
		17					
				1604878A.17.01.20090812	Summer 2009	12.08.2009	☐
				1604879.17.2.semaine 22 2008	Summer 2008	03.07.2008	☑
		18					
				1604878A.18.01.20090812	Summer 2009	12.08.2009	☐
				1604878.18.2.semaine 22 2008	Summer 2008	03.07.2008	☑
	1604879A						
		19					
				1604879A.19.01.20090812	Summer 2009	12.08.2009	☐
				1604879.19.1.semaine 22 2008	Summer 2008	03.07.2008	☑
		63					
				1604879A.63.01.20090812	Summer 2009	12.08.2009	☐
		64					
				1604879A.64.01.20090812	Summer 2009	12.08.2009	☐
		65					
				1604879A.65.01.20090812	Summer 2009	12.08.2009	☐

Point LHC	Cable number	Label		Photo name	Period	Date	Old
	1604880A						
		13					
				1604880A.13.01.20090812	Summer 2009	12.08.2009	☐
				1604880.13.semaine 22 2008	Summer 2008	03.07.2008	☑
		14					
				1604880A.14.01.20090812	Summer 2009	12.08.2009	☐
				1604880.14.semaine 22 2008	Summer 2008	03.07.2008	☑
		79					
				Picture 353	Winter 2008	21.02.2008	☐

A.11 Monitoring history Point 6R

Photos

Point LHC	Cable number	Label		Photo name	Period	Date	Old
6R							
	1604892C						
		45					
				Picture 003	Winter 2008	12.03.2008	☐
	1604893A						
		22					
				1604893A.22.01.20100831	Summer 2010	31.08.2010	☐
				1604893A.22.01.20090811	Summer 2009	11.08.2009	☑
				1604893.22	Summer 2008	26.06.2008	☑
		23					
				1604893A.23.01.20100831	Summer 2010	31.08.2010	☐
				1604893A.23.01.20090811	Summer 2009	11.08.2009	☑
				1604893.23	Summer 2008	26.06.2008	☑
	1604894A						
		25					
				1604894A.25.01.20100831	Summer 2010	31.08.2010	☐
				1604894A.25.01.20090811	Summer 2009	11.08.2009	☑
				1604894.25	Summer 2008	26.06.2008	☑
		27					
				1604894A.27.01.20100831	Summer 2010	31.08.2010	☐
				1604894A.27.01.20090811	Summer 2009	11.08.2009	☑
				1604894.27	Summer 2008	26.06.2008	☑
		30					
				1604894A.30.01.20100831	Summer 2010	31.08.2010	☐
				1604894A.30.01.20090811	Summer 2009	11.08.2009	☑
		31					
				1604894A.31.01.20100831	Summer 2010	31.08.2010	☐
				1604894A.31.01.20090811	Summer 2009	11.08.2009	☑
	1604895A						
		28					
				1604895A.28.01.20100831	Summer 2010	31.08.2010	☐
				1604895A.28.01.20090811	Summer 2009	11.08.2009	☑
				1604895.29	Summer 2008	26.06.2008	☑
		29					
				1604895A.29.01.20100831	Summer 2010	31.08.2010	☐
				1604895A.29.01.20090811	Summer 2009	11.08.2009	☑
				1604895.28	Summer 2008	26.06.2008	☑

Point LHC	Cable number	Label		Photo name	Period	Date	Old
	1604896A						
		5					
				1604896A.05.01.20100831	Summer 2010	31.08.2010	☐
				1604896A.05.01.20090811	Summer 2009	11.08.2009	☑
				1604896.3	Summer 2008	26.06.2008	☑
		32					
				1604896A.32.01.20100831	Summer 2010	31.08.2010	☐
				1604896A.32.01.20090811	Summer 2009	11.08.2009	☑
		33					
				1604896A.33.01.20100831	Summer 2010	31.08.2010	☐
				1604896A.33.01.20090811	Summer 2009	11.08.2009	☑
	1604897A						
		4					
				1604897A.04.01.20100831	Summer 2010	31.08.2010	☐
				1604897A.04.01.20090811	Summer 2009	11.08.2009	☑
				1604897.4	Summer 2008	26.06.2008	☑
		34					
				1604897A.34.01.20100831	Summer 2010	31.08.2010	☐
				1604897A.34.01.20090811	Summer 2009	11.08.2009	☑
		35					
				1604897A.35.01.20100831	Summer 2010	31.08.2010	☐
				1604897A.35.01.20090811	Summer 2009	11.08.2009	☑
	1604898A						
		6					
				1604898A.06.01.20100831	Summer 2010	31.08.2010	☐
				1604898A.06.01.20090811	Summer 2009	11.08.2009	☑
				1604898.6	Summer 2008	26.06.2008	☑
		7					
				1604898A.07.01.20100831	Summer 2010	31.08.2010	☐
				1604898A.07.01.20090811	Summer 2009	11.08.2009	☑
				1604898.7	Summer 2008	26.06.2008	☑
		8					
				1604898A.08.01.20100831	Summer 2010	31.08.2010	☐
				1604898A.08.01.20090811	Summer 2009	11.08.2009	☑
				1604898.8	Summer 2008	26.06.2008	☑
		43					
				1604898A.43.01.Observation	Winter 2008		☐

Point LHC	Cable number	Label		Photo name	Period	Date	Old
	1604905A						
		18					
				1604905A.18.01.20100831	Summer 2010	31.08.2010	☐
				1604905A.18.01.20090811	Summer 2009	11.08.2009	☑
				1604905.18	Summer 2008	26.06.2008	☑
		19					
				1604905A.19.01.20100831	Summer 2010	31.08.2010	☐
				1604905A.19.01.20090811	Summer 2009	11.08.2009	☑
				1604905.19	Summer 2008	26.06.2008	☑
		20					
				1604905A.20.01.20100831	Summer 2010	31.08.2010	☐
				1604905A.20.01.20090811	Summer 2009	11.08.2009	☑
				1604905.21	Summer 2008	26.06.2008	☑
		21					
				1604905A.21.01.20100831	Summer 2010	31.08.2010	☐
				1604905A.21.01.20090811	Summer 2009	11.08.2009	☑
	1604906A						
		15					
				1604906A.15.01.20100831	Summer 2010	31.08.2010	☐
				1604906A.15.01.20090811	Summer 2009	11.08.2009	☑
				1604906.16	Summer 2008	26.06.2008	☑
		16					
				1604906A.16.01.20100831	Summer 2010	31.08.2010	☐
				1604906A.16.01.20090811	Summer 2009	11.08.2009	☑
				1604906.17	Summer 2008	26.06.2008	☑
		17					
				1604906A.17.01.20100831	Summer 2010	31.08.2010	☐
				1604906A.17.01.20090811	Summer 2009	11.08.2009	☑
				1604906.15	Summer 2008	26.06.2008	☑
		36					
				1604906A.36.01.20090812	Summer 2009	12.08.2009	☐
		38,1					
				1604906A.38.01.20090812	Summer 2009	12.08.2009	☐
		38,2					
				1604906A.38.02.20090812	Summer 2009	12.08.2009	☐

Point LHC	Cable number	Label		Photo name	Period	Date	Old
	1604907A						
		10					
				1604907A.10.01.20100831	Summer 2010	31.08.2010	☐
				1604907A.10.01.20090811	Summer 2009	11.08.2009	☑
				1604907.10	Summer 2008	26.06.2008	☑
		11					
				1604907A.11.01.20100831	Summer 2010	31.08.2010	☐
				1604907A.11.01.20090811	Summer 2009	11.08.2009	☑
				1604907.11	Summer 2008	26.06.2008	☑
		12					
				1604907A.12.01.20100831	Summer 2010	31.08.2010	☐
				1604907A.12.01.20090811	Summer 2009	11.08.2009	☐
				1604907.12	Summer 2008	26.06.2008	☑
		37					
				1604907A.37.01.20090812	Summer 2009	12.08.2009	☐
		44					
				1604907A.44.01.Observation	Winter 2008		☐
	1604911A						
		39					
				Picture 407	Winter 2008	21.02.2008	☐
		40					
				1604911A.40.01.Observation	Winter 2008		☐
	1604912A						
		41					
				Picture 408	Winter 2008	21.02.2008	☐
		42					
				1604912A.42.01.Observation	Winter 2008		☐

Appendix B

Reinforcement layer measurement records

Disque en caoutchouc Ø76mm

Unité des mesures: mm

Moyens de mesures utilisés: loupe graduée

Précision des mesures: 0.05mm

En jaune: distance mini

En orange: distance maxi

	Disque No1	Disque No2	Disque No3
1	3.90	3.70	3.10
2	3.90	3.60	3.20
3	4.25	3.90	3.70
4	4.30	4.20	3.90
5	4.60	4.20	4.35
6	4.40	4.15	4.25
7	4.25	4.50	4.20
8	4.50	4.50	4.20
9	4.70	4.30	3.90
10	4.30	4.20	4.10
11	4.00	3.50	4.30
12	4.20	3.60	4.10
13	4.40	3.50	4.10
14	4.20	3.50	4.10
15	4.20	4.00	4.20
16	4.35	4.20	4.10
17	4.30	4.30	3.70
18	3.75	4.50	3.60
19	4.10	4.50	3.60
20	4.00	4.00	3.50
21	3.75	3.70	
22	3.70	3.80	
23	3.60	3.60	
24	3.40	3.70	

Disque en caoutchouc Ø86mm

Unité des mesures: mm

Moyens de mesures utilisés: loupe graduée

Précision des mesures: 0.05mm

En jaune: distance mini

En orange: distance maxi

	Disque No1	Disque No2	Disque No3
1	3.45	3.50	3.90
2	3.60	3.60	3.90
3	3.80	3.10	4.30
4	3.60	3.10	3.70
5	3.45	3.50	3.60
6	3.40	3.80	4.00
7	3.75	4.10	3.90
8	4.00	4.30	4.40
9	4.00	3.70	4.50
10	4.30	4.15	4.60
11	4.40	4.00	4.00
12	4.10	4.30	3.50
13	3.90	4.05	3.70
14	4.10	4.25	3.75
15	4.30	4.20	3.80
16	3.80	4.20	3.45
17	3.80	4.40	3.40
18	3.70	4.00	3.40
19	4.30	4.00	3.60
20	4.00	3.70	3.70
21	4.50		
22	4.10		
23	3.80		
24	3.75		

Disque en caoutchouc Ø106mm

Unité des mesures: mm

Moyens de mesures utilisés: loupe graduée

Précision des mesures: 0.05mm

En jaune: distance mini

En orange: distance maxi

	Disque No1	Disque No2	Disque No3
1	3.10	3.00	3.10
2	2.55	3.10	3.20
3	2.50	2.90	3.20
4	2.70	3.20	3.00
5	2.70	3.20	3.00
6	3.00	3.40	2.50
7	2.90	3.30	2.50
8	2.55	3.00	2.80
9	3.00	2.30	2.60
10	3.30	2.70	2.60
11	2.60	2.40	2.60
12	3.20	2.50	2.40
13	2.90	2.70	2.60
14	3.20	2.60	2.40
15	3.20	2.60	3.10
16	3.10	2.30	2.90
17	2.50	2.70	2.40
18	2.80	2.50	2.30
19	2.60	3.00	3.00
20	2.40	3.20	2.90
21	2.80	3.10	3.00
22	2.80	3.00	3.30
23	2.90	2.90	3.10
24	2.80	3.10	3.10
25	3.00	3.50	3.10
26	2.50	3.50	3.20
27	2.50		3.00
28	2.90		2.80
29	2.80		2.80
30	3.00		2.70
31	3.50		3.30

Appendix C

Pressure test profiles

Pressure pattern during initial test

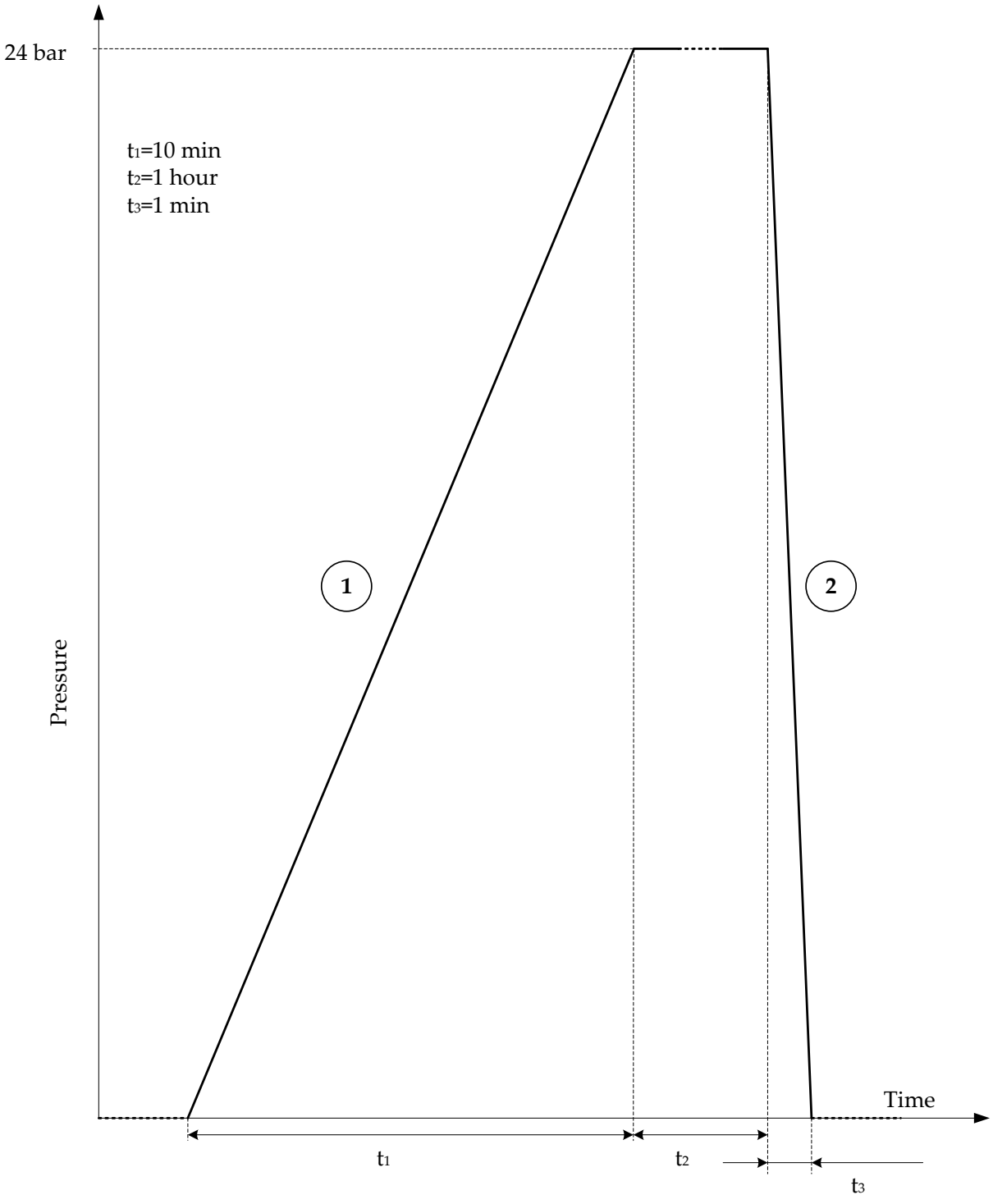

Pressure pattern during commissioning

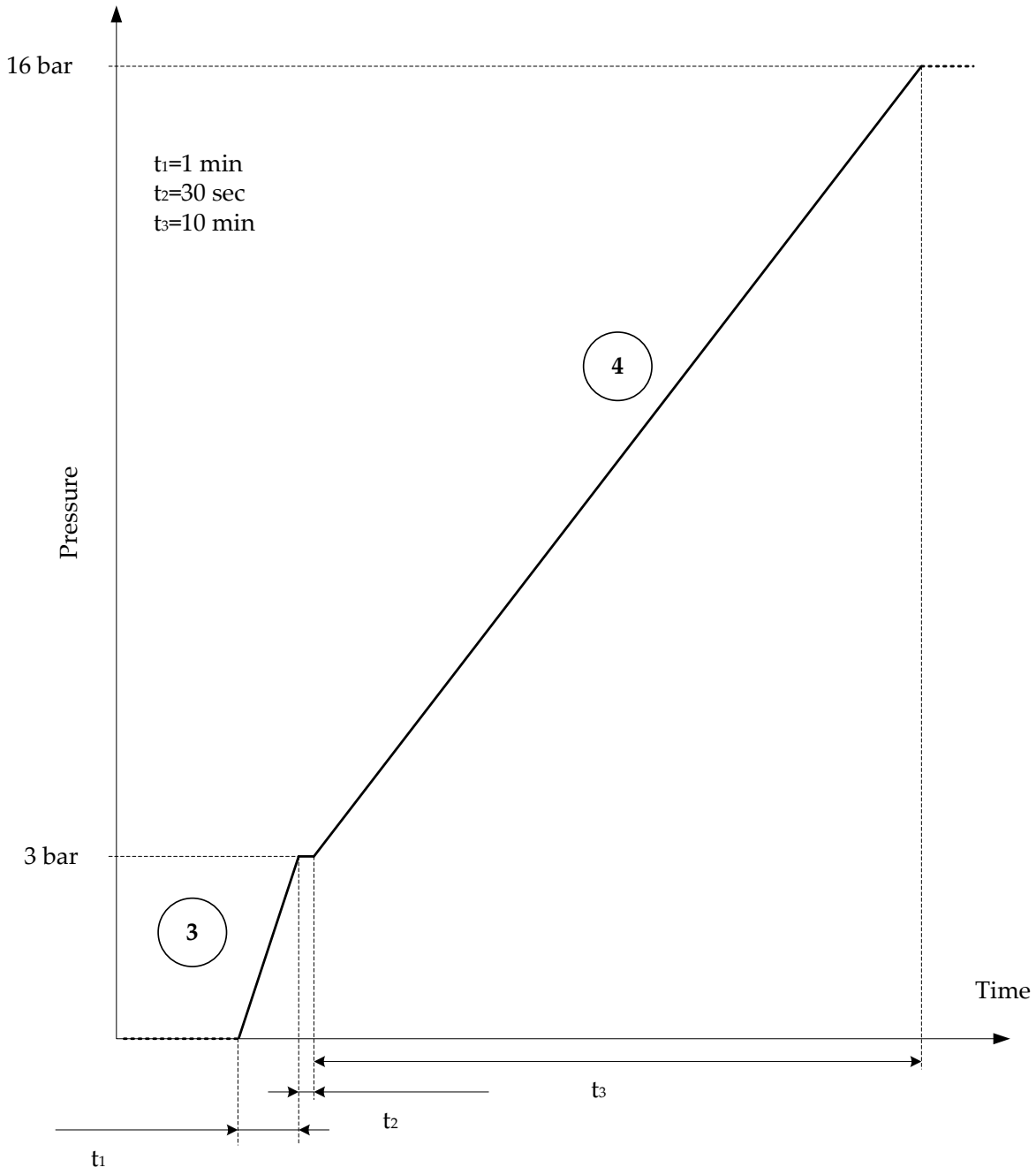

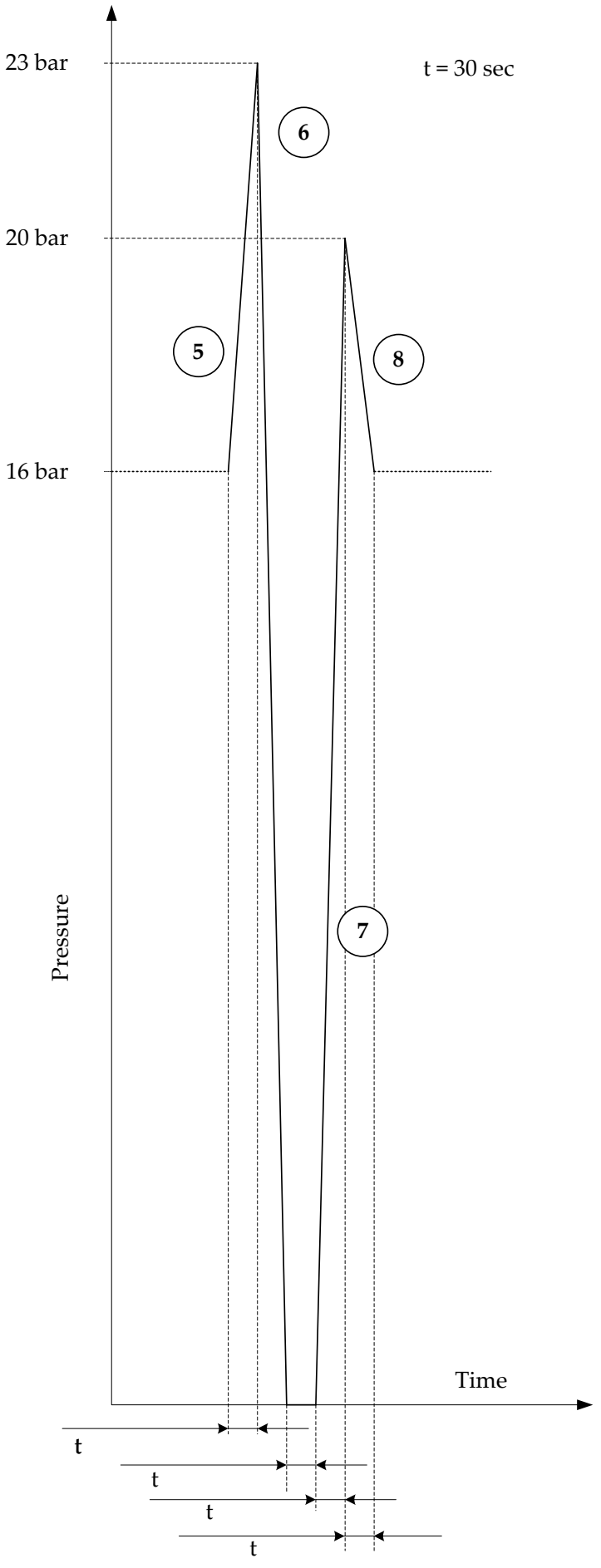

Pressure pattern during maintenance of hydraulic system

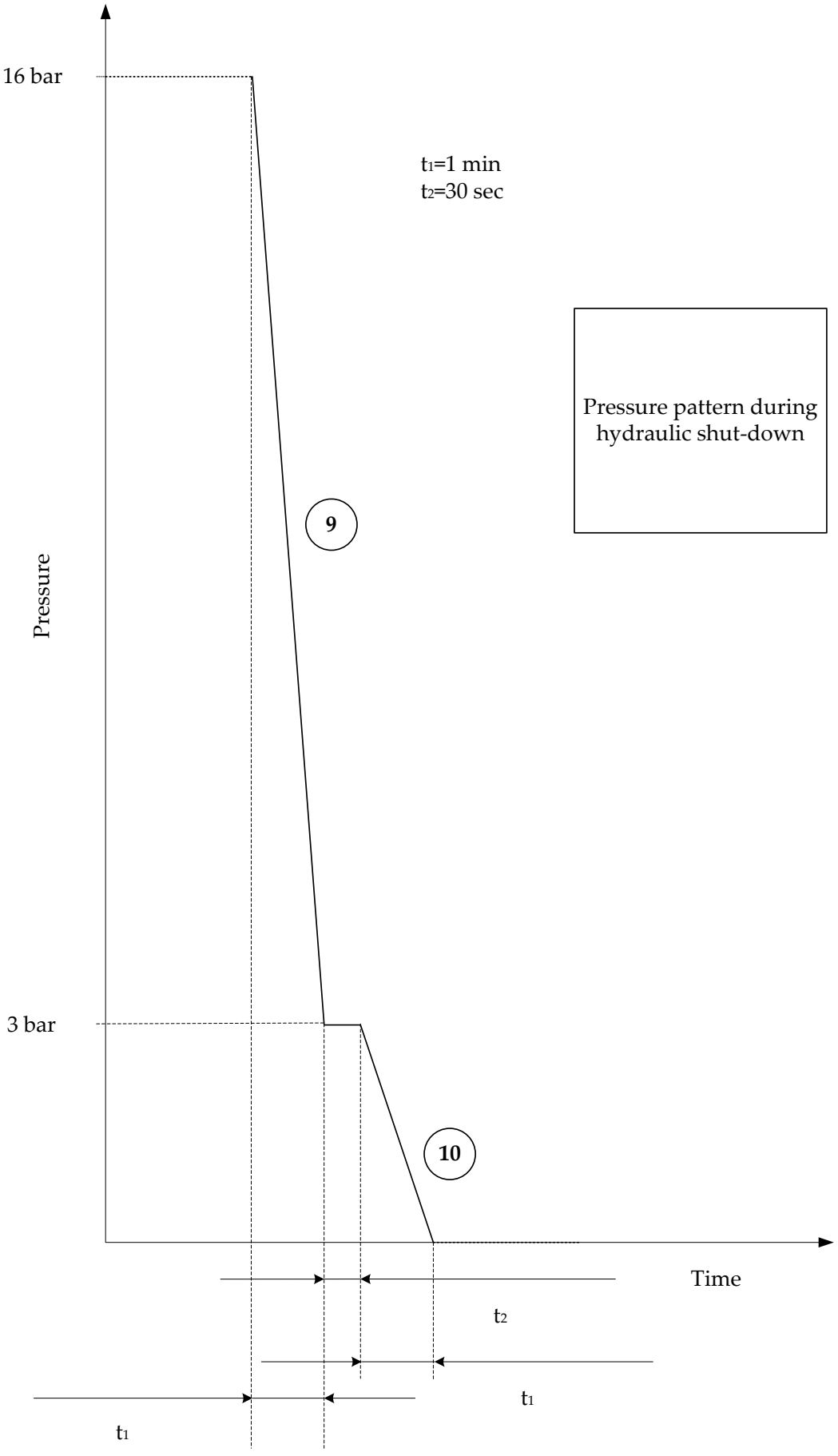
16 bar
t1=1 min
t2=30 sec
Pressure pattern during hydraulic shut-down
9
Pressure
3 bar
10
Time
t2
t1
t1

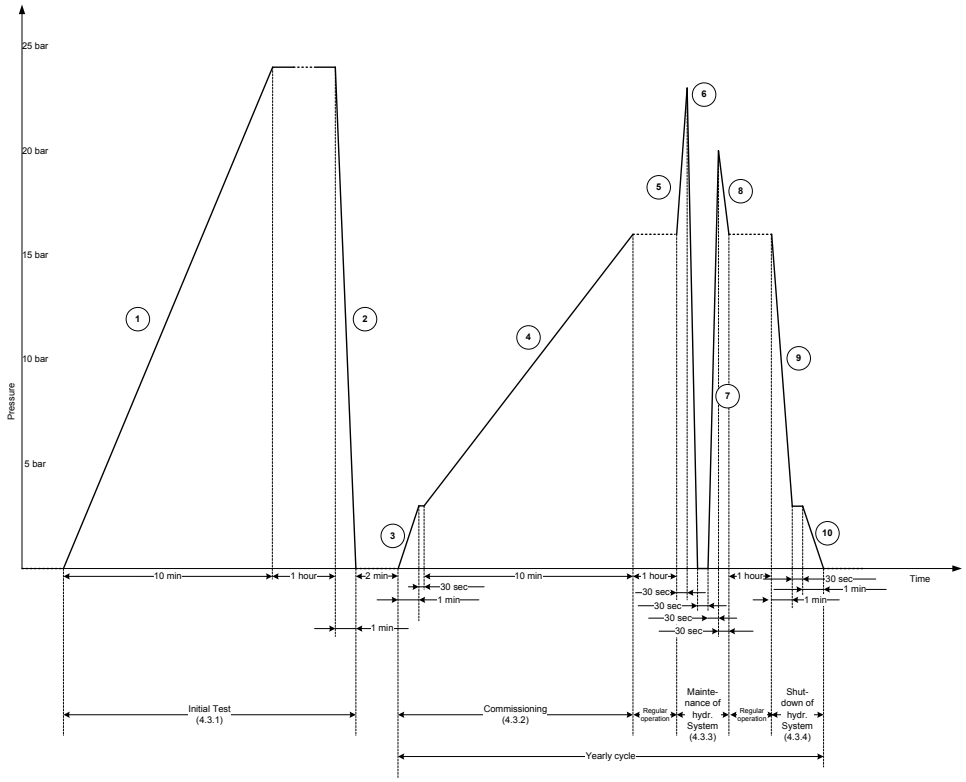
25 bar
20 bar
15 bar
10 bar
5 bar
Pressure
Time
1
2
3
4
5
6
7
8
9
10
10 min
1 hour
2 min
30 sec
1 min
Initial Test
(4.3.1)
Commissioning
(4.3.2)
Regular operation
Mainte-
nance of
hydr.
System
(4.3.3)
Shut-
down of
hydr.
System
(4.3.4)
Yearly cycle

Appendix D

Tensile test results of irradiated rubber hose samples

CERN - EN/MME/MM

Test Report

-

Engineering Department

Customer: J-C. Guillaume EN/EL
Material: Rubber + reinforcement
Operator: Ph.D
Preparation: 0 kGy
Teststandard ISO 37

Speed Step1 50.00 mm/min

Testdate: 09.04.2010
Spare Field LHC
Type of test: Tensile
Groupe of sample WCC-ALG-75-0

Gaine cable LHC	B [mm]	H [mm]	Rm [MPa]	Agt [%]
WCC-ALG-75-0	5.80	6.65	5.91	249.06
WCC-ALG-75-0-2	6.00	6.30	6.12	257.25
WCC-ALG-75-0-3	5.80	6.80	5.57	236.61
-	--			
	B [mm]	H [mm]	Rm [MPa]	Agt [%]
min	5.80	6.30	5.57	236.61
max	6.00	6.80	6.12	257.25
AM	5.87	6.58	5.87	247.64
s	0.12	0.26	0.27	10.39

Set-up

Broken sample

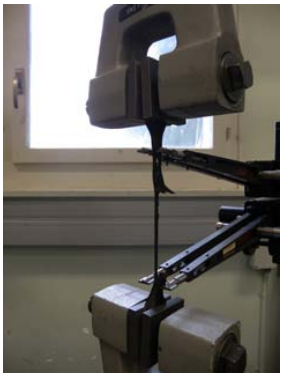

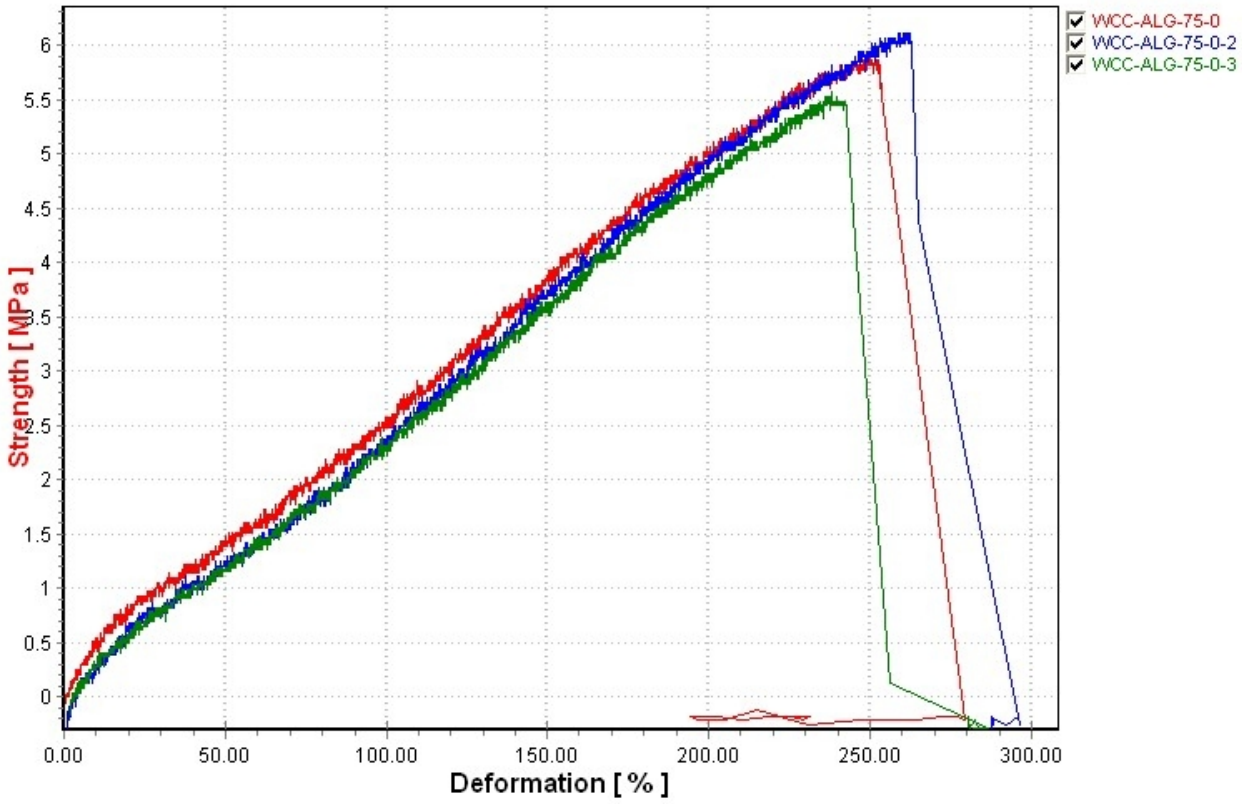

CERN - EN/MME/MM

Test Report

-

EN Engineering Department

Customer:	J-C. Guillaume EN/EL
Material:	Rubber + reinforcement
Operator:	Ph.D
Preparation:	22 kGy
Teststandard	ISO 37
Speed Step1	50.00 mm/min

Testdate:	09.06.2010
Spare Field	LHC
Type of test:	Tensile
Groupe of sample	WCC-ALG-75-22

Gaine cable LHC	B [mm]	H [mm]	Rm [MPa]	Agt [%]
WCC-ALG-75-22-1	6.09	6.30	5.86	218.14
WCC-ALG-75-22-2	6.06	6.55	5.29	188.95
WCC-ALG-75-22-3	6.00	6.30	6.33	210.09
-	--			
	B [mm]	H [mm]	Rm [MPa]	Agt [%]
min	6.00	6.30	5.29	188.95
max	6.09	6.55	6.33	218.14
AM	6.05	6.38	5.83	205.73
s	0.05	0.14	0.52	15.07

Set-up

Broken sample

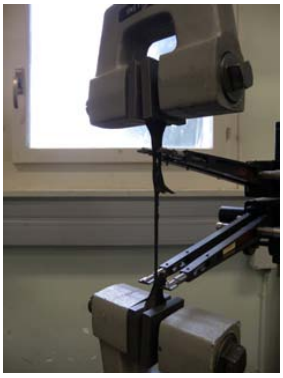

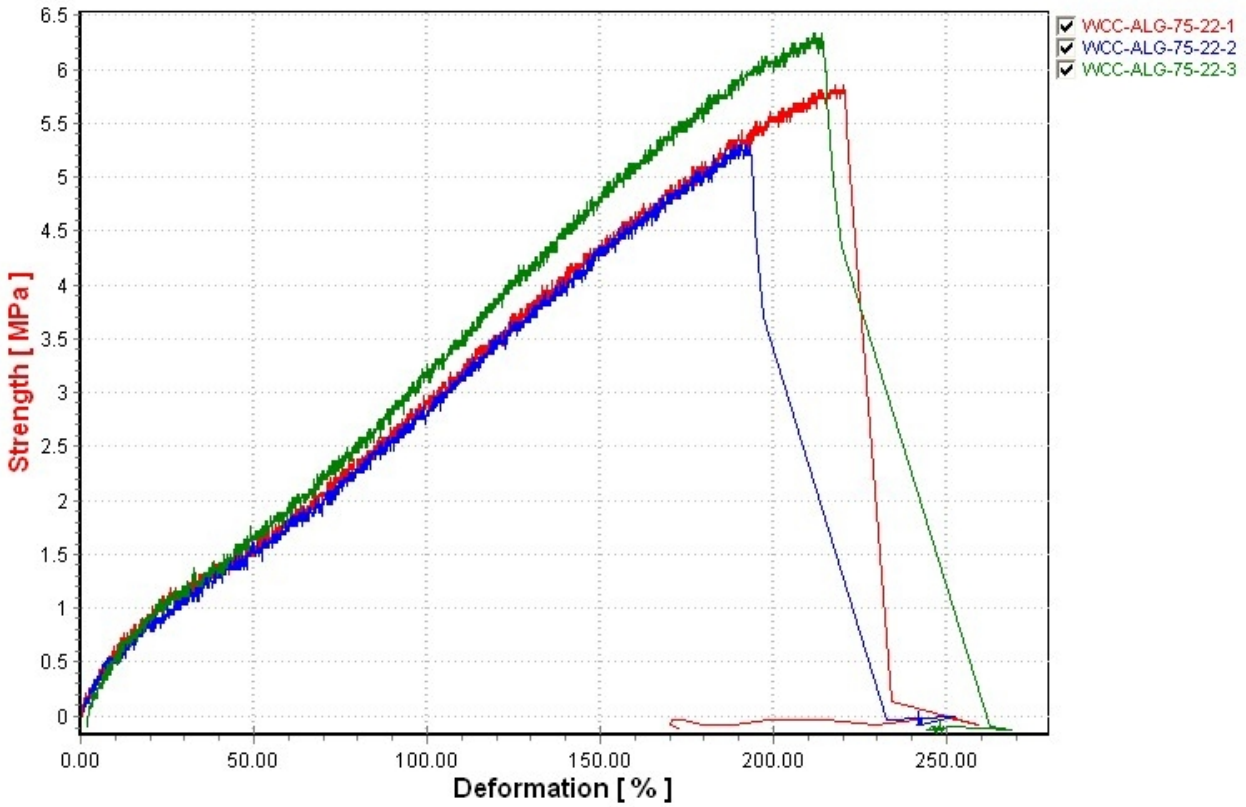

CERN - EN/MME/MM

Test Report

-

Engineering Department

Customer:	J-C. Guillaume EN/EL
Material:	Rubber + reinforcement
Operator:	Ph.D
Preparation:	100 kGy
Teststandard	ISO 37
Speed Step1	50.00 mm/min

Testdate:	09.06.2010
Spare Field	LHC
Type of test:	Tensile
Groupe of sample	WCC-ALG-75-100

Gaine cable LHC	B [mm]	H [mm]	Rm [MPa]	Agt [%]
WCC-ALG-75-100-1	6.00	6.10	6.22	211.61
WCC-ALG-75-100-2	6.00	6.55	5.42	190.37
WCC-ALG-75-100-3	6.00	6.25	5.82	203.40
-	--			
	B [mm]	H [mm]	Rm [MPa]	Agt [%]
min	6.00	6.10	5.42	190.37
max	6.00	6.55	6.22	211.61
AM	6.00	6.30	5.82	201.80
s	0.00	0.23	0.40	10.71

Set-up

Broken sample

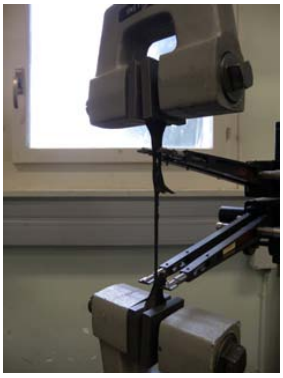

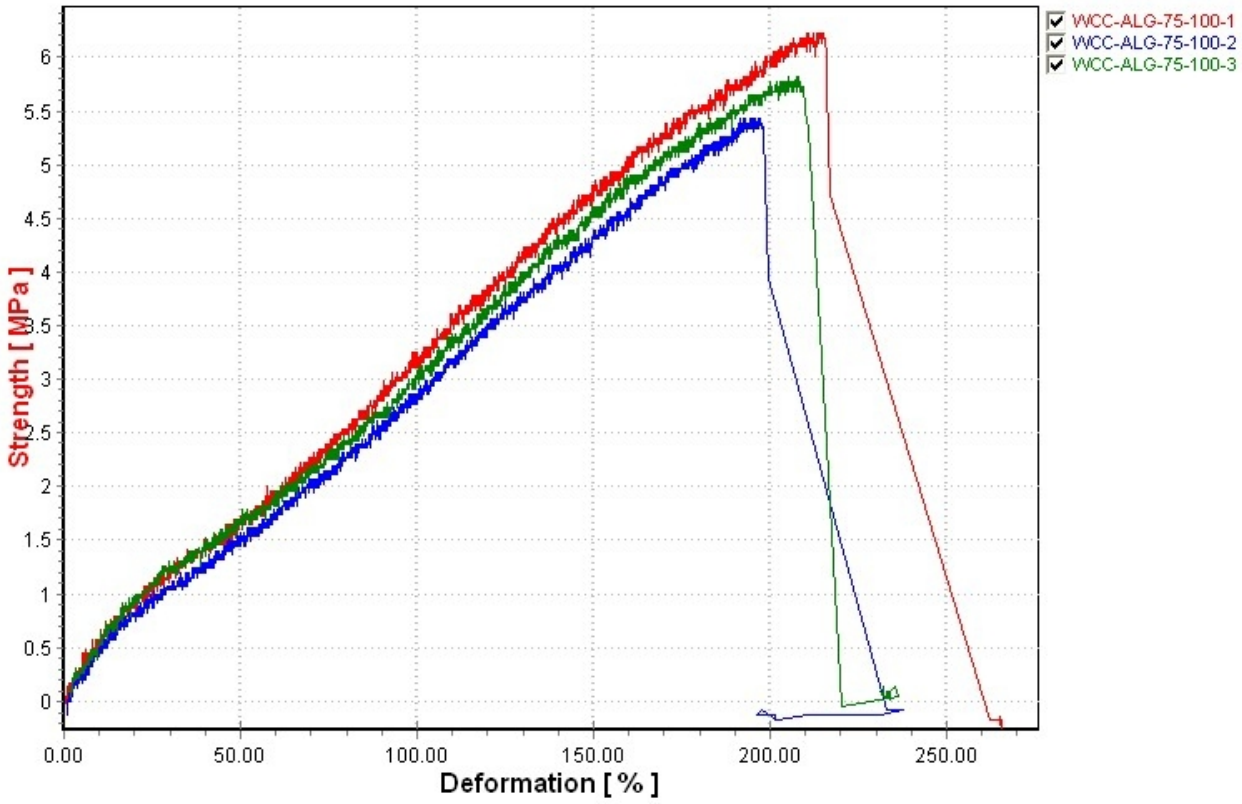

CERN - EN/MME/MM

Test Report

-

Engineering Department

Customer:	J-C. Guillaume EN/EL
Material:	Rubber + reinforcement
Operator:	Ph.D
Preparation:	250 kGy
Teststandard	ISO 37
Speed Step1	50.00 mm/min

Testdate:	16.09.2010
Spare Field	LHC
Type of test:	Tensile
Groupe of sample	WCC-ALG-75-250

Gaine cable LHC	B [mm]	H [mm]	Rm [MPa]	Agt [%]
WCC-ALG-75-250-1	6.25	6.50	5.13	164.21
WCC-ALG-75-250-2	6.15	6.45	5.13	176.25
WCC-ALG-75-250-3	6.30	6.25	5.41	165.75
-	--			
	B [mm]	H [mm]	Rm [MPa]	Agt [%]
min	6.15	6.25	5.13	164.21
max	6.30	6.50	5.41	176.25
AM	6.23	6.40	5.22	168.74
s	0.08	0.13	0.17	6.55

Set-up

Broken sample

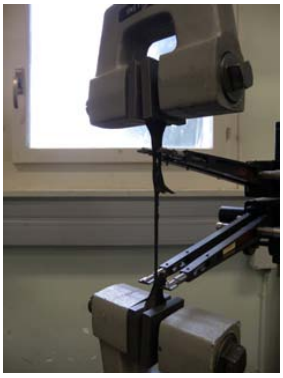

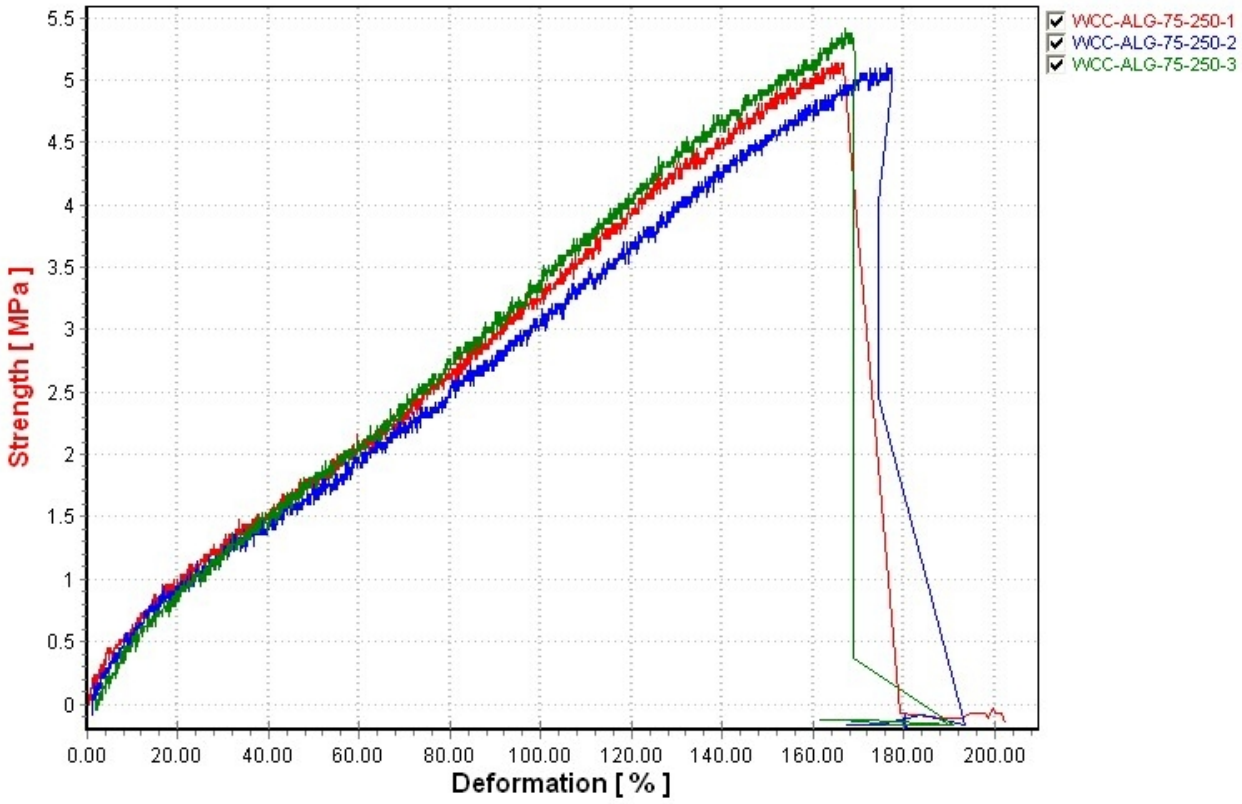

CERN - EN/MME/MM

Test Report

-

Engineering Department

Customer: J-C. Guillaume EN/EL
Material: Rubber + reinforcement
Operator: Ph.D
Preparation: 300 kGy
Teststandard ISO 37

Speed Step1 50.00 mm/min

Testdate: 16.09.2010
Spare Field LHC
Type of test: Tensile
Groupe of sample WCC-ALG-75-300

Gaine cable LHC	B [mm]	H [mm]	Rm [MPa]	Agt [%]
WCC-ALG-75-300-1	6.10	6.45	5.50	162.81
WCC-ALG-75-300-2	6.20	6.50	4.89	153.39
WCC-ALG-75-300-3	6.27	6.50	5.23	161.13
-	--			
	B [mm]	H [mm]	Rm [MPa]	Agt [%]
min	6.10	6.45	4.89	153.39
max	6.27	6.50	5.50	162.81
AM	6.19	6.48	5.21	159.11
s	0.09	0.03	0.31	5.03

Set-up

Broken sample

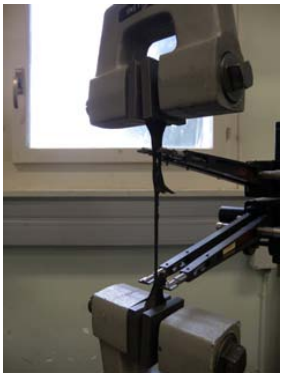

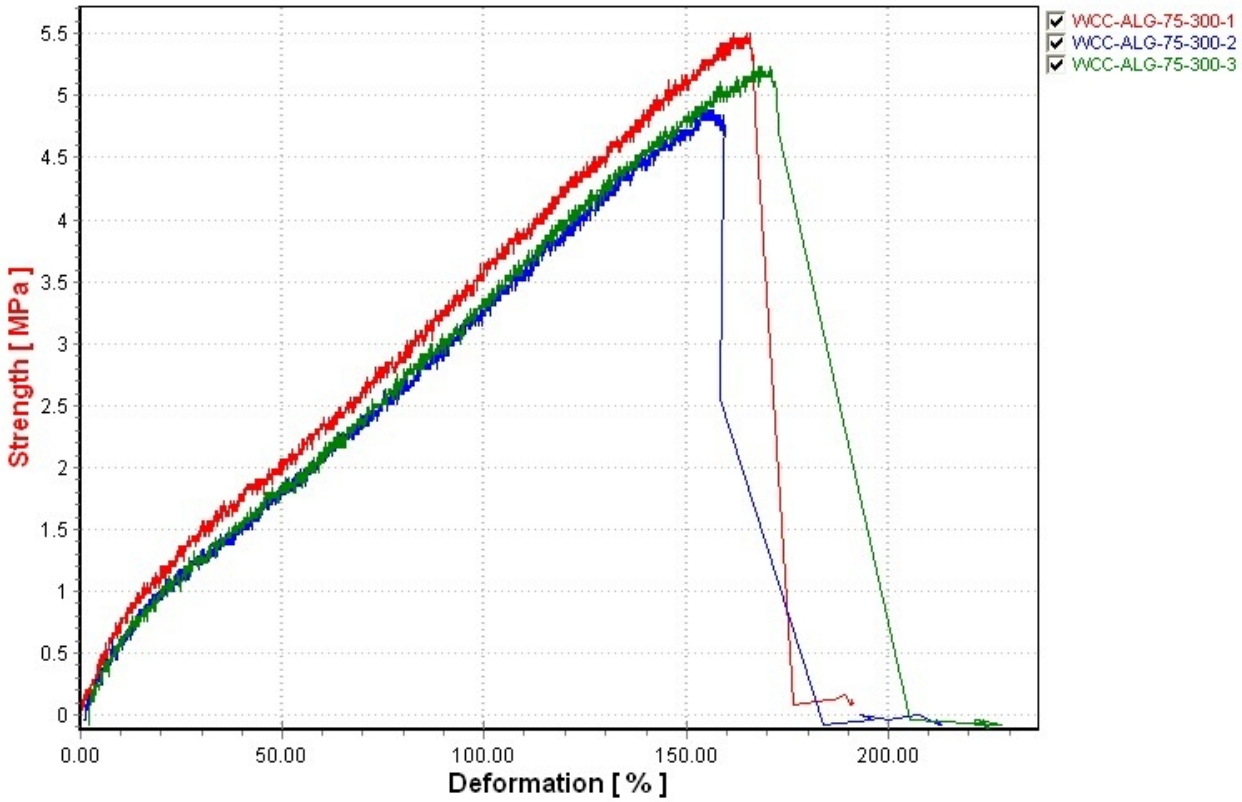

CERN - EN/MME/MM

Test Report

-

Engineering Department

Customer:	J-C. Guillaume EN/EL
Material:	Rubber + reinforcement
Operator:	Ph.D
Preparation:	330 kGy
Teststandard	ISO 37
Speed Step1	50.00 mm/min

Testdate:	17.09.2010
Spare Field	LHC
Type of test:	Tensile
Groupe of sample	WCC-ALG-75-330

Gaine cable LHC	B [mm]	H [mm]	Rm [MPa]	Agt [%]
WCC-ALG-75-330-1	6.15	6.35	4.96	145.18
WCC-ALG-75-330-2	6.10	6.40	5.05	155.52
WCC-ALG-75-330-3	6.10	6.30	5.16	144.54
-	--			
	B [mm]	H [mm]	Rm [MPa]	Agt [%]
min	6.10	6.30	4.96	144.54
max	6.15	6.40	5.16	155.52
AM	6.12	6.35	5.06	148.41
s	0.03	0.05	0.10	6.16

Set-up

Broken sample

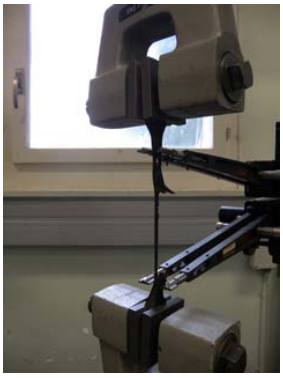

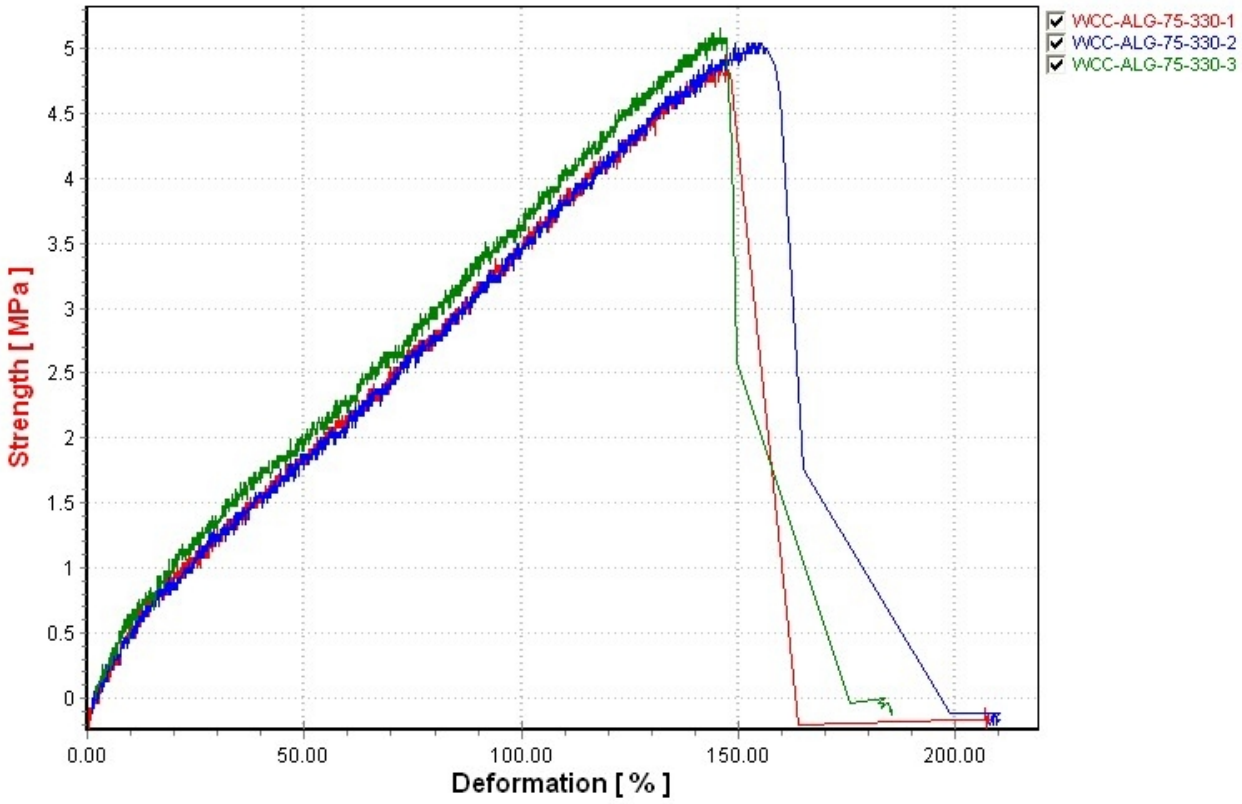

CERN - EN/MME/MM

Test Report

-

Engineering Department

Customer: J-C. Guillaume EN/EL
Material: Rubber + reinforcement
Operator: Ph.D
Preparation: 0 kGy
Teststandard ISO 37

Speed Step1 50.00 mm/min

Testdate: 09.04.2010
Spare Field LHC
Type of test: Tensile
Groupe of sample WCC-ALG-100-0

Gaine cable LHC	B [mm]	H [mm]	Rm [MPa]	Agt [%]
WCC-ALG-100-0	6.10	7.40	4.47	246.79
WCC-ALG-100-0-2	6.10	7.40	4.79	224.40
WCC-ALG-100-0-3	6.00	7.15	4.67	258.71
-	--			
	B [mm]	H [mm]	Rm [MPa]	Agt [%]
min	6.00	7.15	4.47	224.40
max	6.10	7.40	4.79	258.71
AM	6.07	7.32	4.64	243.30
s	0.06	0.14	0.16	17.42

Set-up

Broken sample

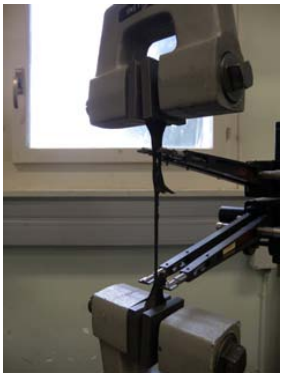

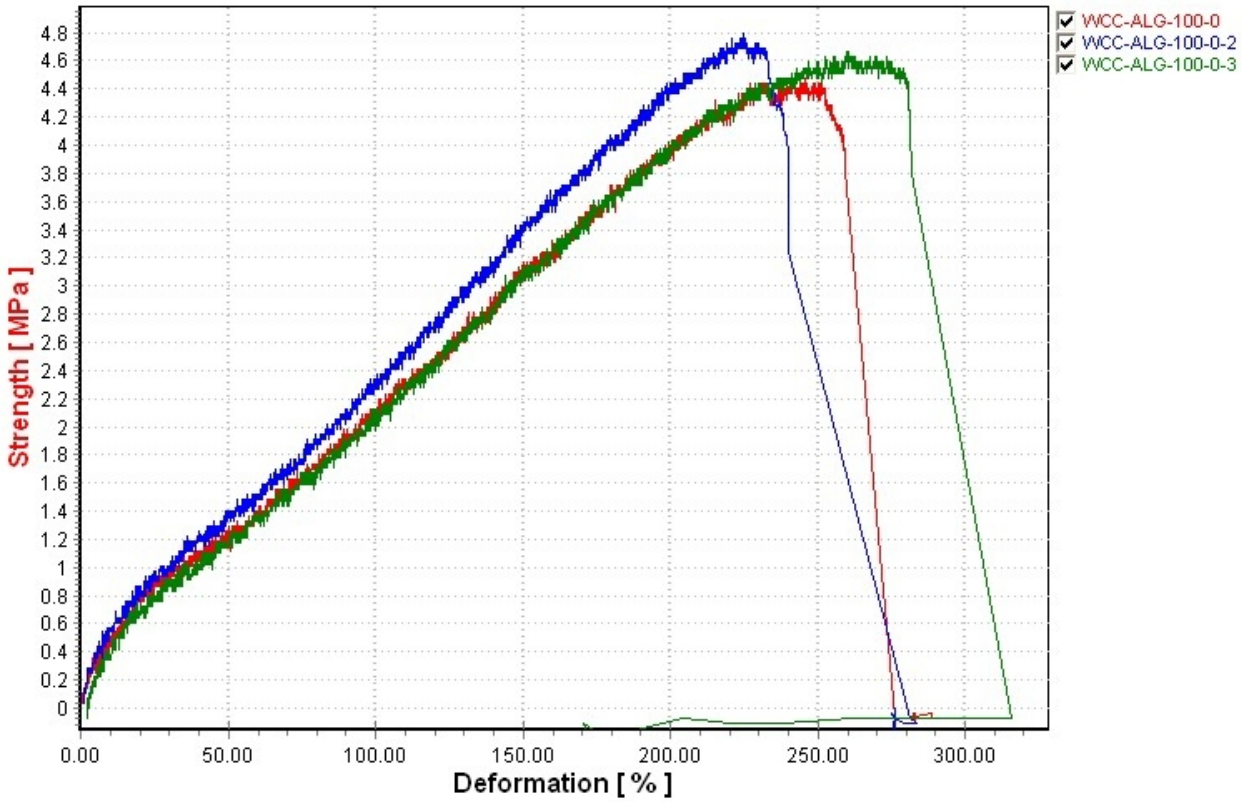

CERN - EN/MME/MM

Test Report

-

Engineering Department

Customer:	J-C. Guillaume EN/EL
Material:	Rubber + reinforcement
Operator:	Ph.D
Preparation:	100 kGy
Teststandard	ISO 37
Speed Step1	50.00 mm/min

Testdate:	09.06.2010
Spare Field	LHC
Type of test:	Tensile
Groupe of sample	WCC-ALG-100-22

Gaine cable LHC	B [mm]	H [mm]	Rm [MPa]	Agt [%]
WCC-ALG-100-22-1	6.00	7.20	4.56	185.17
WCC-ALG-100-22-2	6.10	7.30	4.50	209.12
WCC-ALG-100-22-3	6.04	7.20	4.71	228.61
-	--			
	B [mm]	H [mm]	Rm [MPa]	Agt [%]
min	6.00	7.20	4.50	185.17
max	6.10	7.30	4.71	228.61
AM	6.05	7.23	4.59	207.63
s	0.05	0.06	0.11	21.76

Set-up

Broken sample

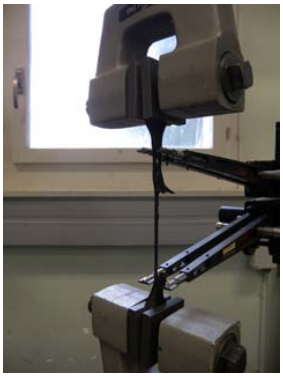

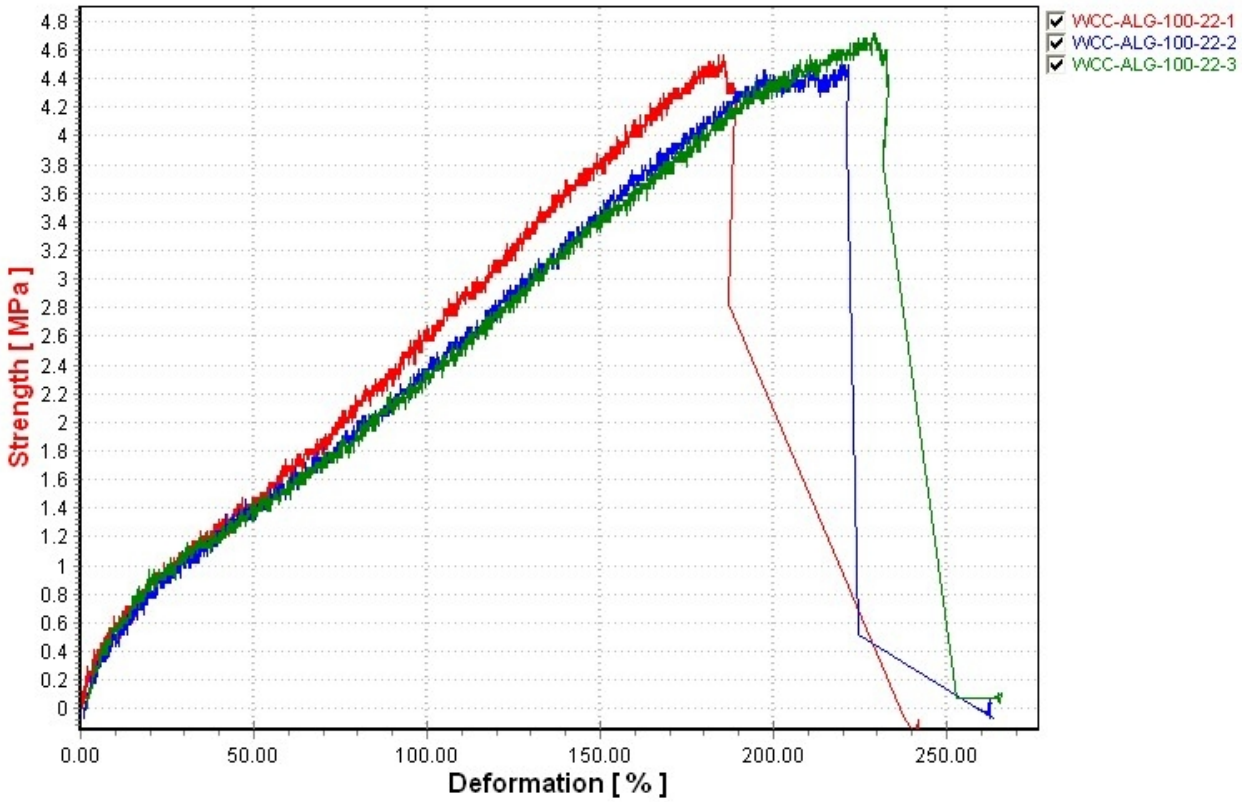

CERN - EN/MME/MM

Test Report

-

EN Engineering Department

Customer:	J-C. Guillaume EN/EL
Material:	Rubber + reinforcement
Operator:	Ph.D
Preparation:	100 kGy
Teststandard	ISO 37
Speed Step1	50.00 mm/min

Testdate:	09.06.2010
Spare Field	LHC
Type of test:	Tensile
Groupe of sample	WCC-ALG-100-100

Gaine cable LHC	B [mm]	H [mm]	Rm [MPa]	Agt [%]
WCC-ALG-100-100-1	6.05	7.00	4.31	199.47
WCC-ALG-100-100-2	6.00	7.25	4.38	174.79
WCC-ALG-100-100-3	6.10	6.95	4.49	192.04
-	--			
	B [mm]	H [mm]	Rm [MPa]	Agt [%]
min	6.00	6.95	4.31	174.79
max	6.10	7.25	4.49	199.47
AM	6.05	7.07	4.39	188.77
s	0.05	0.16	0.09	12.66

Set-up

Broken sample

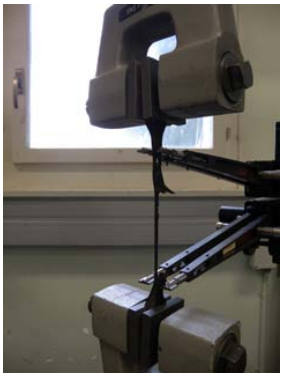

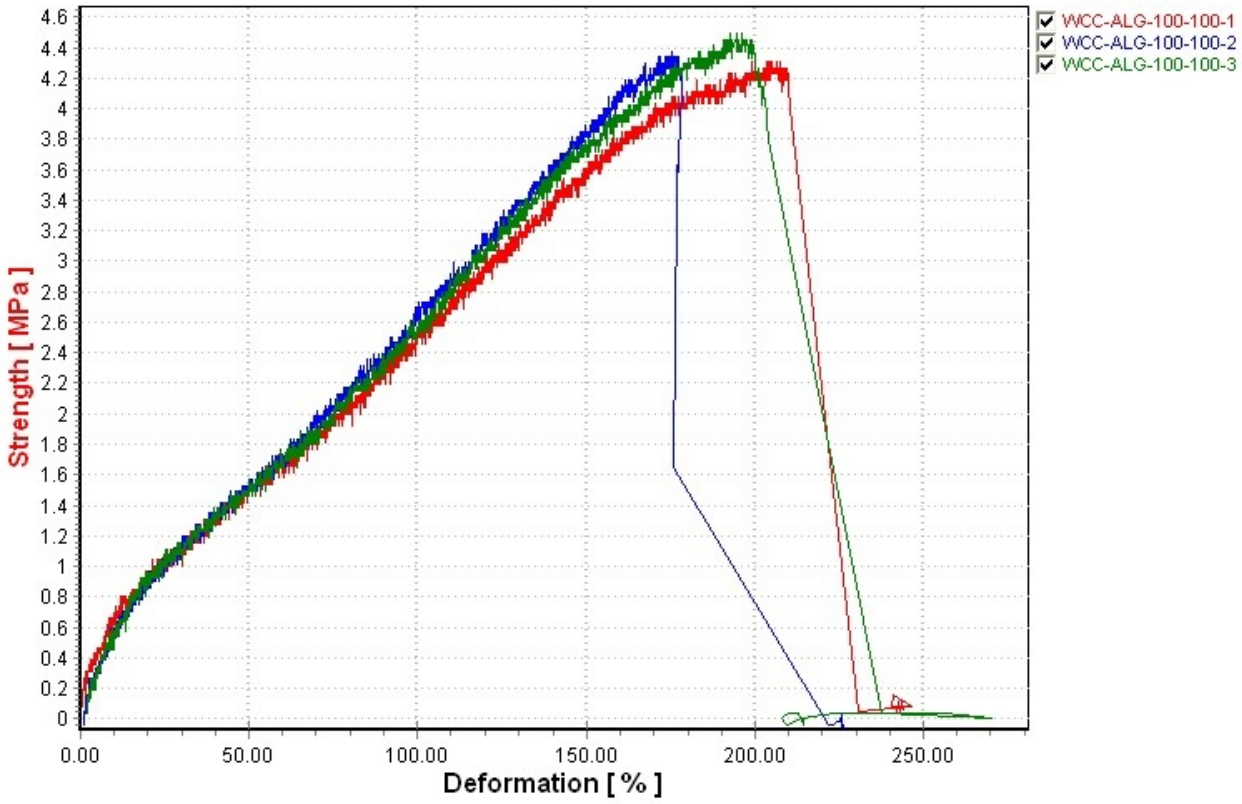

CERN - EN/MME/MM

Test Report

-

EN Engineering Department

Customer:	J-C. Guillaume EN/EL
Material:	Rubber + reinforcement
Operator:	Ph.D
Preparation:	250 kGy
Teststandard	ISO 37
Speed Step1	50.00 mm/min

Testdate:	16.09.2010
Spare Field	LHC
Type of test:	Tensile
Groupe of sample	WCC-ALG-100-250

Gaine cable LHC	B [mm]	H [mm]	Rm [MPa]	Agt [%]
WCC-ALG-100-250-1	6.10	7.10	3.87	164.98
WCC-ALG-100-250-2	6.10	7.25	4.05	182.61
WCC-ALG-100-250-3	6.10	7.20	3.97	163.14
-	--			
	B [mm]	H [mm]	Rm [MPa]	Agt [%]
min	6.10	7.10	3.87	163.14
max	6.10	7.25	4.05	182.61
AM	6.10	7.18	3.96	170.24
s	0.00	0.08	0.09	10.75

Set-up

Broken sample

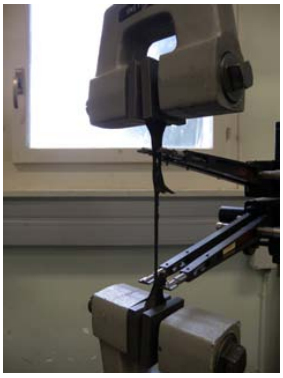

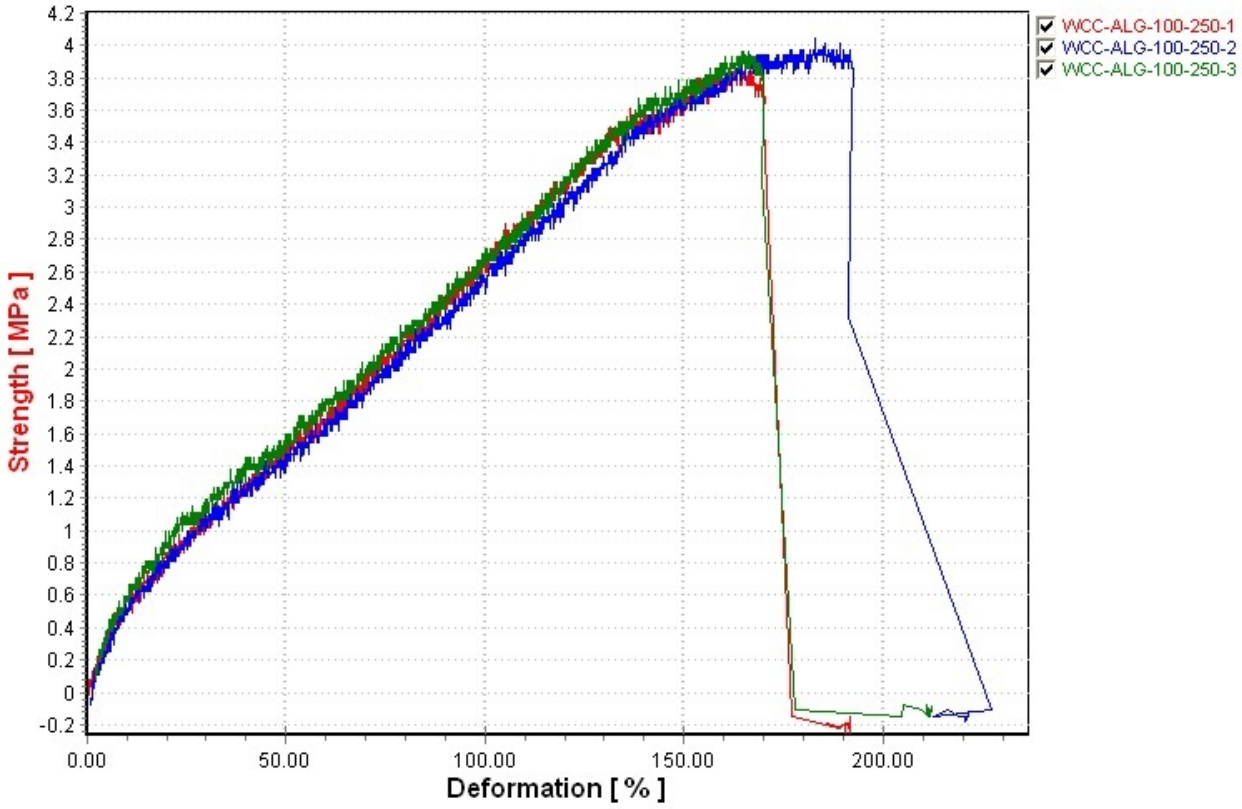

CERN - EN/MME/MM

Test Report

-

EN Engineering Department

Customer:	J-C. Guillaume EN/EL		
Material:	Rubber + reinforcement		
Operator:	Ph.D		
Preparation:	300 kGy	Testdate:	16.09.2010
Teststandard	ISO 37	Spare Field	LHC
		Type of test:	Tensile
Speed Step1	50.00 mm/min	Groupe of sample	WCC-ALG-100-300

Gaine cable LHC	B [mm]	H [mm]	Rm [MPa]	Agt [%]
WCC-ALG-100-300-1	6.10	7.55	3.99	152.54
WCC-ALG-100-300-2	6.04	7.50	4.31	179.53
WCC-ALG-100-300-3	6.25	7.50	3.78	172.92
-	--			
	B [mm]	H [mm]	Rm [MPa]	Agt [%]
min	6.04	7.50	3.78	152.54
max	6.25	7.55	4.31	179.53
AM	6.13	7.52	4.03	168.33
s	0.11	0.03	0.26	14.07

Set-up

Broken sample

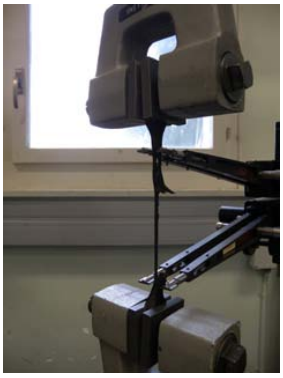

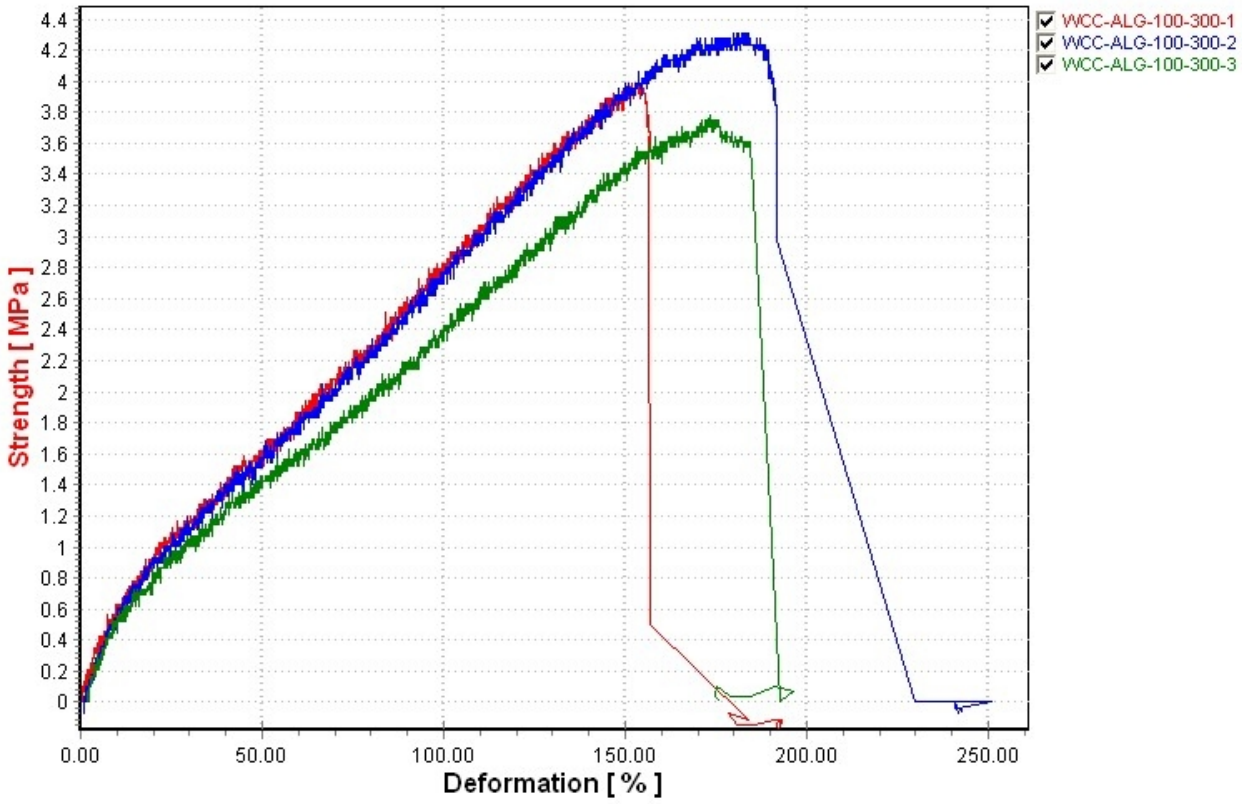

CERN - EN/MME/MM

Test Report

-

Engineering Department

Customer:	J-C. Guillaume EN/EL
Material:	Rubber + reinforcement
Operator:	Ph.D
Preparation:	330 kGy
Teststandard	ISO 37
Speed Step1	50.00 mm/min

Testdate:	17.09.2010
Spare Field	LHC
Type of test:	Tensile
Groupe of sample	WCC-ALG-100-330

Gaine cable LHC	B [mm]	H [mm]	Rm [MPa]	Agt [%]
WCC-ALG-100-330-1	6.20	7.00	3.45	162.19
WCC-ALG-100-330-2	6.20	7.25	3.91	140.28
WCC-ALG-100-330-3	6.20	7.25	3.40	157.40
-	--			
	B [mm]	H [mm]	Rm [MPa]	Agt [%]
min	6.20	7.00	3.40	140.28
max	6.20	7.25	3.91	162.19
AM	6.20	7.17	3.59	153.29
s	0.00	0.14	0.28	11.52

Set-up

Broken sample

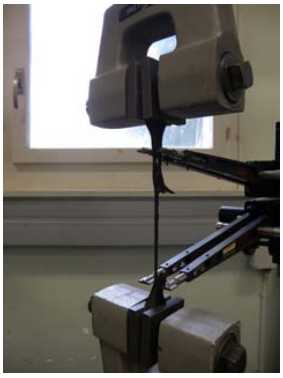

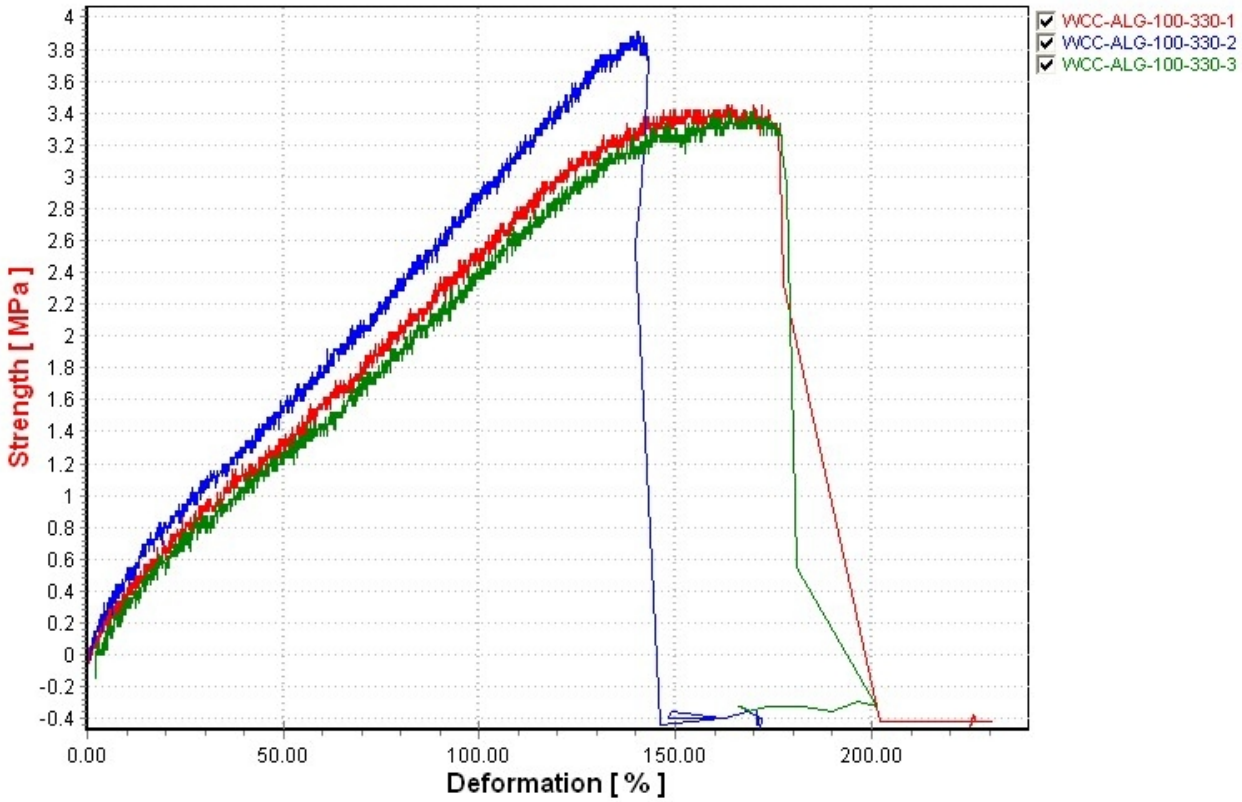

CERN - EN/MME/MM

Test Report

-

Engineering Department

Customer:	J-C. Guillaume EN/EL
Material:	Rubber + reinforcement
Operator:	Ph.D
Preparation:	0 kGy
Teststandard	ISO 37
Speed Step1	50.00 mm/min

Testdate:	09.04.2010
Spare Field	LHC
Type of test:	Tensile
Groupe of sample	WCC-CON-60-0

Gaine cable LHC	B [mm]	H [mm]	Rm [MPa]	Agt [%]
WCC-CON-60-0	6.13	8.15	2.80	274.71
WCC-CON-60-0-2	6.07	6.70	2.48	234.82
WCC-CON-60-0-3	6.25	8.30	2.42	254.93
-	--			

	B [mm]	H [mm]	Rm [MPa]	Agt [%]
min	6.07	6.70	2.42	234.82
max	6.25	8.30	2.80	274.71
AM	6.15	7.72	2.57	254.82
s	0.09	0.88	0.21	19.95

Set-up

Broken sample

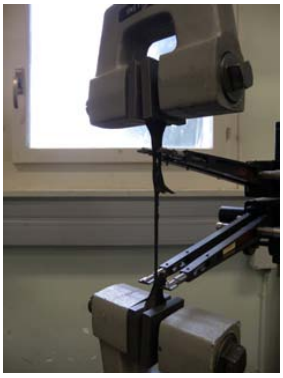

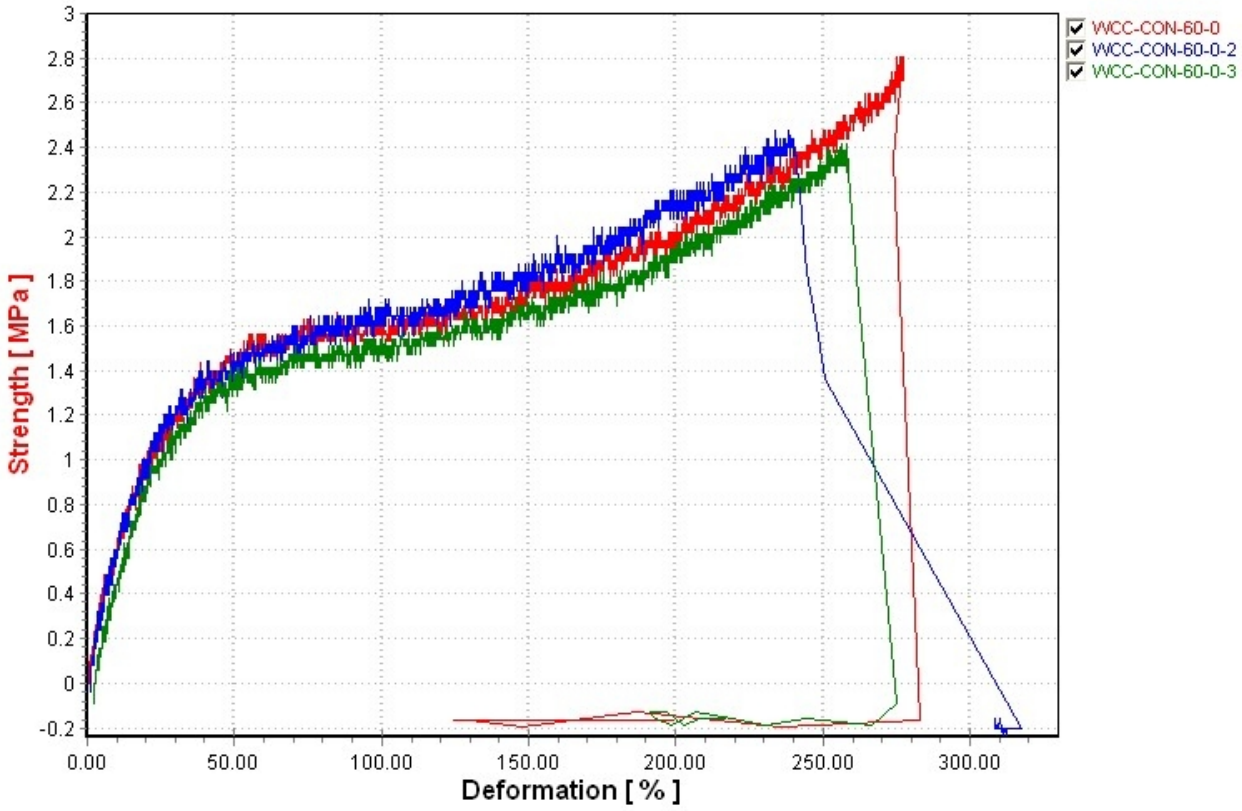

CERN - EN/MME/MM

Test Report

-

Engineering Department

Customer: J-C. Guillaume EN/EL
Material: Rubber + reinforcement
Operator: Ph.D
Preparation: 22 kGy
Teststandard ISO 37

Speed Step1 50.00 mm/min

Testdate: 21.04.2010
Spare Field LHC
Type of test: Tensile
Groupe of sample WCC-CON-60-22

Gaine cable LHC	B [mm]	H [mm]	Rm [MPa]	Agt [%]
WCC-CON-60-22	6.30	7.70	2.35	250.34
WCC-CON-60-22-2	6.10	8.15	2.75	242.15
WCC-CON-60-22-3	6.20	7.80	2.76	233.19
-	--			

	B [mm]	H [mm]	Rm [MPa]	Agt [%]
min	6.10	7.70	2.35	233.19
max	6.30	8.15	2.76	250.34
AM	6.20	7.88	2.62	241.89
s	0.10	0.24	0.23	8.58

Set-up

Broken sample

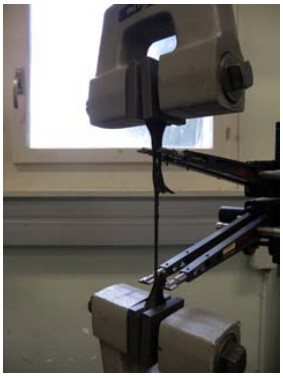

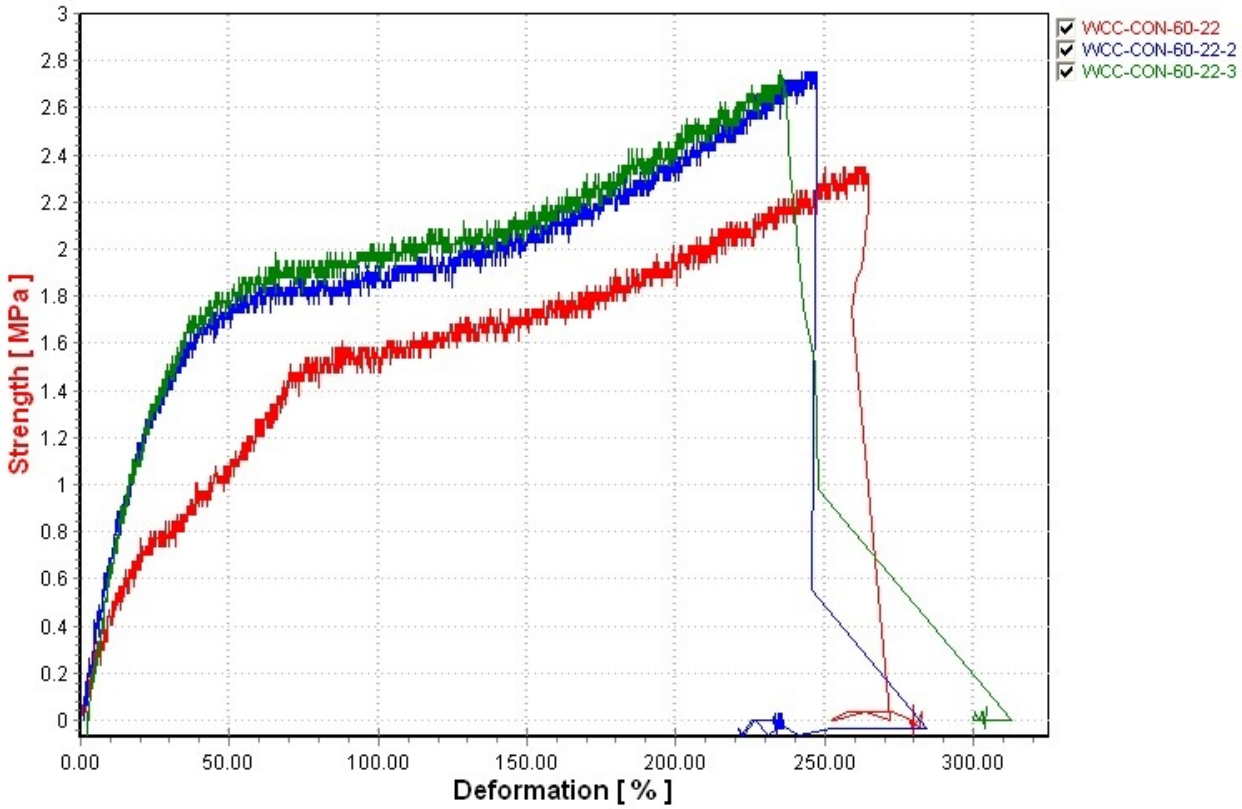

CERN - EN/MME/MM

Test Report

-

EN Engineering Department

Customer: J-C. Guillaume EN/EL
Material: Rubber + reinforcement
Operator: Ph.D
Preparation: Total Dose Point
Teststandard ISO 37

Speed Step1 50.00 mm/min

Testdate: 21.04.2010
Spare Field LHC
Type of test: Tensile
Groupe of sample WCC-CON-60-100

Gaine cable LHC	B [mm]	H [mm]	Rm [MPa]	Agt [%]
WCC-CON-60-100	6.25	6.70	2.72	216.90
WCC-CON-60-100-2	6.14	7.50	2.48	166.83
WCC-CON-60-100-3	6.20	6.60	2.46	143.67
-	--			
	B [mm]	H [mm]	Rm [MPa]	Agt [%]
min	6.14	6.60	2.46	143.67
max	6.25	7.50	2.72	216.90
AM	6.20	6.93	2.55	175.80
s	0.06	0.49	0.15	37.43

Set-up

Broken sample

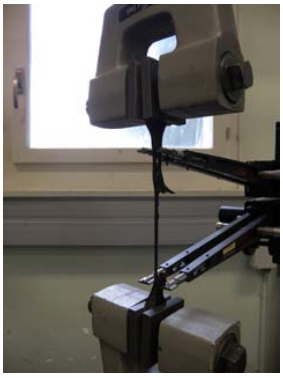

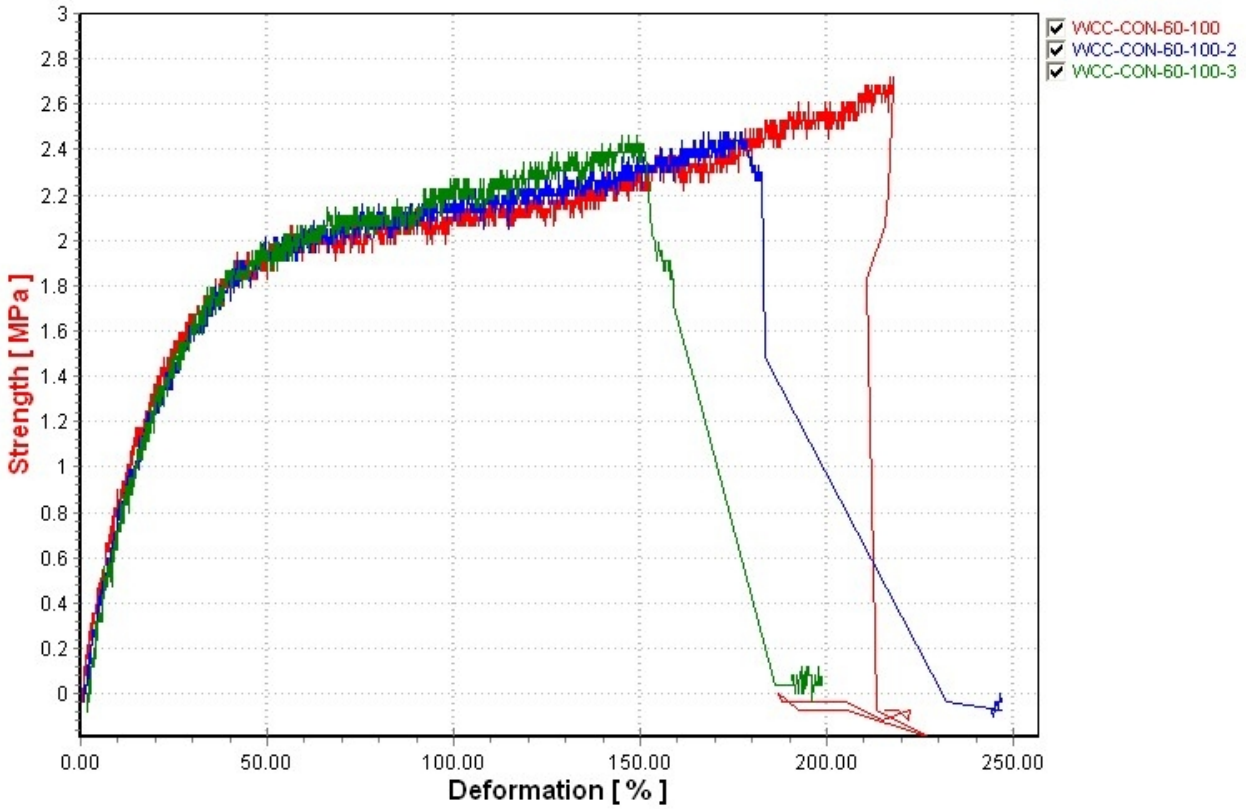

CERN - EN/MME/MM

Test Report

-

EN Engineering Department

Customer:	J-C. Guillaume EN/EL
Material:	Rubber + reinforcement
Operator:	Ph.D
Preparation:	250 kGy
Teststandard	ISO 37
Speed Step1	50.00 mm/min

Testdate:	21.04.2010
Spare Field	LHC
Type of test:	Tensile
Groupe of sample	WCC-CON-60-250

Gaine cable LHC	B [mm]	H [mm]	Rm [MPa]	Agt [%]
WCC-CON-60-250	6.15	8.10	2.71	97.99
WCC-CON-60-250-2	6.15	7.40	2.65	98.97
WCC-CON-60-250-3	6.10	7.30	2.78	116.19
-	--			
	B [mm]	H [mm]	Rm [MPa]	Agt [%]
min	6.10	7.30	2.65	97.99
max	6.15	8.10	2.78	116.19
AM	6.13	7.60	2.71	104.38
s	0.03	0.44	0.07	10.24

Set-up

Broken sample

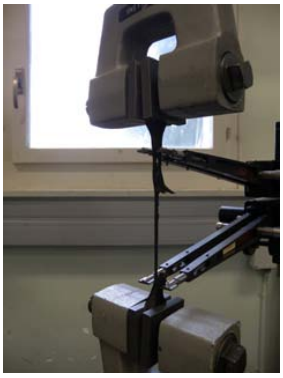

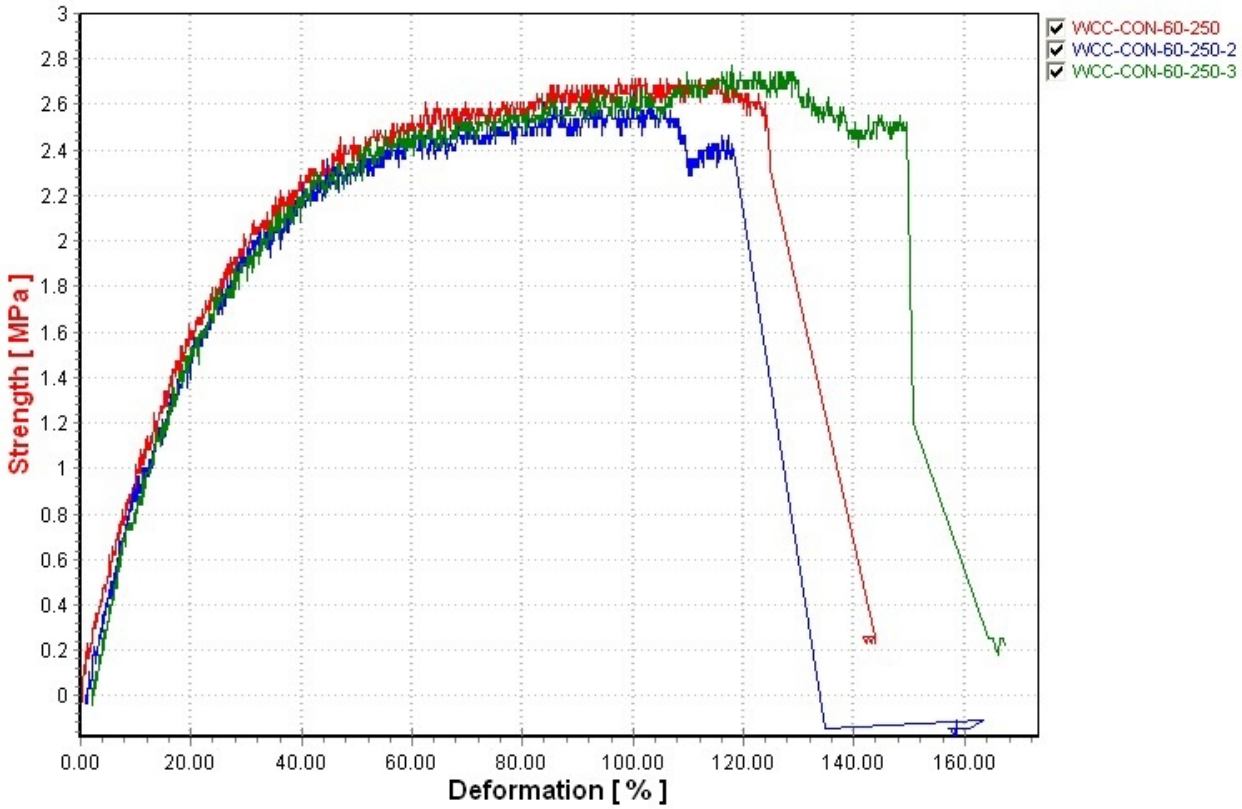

CERN - EN/MME/MM

Test Report

-

EN Engineering Department

Customer:	J-C. Guillaume EN/EL
Material:	Rubber + reinforcement
Operator:	Ph.D
Preparation:	300 kGy
Teststandard	ISO 37
Speed Step1	50.00 mm/min

Testdate:	21.04.2010
Spare Field	LHC
Type of test:	Tensile
Groupe of sample	WCC-CON-60-300

Gaine cable LHC	B [mm]	H [mm]	Rm [MPa]	Agt [%]
WCC-CON-60-300	6.10	6.70	2.59	71.36
WCC-CON-60-300-2	6.20	8.00	2.56	112.52
WCC-CON-60-300-3	6.30	7.80	2.71	172.72
-	--			
	B [mm]	H [mm]	Rm [MPa]	Agt [%]
min	6.10	6.70	2.56	71.36
max	6.30	8.00	2.71	172.72
AM	6.20	7.50	2.62	118.87
s	0.10	0.70	0.08	50.98

Set-up

Broken sample

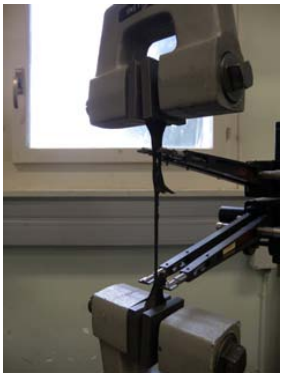

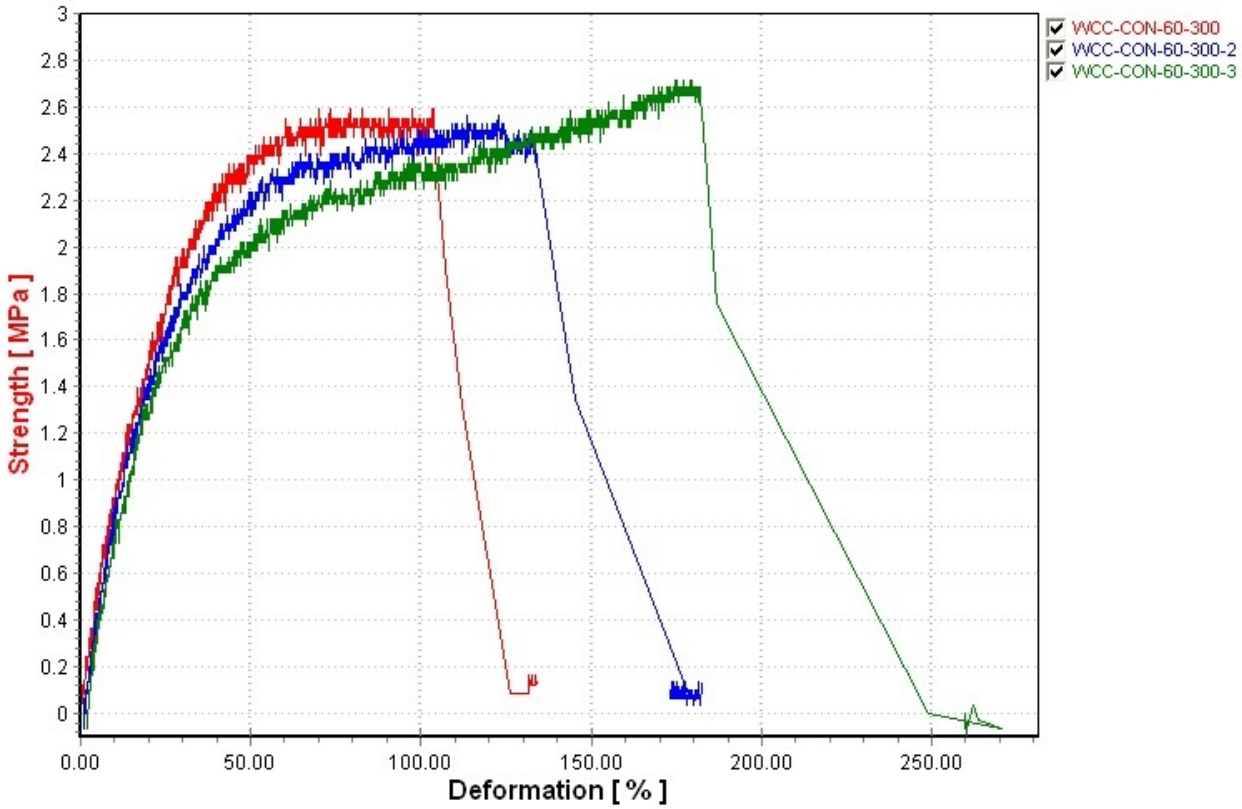

CERN - EN/MME/MM

Test Report

-

Engineering Department

Customer:	J-C. Guillaume EN/EL		
Material:	Rubber + reinforcement		
Operator:	Ph.D		
Preparation:	330 kGy	Testdate:	21.04.2010
Teststandard	ISO 37	Spare Field	LHC
		Type of test:	Tensile
Speed Step1	50.00 mm/min	Groupe of sample	WCC-CON-60-330

Gaine cable LHC	B [mm]	H [mm]	Rm [MPa]	Agt [%]
WCC-CON-60-330	6.04	6.04	2.81	83.75
WCC-CON-60-330-2	6.10	7.90	2.60	161.65
WCC-CON-60-330-3	5.90	7.85	2.85	99.25
-	--			

	B [mm]	H [mm]	Rm [MPa]	Agt [%]
min	5.90	6.04	2.60	83.75
max	6.10	7.90	2.85	161.65
AM	6.01	7.26	2.75	114.88
s	0.10	1.06	0.13	41.24

Set-up

Broken sample

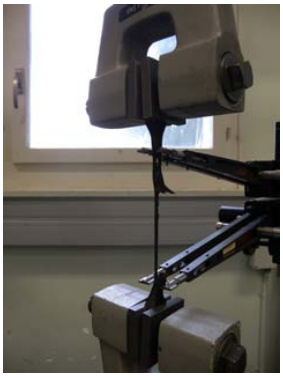

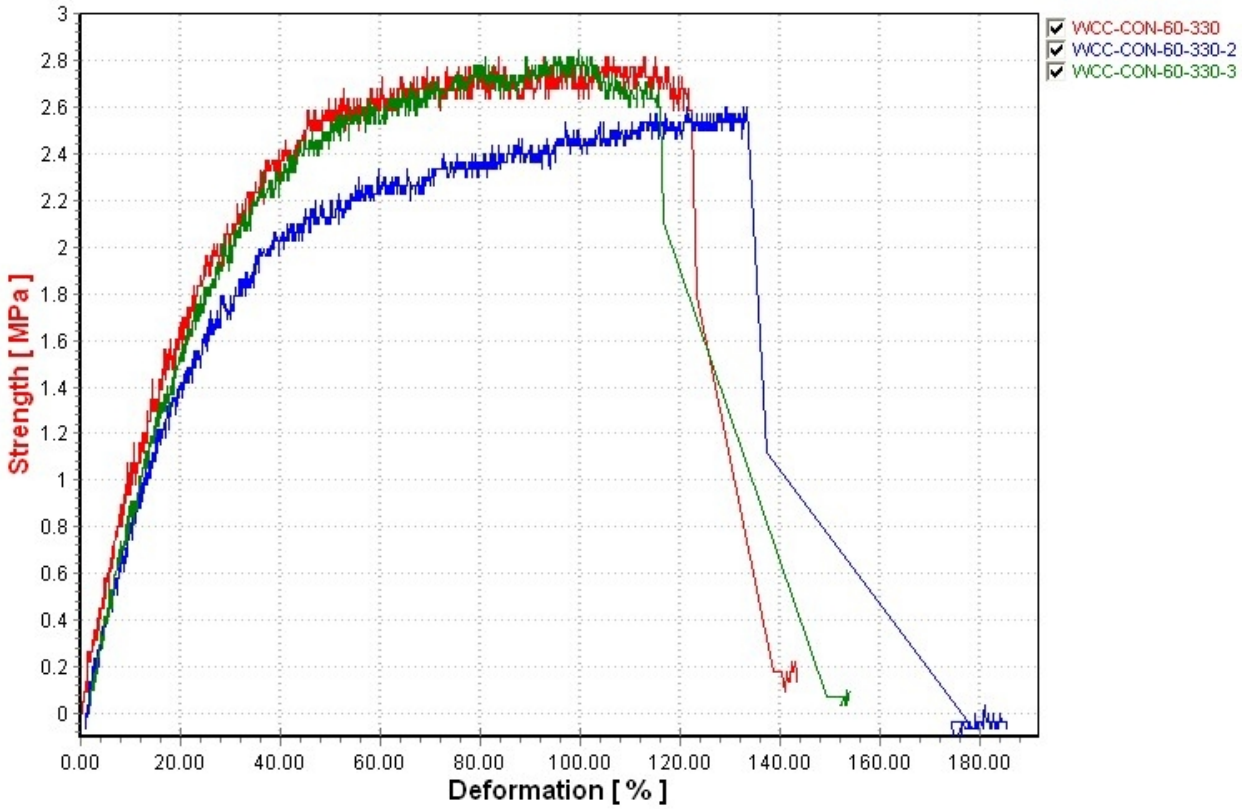

CERN - EN/MME/MM

Test Report

-

EN Engineering Department

Customer:	J-C. Guillaume EN/EL
Material:	Rubber + reinforcement
Operator:	Ph.D
Preparation:	0 kGy
Teststandard	ISO 37
Speed Step1	50.00 mm/min

Testdate:	09.04.2010
Spare Field	LHC
Type of test:	Tensile
Groupe of sample	WCC-CON-70-0

Gaine cable LHC	B [mm]	H [mm]	Rm [MPa]	Agt [%]
WCC-CON-70-0	5.80	7.15	2.63	267.86
WCC-CON-70-0-2	5.90	7.15	3.12	281.77
WCC-CON-70-0-3	5.90	7.15	2.85	263.58
-	--			
	B [mm]	H [mm]	Rm [MPa]	Agt [%]
min	5.80	7.15	2.63	263.58
max	5.90	7.15	3.12	281.77
AM	5.87	7.15	2.87	271.07
s	0.06	0.00	0.25	9.51

Set-up

Broken sample

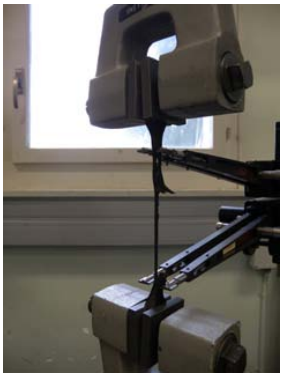

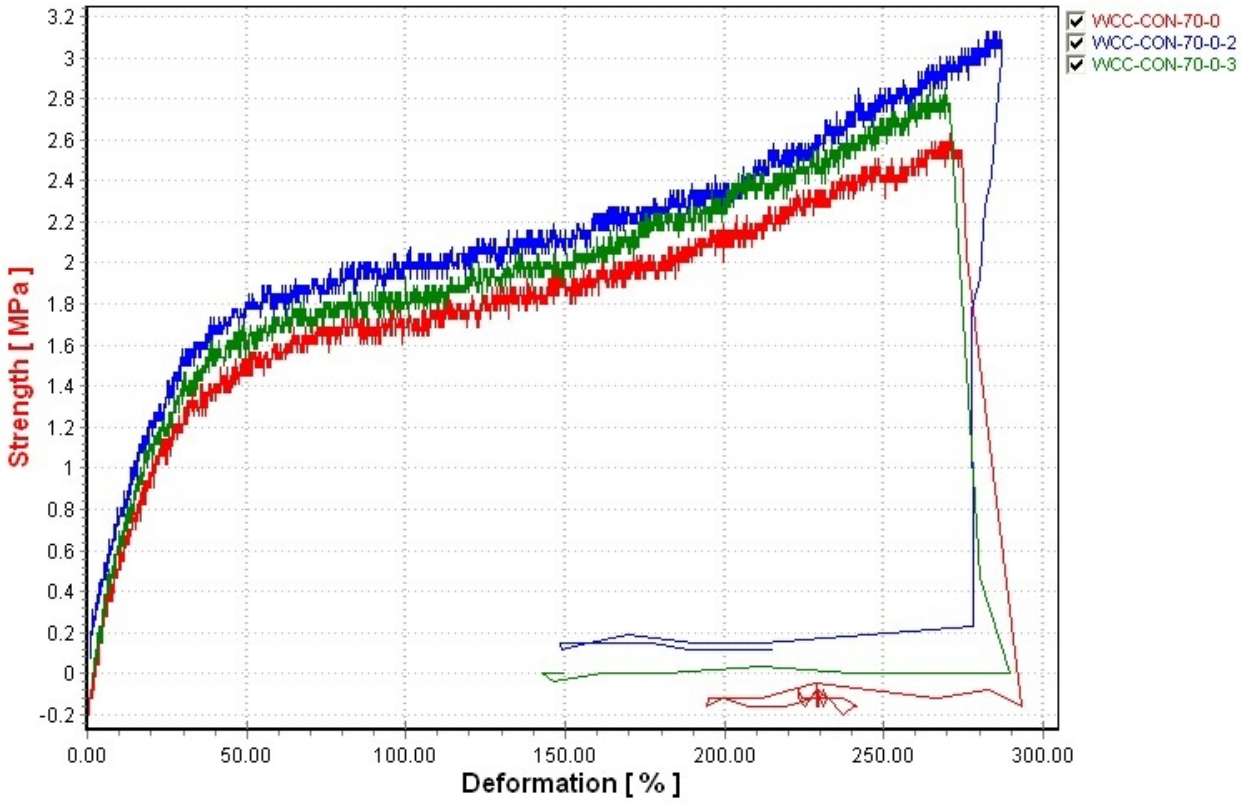

CERN - EN/MME/MM

Test Report

-

EN Engineering Department

Customer:	J-C. Guillaume EN/EL
Material:	Rubber + reinforcement
Operator:	Ph.D
Preparation:	22 kGy
Teststandard	ISO 37
Speed Step1	50.00 mm/min

Testdate:	21.04.2010
Spare Field	LHC
Type of test:	Tensile
Groupe of sample	WCC-CON-70-22

Gaine cable LHC	B [mm]	H [mm]	Rm [MPa]	Agt [%]
WCC-CON-70-22	6.10	7.10	2.44	207.40
WCC-CON-70-22-2	6.10	7.15	2.91	226.04
WCC-CON-70-22-3	6.10	7.50	2.46	236.41
-	--			
	B [mm]	H [mm]	Rm [MPa]	Agt [%]
min	6.10	7.10	2.44	207.40
max	6.10	7.50	2.91	236.41
AM	6.10	7.25	2.60	223.29
s	0.00	0.22	0.27	14.70

Set-up

Broken sample

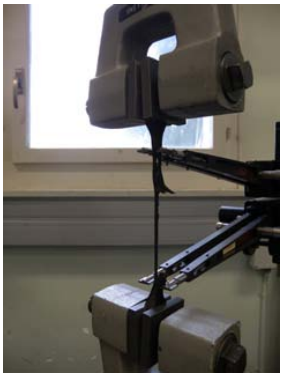

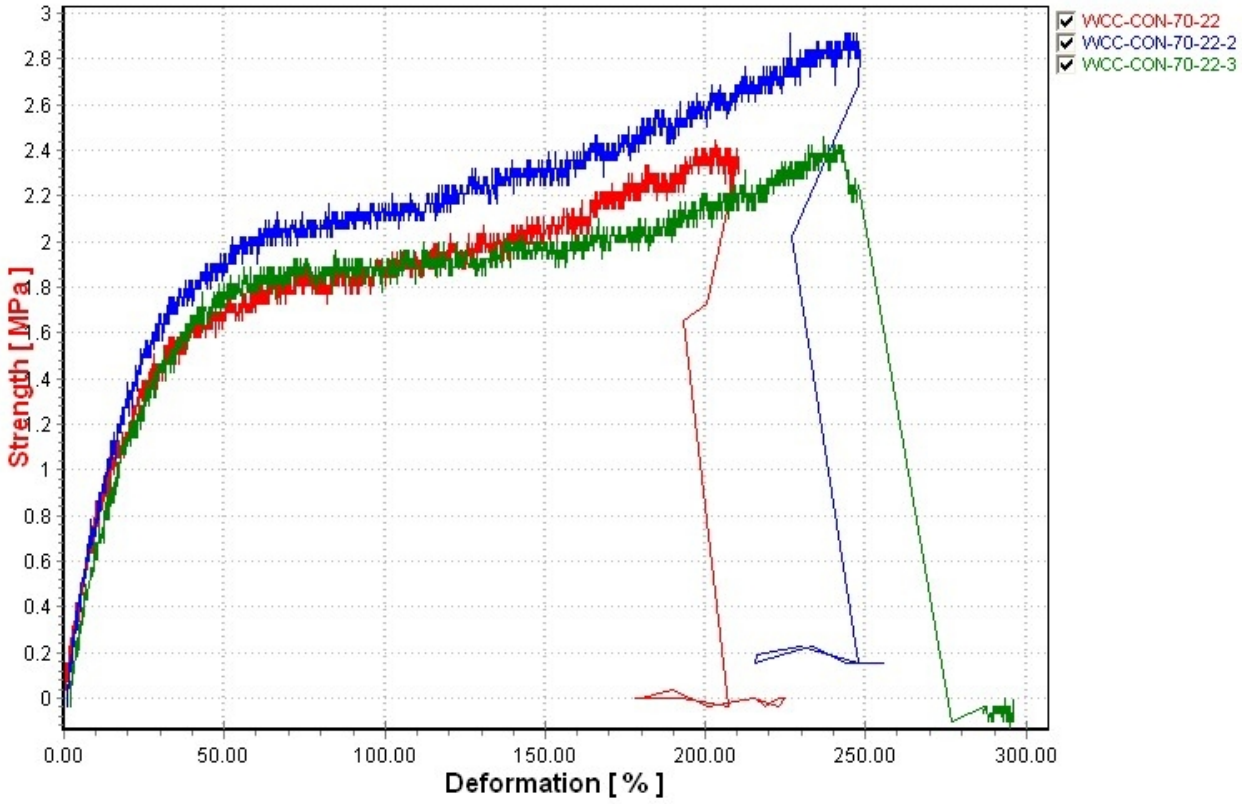

CERN - EN/MME/MM

Test Report

-

Engineering Department

Customer:	J-C. Guillaume EN/EL
Material:	Rubber + reinforcement
Operator:	Ph.D
Preparation:	100 kGy
Teststandard	ISO 37
Speed Step1	50.00 mm/min

Testdate:	09.06.2010
Spare Field	LHC
Type of test:	Tensile
Groupe of sample	WCC-CON-70-100

Gaine cable LHC	B [mm]	H [mm]	Rm [MPa]	Agt [%]
WCC-CON-70-100-1	6.10	7.22	2.62	201.79
WCC-CON-70-100-2	6.10	7.30	2.34	182.16
WCC-CON-70-100-3	5.90	7.30	2.27	179.05
-	--			
	B [mm]	H [mm]	Rm [MPa]	Agt [%]
min	5.90	7.22	2.27	179.05
max	6.10	7.30	2.62	201.79
AM	6.03	7.27	2.41	187.67
s	0.12	0.05	0.19	12.33

Set-up

Broken sample

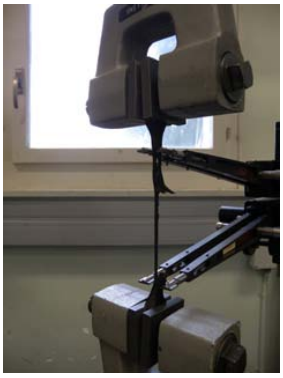

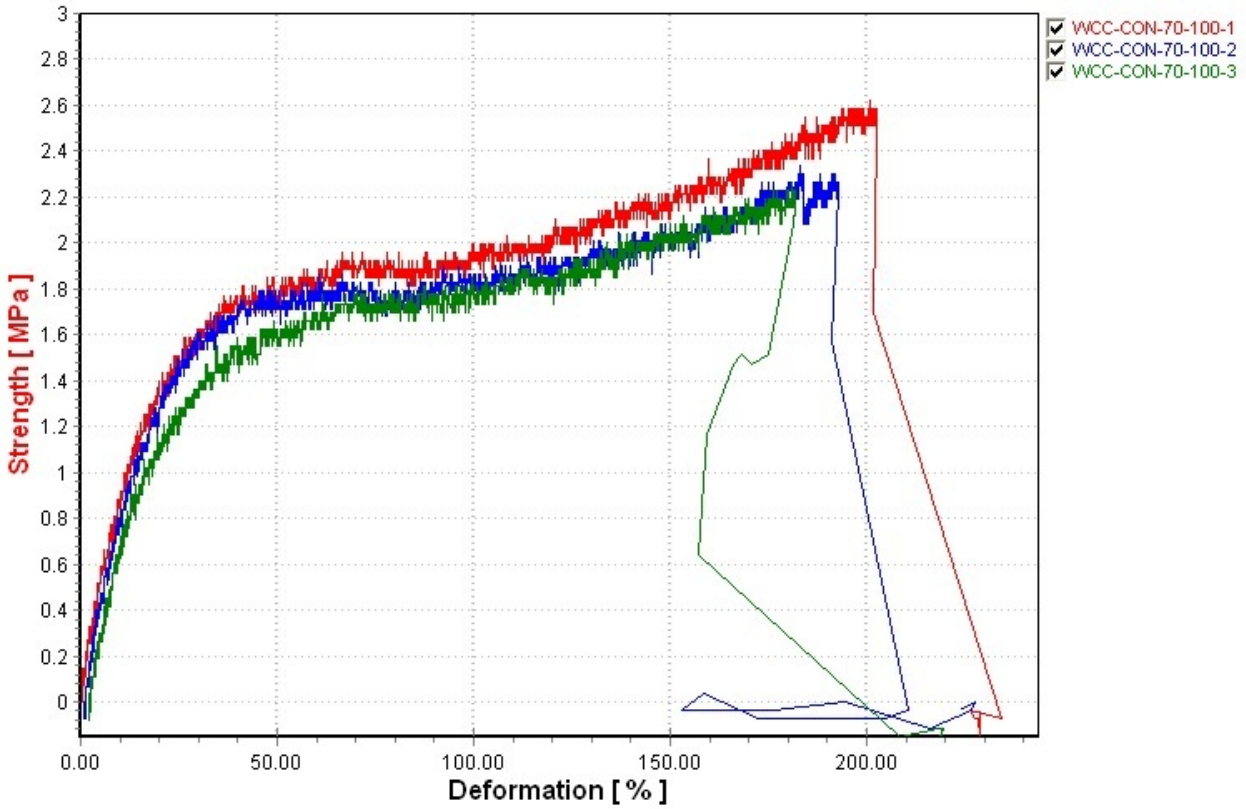

CERN - EN/MME/MM

Test Report

-

Engineering Department

Customer:	J-C. Guillaume EN/EL
Material:	Rubber + reinforcement
Operator:	Ph.D
Preparation:	250 kGy
Teststandard	ISO 37
Speed Step1	50.00 mm/min

Testdate:	21.04.2010
Spare Field	LHC
Type of test:	Tensile
Groupe of sample	WCC-CON-70-250

Gaine cable LHC	B [mm]	H [mm]	Rm [MPa]	Agt [%]
WCC-CON-70-250	6.15	7.75	2.56	77.21
WCC-CON-70-250-2	6.20	7.20	2.80	138.26
WCC-CON-70-250-3	5.70	7.15	2.67	126.29
-	--			
	B [mm]	H [mm]	Rm [MPa]	Agt [%]
min	5.70	7.15	2.56	77.21
max	6.20	7.75	2.80	138.26
AM	6.02	7.37	2.68	113.92
s	0.28	0.33	0.12	32.35

Set-up

Broken sample

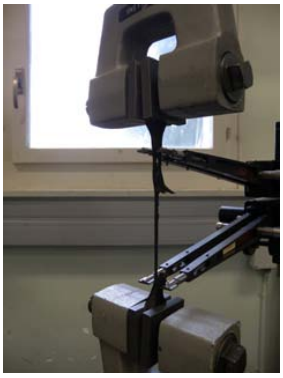

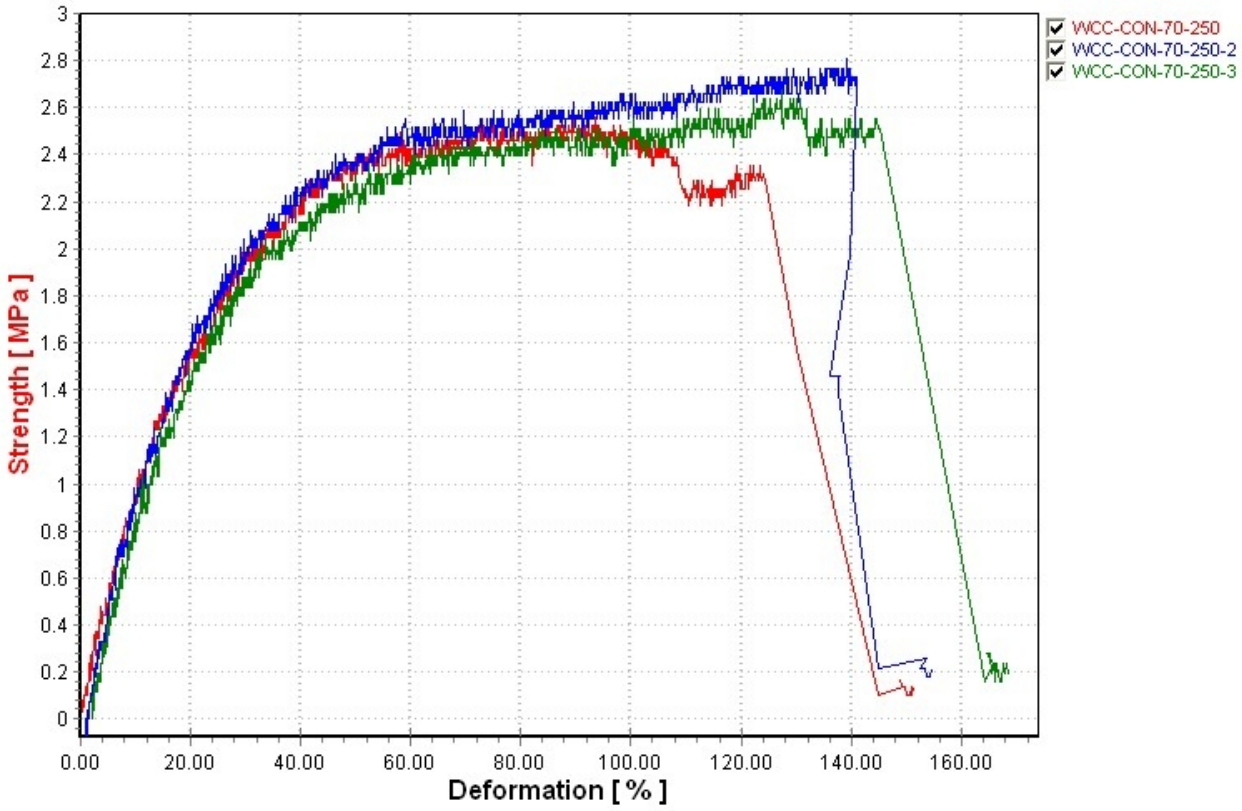

CERN - EN/MME/MM

Test Report

-

EN Engineering Department

Customer:	J-C. Guillaume EN/EL		
Material:	Rubber + reinforcement		
Operator:	Ph.D		
Preparation:	300 kGy	Testdate:	21.04.2010
Teststandard	ISO 37	Spare Field	LHC
		Type of test:	Tensile
Speed Step1	50.00 mm/min	Groupe of sample	WCC-CON-70-300

Gaine cable LHC	B [mm]	H [mm]	Rm [MPa]	Agt [%]
WCC-CON-70-300	6.00	7.90	2.58	115.27
WCC-CON-70-300-2	6.04	7.75	2.71	95.04
WCC-CON-70-300-3	6.15	7.00	2.54	67.37
-	--			

	B [mm]	H [mm]	Rm [MPa]	Agt [%]
min	6.00	7.00	2.54	67.37
max	6.15	7.90	2.71	115.27
AM	6.06	7.55	2.61	92.56
s	0.08	0.48	0.09	24.05

Set-up

Broken sample

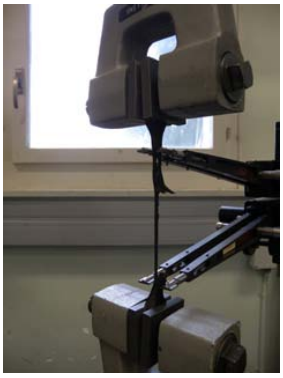

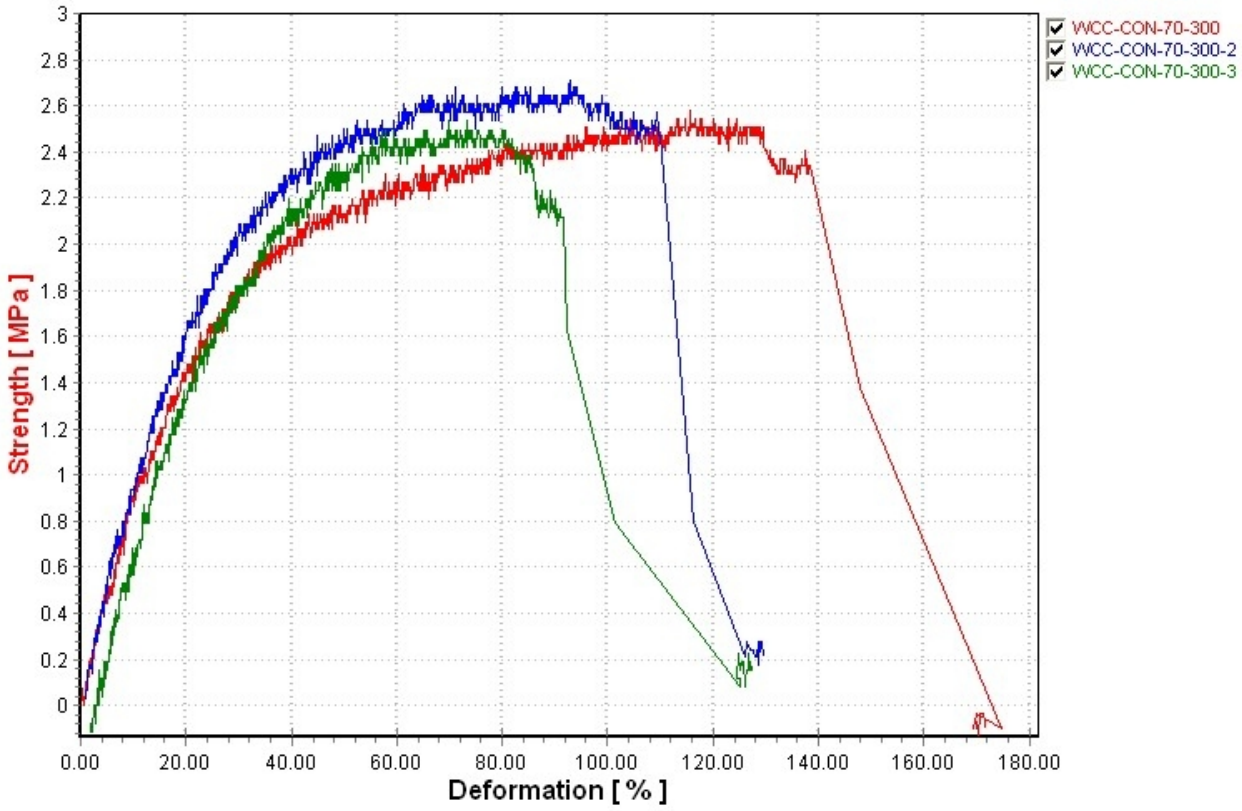

CERN - EN/MME/MM

Test Report

-

EN Engineering Department

Customer:	J-C. Guillaume EN/EL		
Material:	Rubber + reinforcement		
Operator:	Ph.D		
Preparation:	330 kGy	Testdate:	21.04.2010
Teststandard	ISO 37	Spare Field	LHC
		Type of test:	Tensile
Speed Step1	50.00 mm/min	Groupe of sample	WCC-CON-70-330

Gaine cable LHC	B [mm]	H [mm]	Rm [MPa]	Agt [%]
WCC-CON-70-330	6.10	7.75	2.61	73.52
WCC-CON-70-330-2	5.95	7.10	2.55	57.60
WCC-CON-70-330-3	5.86	7.10	2.66	64.41
-	--			

	B [mm]	H [mm]	Rm [MPa]	Agt [%]
min	5.86	7.10	2.55	57.60
max	6.10	7.75	2.66	73.52
AM	5.97	7.32	2.61	65.18
s	0.12	0.38	0.06	7.98

Set-up

Broken sample

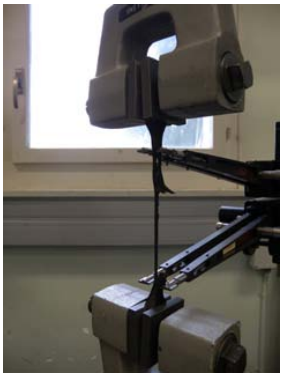

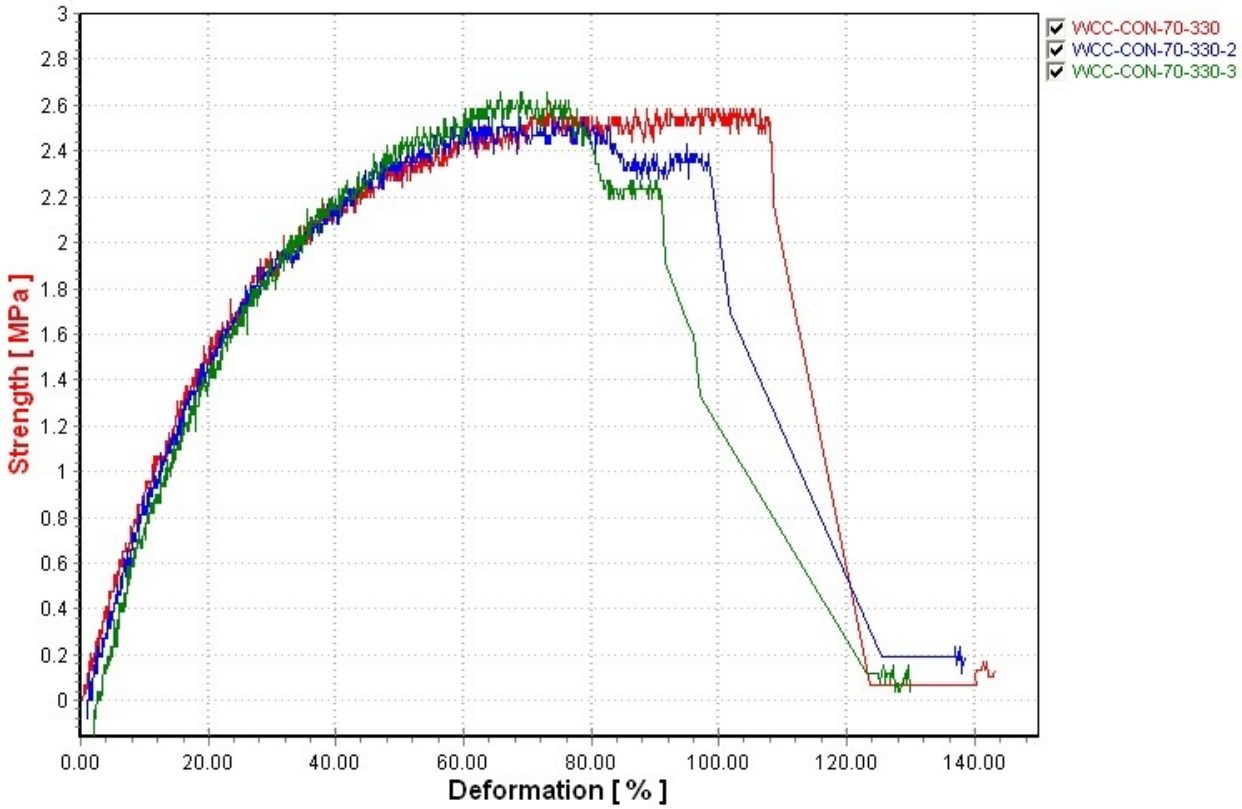

CERN - EN/MME/MM

Test Report

-

Engineering Department

Customer:	J-C. Guillaume EN/EL
Material:	Rubber + reinforcement
Operator:	Ph.D
Preparation:	0 kGy
Teststandard	ISO 37
Speed Step1	50.00 mm/min

Testdate:	09.04.2010
Spare Field	LHC
Type of test:	Tensile
Groupe of sample	WCC-CON-90-0

Gaine cable LHC	B [mm]	H [mm]	Rm [MPa]	Agt [%]
WCC-CON-90-0	6.00	8.10	2.41	254.18
WCC-CON-90-0-2	6.15	7.60	2.30	219.45
WCC-CON-90-0-3	6.00	7.94	2.56	253.17
-	--			
	B [mm]	H [mm]	Rm [MPa]	Agt [%]
min	6.00	7.60	2.30	219.45
max	6.15	8.10	2.56	254.18
AM	6.05	7.88	2.42	242.27
s	0.09	0.26	0.13	19.77

Set-up

Broken sample

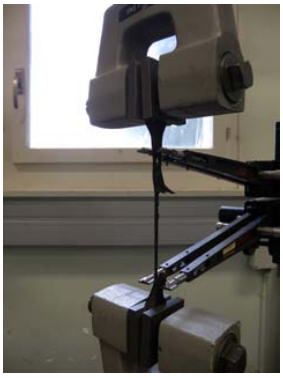

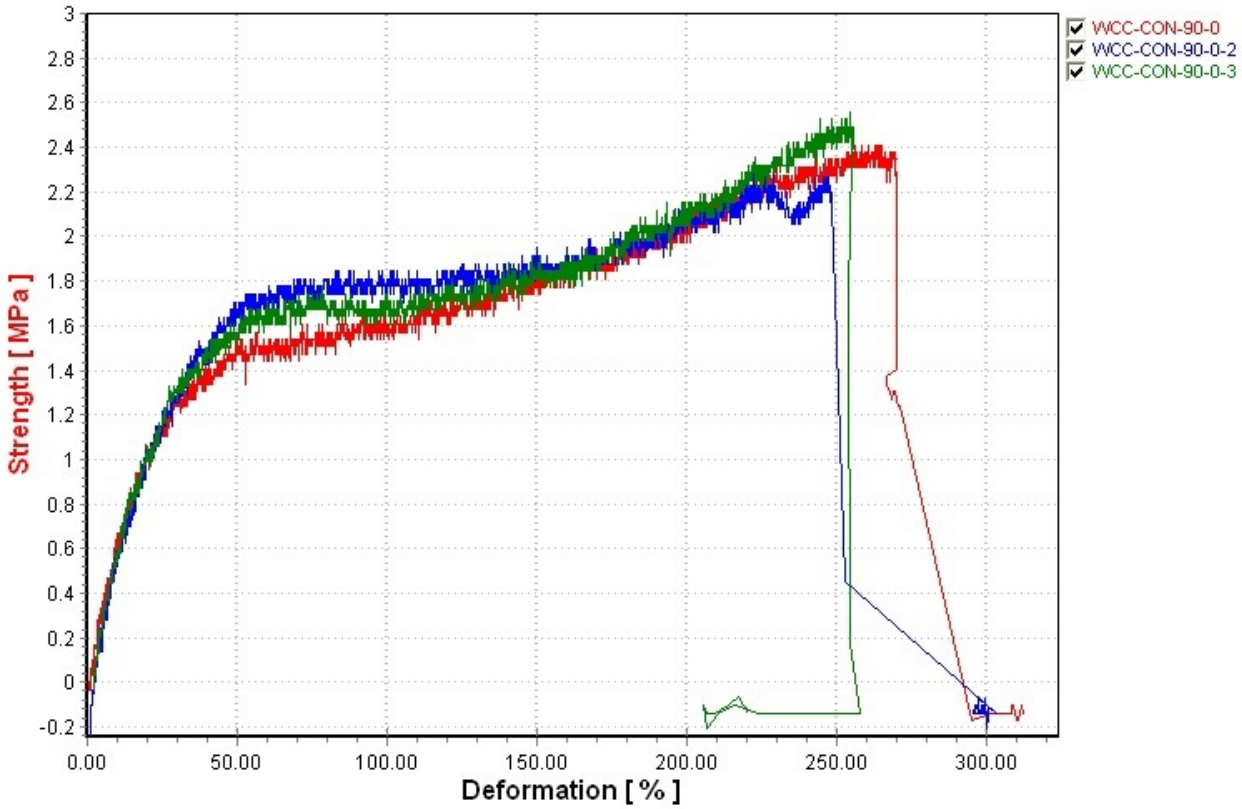

CERN - EN/MME/MM

Test Report

-

Engineering Department

Customer: J-C. Guillaume EN/EL
Material: Rubber + reinforcement
Operator: Ph.D
Preparation: 22 kGy
Teststandard ISO 37

Speed Step1 50.00 mm/min

Testdate: 21.04.2010
Spare Field LHC
Type of test: Tensile
Groupe of sample WCC-CON-90-22

Gaine cable LHC	B [mm]	H [mm]	Rm [MPa]	Agt [%]
WCC-CON-90-22	6.20	7.80	2.76	229.44
WCC-CON-90-22-2	6.20	7.50	2.28	163.12
WCC-CON-90-22-3	6.20	7.40	2.73	240.39
-	--			
	B [mm]	H [mm]	Rm [MPa]	Agt [%]
min	6.20	7.40	2.28	163.12
max	6.20	7.80	2.76	240.39
AM	6.20	7.57	2.59	210.98
s	0.00	0.21	0.27	41.81

Set-up

Broken sample

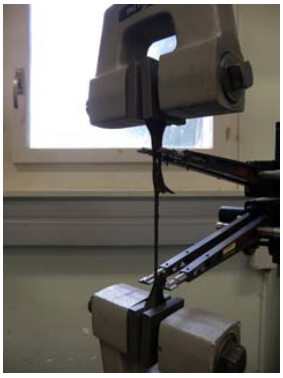

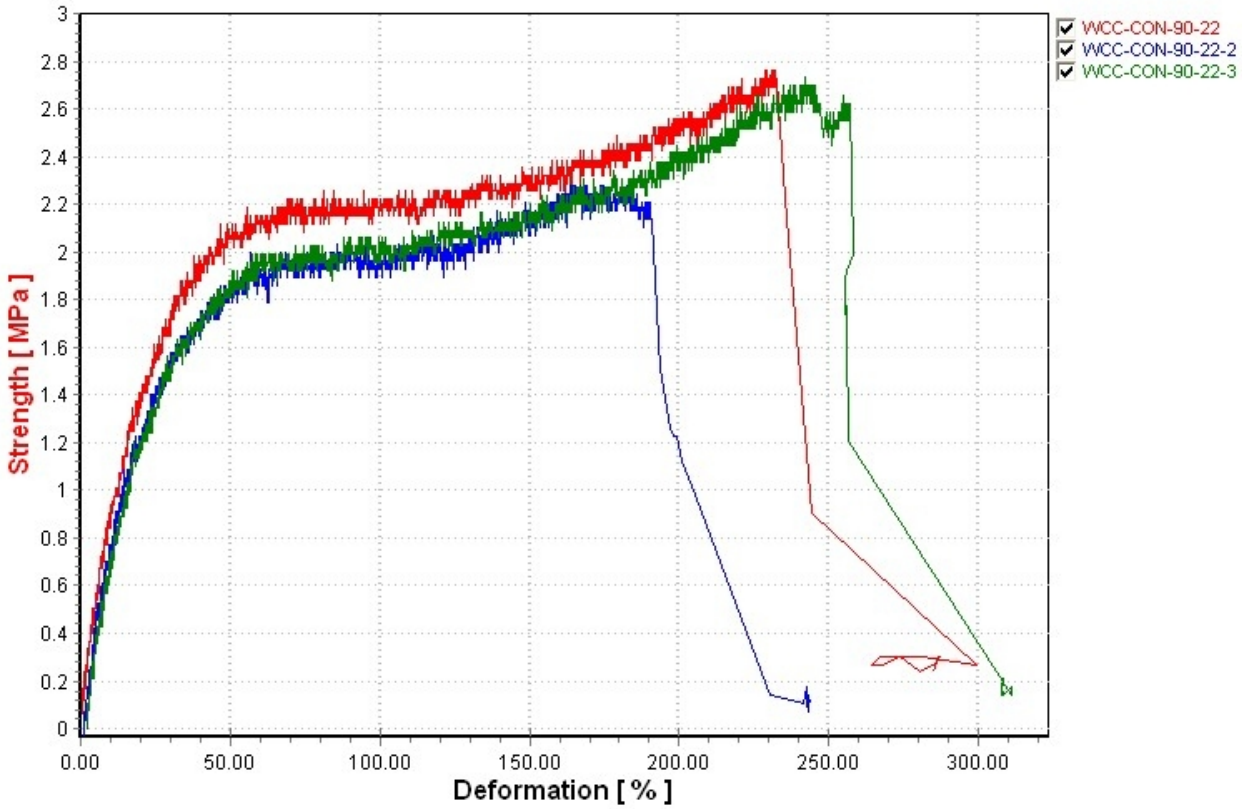

CERN - EN/MME/MM

Test Report

-

EN Engineering Department

Customer:	J-C. Guillaume EN/EL
Material:	Rubber + reinforcement
Operator:	Ph.D
Preparation:	Total Dose Point
Teststandard	ISO 37
Speed Step1	50.00 mm/min

Testdate:	21.04.2010
Spare Field	LHC
Type of test:	Tensile
Groupe of sample	WCC-CON-90-100

Gaine cable LHC	B [mm]	H [mm]	Rm [MPa]	Agt [%]
WCC-CON-90-100	5.70	8.05	2.48	170.01
WCC-CON-90-100-2	6.15	7.75	2.53	187.98
WCC-CON-90-100-3	6.30	7.70	2.31	152.98
-	--			
	B [mm]	H [mm]	Rm [MPa]	Agt [%]
min	5.70	7.70	2.31	152.98
max	6.30	8.05	2.53	187.98
AM	6.05	7.83	2.44	170.32
s	0.31	0.19	0.11	17.50

Set-up

Broken sample

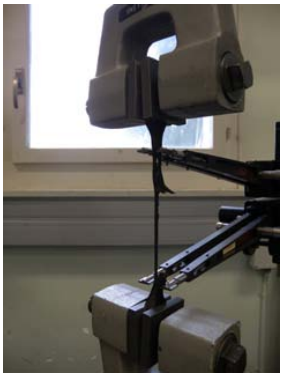

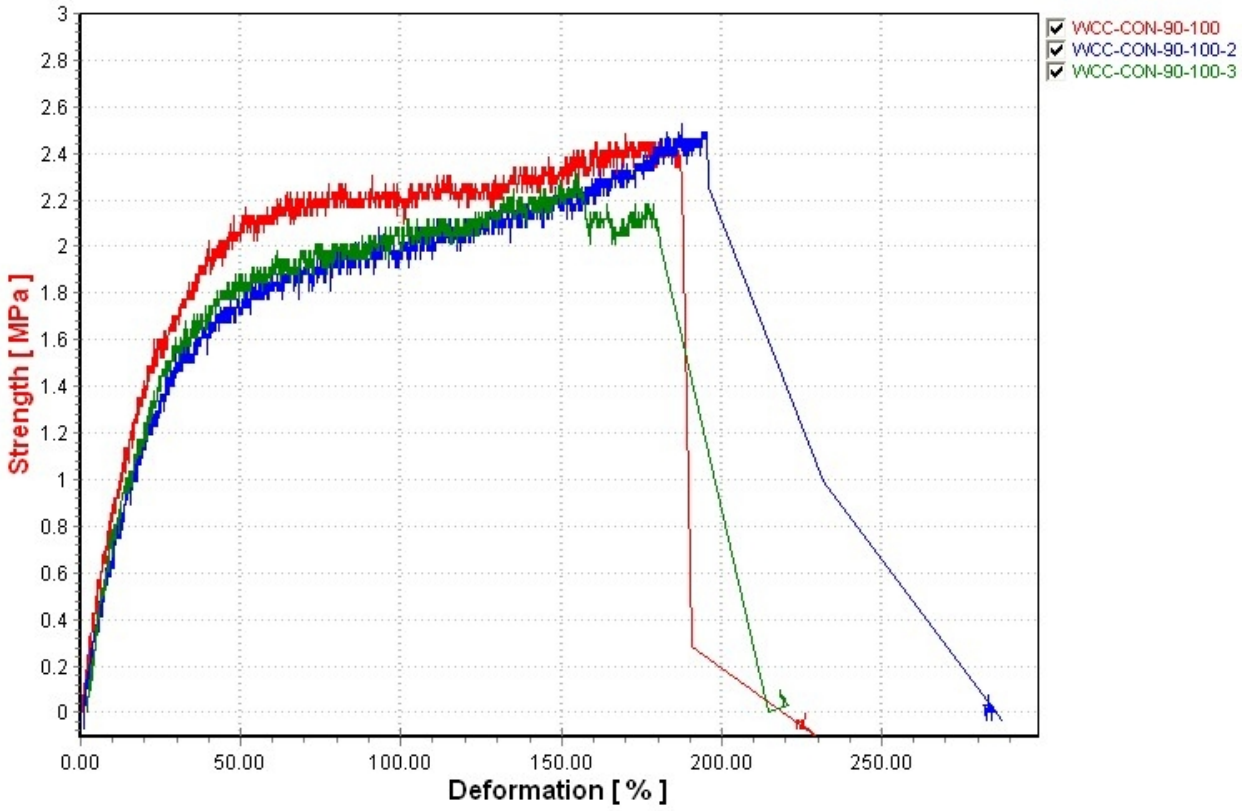

CERN - EN/MME/MM

Test Report

-

Engineering Department

Customer:	J-C. Guillaume EN/EL
Material:	Rubber + reinforcement
Operator:	Ph.D
Preparation:	250 kGy
Teststandard	ISO 37
Speed Step1	50.00 mm/min

Testdate:	21.04.2010
Spare Field	LHC
Type of test:	Tensile
Groupe of sample	WCC-CON-90-250

Gaine cable LHC	B [mm]	H [mm]	Rm [MPa]	Agt [%]
WCC-CON-90-250	6.30	7.40	1.85	104.70
WCC-CON-90-250-2	6.00	7.90	2.23	129.77
WCC-CON-90-250-3	6.10	8.10	2.27	130.31
-	--			
	B [mm]	H [mm]	Rm [MPa]	Agt [%]
min	6.00	7.40	1.85	104.70
max	6.30	8.10	2.27	130.31
AM	6.13	7.80	2.12	121.59
s	0.15	0.36	0.23	14.63

Set-up

Broken sample

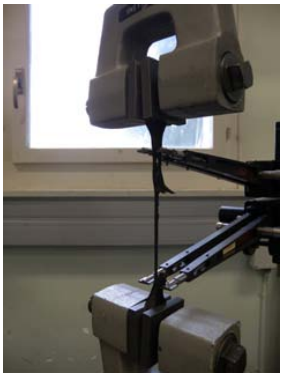

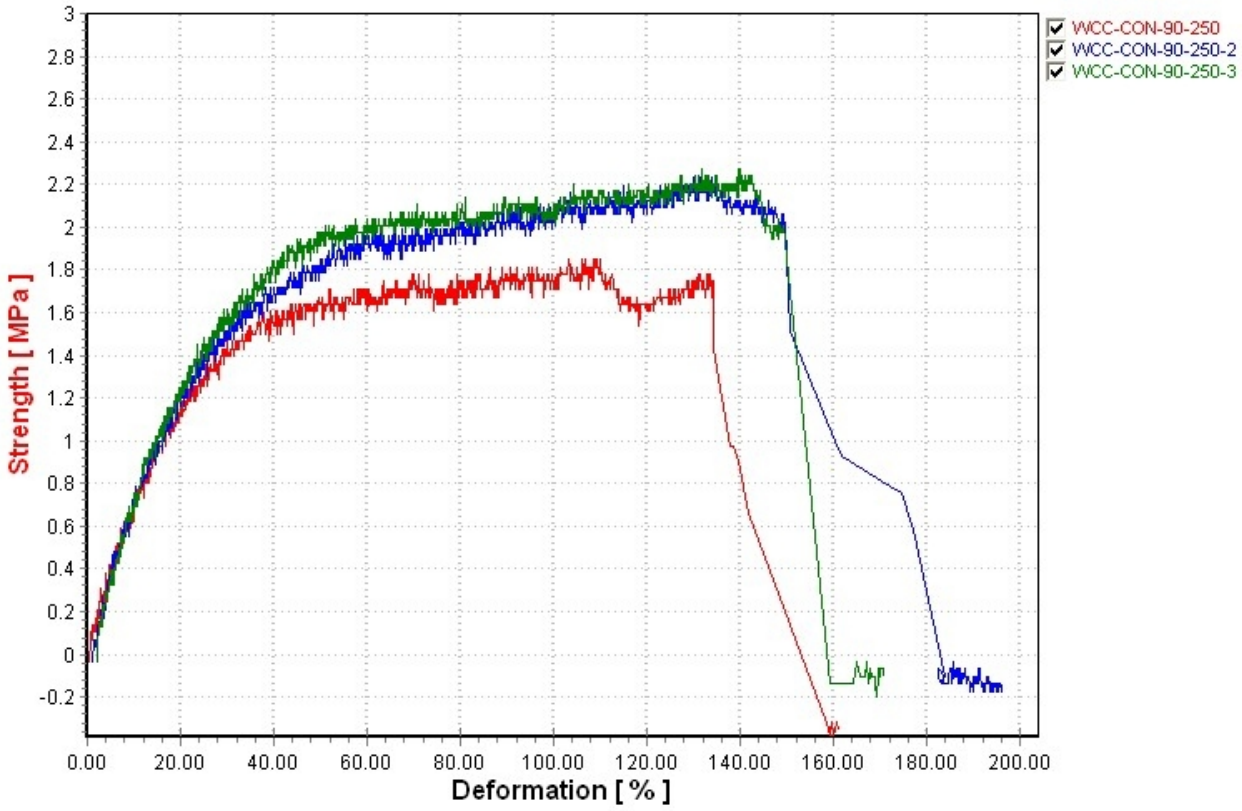

CERN - EN/MME/MM

Test Report

-

EN Engineering Department

Customer:	J-C. Guillaume EN/EL
Material:	Rubber + reinforcement
Operator:	Ph.D
Preparation:	300 kGy
Teststandard	ISO 37
Speed Step1	50.00 mm/min

Testdate:	21.04.2010
Spare Field	LHC
Type of test:	Tensile
Groupe of sample	WCC-CON-90-300

Gaine cable LHC	B [mm]	H [mm]	Rm [MPa]	Agt [%]
WCC-CON-90-300	6.15	7.50	2.44	103.07
WCC-CON-90-300-2	6.10	7.55	3.11	84.81
WCC-CON-90-300-3	6.10	8.05	2.78	99.65
-	--			

	B [mm]	H [mm]	Rm [MPa]	Agt [%]
min	6.10	7.50	2.44	84.81
max	6.15	8.05	3.11	103.07
AM	6.12	7.70	2.78	95.84
s	0.03	0.30	0.34	9.71

Set-up

Broken sample

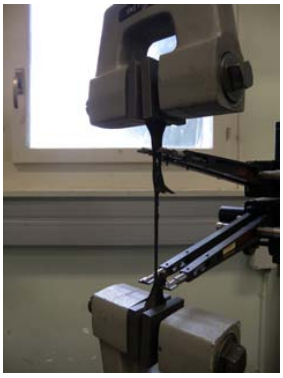

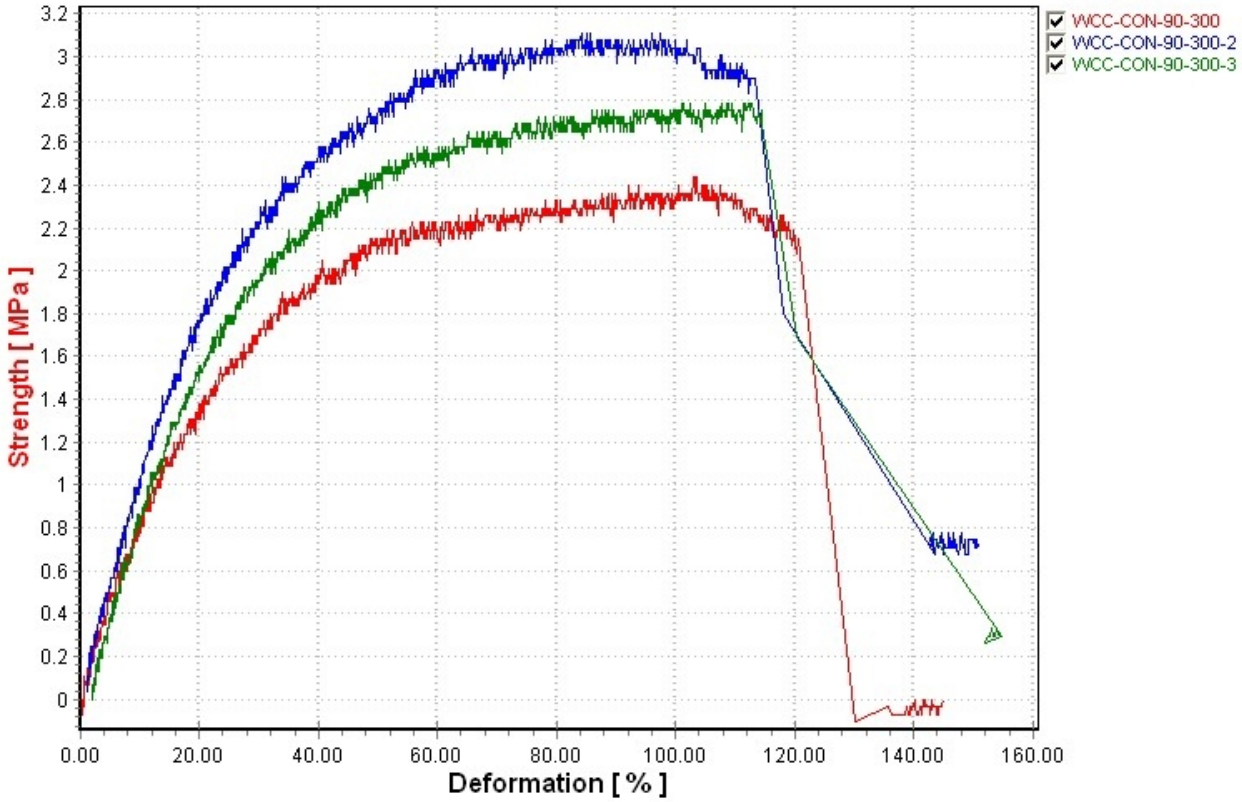

CERN - EN/MME/MM

Test Report

-

Engineering Department

Customer:	J-C. Guillaume EN/EL
Material:	Rubber + reinforcement
Operator:	Ph.D
Preparation:	330 kGy
Teststandard	ISO 37
Speed Step1	50.00 mm/min

Testdate:	21.04.2010
Spare Field	LHC
Type of test:	Tensile
Groupe of sample	WCC-CON-90-330

Gaine cable LHC	B [mm]	H [mm]	Rm [MPa]	Agt [%]
WCC-CON-90-330	6.10	8.10	2.53	67.38
WCC-CON-90-330-2	6.06	8.00	2.58	97.24
WCC-CON-90-330-3	6.10	8.00	2.64	83.34
-	--			
	B [mm]	H [mm]	Rm [MPa]	Agt [%]
min	6.06	8.00	2.53	67.38
max	6.10	8.10	2.64	97.24
AM	6.09	8.03	2.58	82.66
s	0.02	0.06	0.05	14.94

Set-up

Broken sample

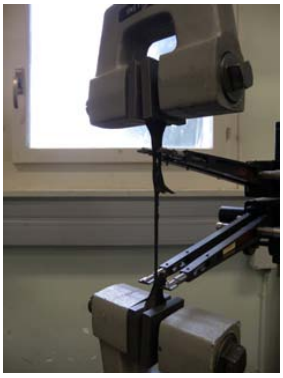

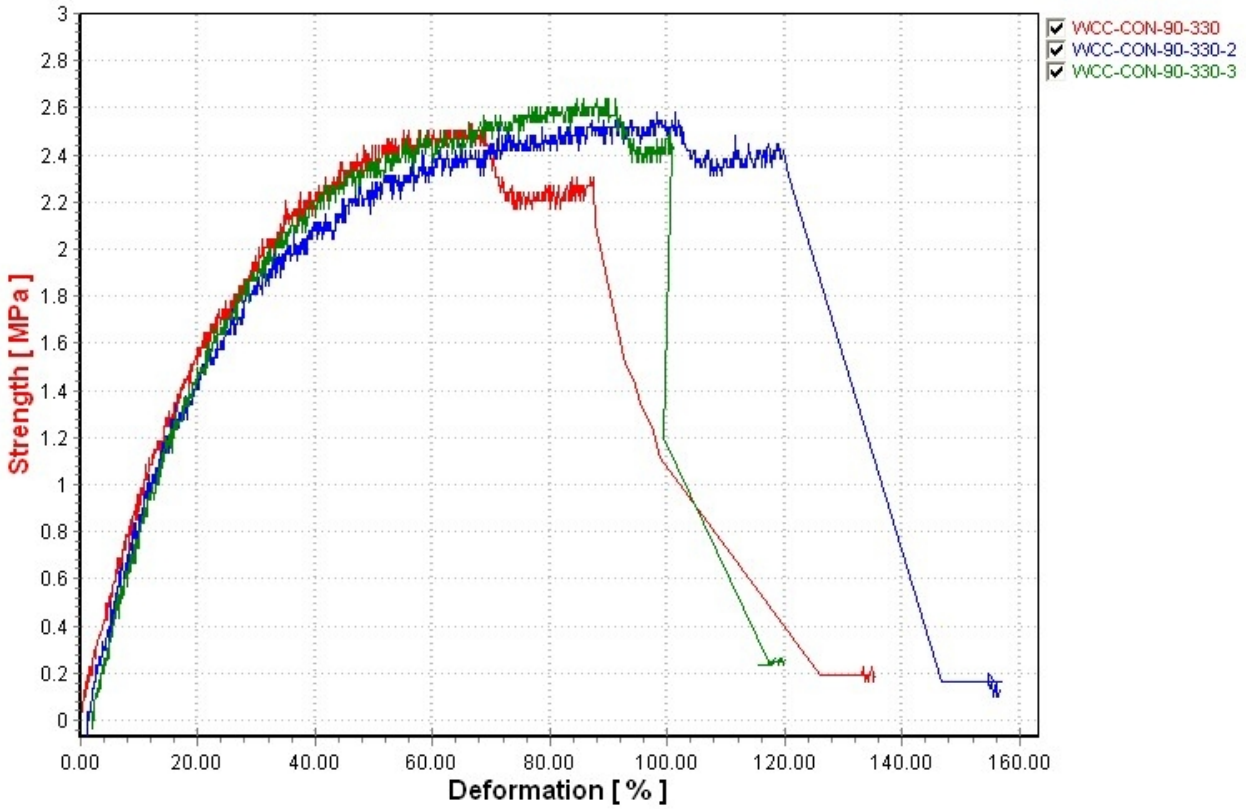

CERN - EN/MME/MM

Test Report

-

EN Engineering Department

Customer:	J-C. Guillaume EN/EL
Material:	Rubber + Nylon reinforcement
Operator:	AG
Preparation:	0 kGy
Teststandard	ISO 37
Speed Step1	50.00 mm/min

Testdate:	07.04.2010
Spare Field	LHC
Type of test:	Tensile
Groupe of sample	WCC-IVG-N-42-0

Gaine cable LHC	B [mm]	H [mm]	Rm [MPa]	Agt [%]
WCC-IVG-N-42-0	5.84	10.50	3.00	108.54
WCC-IVG-N-42-0-2	5.84	10.10	3.04	113.68
WCC-IVG-N-42-0-3	5.86	10.10	2.91	107.09
-	--			
	B [mm]	H [mm]	Rm [MPa]	Agt [%]
min	5.84	10.10	2.91	107.09
max	5.86	10.50	3.04	113.68
AM	5.85	10.23	2.98	109.77
s	0.01	0.23	0.06	3.46

Set-up

Broken sample

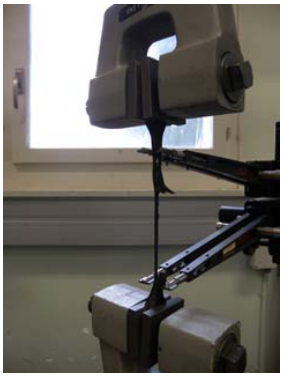

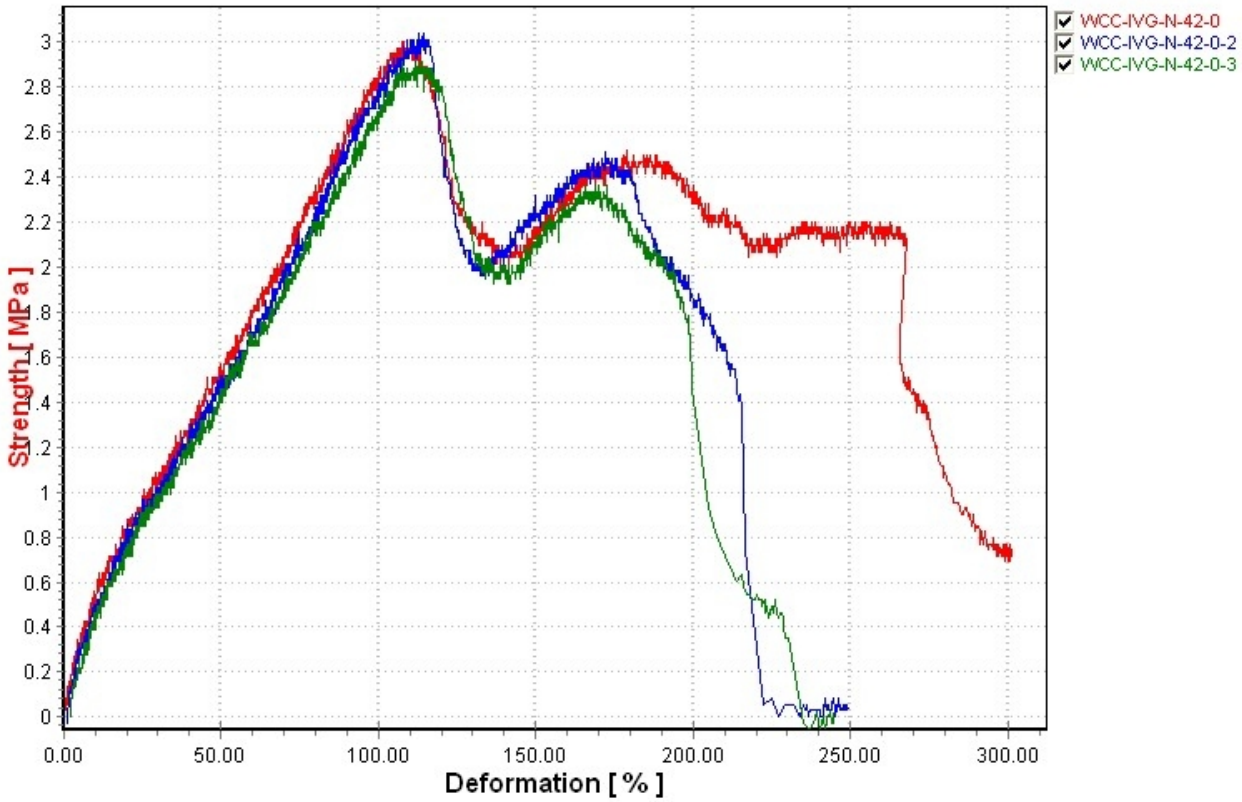

CERN - EN/MME/MM

Test Report

-

EN Engineering Department

Customer:	J-C. Guillaume EN/EL
Material:	Rubber + reinforcement
Operator:	AG
Preparation:	22 kGy
Teststandard	ISO 37
Speed Step1	50.00 mm/min

Testdate:	14.04.2010
Spare Field	LHC
Type of test:	Tensile
Groupe of sample	WCC-IVG-N-42-22

Gaine cable LHC	B [mm]	H [mm]	Rm [MPa]	Agt [%]
WCC-IVG-N-42-22	6.02	9.90	2.95	103.65
WCC-IVG-N-42-22-2	5.95	10.35	2.94	103.35
WCC-IVG-N-42-22-3	5.83	10.30	2.98	100.85
-	--			
	B [mm]	H [mm]	Rm [MPa]	Agt [%]
min	5.83	9.90	2.94	100.85
max	6.02	10.35	2.98	103.65
AM	5.93	10.18	2.96	102.62
s	0.10	0.25	0.02	1.53

Set-up

Broken sample

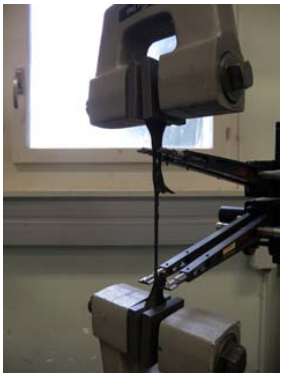

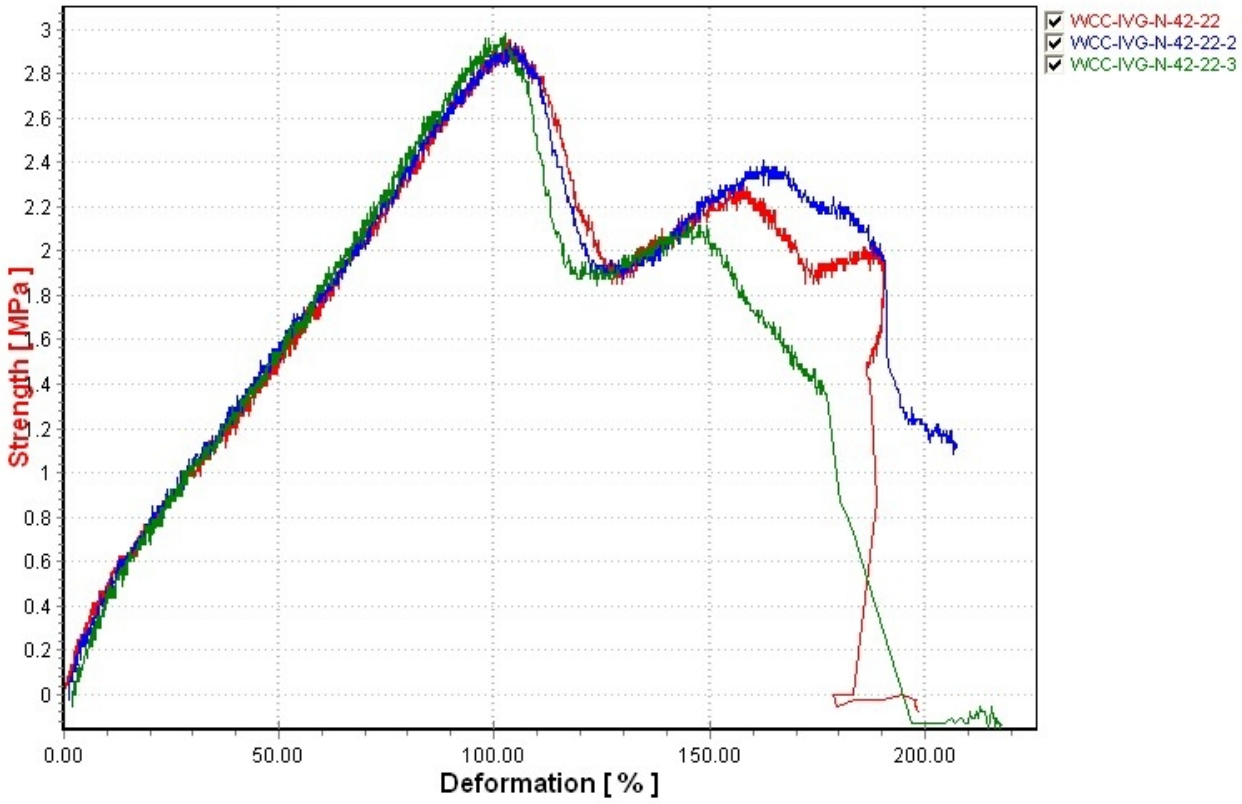

CERN - EN/MME/MM

Test Report

-

EN Engineering Department

Customer:	J-C. Guillaume EN/EL
Material:	Rubber + reinforcement
Operator:	Ph.D
Preparation:	Total Dose Point
Teststandard	ISO 37
Speed Step1	50.00 mm/min

Testdate:	21.04.2010
Spare Field	LHC
Type of test:	Tensile
Groupe of sample	WCC-IVG-N-42-100

Gaine cable LHC	B [mm]	H [mm]	Rm [MPa]	Agt [%]
WCC-IVG-N-42-100	5.86	9.80	3.32	82.07
WCC-IVG-N-42-100-2	6.00	10.15	3.13	79.52
WCC-IVG-N-42-100-3	5.80	9.90	3.32	84.06
-	--			
	B [mm]	H [mm]	Rm [MPa]	Agt [%]
min	5.80	9.80	3.13	79.52
max	6.00	10.15	3.32	84.06
AM	5.89	9.95	3.25	81.88
s	0.10	0.18	0.11	2.27

Set-up

Broken sample

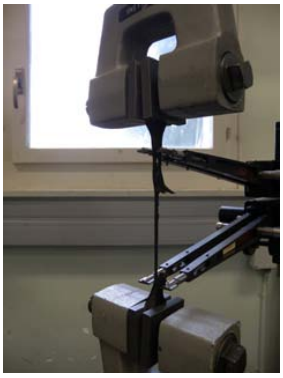

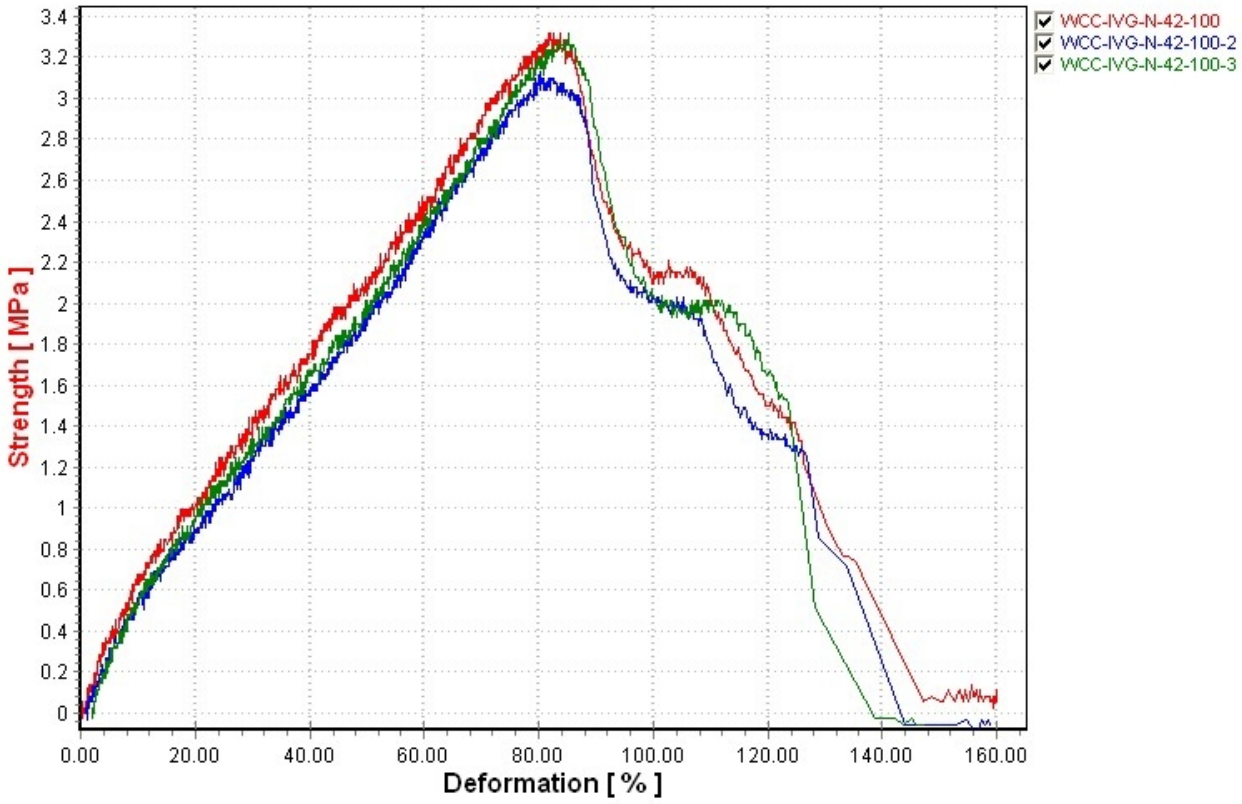

CERN - EN/MME/MM

Test Report

-

EN Engineering Department

Customer:	J-C. Guillaume EN/EL
Material:	Rubber + reinforcement
Operator:	Ph.D
Preparation:	250 kGy
Teststandard	ISO 37
Speed Step1	50.00 mm/min

Testdate:	21.04.2010
Spare Field	LHC
Type of test:	Tensile
Groupe of sample	WCC-IVG-N-42-250

Gaine cable LHC	B [mm]	H [mm]	Rm [MPa]	Agt [%]
WCC-IVG-N-42-250	5.80	10.30	3.84	64.28
WCC-IVG-N-42-250-2	5.80	10.30	3.65	66.49
WCC-IVG-N-42-250-3	6.00	10.20	3.64	65.71
-	--			
	B [mm]	H [mm]	Rm [MPa]	Agt [%]
min	5.80	10.20	3.64	64.28
max	6.00	10.30	3.84	66.49
AM	5.87	10.27	3.71	65.49
s	0.12	0.06	0.11	1.12

Set-up

Broken sample

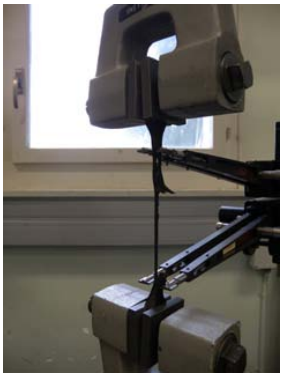

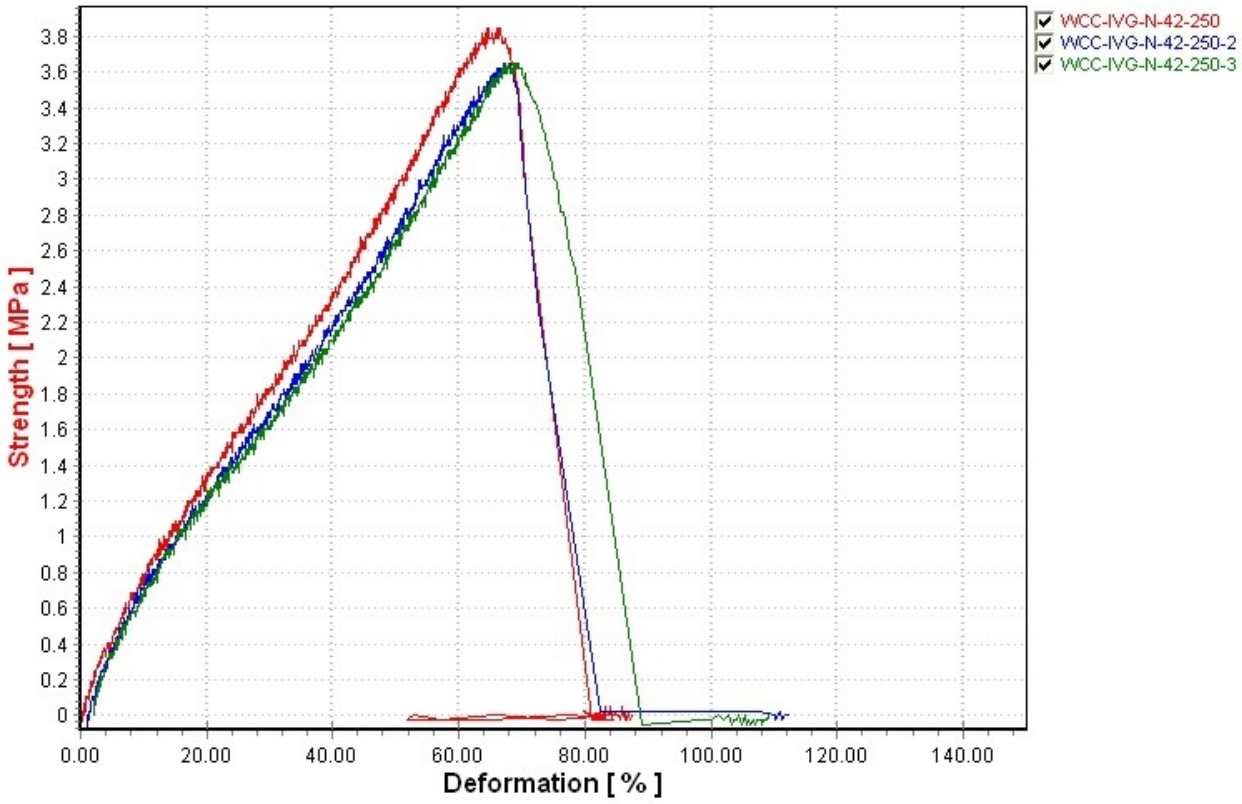

CERN - EN/MME/MM

Test Report

-

EN Engineering Department

Customer:	J-C. Guillaume EN/EL
Material:	Rubber + reinforcement
Operator:	Ph.D
Preparation:	300 kGy
Teststandard	ISO 37
Speed Step1	50.00 mm/min

Testdate:	21.04.2010
Spare Field	LHC
Type of test:	Tensile
Groupe of sample	WCC-IVG-N-42-300

Gaine cable LHC	B [mm]	H [mm]	Rm [MPa]	Agt [%]
WCC-IVG-N-42-300	5.90	10.25	3.50	67.06
WCC-IVG-N-42-300-2	5.90	10.25	3.58	72.22
WCC-IVG-N-42-300-3	5.90	10.10	3.42	69.68
-	--			
	B [mm]	H [mm]	Rm [MPa]	Agt [%]
min	5.90	10.10	3.42	67.06
max	5.90	10.25	3.58	72.22
AM	5.90	10.20	3.50	69.65
s	0.00	0.09	0.08	2.58

Set-up

Broken sample

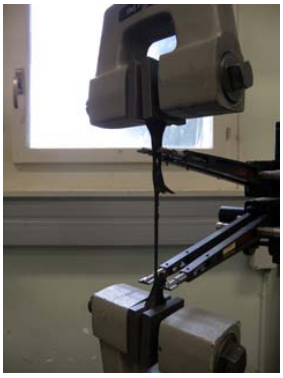

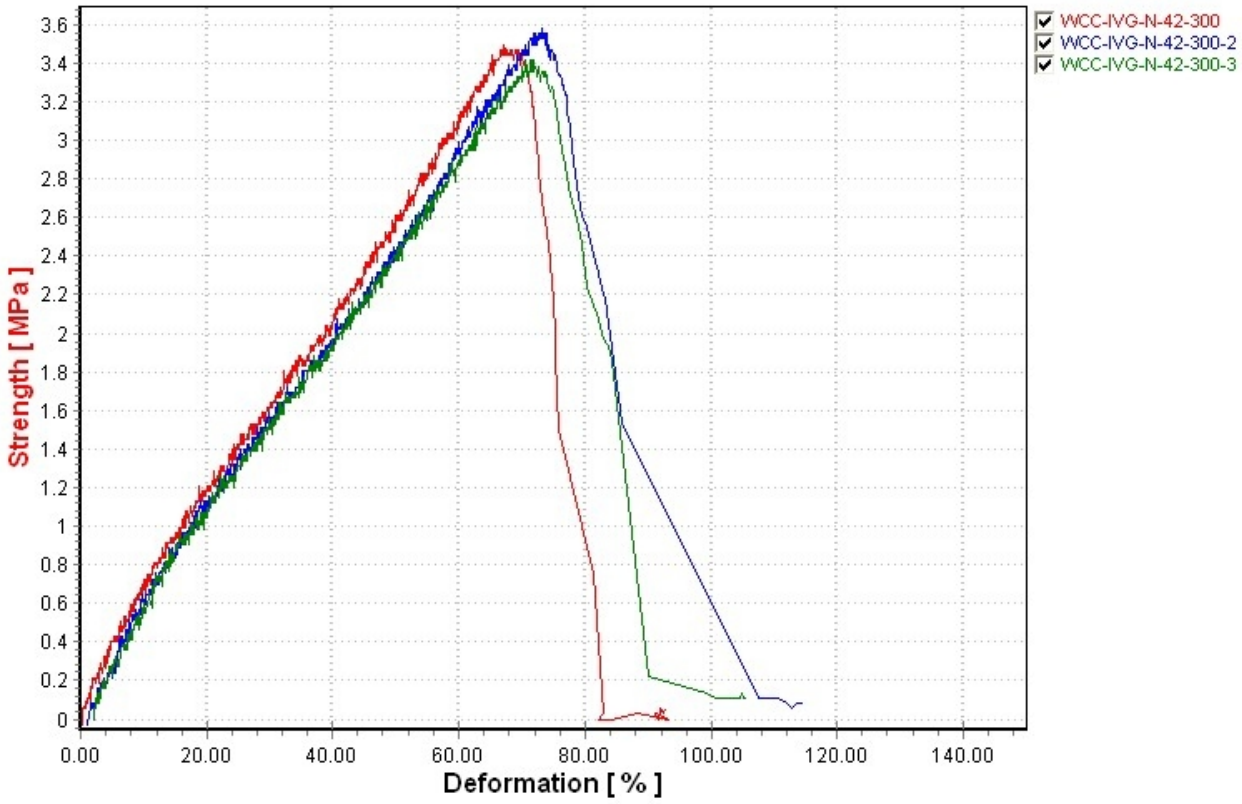

CERN - EN/MME/MM

Test Report

-

EN Engineering Department

Customer:	J-C. Guillaume EN/EL
Material:	Rubber + reinforcement
Operator:	Ph.D
Preparation:	330 kGy
Teststandard	ISO 37
Speed Step1	50.00 mm/min

Testdate:	21.04.2010
Spare Field	LHC
Type of test:	Tensile
Groupe of sample	WCC-IVG-N-42-330

Gaine cable LHC	B [mm]	H [mm]	Rm [MPa]	Agt [%]
WCC-IVG-N-42-330	5.96	9.90	3.45	62.36
WCC-IVG-N-42-330-2	5.80	9.85	3.25	62.40
WCC-IVG-N-42-330-3	5.80	9.95	3.50	65.61
-	--			
	B [mm]	H [mm]	Rm [MPa]	Agt [%]
min	5.80	9.85	3.25	62.36
max	5.96	9.95	3.50	65.61
AM	5.85	9.90	3.40	63.46
s	0.09	0.05	0.13	1.86

Set-up

Broken sample

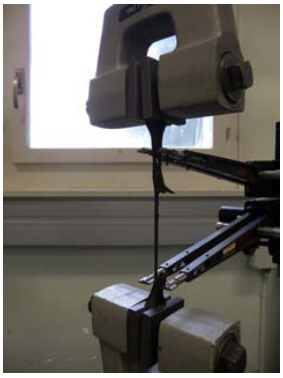

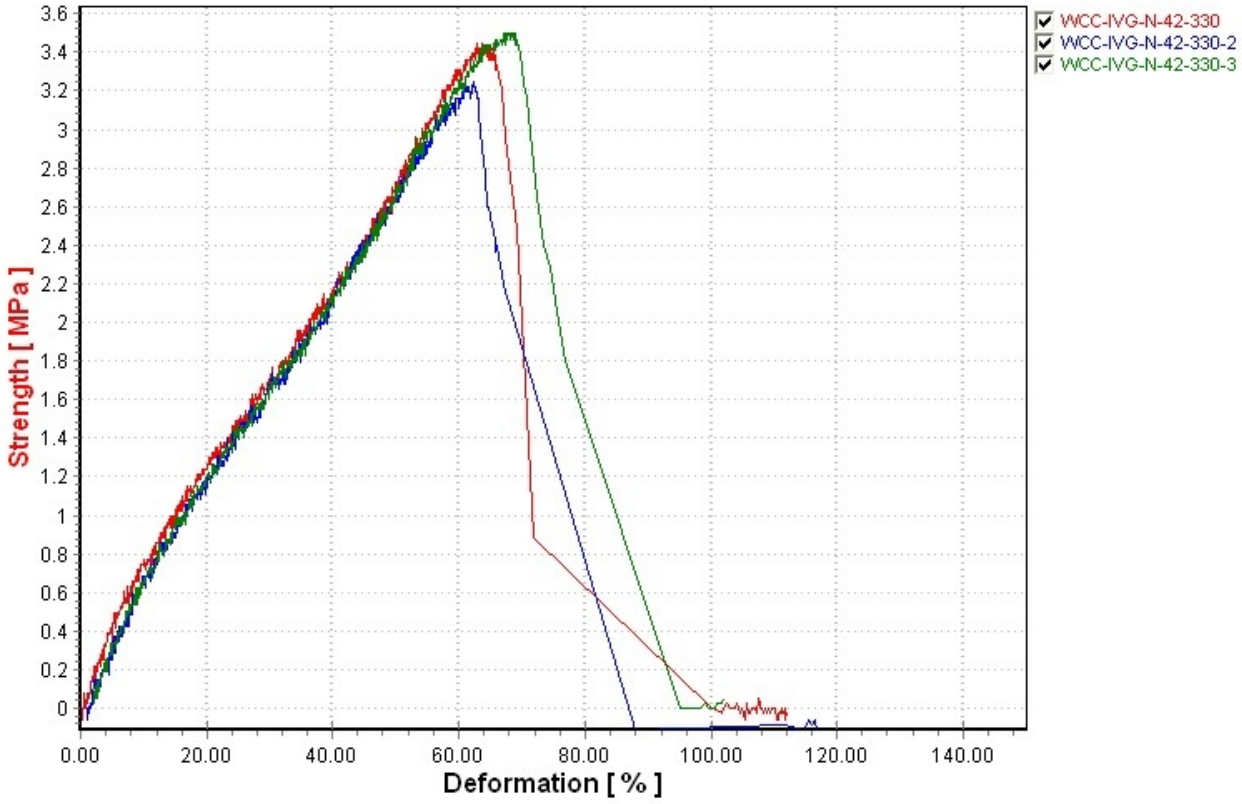

CERN - EN/MME/MM

Test Report

-

EN Engineering Department

Customer:	J-C. Guillaume EN/EL
Material:	Rubber + Nylon reinforcement
Operator:	AG
Preparation:	0 kGy
Teststandard	ISO 37
Speed Step1	50.00 mm/min

Testdate:	08.04.2010
Spare Field	LHC
Type of test:	Tensile
Groupe of sample	WCC-IVG-N-70-0

Gaine cable LHC	B [mm]	H [mm]	Rm [MPa]	Agt [%]
WCC-IVG-N-70-0	5.89	10.04	2.97	141.51
WCC-IVG-N-70-0-2	5.89	10.04	2.73	115.51
WCC-IVG-N-70-0-3	5.50	10.05	3.54	127.60
-	--			
	B [mm]	H [mm]	Rm [MPa]	Agt [%]
min	5.50	10.04	2.73	115.51
max	5.89	10.05	3.54	141.51
AM	5.76	10.04	3.08	128.21
s	0.23	0.01	0.41	13.01

Set-up

Broken sample

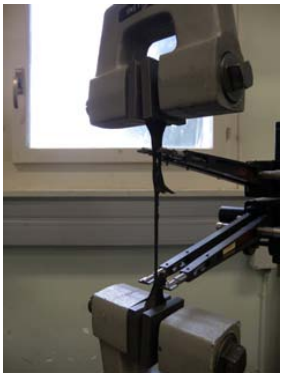

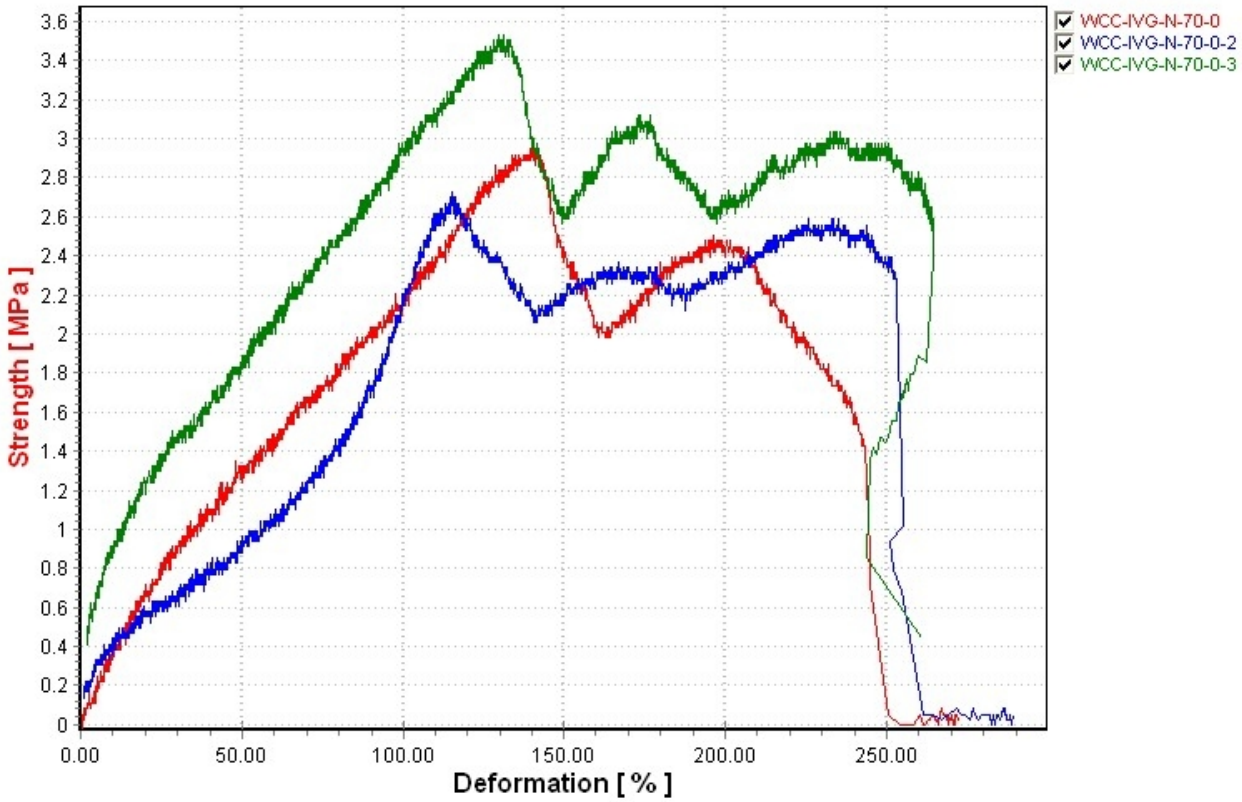

CERN - EN/MME/MM

Test Report

-

EN Engineering Department

Customer:	J-C. Guillaume EN/EL		
Material:	Rubber + reinforcement		
Operator:	AG		
Preparation:	22 kGy	Testdate:	14.04.2010
Teststandard	ISO 37	Spare Field	LHC
		Type of test:	Tensile
Speed Step1	50.00 mm/min	Groupe of sample	WCC-IVG-N-70-22

Gaine cable LHC	B [mm]	H [mm]	Rm [MPa]	Agt [%]
WCC-IVG-N-70-22	5.90	10.00	2.95	119.31
WCC-IVG-N-70-22-2	5.85	10.20	3.00	124.01
WCC-IVG-N-70-22-3	5.92	10.10	2.99	123.54
-	--			

	B [mm]	H [mm]	Rm [MPa]	Agt [%]
min	5.85	10.00	2.95	119.31
max	5.92	10.20	3.00	124.01
AM	5.89	10.10	2.98	122.28
s	0.04	0.10	0.03	2.59

Set-up

Broken sample

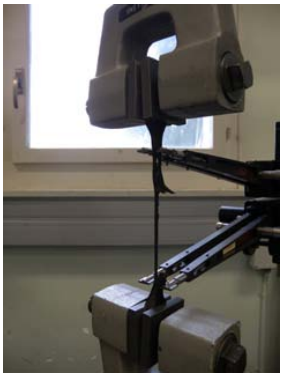

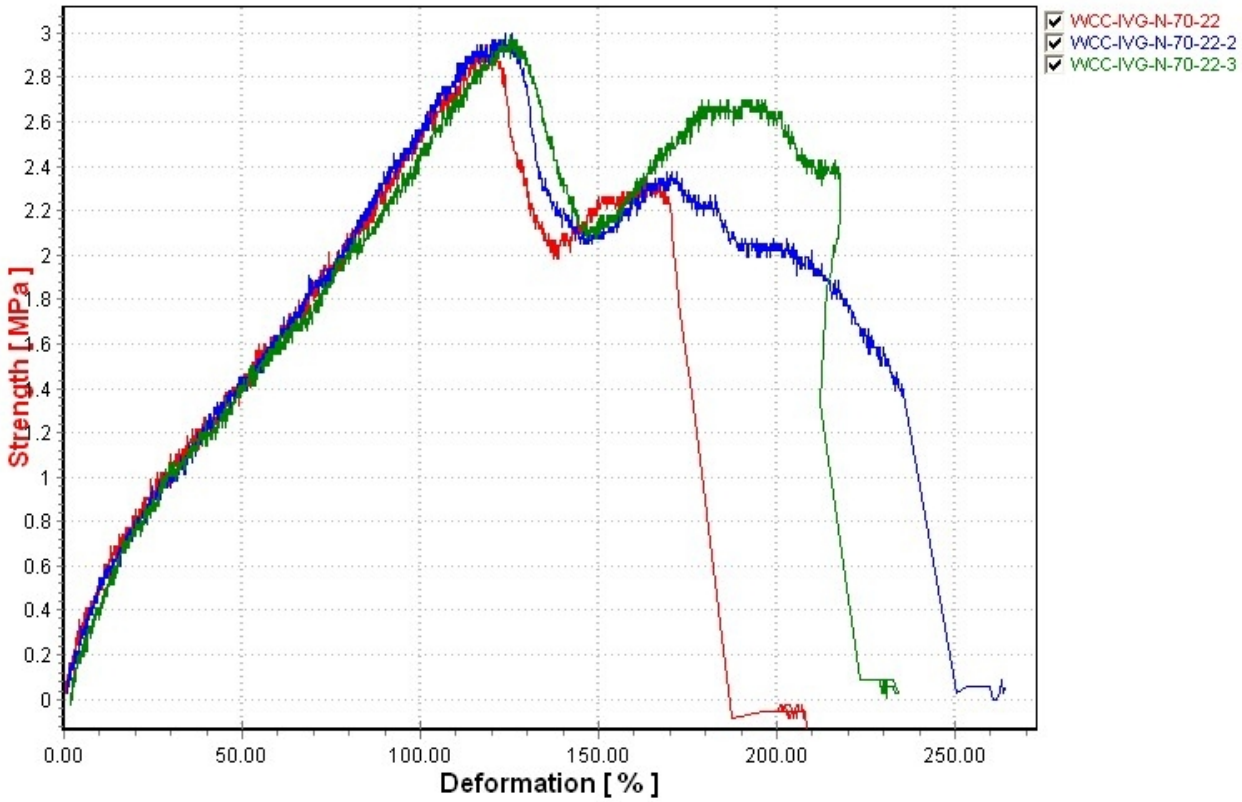

CERN - EN/MME/MM

Test Report

-

EN Engineering Department

Customer:	J-C. Guillaume EN/EL		
Material:	Rubber + reinforcement		
Operator:	Ph.D		
Preparation:	Total Dose Point	Testdate:	27.04.2010
Teststandard	ISO 37	Spare Field	LHC
		Type of test:	Tensile
Speed Step1	50.00 mm/min	Groupe of sample	WCC-IVG-N-70-100

Gaine cable LHC	B [mm]	H [mm]	Rm [MPa]	Agt [%]
WCC-IVG-N-70-100	5.50	9.95	3.27	89.27
WCC-IVG-N-70-100-2	5.80	10.00	3.12	93.59
WCC-IVG-N-70-100-3	5.30	9.90	3.38	96.74
-	--			
	B [mm]	H [mm]	Rm [MPa]	Agt [%]
min	5.30	9.90	3.12	89.27
max	5.80	10.00	3.38	96.74
AM	5.53	9.95	3.26	93.20
s	0.25	0.05	0.13	3.75

Set-up

Broken sample

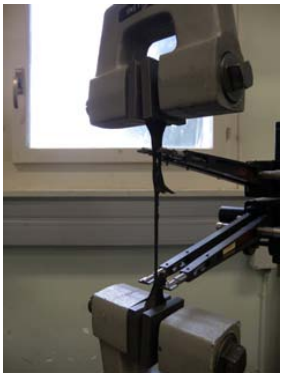

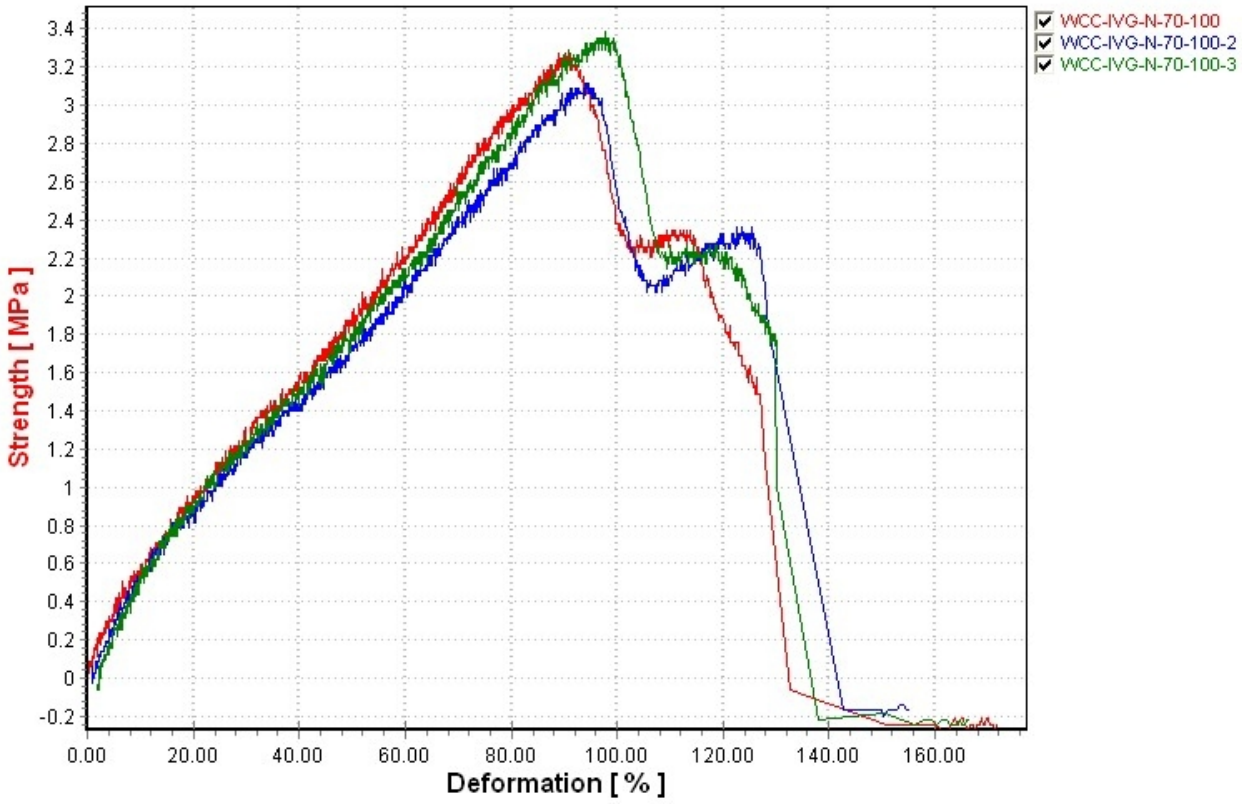

CERN - EN/MME/MM

Test Report

-

EN Engineering Department

Customer:	J-C. Guillaume EN/EL
Material:	Rubber + reinforcement
Operator:	Ph.D
Preparation:	250 kGy
Teststandard	ISO 37
Speed Step1	50.00 mm/min

Testdate:	21.04.2010
Spare Field	LHC
Type of test:	Tensile
Groupe of sample	WCC-IVG-N-70-250

Gaine cable LHC	B [mm]	H [mm]	Rm [MPa]	Agt [%]
WCC-IVG-N-70-250	5.70	10.05	3.44	79.11
WCC-IVG-N-70-250-2	5.60	10.00	3.60	86.02
WCC-IVG-N-70-250-3	5.60	9.95	3.53	80.55
-	--			
	B [mm]	H [mm]	Rm [MPa]	Agt [%]
min	5.60	9.95	3.44	79.11
max	5.70	10.05	3.60	86.02
AM	5.63	10.00	3.52	81.89
s	0.06	0.05	0.08	3.64

Set-up

Broken sample

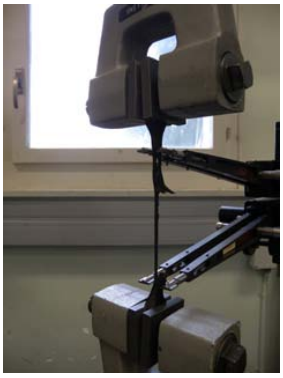

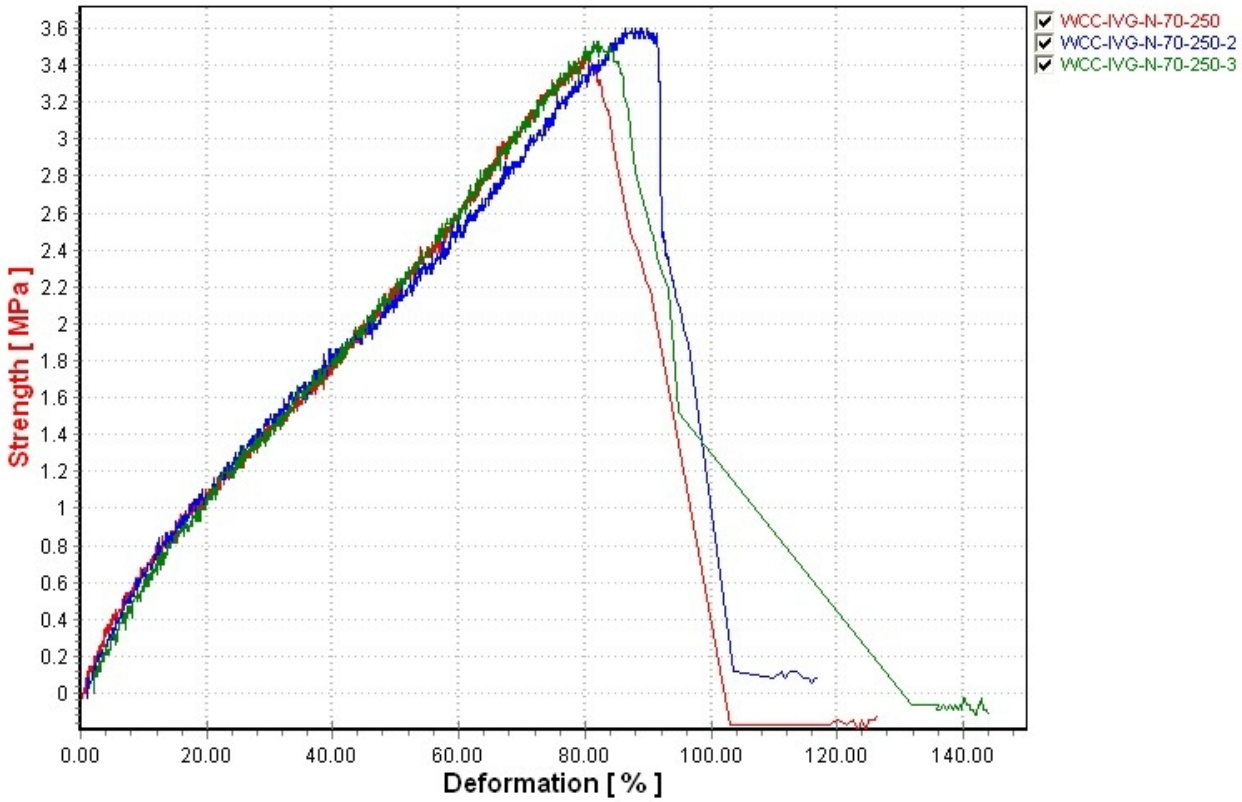

CERN - EN/MME/MM

Test Report

-

EN Engineering Department

Customer:	J-C. Guillaume EN/EL		
Material:	Rubber + reinforcement		
Operator:	Ph.D		
Preparation:	300 kGy	Testdate:	21.04.2010
Teststandard	ISO 37	Spare Field	LHC
		Type of test:	Tensile
Speed Step1	50.00 mm/min	Groupe of sample	WCC-IVG-N-70-300

Gaine cable LHC	B [mm]	H [mm]	Rm [MPa]	Agt [%]
WCC-IVG-N-70-300	6.00	10.10	3.25	67.89
WCC-IVG-N-70-300-2	5.70	10.25	3.51	67.37
WCC-IVG-N-70-300-3	5.90	10.05	3.43	68.69
-	--			
	B [mm]	H [mm]	Rm [MPa]	Agt [%]
min	5.70	10.05	3.25	67.37
max	6.00	10.25	3.51	68.69
AM	5.87	10.13	3.40	67.98
s	0.15	0.10	0.13	0.66

Set-up

Broken sample

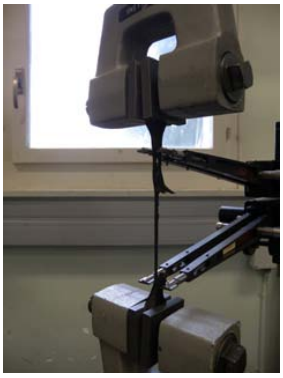

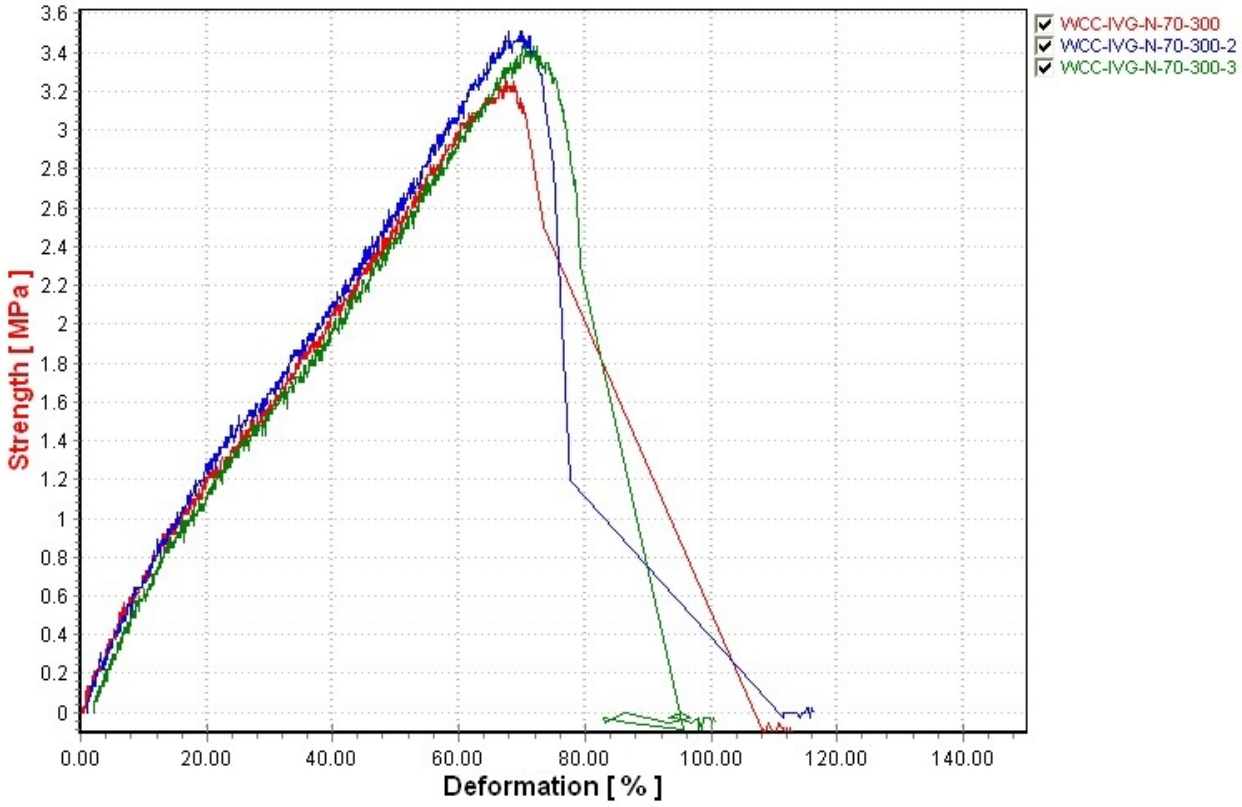

CERN - EN/MME/MM

Test Report

-

EN Engineering Department

Customer:	J-C. Guillaume EN/EL
Material:	Rubber + reinforcement
Operator:	Ph.D
Preparation:	330 kGy
Teststandard	ISO 37
Speed Step1	50.00 mm/min

Testdate:	21.04.2010
Spare Field	LHC
Type of test:	Tensile
Groupe of sample	WCC-IVG-N-70-330

Gaine cable LHC	B [mm]	H [mm]	Rm [MPa]	Agt [%]
WCC-IVG-N-70-330	5.70	10.05	3.55	70.57
WCC-IVG-N-70-330-2	6.00	10.05	3.51	69.80
WCC-IVG-N-70-330-3	6.00	10.05	3.37	67.88
-	--			
	B [mm]	H [mm]	Rm [MPa]	Agt [%]
min	5.70	10.05	3.37	67.88
max	6.00	10.05	3.55	70.57
AM	5.90	10.05	3.48	69.42
s	0.17	0.00	0.09	1.39

Set-up

Broken sample

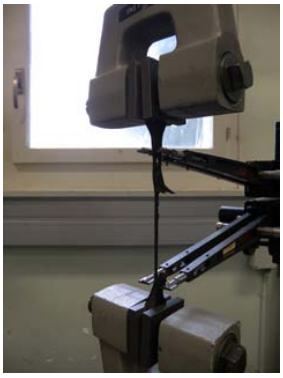

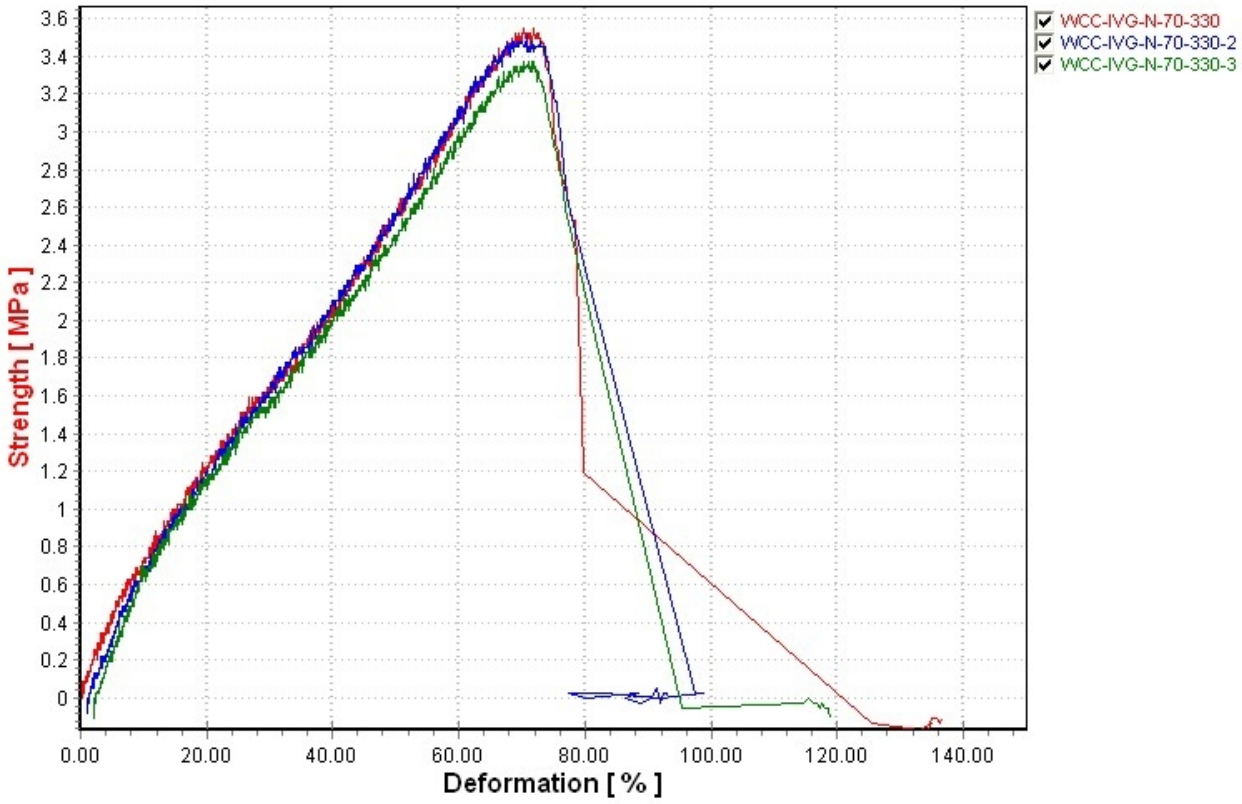

CERN - EN/MME/MM

Test Report

-

Engineering Department

Customer: J-C. Guillaume EN/EL

Material: Rubber + Nylon reinforcement

Operator: Ph.D

Preparation: 0 kGy

Teststandard ISO 37

Speed Step1 50.00 mm/min

Testdate: 08.04.2010

Spare Field LHC

Type of test: Tensile

Groupe of sample WCC-IVG-N-90-0

Gaine cable LHC	B [mm]	H [mm]	Rm [MPa]	Agt [%]
WCC-IVG-N-90-0	5.65	10.00	3.28	119.02
WCC-IVG-N-90-0-2	5.40	10.07	3.35	109.31
WCC-IVG-N-90-0-3	5.40	10.07	3.32	112.44
-	--			
	B [mm]	H [mm]	Rm [MPa]	Agt [%]
min	5.40	10.00	3.28	109.31
max	5.65	10.07	3.35	119.02
AM	5.48	10.05	3.32	113.59
s	0.14	0.04	0.03	4.95

Set-up

Broken sample

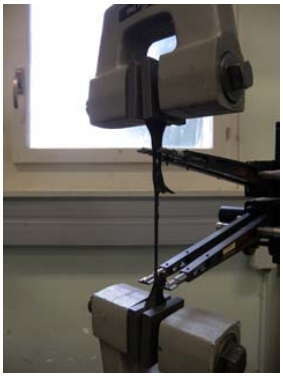

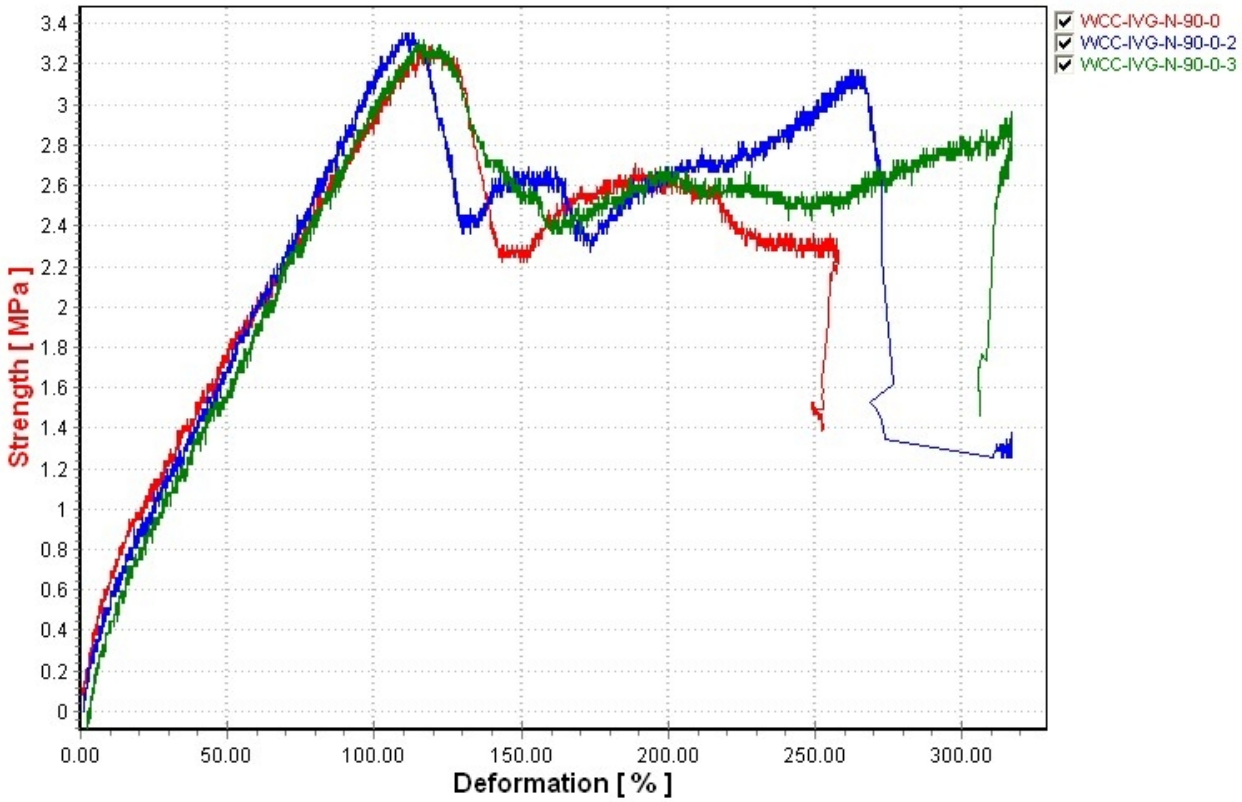

CERN - EN/MME/MM

Test Report

-

EN Engineering Department

Customer:	J-C. Guillaume EN/EL
Material:	Rubber + reinforcement
Operator:	Ph.D
Preparation:	22 kGy
Teststandard	ISO 37
Speed Step1	50.00 mm/min

Testdate:	08.06.2010
Spare Field	LHC
Type of test:	Tensile
Groupe of sample	WCC-IVG-N-90-22

Gaine cable LHC	B [mm]	H [mm]	Rm [MPa]	Agt [%]
WCC-IVG-N-90-22-1	5.55	10.00	2.84	82.36
WCC-IVG-N-90-22-2	5.50	10.00	2.96	88.71
WCC-IVG-N-90-22-3	5.46	9.95	3.09	90.67
-	--			
	B [mm]	H [mm]	Rm [MPa]	Agt [%]
min	5.46	9.95	2.84	82.36
max	5.55	10.00	3.09	90.67
AM	5.50	9.98	2.96	87.25
s	0.05	0.03	0.12	4.34

Set-up

Broken sample

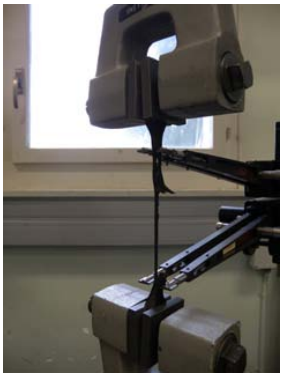

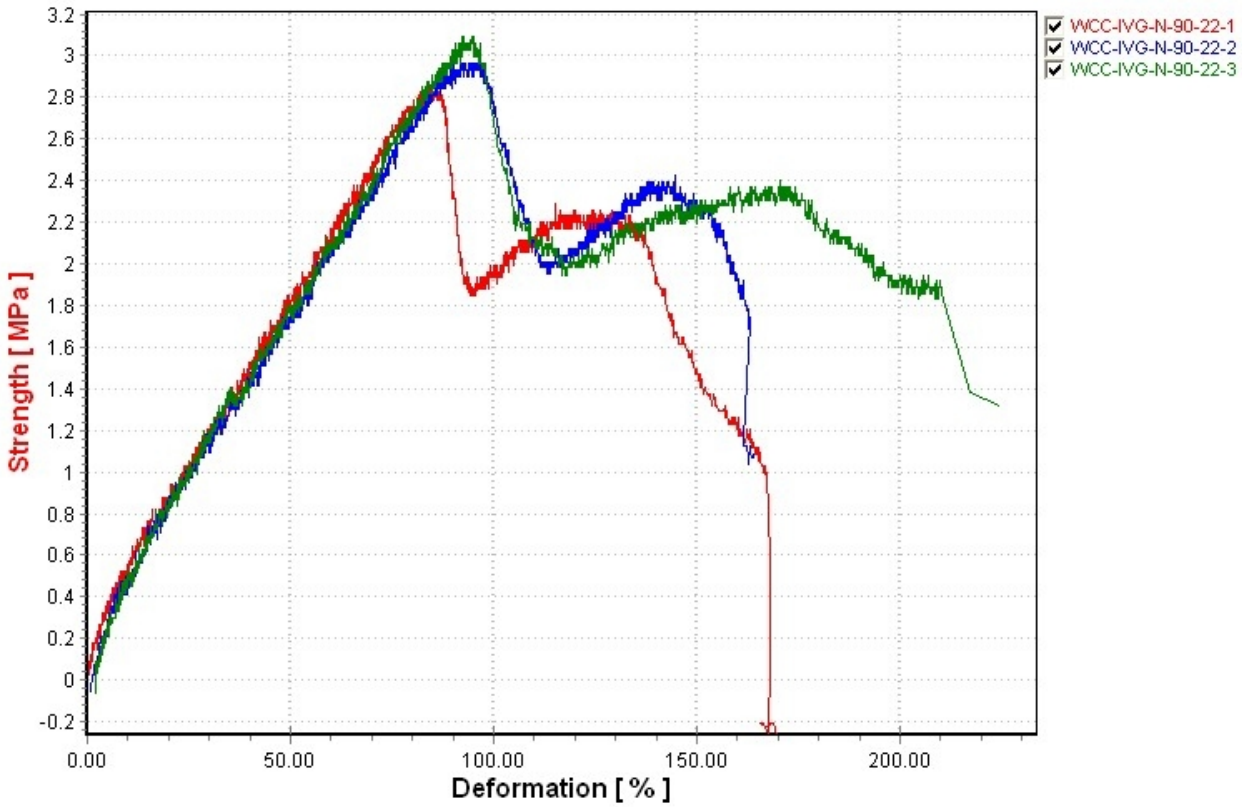

CERN - EN/MME/MM

Test Report

-

EN Engineering Department

Customer:	J-C. Guillaume EN/EL
Material:	Rubber + reinforcement
Operator:	Ph.D
Preparation:	100 kGy
Teststandard	ISO 37
Speed Step1	50.00 mm/min

Testdate:	08.06.2010
Spare Field	LHC
Type of test:	Tensile
Groupe of sample	WCC-IVG-N-90-100

Gaine cable LHC	B [mm]	H [mm]	Rm [MPa]	Agt [%]
WCC-IVG-N-90-100-1	5.70	10.10	3.25	81.29
WCC-IVG-N-90-100-2	5.45	9.95	3.45	82.86
WCC-IVG-N-90-100-3	5.70	10.05	3.01	74.64
-	--			
	B [mm]	H [mm]	Rm [MPa]	Agt [%]
min	5.45	9.95	3.01	74.64
max	5.70	10.10	3.45	82.86
AM	5.62	10.03	3.24	79.60
s	0.14	0.08	0.22	4.37

Set-up

Broken sample

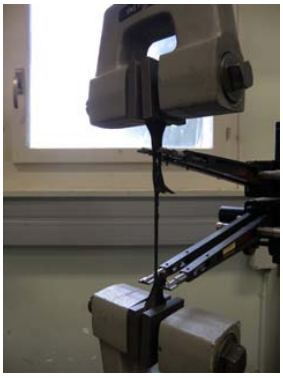

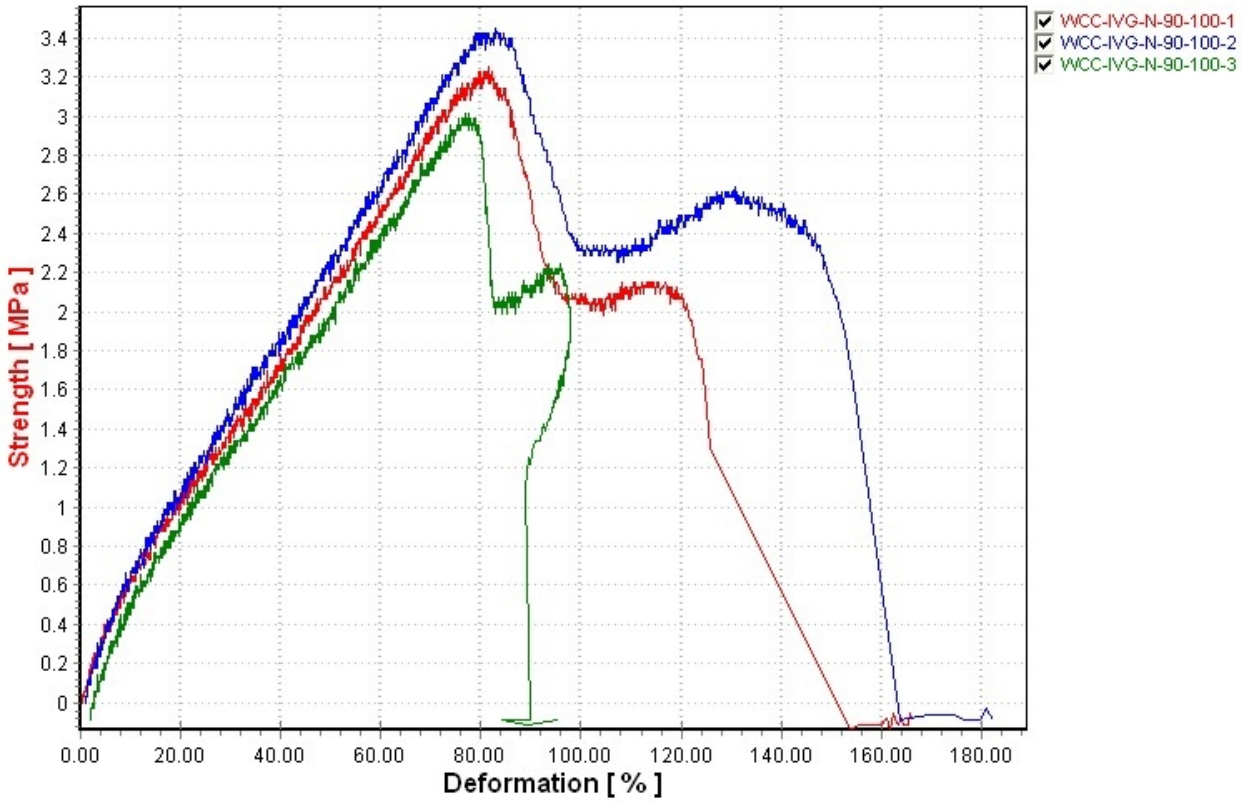

CERN - EN/MME/MM

Test Report

-

EN Engineering Department

Customer:	J-C. Guillaume EN/EL		
Material:	Rubber + reinforcement		
Operator:	Ph.D		
Preparation:	250 kGy	Testdate:	16.09.2010
Teststandard	ISO 37	Spare Field	LHC
		Type of test:	Tensile
Speed Step1	50.00 mm/min	Groupe of sample	WCC-IVG-N-90-250

Gaine cable LHC	B [mm]	H [mm]	Rm [MPa]	Agt [%]
WCC-IVG-N-90-250-1	5.70	10.12	3.50	63.76
WCC-IVG-N-90-250-2	5.70	10.25	3.37	59.06
WCC-IVG-N-90-250-3	5.60	10.15	3.58	58.87
-	--			
	B [mm]	H [mm]	Rm [MPa]	Agt [%]
min	5.60	10.12	3.37	58.87
max	5.70	10.25	3.58	63.76
AM	5.67	10.17	3.48	60.57
s	0.06	0.07	0.10	2.77

Set-up

Broken sample

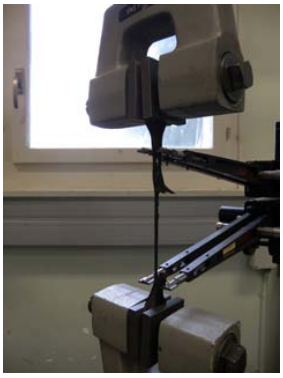

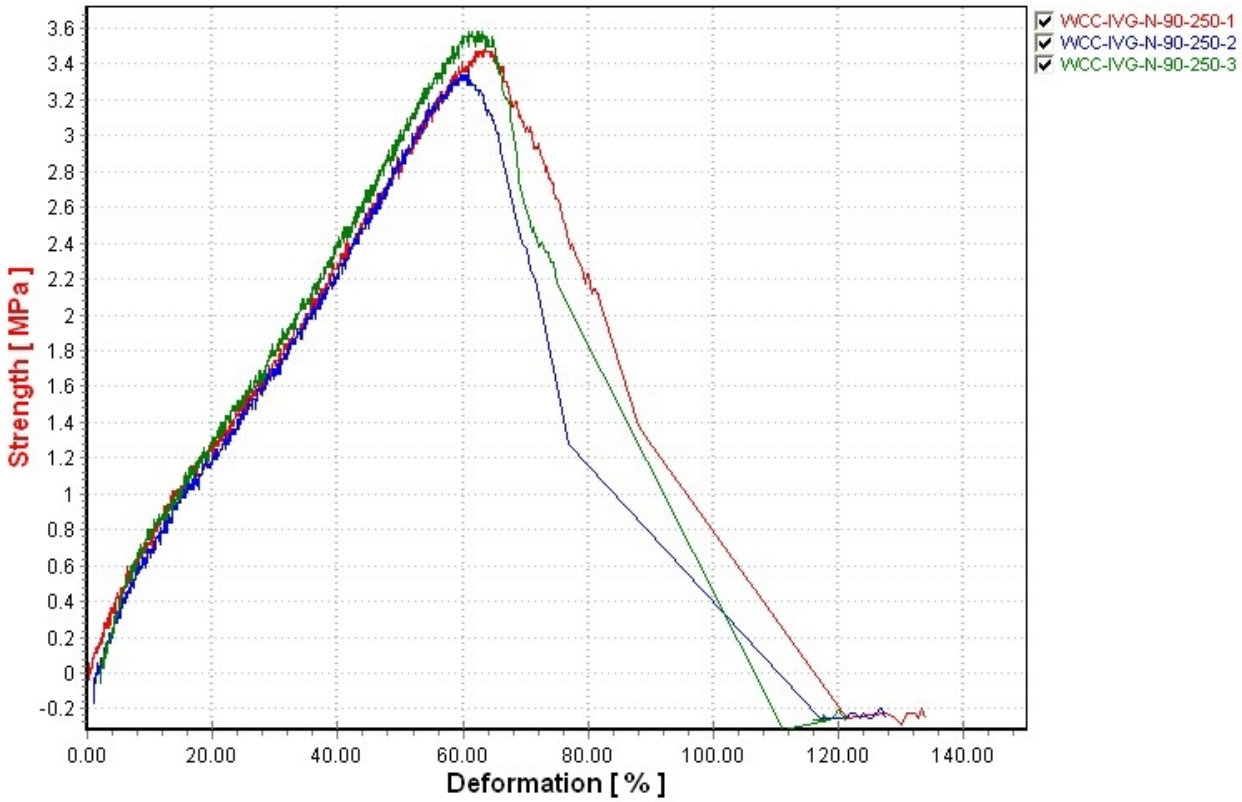

CERN - EN/MME/MM

Test Report

-

EN Engineering Department

Customer:	J-C. Guillaume EN/EL		
Material:	Rubber + reinforcement		
Operator:	Ph.D		
Preparation:	300 kGy	Testdate:	16.09.2010
Teststandard	ISO 37	Spare Field	LHC
		Type of test:	Tensile
Speed Step1	50.00 mm/min	Groupe of sample	WCC-IVG-N-90-300

Gaine cable LHC	B [mm]	H [mm]	Rm [MPa]	Agt [%]
WCC-IVG-N-90-300-1	5.70	10.00	3.43	62.34
WCC-IVG-N-90-300-2	5.70	10.06	3.58	61.11
WCC-IVG-N-90-300-3	5.70	10.06	3.58	64.02
-	--			
	B [mm]	H [mm]	Rm [MPa]	Agt [%]
min	5.70	10.00	3.43	61.11
max	5.70	10.06	3.58	64.02
AM	5.70	10.04	3.53	62.49
s	0.00	0.03	0.09	1.46

Set-up

Broken sample

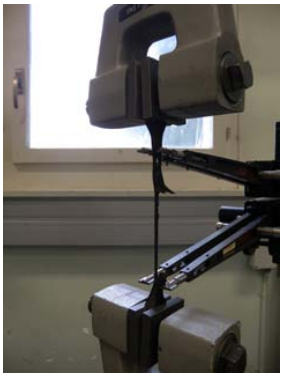

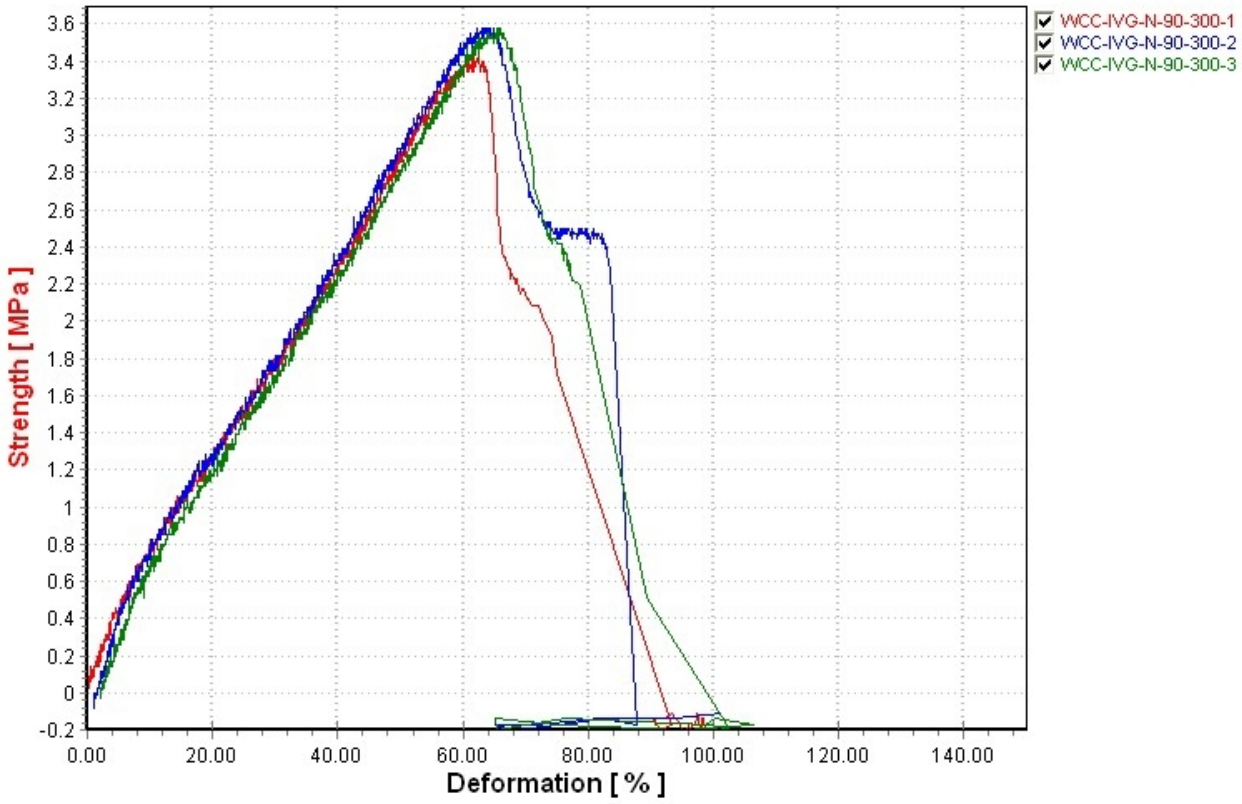

CERN - EN/MME/MM

Test Report

-

EN Engineering Department

Customer:	J-C. Guillaume EN/EL
Material:	Rubber + reinforcement
Operator:	Ph.D
Preparation:	330 kGy
Teststandard	ISO 37
Speed Step1	50.00 mm/min

Testdate:	17.09.2010
Spare Field	LHC
Type of test:	Tensile
Groupe of sample	WCC-IVG-N-90-330

Gaine cable LHC	B [mm]	H [mm]	Rm [MPa]	Agt [%]
WCC-IVG-N-90-330-1	5.85	10.05	3.91	65.51
WCC-IVG-N-90-330-2	5.80	10.10	3.67	60.00
WCC-IVG-N-90-330-3	5.60	10.00	3.92	59.91
-	--			
	B [mm]	H [mm]	Rm [MPa]	Agt [%]
min	5.60	10.00	3.67	59.91
max	5.85	10.10	3.92	65.51
AM	5.75	10.05	3.83	61.81
s	0.13	0.05	0.14	3.21

Set-up

Broken sample

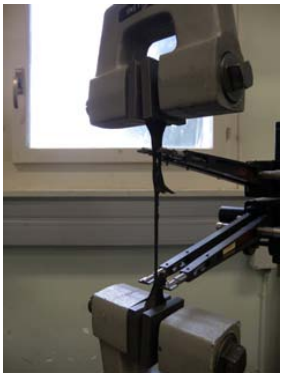

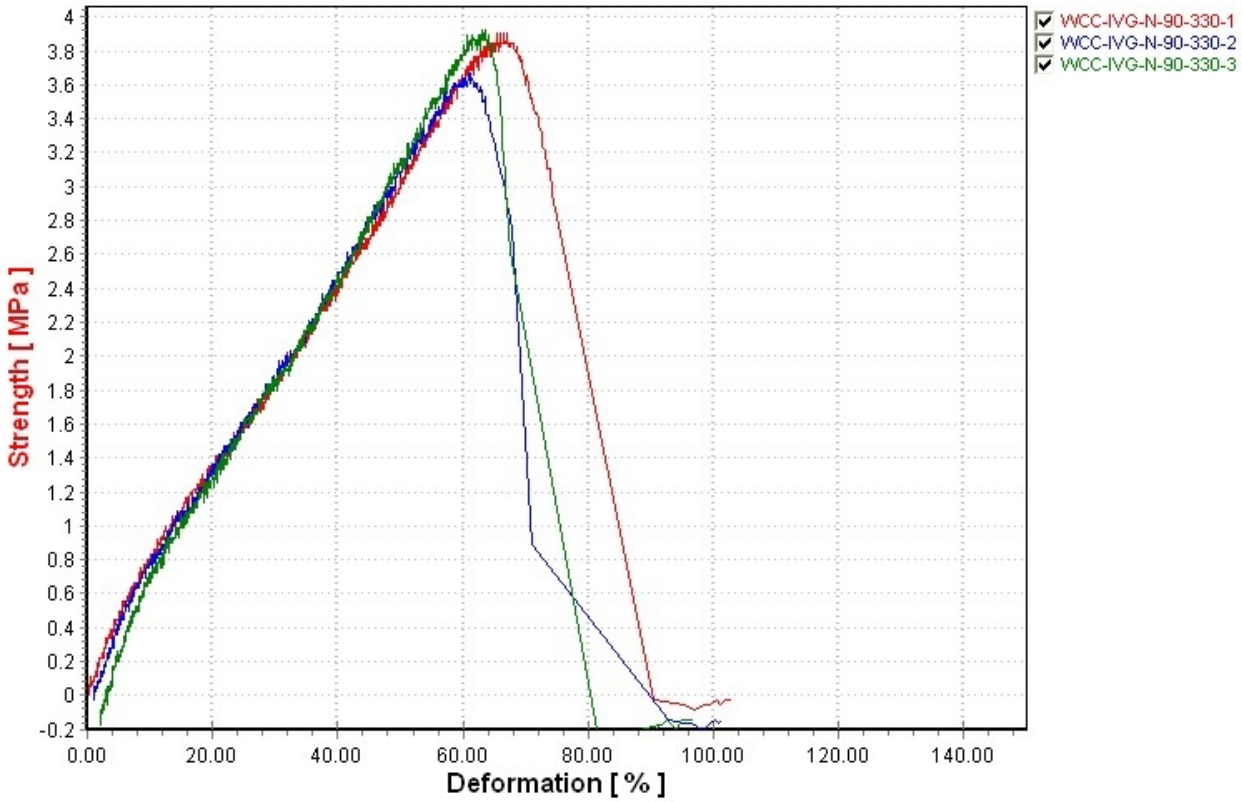

CERN - EN/MME/MM

Test Report

-

Engineering Department

Customer: J-C. Guillaume EN/EL
Material: Rubber + Rayon reinforcement
Operator: AG
Preparation: 0 kGy
Teststandard ISO 37

Speed Step1 50.00 mm/min

Testdate: 07.04.2010
Spare Field LHC
Type of test: Tensile
Groupe of sample WCC-IVG-R-42-0

Gaine cable LHC	B [mm]	H [mm]	Rm [MPa]	Agt [%]
WCC-IVG-R-42-0	5.94	9.80	2.93	99.20
WCC-IVG-R-42-0-2	6.02	9.89	2.62	88.24
WCC-IVG-R-42-0-3	6.08	9.92	2.83	99.40
-	--			
	B [mm]	H [mm]	Rm [MPa]	Agt [%]
min	5.94	9.80	2.62	88.24
max	6.08	9.92	2.93	99.40
AM	6.01	9.87	2.80	95.61
s	0.07	0.06	0.16	6.39

Set-up

Broken sample

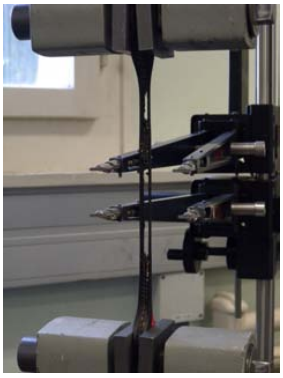

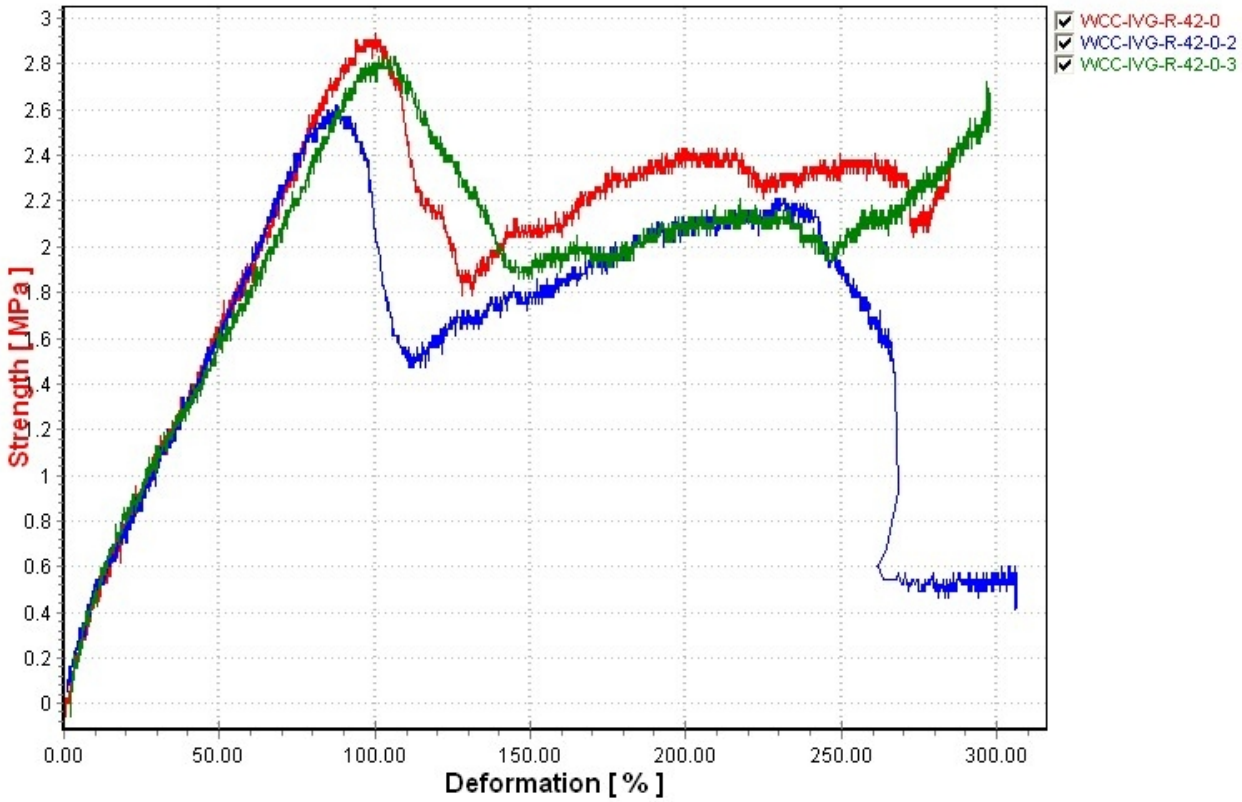

CERN - EN/MME/MM

Test Report

-

EN Engineering Department

Customer:	J-C. Guillaume EN/EL
Material:	Rubber + reinforcement
Operator:	AG
Preparation:	22 kGy
Teststandard	ISO 37
Speed Step1	50.00 mm/min

Testdate:	15.04.2010
Spare Field	LHC
Type of test:	Tensile
Groupe of sample	WCC-IVG-R-42-22

Gaine cable LHC	B [mm]	H [mm]	Rm [MPa]	Agt [%]
WCC-IVG-R-42-22	6.12	9.82	2.90	92.42
WCC-IVG-R-42-22-2	6.15	9.75	3.15	87.44
WCC-IVG-R-42-22-3	6.09	9.74	2.99	90.79
-	--			

	B [mm]	H [mm]	Rm [MPa]	Agt [%]
min	6.09	9.74	2.90	87.44
max	6.15	9.82	3.15	92.42
AM	6.12	9.77	3.01	90.22
s	0.03	0.04	0.13	2.54

Set-up

Broken sample

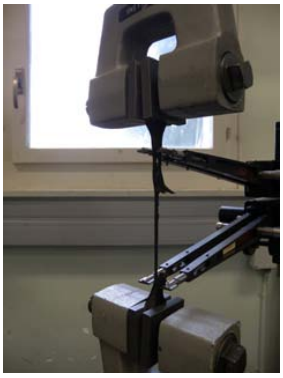

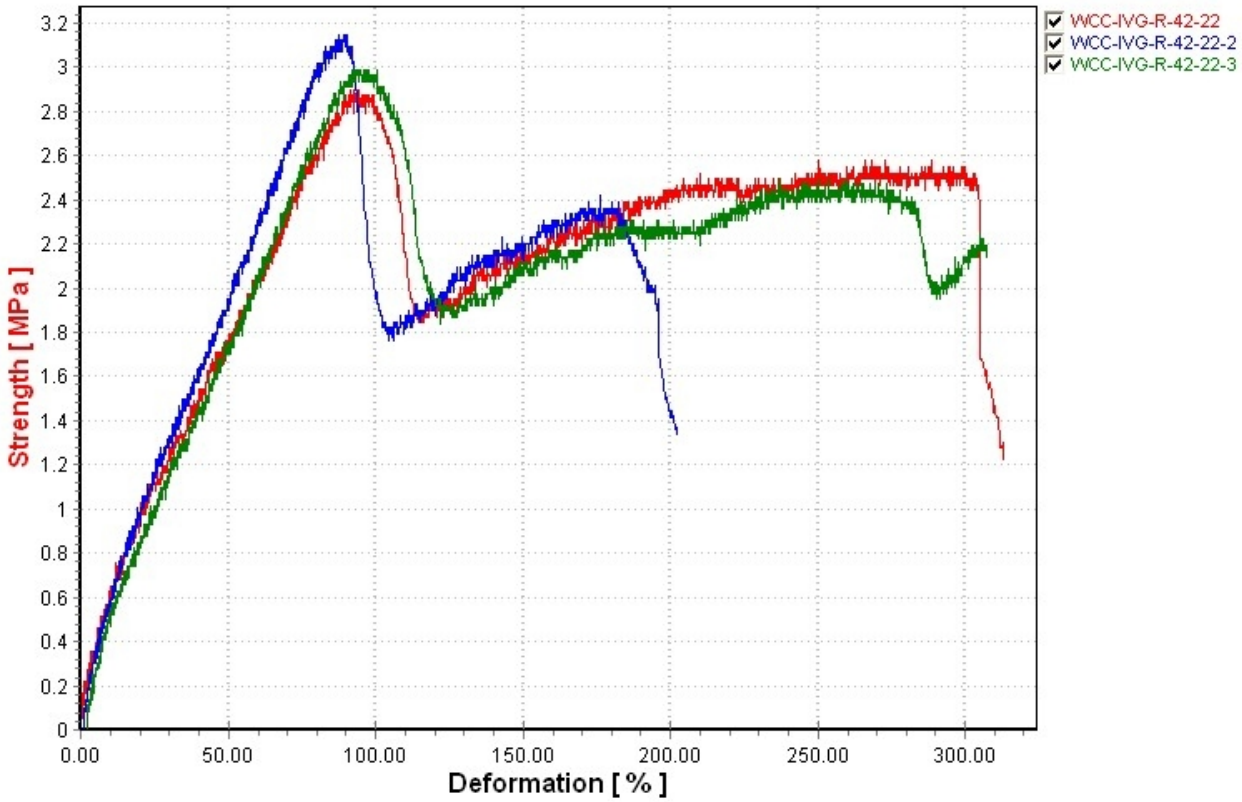

CERN - EN/MME/MM

Test Report

-

EN Engineering Department

Customer:	J-C. Guillaume EN/EL
Material:	Rubber + reinforcement
Operator:	Ph.D
Preparation:	Total Dose Point
Teststandard	ISO 37
Speed Step1	50.00 mm/min

Testdate:	27.04.2010
Spare Field	LHC
Type of test:	Tensile
Groupe of sample	WCC-IVG-R-42-100

Gaine cable LHC	B [mm]	H [mm]	Rm [MPa]	Agt [%]
WCC-IVG-R-42-100	6.00	9.65	3.29	74.38
WCC-IVG-R-42-100-2	6.00	9.65	3.34	77.61
WCC-IVG-R-42-100-3	6.00	9.65	3.26	71.82
-	--			
	B [mm]	H [mm]	Rm [MPa]	Agt [%]
min	6.00	9.65	3.26	71.82
max	6.00	9.65	3.34	77.61
AM	6.00	9.65	3.30	74.60
s	0.00	0.00	0.04	2.90

Set-up

Broken sample

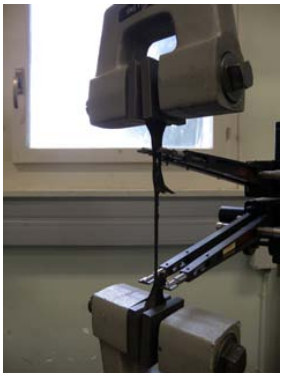

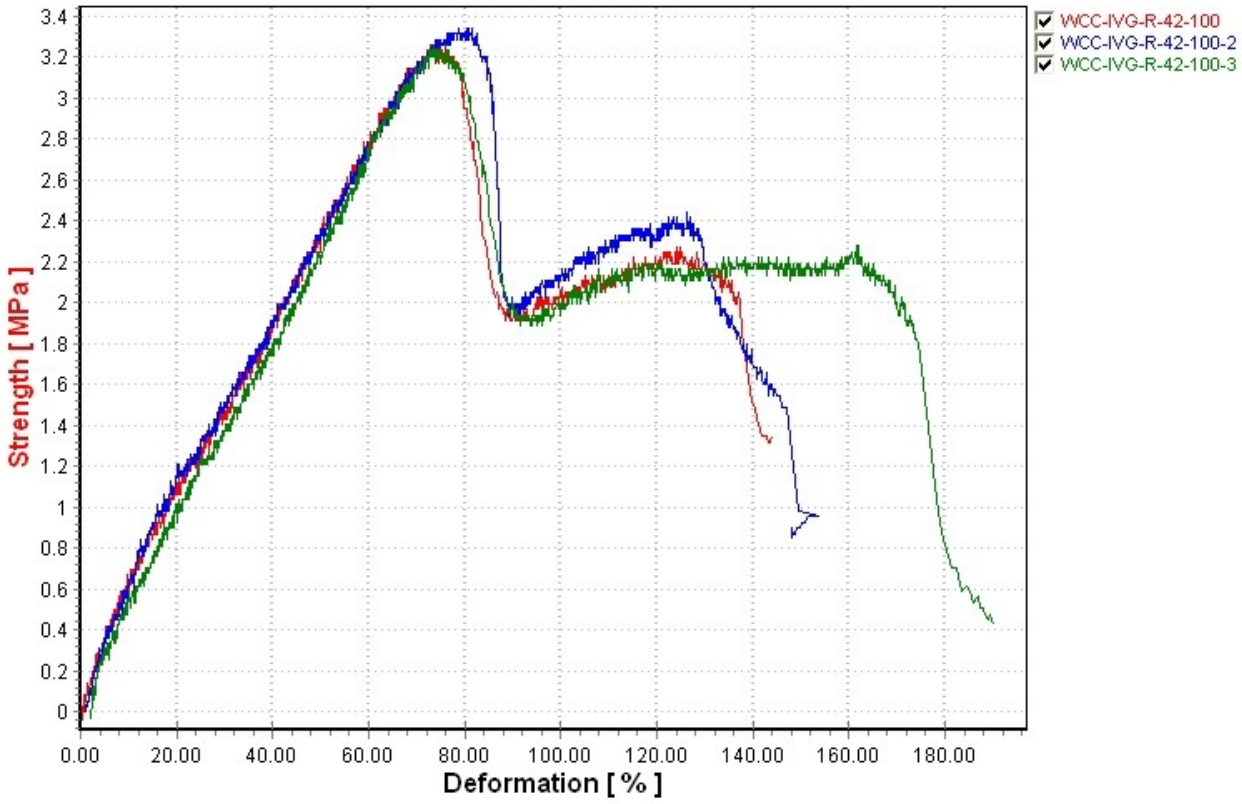

CERN - EN/MME/MM

Test Report

-

EN Engineering Department

Customer:	J-C. Guillaume EN/EL
Material:	Rubber + reinforcement
Operator:	Ph.D
Preparation:	250 kGy
Teststandard	ISO 37
Speed Step1	50.00 mm/min

Testdate:	21.04.2010
Spare Field	LHC
Type of test:	Tensile
Groupe of sample	WCC-IVG-R-42-250

Gaine cable LHC	B [mm]	H [mm]	Rm [MPa]	Agt [%]
WCC-IVG-R-42-250	6.05	9.60	3.33	65.14
WCC-IVG-R-42-250-2	6.10	9.45	3.28	63.51
WCC-IVG-R-42-250-3	6.00	9.70	3.16	59.99
-	--			
	B [mm]	H [mm]	Rm [MPa]	Agt [%]
min	6.00	9.45	3.16	59.99
max	6.10	9.70	3.33	65.14
AM	6.05	9.58	3.26	62.88
s	0.05	0.13	0.09	2.63

Set-up

Broken sample

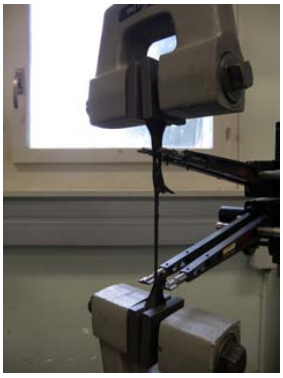

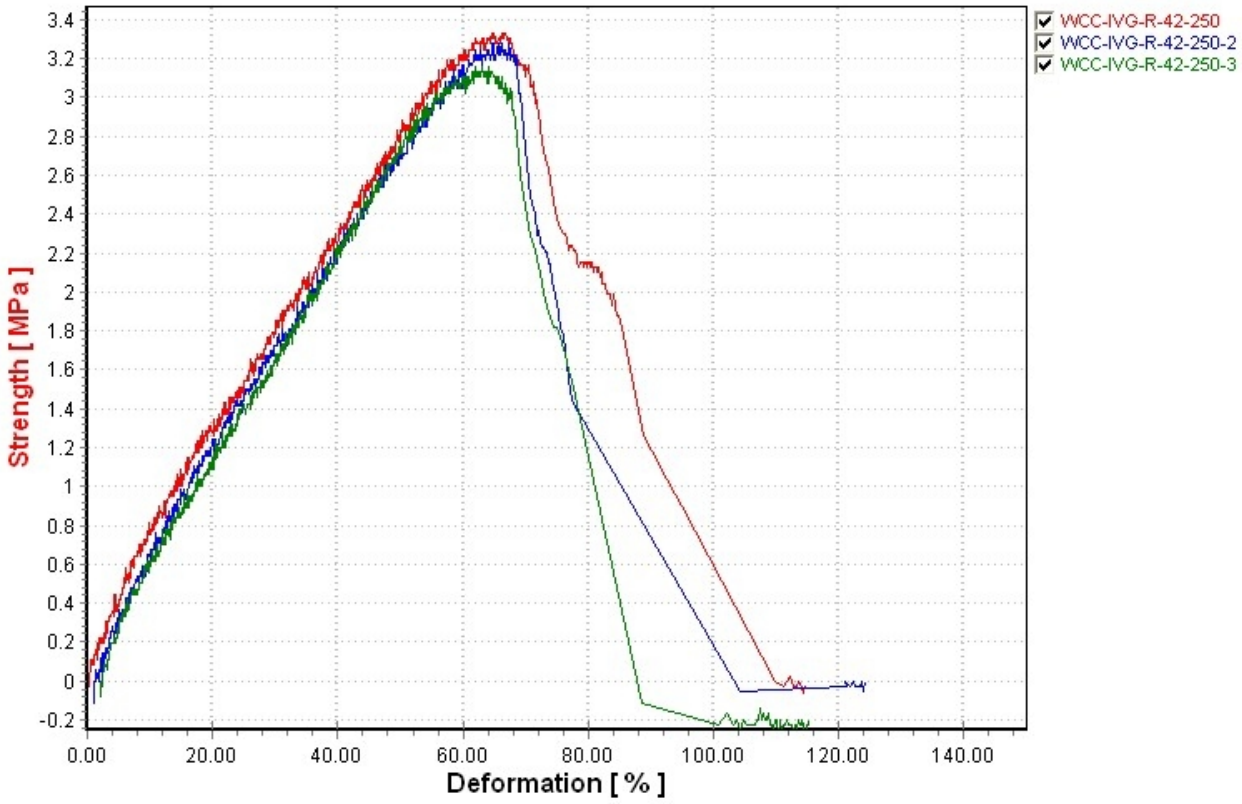

CERN - EN/MME/MM

Test Report

-

Engineering Department

Customer:	J-C. Guillaume EN/EL
Material:	Rubber + reinforcement
Operator:	Ph.D
Preparation:	300 kGy
Teststandard	ISO 37
Speed Step1	50.00 mm/min

Testdate:	21.04.2010
Spare Field	LHC
Type of test:	Tensile
Groupe of sample	WCC-IVG-R-42-300

Gaine cable LHC	B [mm]	H [mm]	Rm [MPa]	Agt [%]
WCC-IVG-R-42-300	6.13	9.50	3.94	68.53
WCC-IVG-R-42-300-2	6.30	9.70	3.25	61.14
WCC-IVG-R-42-300-3	6.10	10.00	3.23	66.88
-	--			
	B [mm]	H [mm]	Rm [MPa]	Agt [%]
min	6.10	9.50	3.23	61.14
max	6.30	10.00	3.94	68.53
AM	6.18	9.73	3.47	65.51
s	0.11	0.25	0.41	3.88

Set-up

Broken sample

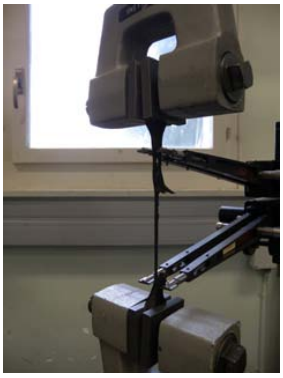

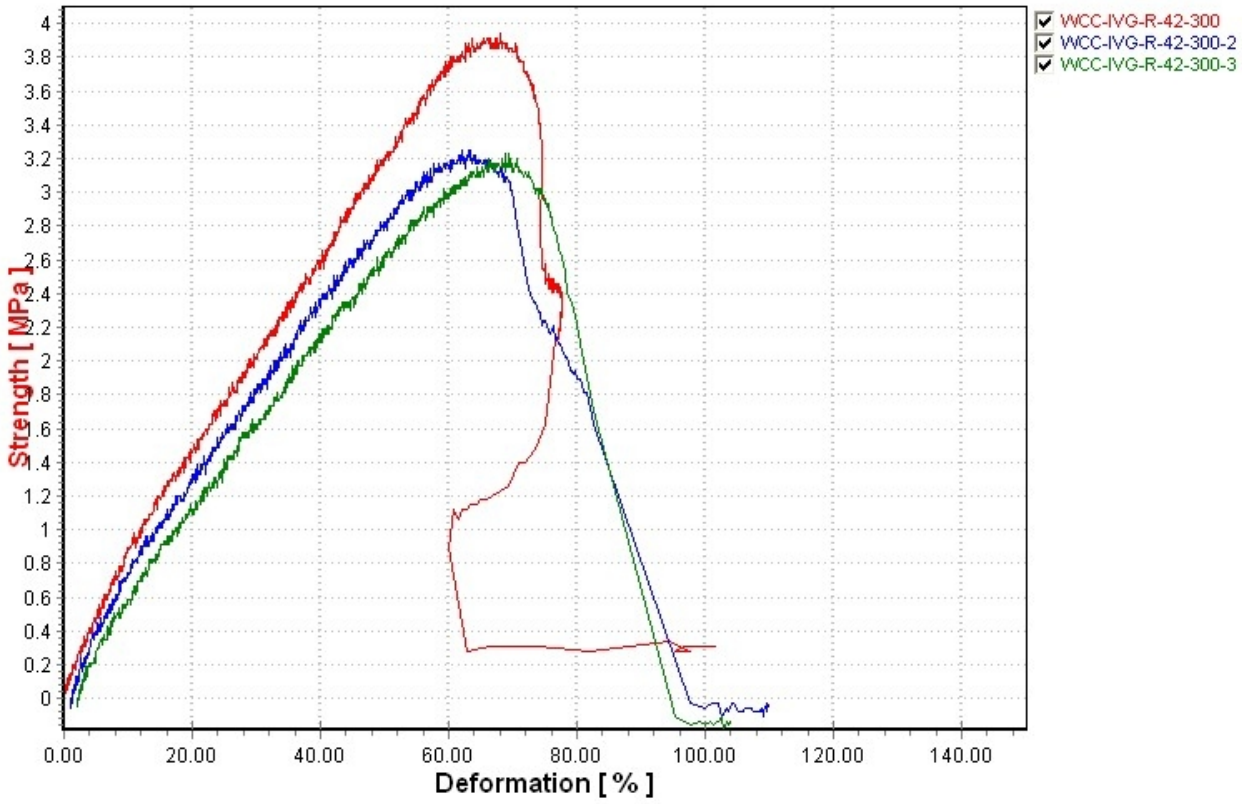

CERN - EN/MME/MM

Test Report

-

EN Engineering Department

Customer:	J-C. Guillaume EN/EL
Material:	Rubber + reinforcement
Operator:	Ph.D
Preparation:	330 kGy
Teststandard	ISO 37
Speed Step1	50.00 mm/min

Testdate:	21.04.2010
Spare Field	LHC
Type of test:	Tensile
Groupe of sample	WCC-IVG-R-42-330

Gaine cable LHC	B [mm]	H [mm]	Rm [MPa]	Agt [%]
WCC-IVG-R-42-330	6.00	9.76	3.22	57.58
WCC-IVG-R-42-330-2	6.00	9.80	3.46	60.22
WCC-IVG-R-42-330-3	6.00	9.70	3.44	61.07
-	--			
	B [mm]	H [mm]	Rm [MPa]	Agt [%]
min	6.00	9.70	3.22	57.58
max	6.00	9.80	3.46	61.07
AM	6.00	9.75	3.38	59.62
s	0.00	0.05	0.13	1.82

Set-up

Broken sample

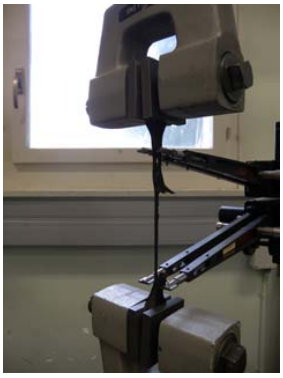

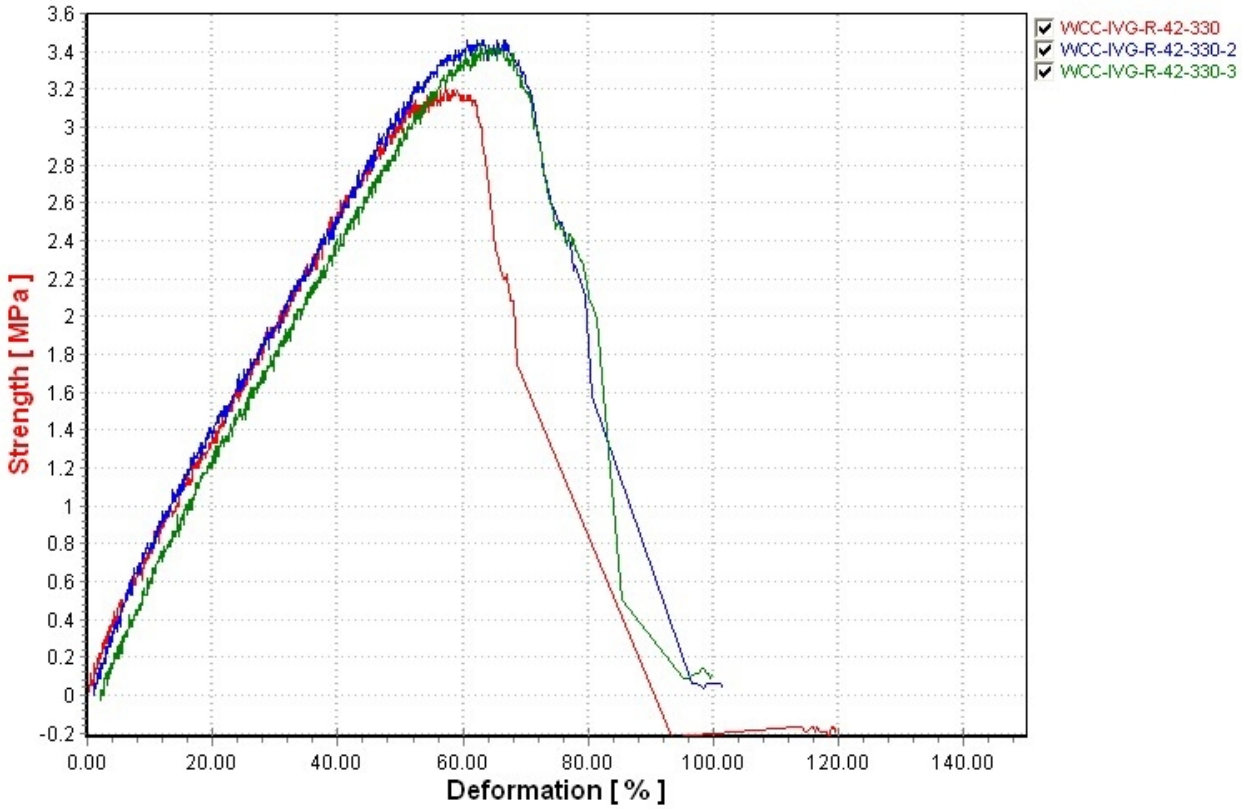

CERN - EN/MME/MM

Test Report

-

Engineering Department

Customer: J-C. Guillaume EN/EL
Material: Rubber + Rayon reinforcement
Operator: AG
Preparation: 0 kGy
Teststandard ISO 37

Speed Step1 50.00 mm/min

Testdate: 07.04.2010
Spare Field LHC
Type of test: Tensile
Groupe of sample WCC-IVG-R-70-0

Gaine cable LHC	B [mm]	H [mm]	Rm [MPa]	Agt [%]
WCC-IVG-R-70-0	6.00	9.80	2.68	101.41
WCC-IVG-R-70-0-2	6.20	9.85	2.56	104.54
WCC-IVG-R-70-0-3	6.20	9.85	2.61	109.75
-	--			
	B [mm]	H [mm]	Rm [MPa]	Agt [%]
min	6.00	9.80	2.56	101.41
max	6.20	9.85	2.68	109.75
AM	6.13	9.83	2.62	105.23
s	0.12	0.03	0.06	4.21

Set-up

Broken sample

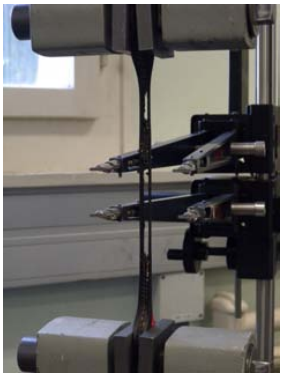

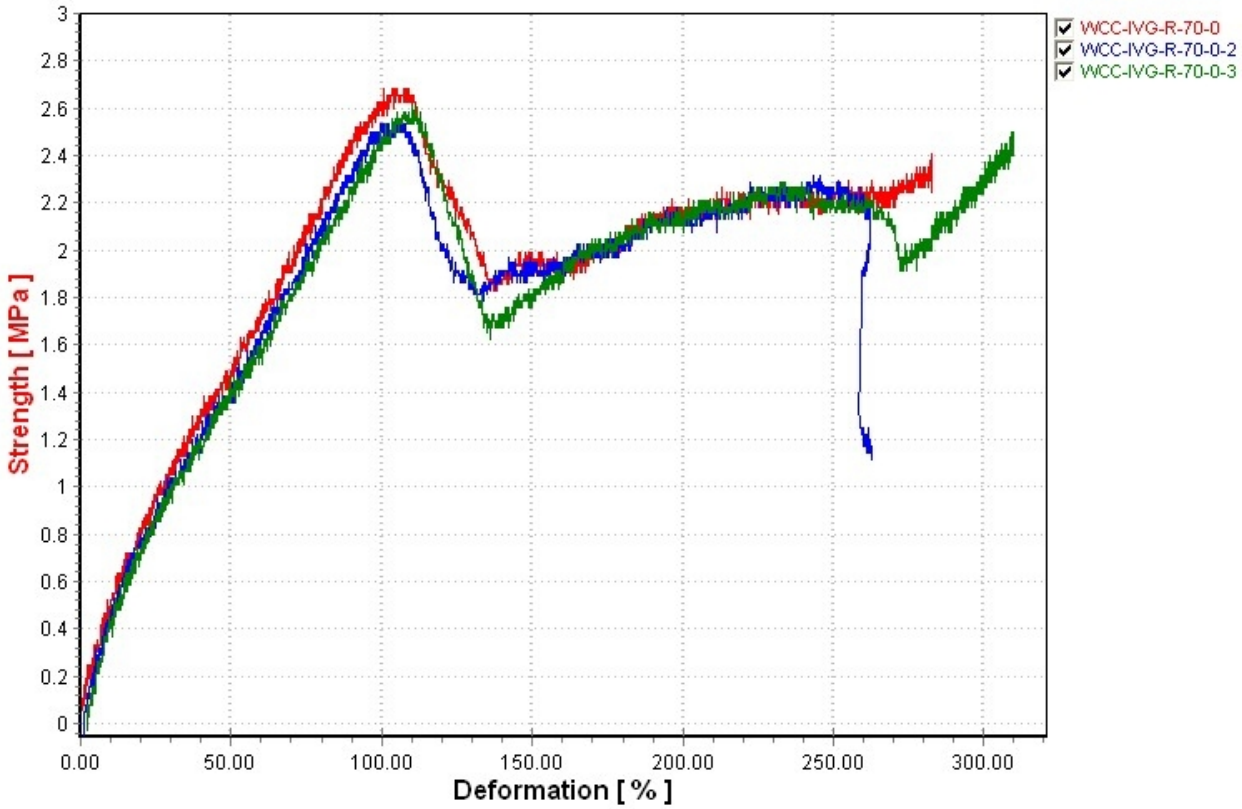

CERN - EN/MME/MM

Test Report

-

Engineering Department

Customer:	J-C. Guillaume EN/EL
Material:	Rubber + reinforcement
Operator:	Ph.D
Preparation:	22 kGy
Teststandard	ISO 37
Speed Step1	50.00 mm/min

Testdate:	08.06.2010
Spare Field	LHC
Type of test:	Tensile
Groupe of sample	WCC-IVG-R-70-22

Gaine cable LHC	B [mm]	H [mm]	Rm [MPa]	Agt [%]
WCC-IVG-R-70-22-1	5.65	9.90	2.71	83.87
WCC-IVG-R-70-22-2	5.90	9.80	2.53	82.44
WCC-IVG-R-70-22-3	5.90	9.80	2.73	85.69
-	--			
	B [mm]	H [mm]	Rm [MPa]	Agt [%]
min	5.65	9.80	2.53	82.44
max	5.90	9.90	2.73	85.69
AM	5.82	9.83	2.66	84.00
s	0.14	0.06	0.11	1.63

Set-up

Broken sample

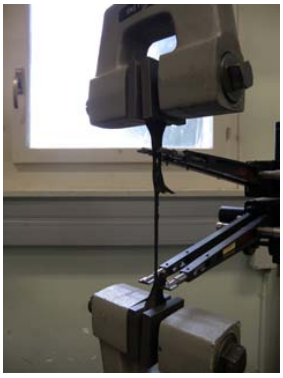

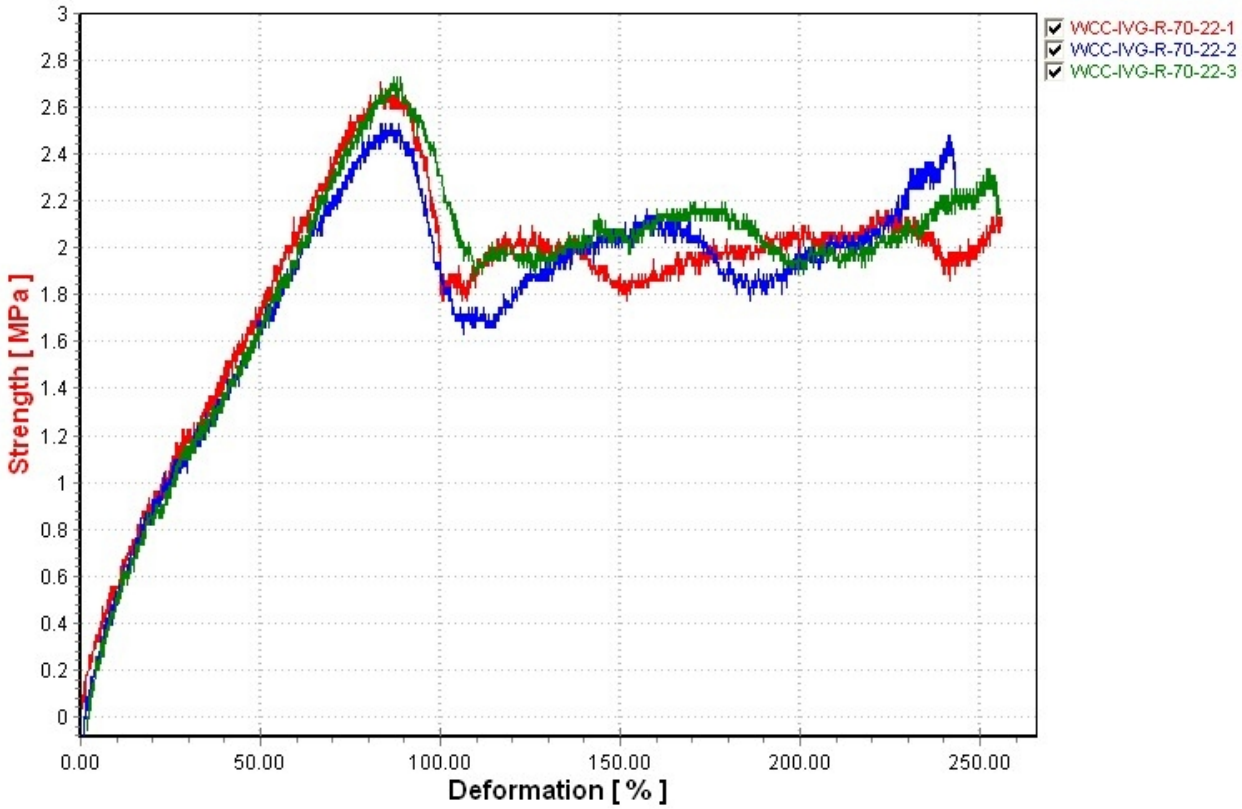

CERN - EN/MME/MM

Test Report

-

Engineering Department

Customer:	J-C. Guillaume EN/EL
Material:	Rubber + reinforcement
Operator:	Ph.D
Preparation:	Total Dose Point
Teststandard	ISO 37
Speed Step1	50.00 mm/min

Testdate:	21.04.2010
Spare Field	LHC
Type of test:	Tensile
Groupe of sample	WCC-IVG-R-70-100

Gaine cable LHC	B [mm]	H [mm]	Rm [MPa]	Agt [%]
WCC-IVG-R-70-100	6.00	9.70	2.77	83.17
WCC-IVG-R-70-100-2	5.80	9.80	2.72	83.65
WCC-IVG-R-70-100-3	5.90	9.80	2.79	79.11
-	--			
	B [mm]	H [mm]	Rm [MPa]	Agt [%]
min	5.80	9.70	2.72	79.11
max	6.00	9.80	2.79	83.65
AM	5.90	9.77	2.76	81.97
s	0.10	0.06	0.04	2.50

Set-up

Broken sample

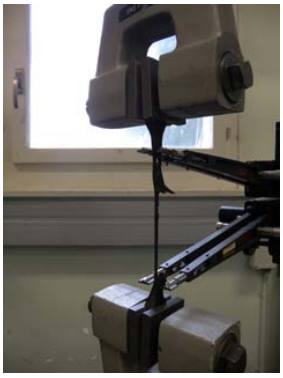

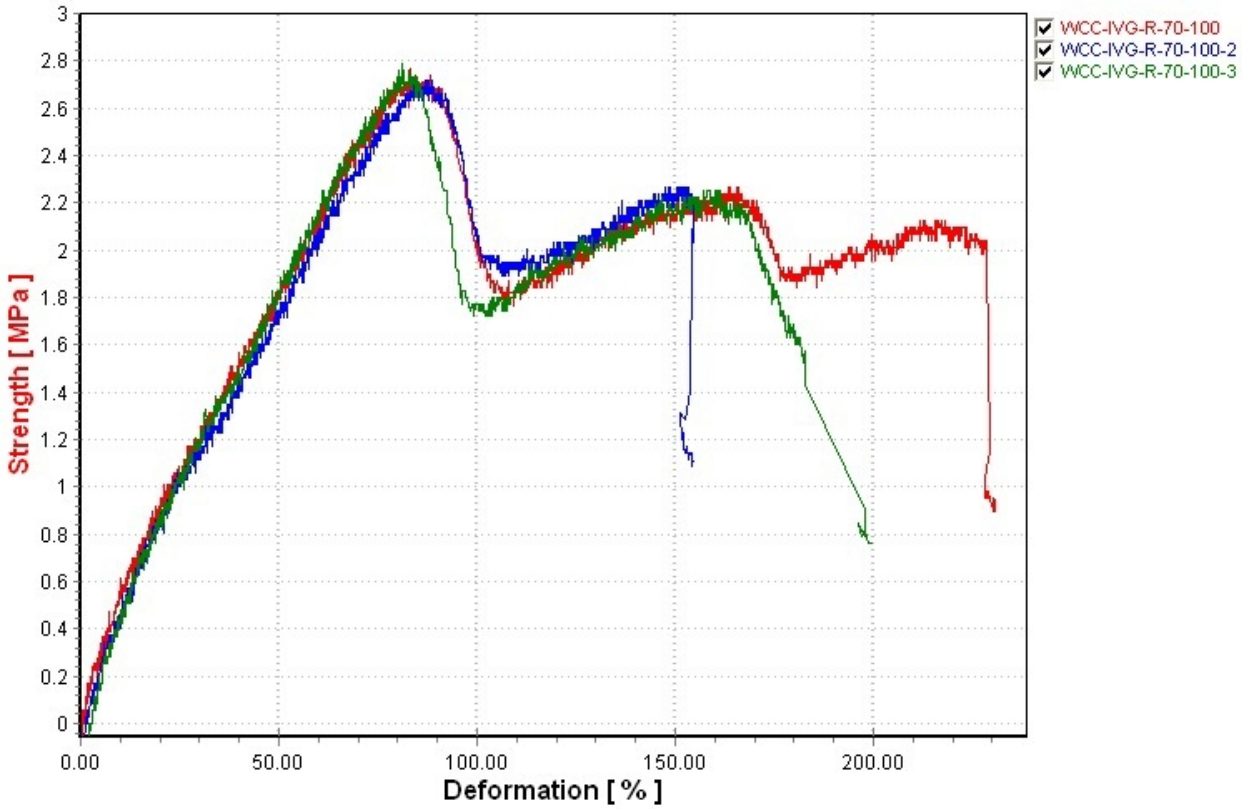

CERN - EN/MME/MM

Test Report

-

EN Engineering Department

Customer:	J-C. Guillaume EN/EL
Material:	Rubber + reinforcement
Operator:	Ph.D
Preparation:	250 kGy
Teststandard	ISO 37
Speed Step1	50.00 mm/min

Testdate:	16.09.2010
Spare Field	LHC
Type of test:	Tensile
Groupe of sample	WCC-IVG-R-70-250

Gaine cable LHC	B [mm]	H [mm]	Rm [MPa]	Agt [%]
WCC-IVG-R-70-250-1	6.15	9.80	3.05	58.67
WCC-IVG-R-70-250-2	6.20	9.65	2.69	53.12
WCC-IVG-R-70-250-3	6.27	9.80	3.02	61.40
-	--			
	B [mm]	H [mm]	Rm [MPa]	Agt [%]
min	6.15	9.65	2.69	53.12
max	6.27	9.80	3.05	61.40
AM	6.21	9.75	2.92	57.73
s	0.06	0.09	0.20	4.22

Set-up

Broken sample

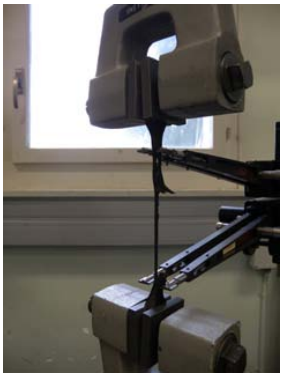

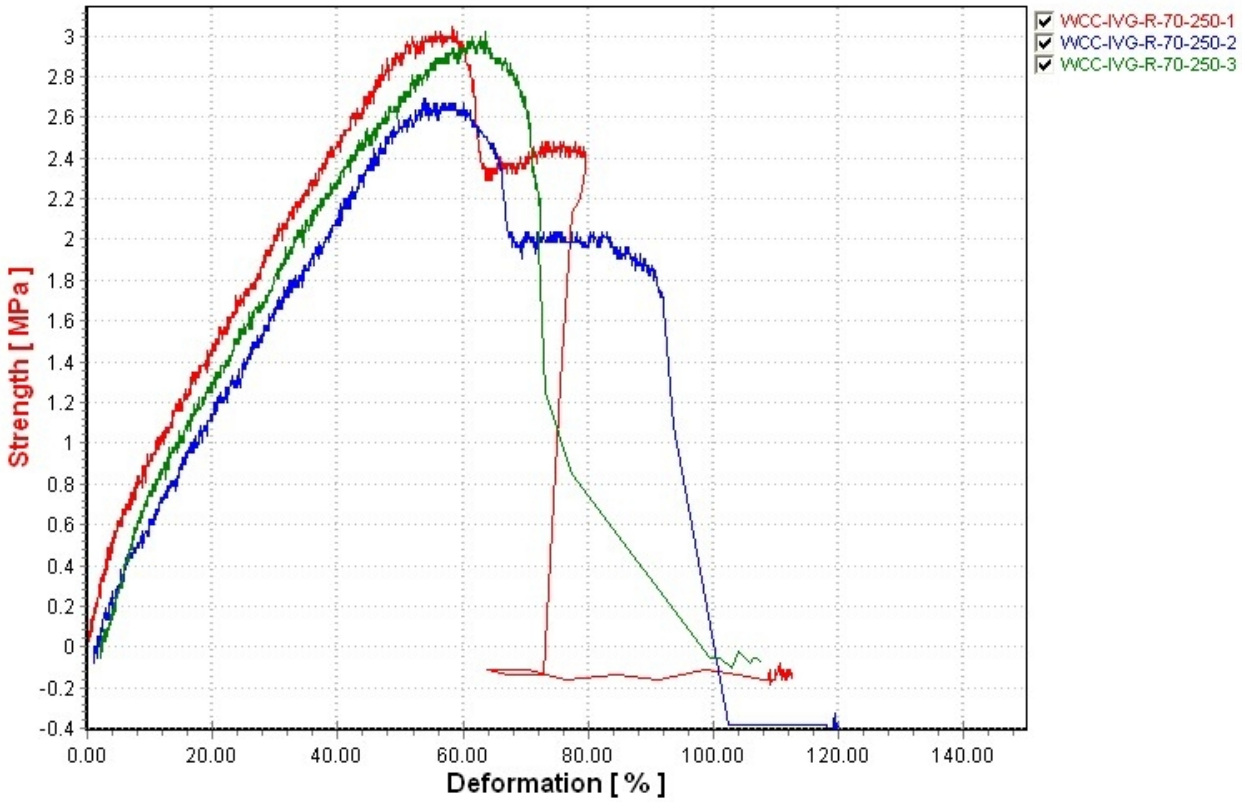

CERN - EN/MME/MM

Test Report

-

EN Engineering Department

Customer:	J-C. Guillaume EN/EL
Material:	Rubber + reinforcement
Operator:	Ph.D
Preparation:	300 kGy
Teststandard	ISO 37
Speed Step1	50.00 mm/min

Testdate:	16.09.2010
Spare Field	LHC
Type of test:	Tensile
Groupe of sample	WCC-IVG-R-70-300

Gaine cable LHC	B [mm]	H [mm]	Rm [MPa]	Agt [%]
WCC-IVG-R-70-300-1	6.10	9.90	2.85	63.74
WCC-IVG-R-70-300-2	6.20	9.85	2.74	60.36
WCC-IVG-R-70-300-3	6.20	9.80	2.68	54.18
-	--			
	B [mm]	H [mm]	Rm [MPa]	Agt [%]
min	6.10	9.80	2.68	54.18
max	6.20	9.90	2.85	63.74
AM	6.17	9.85	2.76	59.43
s	0.06	0.05	0.09	4.85

Set-up

Broken sample

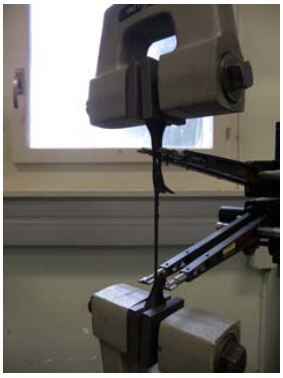

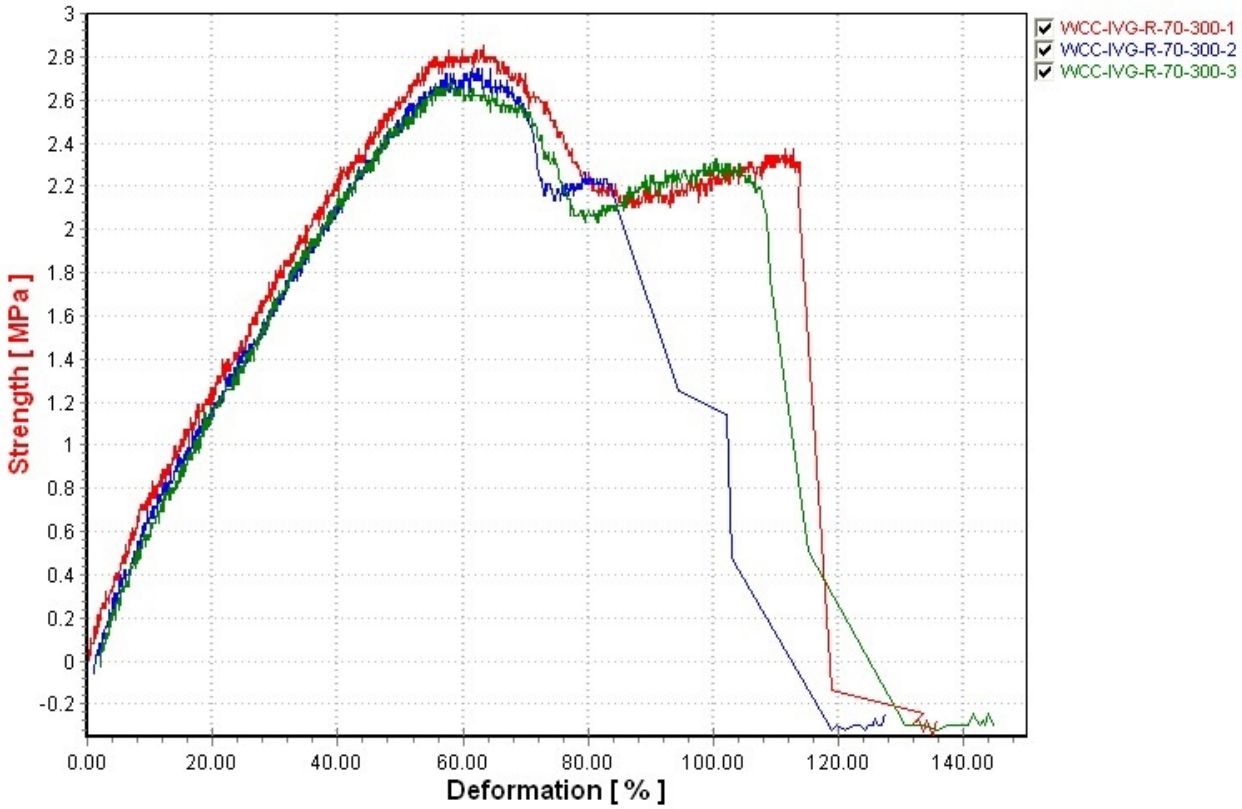

CERN - EN/MME/MM

Test Report

-

EN Engineering Department

Customer:	J-C. Guillaume EN/EL
Material:	Rubber + reinforcement
Operator:	Ph.D
Preparation:	330 kGy
Teststandard	ISO 37
Speed Step1	50.00 mm/min

Testdate:	17.09.2010
Spare Field	LHC
Type of test:	Tensile
Groupe of sample	WCC-IVG-R-70-330

Gaine cable LHC	B [mm]	H [mm]	Rm [MPa]	Agt [%]
WCC-IVG-R-70-330-1	6.10	9.75	2.87	56.35
WCC-IVG-R-70-330-2	5.95	9.65	3.35	61.39
WCC-IVG-R-70-330-3	6.00	9.80	3.24	55.12
-	--			
	B [mm]	H [mm]	Rm [MPa]	Agt [%]
min	5.95	9.65	2.87	55.12
max	6.10	9.80	3.35	61.39
AM	6.02	9.73	3.15	57.62
s	0.08	0.08	0.25	3.32

Set-up

Broken sample

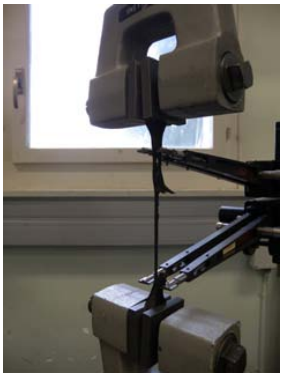

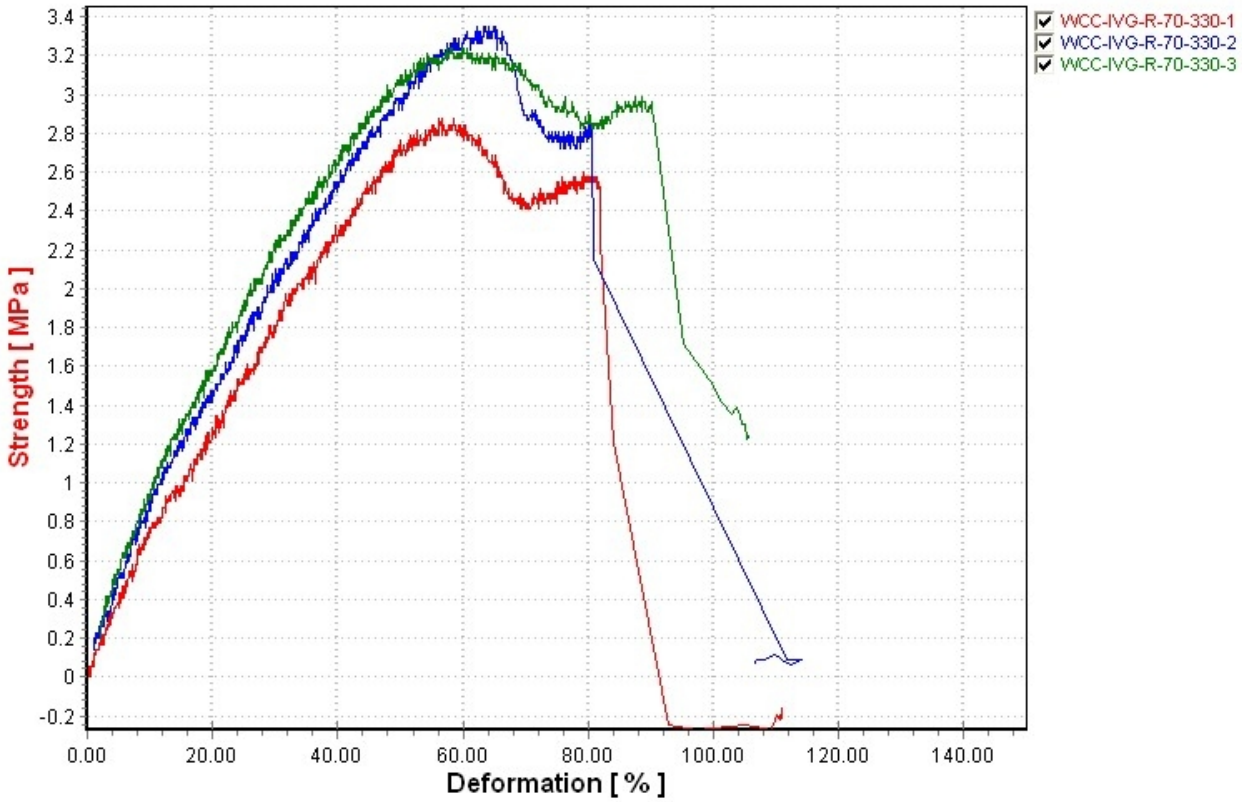

CERN - EN/MME/MM

Test Report

-

Engineering Department

Customer: J-C. Guillaume EN/EL
Material: Rubber + Rayon reinforcement
Operator: AG
Preparation: 0 kGy
Teststandard ISO 37

Speed Step1 50.00 mm/min

Testdate: 07.04.2010
Spare Field LHC
Type of test: Tensile
Groupe of sample WCC-IVG-R-90-0

Gaine cable LHC	B [mm]	H [mm]	Rm [MPa]	Agt [%]
WCC-IVG-R-90-0	6.20	9.69	2.98	88.10
WCC-IVG-R-90-0-2	6.23	9.57	2.89	99.50
WCC-IVG-R-90-0-3	6.20	9.62	3.08	100.97
-	--			
	B [mm]	H [mm]	Rm [MPa]	Agt [%]
min	6.20	9.57	2.89	88.10
max	6.23	9.69	3.08	100.97
AM	6.21	9.63	2.99	96.19
s	0.02	0.06	0.10	7.05

Set-up

Broken sample

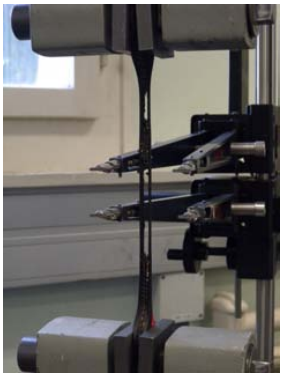

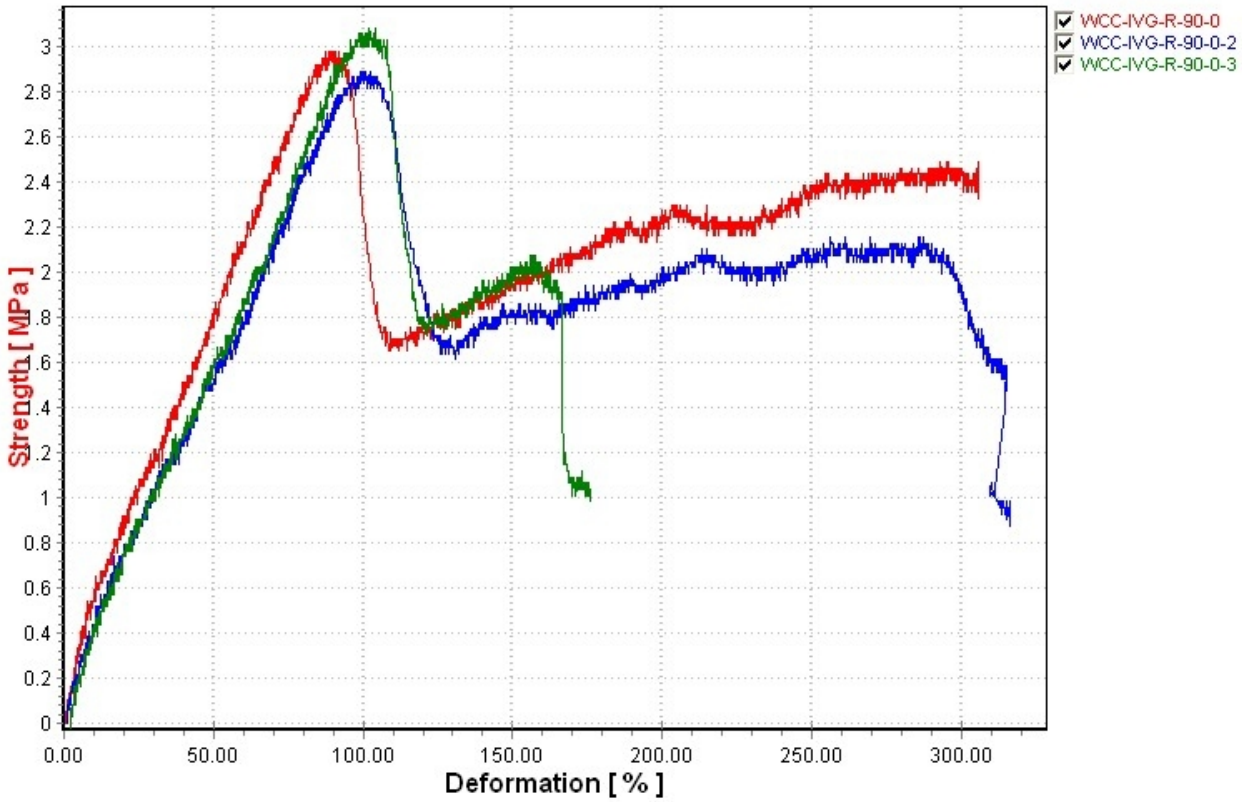

CERN - EN/MME/MM

Test Report

-

EN Engineering Department

Customer:	J-C. Guillaume EN/EL
Material:	Rubber + reinforcement
Operator:	Ph.D
Preparation:	22 kGy
Teststandard	ISO 37
Speed Step1	50.00 mm/min

Testdate:	09.06.2010
Spare Field	LHC
Type of test:	Tensile
Groupe of sample	WCC-IVG-R-90-22

Gaine cable LHC	B [mm]	H [mm]	Rm [MPa]	Agt [%]
WCC-IVG-R-90-22-1	5.90	9.50	2.93	71.41
WCC-IVG-R-90-22-2	6.10	9.80	2.70	72.69
WCC-IVG-R-90-22-3	5.90	9.65	2.86	72.08
-	--			
	B [mm]	H [mm]	Rm [MPa]	Agt [%]
min	5.90	9.50	2.70	71.41
max	6.10	9.80	2.93	72.69
AM	5.97	9.65	2.83	72.06
s	0.12	0.15	0.12	0.64

Set-up

Broken sample

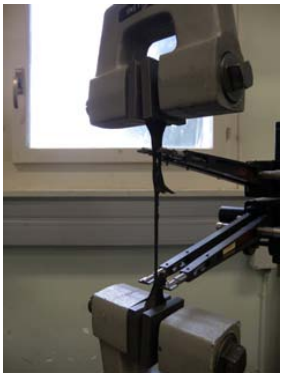

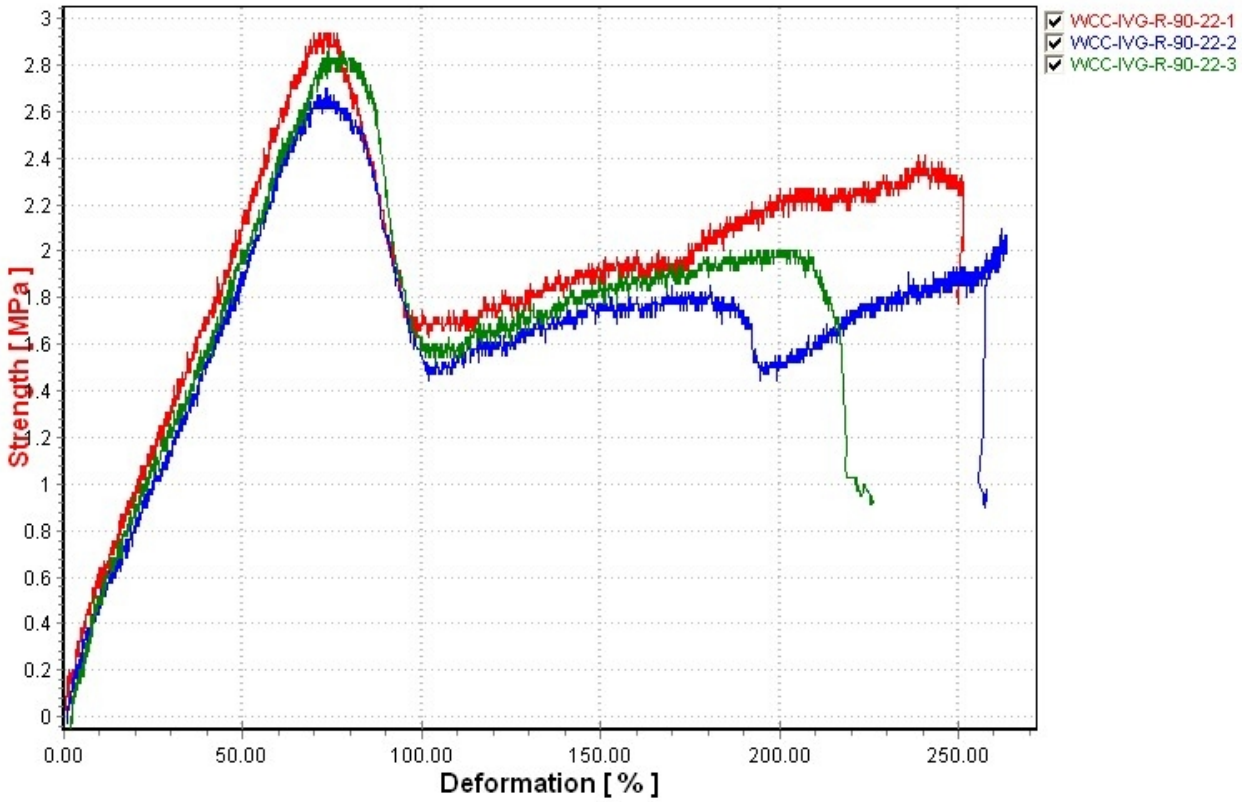

CERN - EN/MME/MM

Test Report

-

EN Engineering Department

Customer:	J-C. Guillaume EN/EL
Material:	Rubber + reinforcement
Operator:	Ph.D
Preparation:	100 kGy
Teststandard	ISO 37
Speed Step1	50.00 mm/min

Testdate:	09.06.2010
Spare Field	LHC
Type of test:	Tensile
Groupe of sample	WCC-IVG-R-90-100

Gaine cable LHC	B [mm]	H [mm]	Rm [MPa]	Agt [%]
WCC-IVG-R-90-100-1	5.98	9.70	2.81	65.70
WCC-IVG-R-90-100-2	5.90	9.80	2.84	64.12
WCC-IVG-R-90-100-3	5.95	9.70	2.85	60.33
-	--			
	B [mm]	H [mm]	Rm [MPa]	Agt [%]
min	5.90	9.70	2.81	60.33
max	5.98	9.80	2.85	65.70
AM	5.94	9.73	2.83	63.38
s	0.04	0.06	0.02	2.76

Set-up

Broken sample

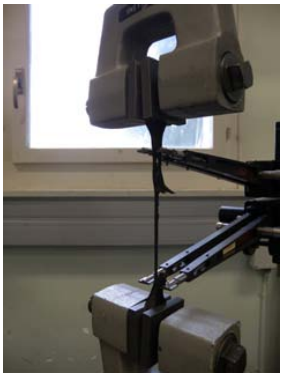

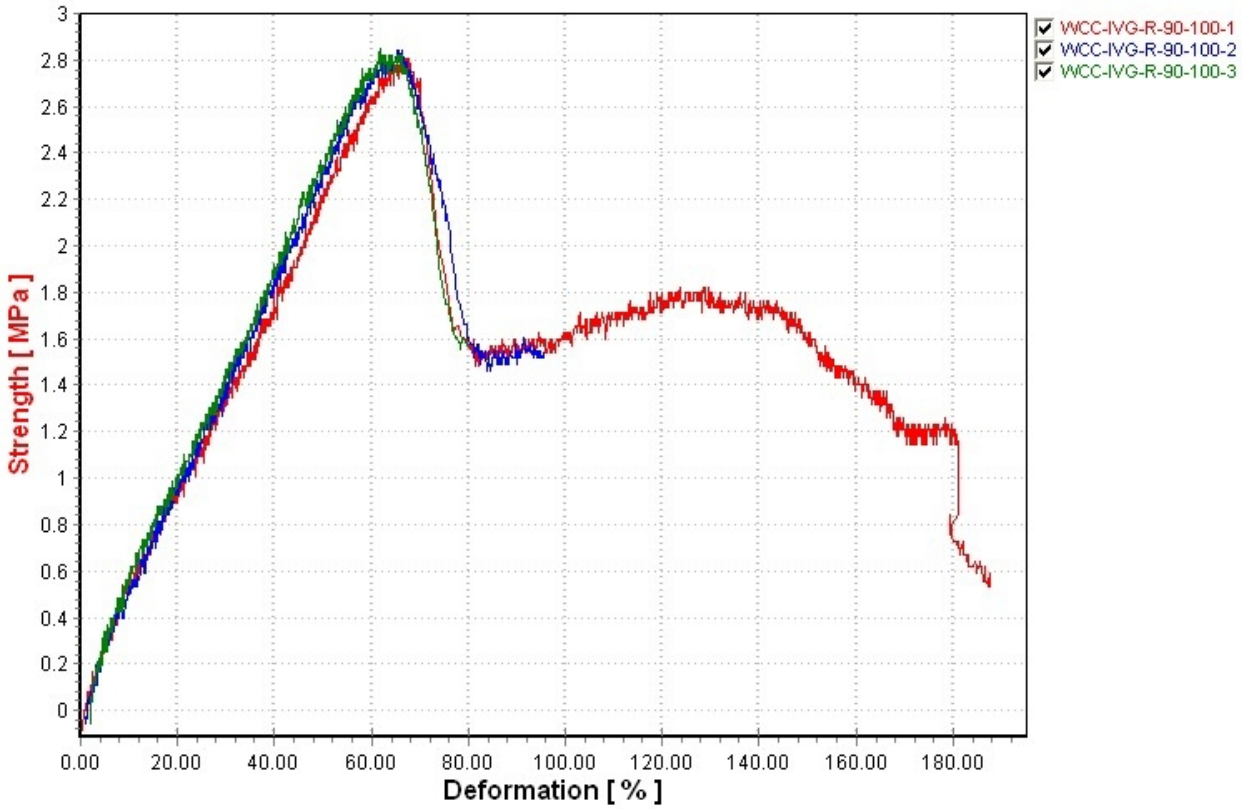

CERN - EN/MME/MM

Test Report

-

EN Engineering Department

Customer:	J-C. Guillaume EN/EL
Material:	Rubber + reinforcement
Operator:	Ph.D
Preparation:	250 kGy
Teststandard	ISO 37
Speed Step1	50.00 mm/min

Testdate:	16.09.2010
Spare Field	LHC
Type of test:	Tensile
Groupe of sample	WCC-IVG-R-90-250

Gaine cable LHC	B [mm]	H [mm]	Rm [MPa]	Agt [%]
WCC-IVG-R-90-250-1	6.27	9.80	3.36	51.11
WCC-IVG-R-90-250-2	6.05	9.75	3.42	49.69
WCC-IVG-R-90-250-3	5.70	9.75	3.51	46.05
-	--			
	B [mm]	H [mm]	Rm [MPa]	Agt [%]
min	5.70	9.75	3.36	46.05
max	6.27	9.80	3.51	51.11
AM	6.01	9.77	3.43	48.95
s	0.29	0.03	0.08	2.61

Set-up

Broken sample

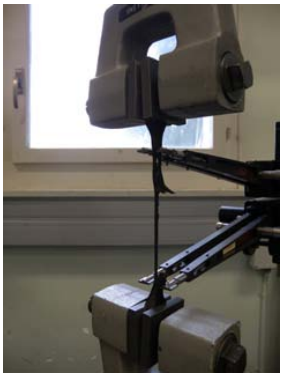

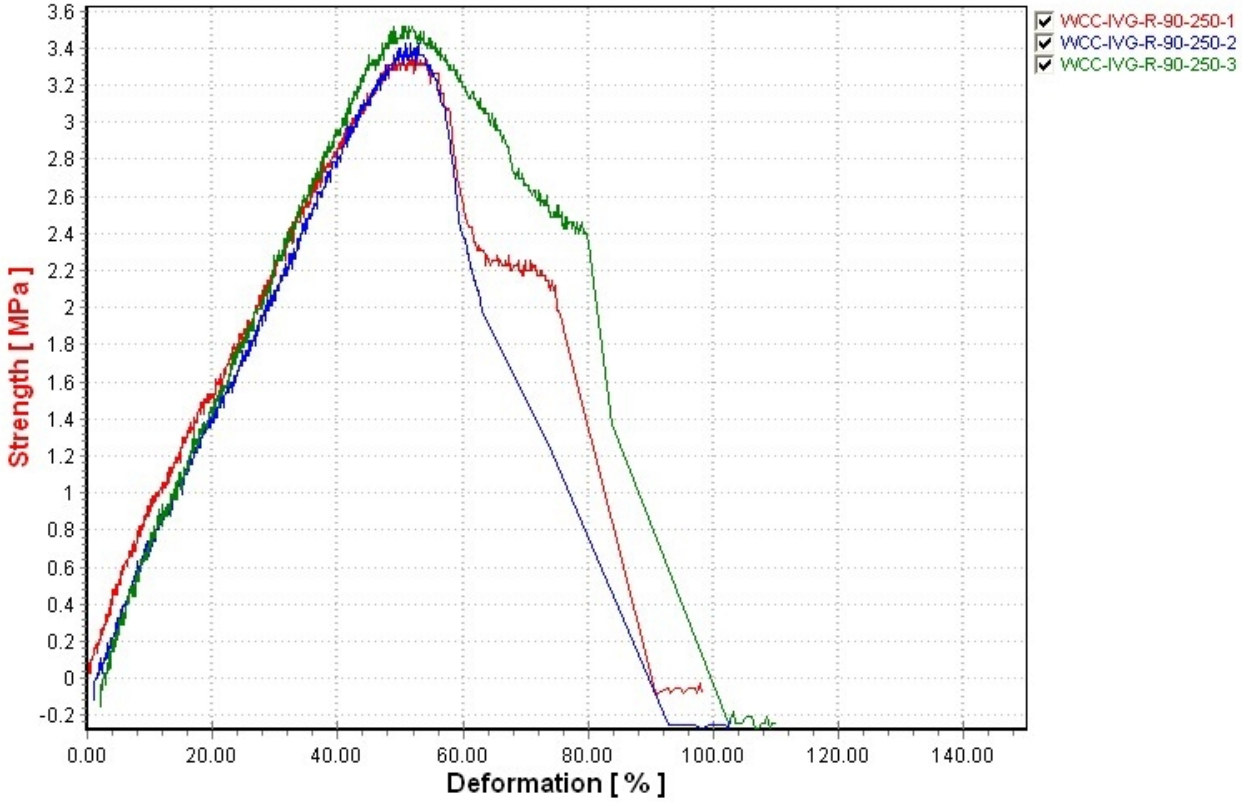

CERN - EN/MME/MM

Test Report

-

EN Engineering Department

Customer:	J-C. Guillaume EN/EL
Material:	Rubber + reinforcement
Operator:	Ph.D
Preparation:	300 kGy
Teststandard	ISO 37
Speed Step1	50.00 mm/min

Testdate:	16.09.2010
Spare Field	LHC
Type of test:	Tensile
Groupe of sample	WCC-IVG-R-90-300

Gaine cable LHC	B [mm]	H [mm]	Rm [MPa]	Agt [%]
WCC-IVG-R-90-300-1	6.20	9.85	3.12	48.14
WCC-IVG-R-90-300-2	6.20	9.80	3.16	52.80
WCC-IVG-R-90-300-3	6.10	9.80	3.35	53.31
-	--			
	B [mm]	H [mm]	Rm [MPa]	Agt [%]
min	6.10	9.80	3.12	48.14
max	6.20	9.85	3.35	53.31
AM	6.17	9.82	3.21	51.41
s	0.06	0.03	0.12	2.85

Set-up

Broken sample

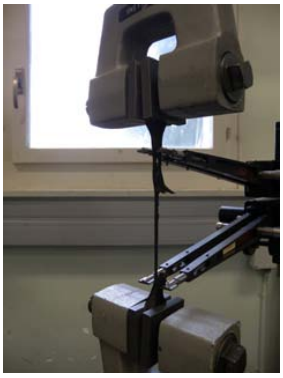

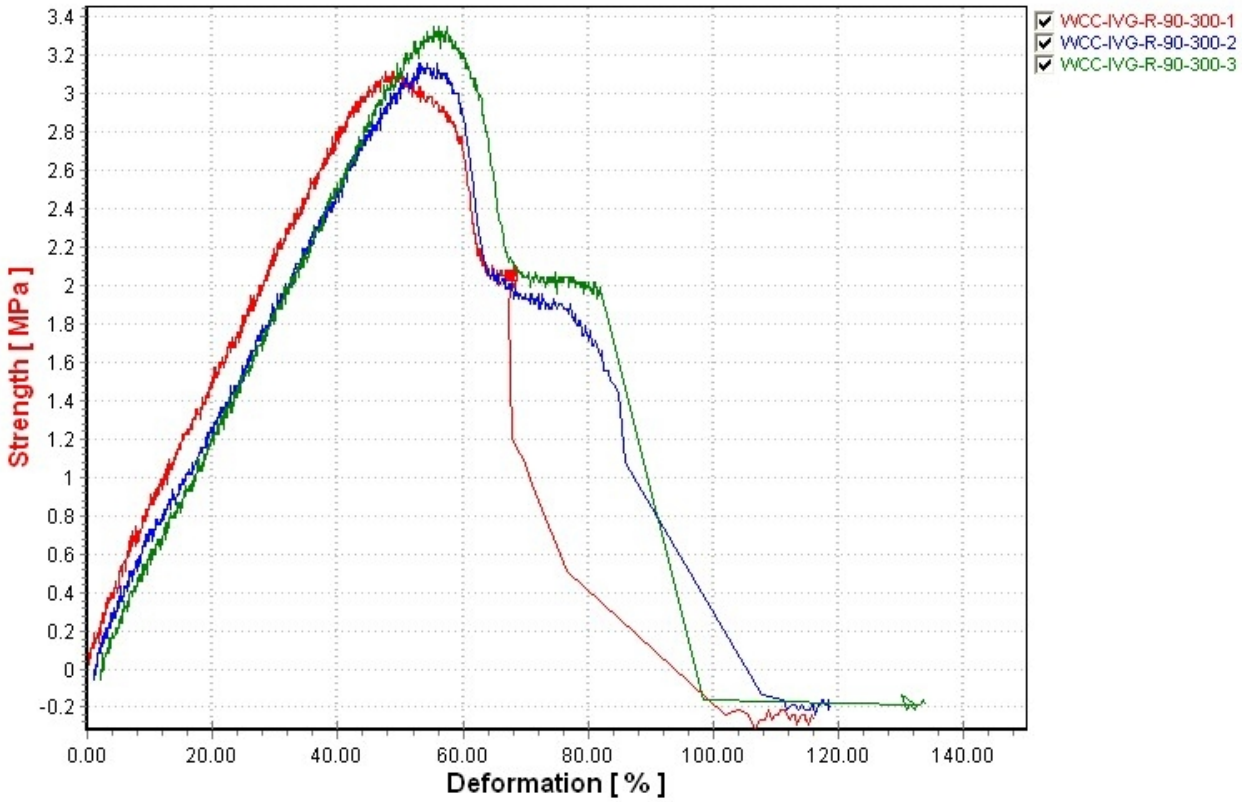

CERN - EN/MME/MM

Test Report

-

EN Engineering Department

Customer:	J-C. Guillaume EN/EL
Material:	Rubber + reinforcement
Operator:	Ph.D
Preparation:	330 kGy
Teststandard	ISO 37
Speed Step1	50.00 mm/min

Testdate:	17.09.2010
Spare Field	LHC
Type of test:	Tensile
Groupe of sample	WCC-IVG-R-90-330

Gaine cable LHC	B [mm]	H [mm]	Rm [MPa]	Agt [%]
WCC-IVG-R-90-330-1	6.30	9.75	3.13	49.88
WCC-IVG-R-90-330-2	6.30	9.65	3.35	55.94
WCC-IVG-R-90-330-3	6.00	9.65	3.40	50.57
-	--			
	B [mm]	H [mm]	Rm [MPa]	Agt [%]
min	6.00	9.65	3.13	49.88
max	6.30	9.75	3.40	55.94
AM	6.20	9.68	3.29	52.13
s	0.17	0.06	0.15	3.32

Set-up

Broken sample